



SAPIENZA
UNIVERSITÀ DI ROMA

PhD School of Pharmaceutical Sciences XXX cycle
"Sapienza" University of Rome

**DESIGN, SYNTHESIS AND BIOLOGICAL EVALUATION OF
NOVEL EPIGENETIC MODULATORS FOR PARASITIC
DISEASES**

Doctoral Dissertation
Submitted by

Gebremedhin Solomon Hailu

Department of Chemistry and Drug Technology
Faculty of Medicine and Pharmacy
"Sapienza" University of Rome

Supervisors:

*Professor **Antonello Mai** Ph.D. (tutor and main supervisor)*

Department of Chemistry and Drug Technology, "Sapienza" University of Rome, P.le Aldo Moro, 5 - 00185 – Rome, Italy.

*Adjunct Professor **A. Ganesan** Ph.D. (foreign supervisor)*

School of Pharmacy, University of East Anglia, Norwich Research Park, Norwich NR4 7JT, UK.

The present doctoral dissertation is based on the following original publications and early stage research projects listed below:

LIST OF PUBLICATIONS:

1. Wapenaar H, van den Bosch T, Leus NGJ¹, van der Wouden PE¹, Eleftheriadis N¹, Hermans J, **Hailu GS**, Rotili D, Mai A, Dömling A, Bischoff R, Haisma HJ, Dekker FJ. **The relevance of Ki calculation for bi-substrate enzymes illustrated by kinetic evaluation of a novel lysine (K) acetyltransferase 8 inhibitors.** Eur J Med Chem. 2017, 18;136:480-486.
2. **Gebremedhin S. Hailu**, Dina Robaa, Mariantonietta Forgione, Wolfgang Sippl, Dante Rotili and Antonello Mai. **Lysine Deacetylase Inhibitors in Parasites: Past, Present, and Future Perspectives.** *J. Med. Chem.*, 2017, 60(12):4780-4804
3. Sébastien Moniot, Mariantonietta Forgione, Alessia Lucidi, **Gebremedhin S. Hailu**, Angela Nebbioso, Vincenzo Carafa, Francesca Baratta, Lucia Altucci, Nicola Giacché, Daniela Passeri, Roberto Pellicciari, Antonello Mai, Clemens Steegborn, and Dante Rotili. **Development of 1,2,4-Oxadiazoles as Potent and Selective Inhibitors of the Human Deacetylase Sirtuin 2: Structure–Activity Relationship, X-ray Crystal Structure, and Anticancer Activity.** *J. Med. Chem.*, 2017, 60 (6), pp 2344–2360.
4. Vincenzo Carafa, Dante Rotili, Mariantonietta Forgione, Francesca Cuomo, Enrica Serretiello, **Gebremedhin Solomon Hailu**, Elina Jarho, Maija Lahtela-Kakkonen, Antonello Mai, and Lucia Altucci. **Sirtuin functions and modulation: from chemistry to the clinic.** *Clin Epigenetics*. 2016; 8: 61.

OTHER RESEARCH PROJECTS:

5. Design, synthesis and biological validation of uracil-based hydroxamides (HDAC inhibitors) as new antimalarial agents.
6. Design, synthesis and preliminary biological validation of *Schistosoma mansoni* Sirt2 inhibitors
7. Design and synthesis of tranylcypromine-based LSD1 inhibitors potentially active against *Schistosoma mansoni*

The main part of synthetic work of the aforementioned publications and projects have been performed by the present PhD student Hailu Gebremedhin Solomon.

Abbreviations

2-ASA, 2-aminosuberic acid;	ncRNAs, non-coding RNAs;
2OG, 2-oxoglutarate;	NFF, neonatal foreskin fibroblast;
2-PCPA,	NTDs, neglected tropical diseases;
trans-2-phenylcyclopropylamine;	OAADPr, O-acetyl-ADP-ribose;
3HPT, 3-hydroxypyridine-2-thione;	PARP, poly ADP-ribose polymerase;
AceCS2, acetyl-CoA synthase 2;	<i>PfEMP1</i> , <i>Plasmodium falciparum</i>
Acetyl-CoA, acetyl-coenzyme A;	erythrocyte membrane protein 1;
ADP, adenosine 5'-diphosphate;	<i>PfGCN5</i> , <i>Plasmodium falciparum</i> GCN5 N
ACT, artemisinin-based combination	acetyltransferase 5;
therapy;	<i>PfHDAC</i> , <i>Plasmodium falciparum</i> histone
AdoHcy, S-adenosyl-L-homocysteine	deacetylase;
AdoMet, S-adenosyl-L-methionine;	<i>PfHP1</i> , <i>Plasmodium falciparum</i>
AMC, Amino-methylcumarin;	heterochromatin protein 1;
AML, acute myeloid leukemia;	<i>PfSir2A/B</i> , <i>Plasmodium falciparum</i>
Aoda, 2-amino-8-oxodecanoic acid;	sirtuins;
AOL, oxidase-like;	PHD2, prolyl hydroxylase domain 2;
APHAs, aroylpyrrolylhydroxamates;	PRCs, polycomb repressive complexes;
ATRA, all- <i>trans</i> retinoic acid;	PRMT, protein arginine
CASP7, apoptosis-related cysteine	methyltransferase;
peptidase;	PTCL, peripheral T-cell lymphoma;
CoREST, corepressor of RE1 silencing	PTMs, post-translational modifications;
transcription factor;	PyBOP, benzotriazol-1-yl-
CQ, chloroquine;	oxytripyrrolidinophosphonium
CTCL, T-cell lymphoma;	hexafluorophosphate;
CU, connection unit;	RDT, rapid diagnostic testing;
DALYs, disability adjusted life-years;	RBC, red blood cells;
BNIP, bisnaphthalimidopropyl;	<i>rPfHDAC1</i> , recombinant <i>Plasmodium</i>
DSβH, double-stranded β-helical;	<i>falciparum</i> histone deacetylase;
EDCI, 1-ethyl-3-(3-	SAM, S-adenosyl-L-methionine;
dimethylaminopropyl)carbodiimide;	SAH, S-Adenosyl-L-Homocysteine;
EZH2, enhancer of zeste 2;	SAR, structure-activity relationship;
FAD, flavin adenine dinucleotide;	SET, [Su(var), E(z), Trithorax];
FDA, US Food and Drug Administration;	SBHA, suberic bishydroxamate;
FIH, factor inhibiting HIF;	SI, Selectivity Index;
FOXO, forkhead box O;	SirReal2, sirtuin 2 rearranging ligand;
GLP, G9a-like protein;	SIRTi, sirtuin inhibitors;
GNATs, histone N-acetyltransferases;	<i>SmHDAC</i> , <i>Schistosoma mansoni</i> histone
HATs, histone acetyltransferases;	deacetylase;
HDAC, histone deacetylase;	<i>smSirt2</i> , <i>Schistosoma mansoni</i> Sirt2;
HDACi, HDAC inhibitors;	STAT3, signal trasducer and activator of
HFF, human foreskin fibroblast cell line;	transcription 3;

HIF, hypoxia inducible factor;	SWI/SNF, (SWItch/Sucrose Non-Fermentable);
HMTs, histone methyltransferases;	SUMO, small ubiquitin-like modifier;
HOBT, 1-Hydroxybenzotriazole hydrate;	TSA, trichostatin A;
HP- β -CD, (2-hydroxypropyl)-beta-cyclodextrin;	TSSs, transcription start sites;
HS, hydrophobic spacer;	UBHAs, uracil-based hydroxamides;
hSIRT, human sirtuins;	VPA, valproic acid;
IC ₅₀ , half maximal inhibitory concentration;	VSGs, variant surface glycoproteins;
IDH, isocitrate dehydrogenase;	ZBG, zinc-binding group;
IRS, indoor residual spraying;	ZBD, zinc-binding domain;
ITNs, insecticides-treated nets;	ZFs, zinc finger;
JmjC, Jumonji C;	ZMAL, Z-Acetyl-Lysine-Amino-methylcumarin;
KDMs, lysine demethylases;	
KMTs, lysine methyltransferases,	
LSD1/2, lysine demethylase 1/2;	
MAOs, mono amine oxidases;	
MDS, myelodysplastic syndromes;	

Contents

1. INTRODUCTION	1
1.1 Epigenetics	1
1.2 DNA Methylation	3
1.3 Histone Modification and Chromatin Remodeling	5
2. HISTONE POSTTRANSLATIONAL MODIFICATIONS (PTMs)	9
2.1 Histone Methylation	9
2.1.1 Histone Methyltransferases	10
2.1.2 Histone Demethylases	12
2.1.2.1 Lysine Specific Demethylase-1 (LSD1)	17
2.1.2.2 Lysine Specific Demethylase-2 (LSD2)	20
2.1.2.3 JmJc Histone Demethylase	21
2.2 Histone Acetylation	24
2.2.1 Histone Acetyltransferases (HATs)	25
2.2.2 Histone Deacetylases	28
2.2.2.1 HDACs	29
2.2.2.2 HDAC Inhibitors	30
2.2.2.3 Sirtuins	33
2.2.2.4 Sirtuin Inhibitors	36
2.3 Histone Phosphorylation	37
2.4 Histone Ubiquitylation	37
2.5 Histone ADP-ribosylation	38
2.6 Histone SUMOylation	39
3. EPIGENETIC TARGETS IN MALARIA AND NEGLECTED TROPICAL DISEASES	40
3.1 Overview of Malaria and Neglected Tropical Diseases	40
3.2 Malaria Epidemiology and Therapeutics	41
3.3 Malaria Life Cycle	43
3.4 The Epidemiology and Distribution of Human Schistosomiasis	45
3.5 <i>Schistosoma mansoni</i> Life Cycle	46
3.6 Control of Schistosomiasis, the Lack of Alternative Therapeutics	48
4. MALARIA EPIGENETICS	49
4.1 Epigenetic Mechanisms as Drug Targets for <i>P. falciparum</i>	49
4.2 <i>Plasmodium falciparum</i> Chromatin Organization and Histone PTMs	53
4.3 Malarial Histone-modifying Enzymes	57
4.3.1 Modifiers of histone acetylation	57
4.3.2 Modifiers of Histone Methylation	60

4.3.3 Consequences of Histone Modifications: “Histone Readers” in Malaria.....	61
4.4 Antimalarial Epi-drugs.....	63
4.4.1 Antimalarial HAT Inhibitors.....	64
4.4.2 Antimalarial HDAC Inhibitors	65
4.4.2.1 Cyclic Tetrapeptide HDAC Inhibitors.....	65
4.4.2.2 Short-chain Fatty Acid HDAC Inhibitors	66
4.4.2.3 Hydroxamate-Based HDAC Inhibitors	67
4.4.2.4 Thiol-based HDAC Inhibitors	74
4.4.2.5 <i>Ortho</i> -Amino-Anilides HDAC Inhibitors.....	74
4.4.2.6 Other Amides as HDAC Inhibitors	77
4.4.3 Antimalarial Sirtuin Inhibitors.....	79
4.4.4 Antimalarial HKMT Inhibitors.....	81
5. EPIGENETIC MECHANISMS AS DRUG TARGETS FOR <i>SCHISTOSOMA MANSONI</i>	84
5.1 DNA Methylation in Schistosomes.....	85
5.2 Schistosome miRNAs.....	85
5.3 Schistosome Histone Modifications.....	86
5.3.1 Schistosome Histone Acetyltransferase.....	88
5.3.2 Schistosoma HDACs	90
5.3.3 Antischistosomal HDAC Inhibitors	90
5.3.4 Schistosoma Sirtuins	92
5.3.5 Schistosoma Sirtuin Inhibitors	93
5.3.6 Histone Methylation and Demethylation	94
6. DESIGN, SYNTHESIS AND BIOLOGICAL VALIDATION OF URACIL-BASED HYDROXAMIDES (HDAC INHIBITORS) AS NEW ANTIMALARIAL AGENTS.....	96
6.1 Research Project	96
6.2 Chemistry	99
6.3 Experimental Section	101
6.4 Biological Evaluation and Results.....	104
6.4.1 Phenotypic screening of epigenetic modulators against 3D7	104
6.4.2 Antiplasmodial activity of analogues derived from active compounds (focused screening)	104
6.4.3 Antiplasmodial activity against W2, a multiresistant strain	107
6.4.4 Selectivity Index (SI) on primary activated cells (splenic murine cells) and on eukaryotic cell line (HFF)	108
6.4.5 Pharmacokinetic analysis.....	108
6.4.6 Effect on histones of treated <i>P. falciparum</i> parasites.....	109

6.4.7 <i>In vivo</i> antimalarial activity in <i>P. berghei</i> infected mice	109
6.5 Discussion and Conclusion	110
6.6 Methods	113
6.6.1 Determination of <i>in vitro</i> activity against <i>P. falciparum</i>	113
6.6.2 <i>In vivo</i> experiments	114
7. DESIGN, SYNTHESIS AND PRELIMINARY BIOLOGICAL VALIDATION OF <i>SCHISTOSOMA MANSONI</i> SIRT2 INHIBITORS	115
7.1 Research Project	115
7.2 Chemistry	123
7.3 Experimental Section	130
7.4 Biological evaluation, results and discussion	139
7.5 Conclusion and perspectives	145
7.6 Methods	147
8. DESIGN AND SYNTHESIS OF TRANSLCYPROMINE-BASED LSD1 INHIBITORS POTENTIALLY ACTIVE AGAINST <i>SCHISTOSOMA MANSONI</i>	150
8.1 Research Project	150
8.2 Chemistry	152
8.3 Experimental Section	157
8.4 Conclusion and perspectives	169
ACKNOWLEDGEMENTS	170
BIBIOLOGRAPGY	171

1. INTRODUCTION

1.1 Epigenetics

Conrad Waddington, who introduced the term epigenetics in the early 1940s [1], defined epigenetics as “the branch of biology which studies the causal interactions between genes and their products which bring the phenotype into being.” In the original sense of this definition, epigenetics referred to all molecular pathways modulating the expression of a genotype into a particular phenotype. Over the following years, the meaning of the word has gradually narrowed, due to drastic progress of genetics [1-3]. By contrast, Arthur Riggs and colleagues defined epigenetics as “the study of mitotically and/or meiotically heritable changes in gene function that cannot be explained by changes in DNA sequence” [4]. Given that there are several existing definitions of epigenetics, the following could be a unifying definition of epigenetic events: the structural adaptation of chromosomal regions so as to register, signal or perpetuate altered activity states. This definition is inclusive of chromosomal marks, because transient modifications associated with both DNA repair or cell-cycle phases and stable changes maintained across multiple cell generations qualify. It focuses on chromosomes and genes, implicitly excluding potential three-dimensional architectural templating of membrane systems and prions, except when these impinge on chromosome function. Also included is the exciting possibility that epigenetic processes are buffers of genetic variation, pending an epigenetic (or mutational) change of state that leads an identical combination of genes to produce a different developmental outcome [5].

In the eukaryotic nucleus, DNA is compacted in a structure defined as chromatin, whose basic unit is the nucleosome. Each nucleosome is formed by protein called histone which in turn surrounded by about 145–147 pairs of DNA bases. Histone is an octamer constituted by four pairs of proteins, called H3, H4, H2A and H2B. The very long molecules of DNA are firstly “supercoiled” and then packaged on to histones, allowing to their compression into a single cell [6-7]. Eukaryotic chromatin is in equilibrium between two distinct higher-order structures: heterochromatin is a more condensed structure, transcriptionally silent, and in regions surrounding centromeres and telomeres; euchromatin is a less condensed structure and transcriptionally competent [8-9]. This feature accomplishes that, starting to the same DNA sequence, cells may differentiate in very different ways. The bidirectional conversion between euchromatin and heterochromatin is determined by epigenetic regulation. Over-all,

three main mechanisms of epigenetic regulation have been identified. Two of them, including DNA methylation and histone covalent modification, influence the type of chromatin, whereas the third is based on the expression of micro-RNAs [10-11]. The most intensely studied epigenetic modification is DNA methylation[12]; however, the most diverse modifications are those that occur on histone proteins [13-14]. In addition to DNA and histone modification, chromatin structure and function are regulated by chromatin remodeling complexes (for example, SWI/SNF and NuRD families), non-coding RNAs (for example, HOX transcript antisense RNA (*HOTAIR*) and HOXA distal transcript antisense RNA (*HOTTIP*)) and mutations in histone proteins themselves [15-16].

These mechanisms together alter the local structural dynamics of chromatin to regulate the functioning of the genome, mostly by regulating its accessibility and compactness. All together, these mechanisms govern the chromatin architecture and gene function in various cell types, developmental and disease states [10, 14, 17-20]. Disruption in the proper maintenance of these heritable epigenetic mechanisms can result in activation or inhibition of various critical cell signaling pathways thus leading to various disease states [21-22]. Importantly, the epigenetic state of a cell is malleable; it evolves in an ordered manner during the cellular differentiation and development of an organism, and epigenetic changes are responsible for cellular plasticity that enables cellular reprogramming and response to the environment. Because epigenetic mechanisms are responsible for the integration of environmental cues at the cellular level, they have important roles in diseases related to diet, lifestyle, early life experience and environmental exposure to toxins [23-24]. Thus, epigenetics is of therapeutic relevance in multiple diseases such as cancer, inflammation, metabolic disease and neurological disorder, as well as in infectious diseases [25-27].

Epigenetic regulators can be divided into distinct groups based on broad functions: epigenetic writers lay down epigenetic marks on DNA or histones; these marks are removed by epigenetic erasers and recognized by epigenetic readers (Fig. 1.1). The enzymatic nature of epigenetic writers and erasers has facilitated the generation of pharmacological inhibitors for many of these enzymes, some of which are clinically approved [15-16]. Inhibitors of epigenetic readers are also in development [16, 28]. These inhibitors show potent anticancer efficacy as well as activity in a range of other disease states. The most successful and long-standing inhibitors of epigenetic processes are the US Food and Drug Administration (FDA)-approved DNA-demethylating agents azacitidine (also known as 5-azacytidine (Vidaza);

Celgene)) and decitabine (also known as 5-aza-2'-deoxycytidine (Dacogen; Eisai)), which are used to treat myelodysplastic syndromes (MDS) and a range of other malignancies [29-30]. Other inhibitors of epigenetic writers, such as the histone methyltransferases DOT1L [31-32] and EZH2 [33-34], have exciting potential for cancer treatment, whereas protein arginine methyltransferase (PRMT) inhibitors show promise for cancer and immune-mediated diseases [35-36].

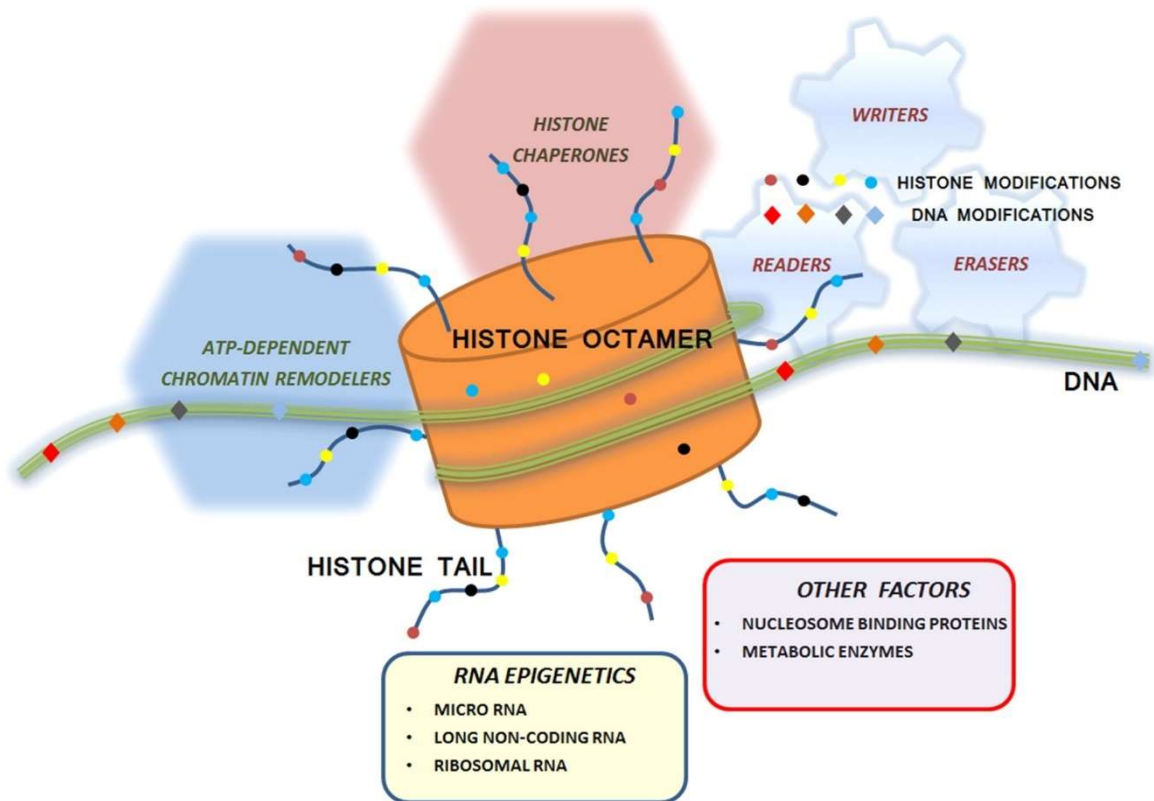


Fig. 1.1: Simplified framework of the various components and mechanisms of the epigenetic machinery. A histone octamer is shown as orange cylinder, and DNA wrapped around the octamer is shown as green ribbon. Chemical modifications to histone surfaces and tails are depicted as filled circles, and modifications to DNA are depicted as filled diamonds [37].

1.2 DNA Methylation

DNA methylation is a common mechanism of epigenetic regulation in eukaryotic organisms ranging from fungi to mammals. DNA methylation is a heritable epigenetic mark involving the covalent transfer of a methyl group to the C-5 position of the cytosine ring of DNA by DNA methyltransferases (DNMTs) [38]. In humans, DNA methylation is a stable epigenetic mark that occurs at the C5 position of cytosines, mainly in a CpG dinucleotide context, but also in non-CpG regions of stem cells[39-40]. More than 50% of genes are associated with CpG islands in their promoter regions. Generally, low levels or a lack of DNA methylation in the promoter region is correlated with an “on” configuration of chromatin that

favors the interaction of DNA with transcription complexes leading to the activation of gene expression. By contrast, methylation of CpG islands in gene promoters is correlated with an “off” configuration of chromatin that leads to gene silencing [41-42]. DNA methylation can maintain differential gene expression patterns in a tissue-specific and developmental-stage-specific manner. The roles of DNA methylation in gene bodies and other regions started to be characterized in the last years [41]. DNA methylation is a highly effective mechanism for silencing of gene expression in vertebrates and plants, either by interfering with the binding of transcription factors, or by attracting methylated DNA-binding proteins (MBDs), able to recruit other proteins and histone modifying enzymes, which leads to formation of a closed chromatin configuration and silencing of gene expression [43-44]. Indeed, most DNA methylation is essential for normal development, and it plays a very important role in a number of key processes including genomic imprinting, X-chromosome inactivation, and suppression of repetitive element transcription and transposition and, when dysregulated, contributes to diseases like cancer [38, 45]. Noteworthy, DNA methylation patterns are altered in the progression of cancer. Both the hypomethylation and hypermethylation of different regions of the genome play a crucial role in tumorigenesis. During the development of tumors, a genome-wide demethylation occurs and this can promote genomic instability possibly by activating silenced retrotransposons [46]. On the other hand, focal hypermethylation of CpG islands has been intensively studied in cancer. Nearly all types of cancers have transcriptional inactivation of tumor suppressor genes due to DNA hypermethylation [12]. However, the exact mechanism responsible for the appearance of DNA methylation in a given promoter is not fully understood.

DNA methylation is regulated by a family of DNMTs: DNMT1, DNMT2, DNMT3A, DNMT3B, and DNMT3L [47-49]. DNMT1 preferentially methylates hemimethylated DNA *in vitro* and is localized to replication foci during S phase. As such, it is the proposed maintenance methyltransferase responsible for copying DNA methylation patterns to the daughter strands during DNA replication [50]. DNMT2 is a methyltransferase homolog that methylates cytosine-38 in the anticodon loop of aspartic acid transfer RNA instead of DNA [51]. DNMT3A and DNMT3B, in contrast to DNMT1, have preference for unmethylated CpG dinucleotides and perform *de novo* methylation during development. Possessing homology to DNMT3A and DNMT3B, DNMT3L assists the *de novo* methyltransferases by increasing their ability to bind to the methyl group donor, S-adenosyl-L-methionine (SAM), and stimulating their activity *in*

vivo [52], although DNMT3L has no catalytic activity itself. Cooperation among different DNMTs is also required in methylating some regions of the genome, particularly repetitive elements. As previously mentioned, it has been widely believed that DNMT1 acts mainly as a “maintenance” methyltransferase during DNA synthesis and that DNMT3A and DNMT3B act as “*de novo*” enzymes in development. However, mounting evidence indicates that DNMT1 may also be required for *de novo* methylation of genomic DNA [53] and that DNMT3A and DNMT3B contribute to *maintenance* methylation during replication [54].

A mechanistic proposal for the DNA methylation at the cytosine C5 position in CpG nucleotide islands catalysed by DNMT is shown in Fig. 1.2. The formation of a reactive enamine intermediate by the addition of a cysteine residue of the DNMT binding pocket to cytosine C6 position following base-flipping [55-56], assisted by the protonation at C3 by a glutamic acid, is followed by the transfer of the methyl group of cofactor SAM to and a β -elimination on the 5-methyl-6-Cys-S-5,6-dihydrocytosine intermediate [57].

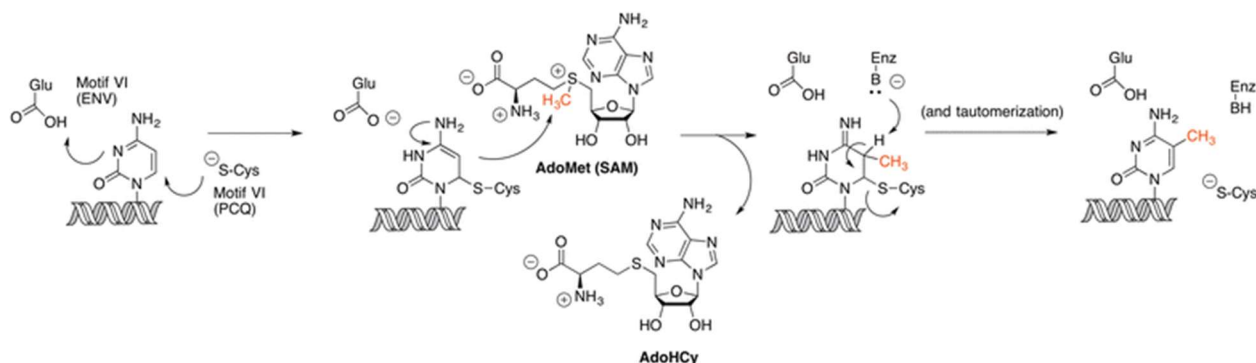


Fig. 1.2: Mechanism of cytosine methylation at C5 catalysed by DNMT, with SAM as electrophile [57].

1.3 Histone Modification and Chromatin Remodeling

Eukaryotic cells organize their genetic material into a DNA-protein complex, called chromatin where its assembly limits the accessibility of genomic sequences, and thus it creates inherent barriers for nuclear events such as transcription, DNA replication, and DNA repair. Consequently, chromatin structure must be dynamic or fluid, and local changes in chromatin structure are utilized to provide the cell with profoundly effective methods for fine-tuning DNA metabolism. Not too surprisingly, disruption of mechanisms that control chromatin dynamics can lead to aberrant gene expression, improper or nonexistent DNA repair, chromosomal translocations, inappropriate proliferation, developmental errors, oncogenesis, or even cell death [58].

Nucleosomes are efficient DNA-packaging units (Fig. 1.3). The fundamental protein unit of the nucleosome is the histone dimer, a simple α -helical domain possessing a highly basic, curved surface that closely matches the phosphate backbone of bent duplex DNA. Two copies each of histone heterodimer, H3/H4 and H2A/H2B, form a histone octamer that is wrapped with approximately 146 bp of duplex DNA in a left-handed spiral [59-60]. Nucleosomes are assembled into long, linear arrays in which each nucleosome is connected by 10–70 bp of linker DNA, with the length varying between species and cell types. The high affinity of the histone octamer for DNA ensures that nucleosome assembly is a significant barrier for enzymes requiring DNA access, and the folding or compaction of nucleosomal arrays can lead to additional constraints on nuclear processes [61].

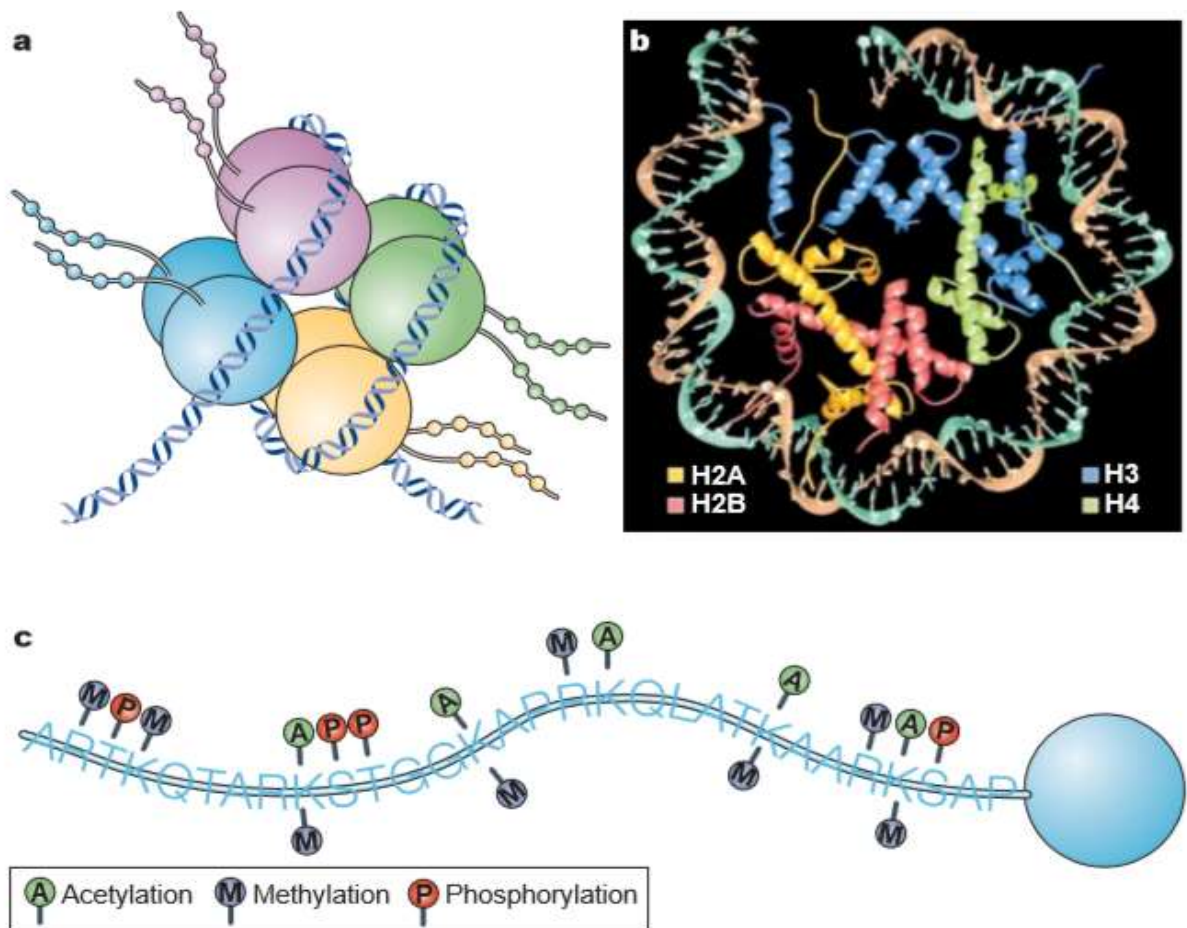


Fig. 1.3: Structure of nucleosome. a) Each nucleosome comprises an octamer of histone molecules, which consists of an H3₂–H4₂ tetramer and two H2A–H2B dimers. The amino (N) termini of histones project out of the nucleosome core and can be epigenetically modified. b) Crystal structure of the nucleosome depicting the interaction of DNA with histones. c) Many sites in the N terminus can be targets for epigenetic tagging [62].

Consequently, in addition to DNA sequence, which influences both preferred nucleosome positioning and unwrapping characteristics [63-66], two distinct mechanisms further modulate nucleosome stability and dynamics. One mechanism involves chemically altering

the histones themselves, which changes the energy landscape of histone–DNA interactions and therefore greatly increases the dynamic range of DNA accessibility. These chemical changes can be in the form of post-translational modifications (PTMs) that can modulate chromatin folding [67-68], and guide the binding of regulatory proteins [69-70]. Non-allelic variants of the core histones, such as H2A.Z or H3.3, can also be incorporated into nucleosomes, and these variant nucleosomes can have altered stability and/or present novel opportunities for PTMs [71-72].

The second, and perhaps most potent mechanism, is the use of ATP-dependent chromatin remodeling enzymes that can lead to a discernible change in histone–DNA contacts. Such changes in contacts can result from the repositioning (sliding) of nucleosomes on DNA, the removal of part or all of the histone octamer from DNA, an induced change in the accessibility of the DNA in chromatin to proteins such as transcription factors or nucleases, and the exchange of histone variants for core histones [73]. Indeed, several chromatin remodeling enzymes use the energy of ATP hydrolysis to catalyze the deposition or removal of histone variants, and thus they play an integral role in regulating their chromosomal distributions. There are four subfamilies of ATP-dependent chromatin remodeling enzymes: SWI/SNF, INO80, ISWI, and CHD [58, 73-74]. Each family is defined by a characteristic ATPase subunit that is related to the DEAD/H superfamily of DNA helicases, but they also possess unique motifs that mediate binding to nucleosomes and individual complex subunits.

In conjunction with histone variants, PTMs not only alter intrinsic dynamics of nucleosomes but also provide chemical signposts to help guide cellular factors to particular locations in the genome. Through recruitment of cellular factors that bind to PTM-marked histones, termed the “histone code,” PTMs play an essential role in defining and maintaining functionally distinct regions of the genome [75-80]. Histone chaperones and chromatin remodelers bind to and sense PTMs as well, and in many cases the specificity of their activities can be traced to PTM-dependent interactions [81-87]. The majority of histone PTMs occur within the 10–30 amino acid N-terminal domains of each of the histones (often called the histone “tails”). These domains extend from the nucleosomal surface, and although they do not directly contribute to the organization of nucleosomal DNA, the N-terminal tails provide interaction surfaces for a host of nucleosome binding proteins, and are essential for chromatin higher order folding [61, 69]. Histone modifications also occur within the globular

domains that organize nucleosomal DNA, and given the remarkable number of histone modifications, it may well be that every solvent-exposed histone residue might be a target for modification. Histone PTMs that can be dynamically added and removed enzymatically, with the best-studied modifications including acetylation, methylation, phosphorylation, ubiquitylation, and ADP-ribosylation (Fig. 1.4) [75-76, 80]. These marks, plus other more recently appreciated modifications such as crotonylation, succinylation, and malonylation [88], have the potential to alter histone–DNA and histone–histone interactions and thus provide a means for transiently targeting changes in nucleosome dynamics [89-91]. Surprisingly, very few histone marks appear to affect chromatin structure dramatically by themselves [69], with the large majority of histone modifications influencing either the binding or activity of other regulatory factors, such as ATP-dependent chromatin remodelling enzymes.

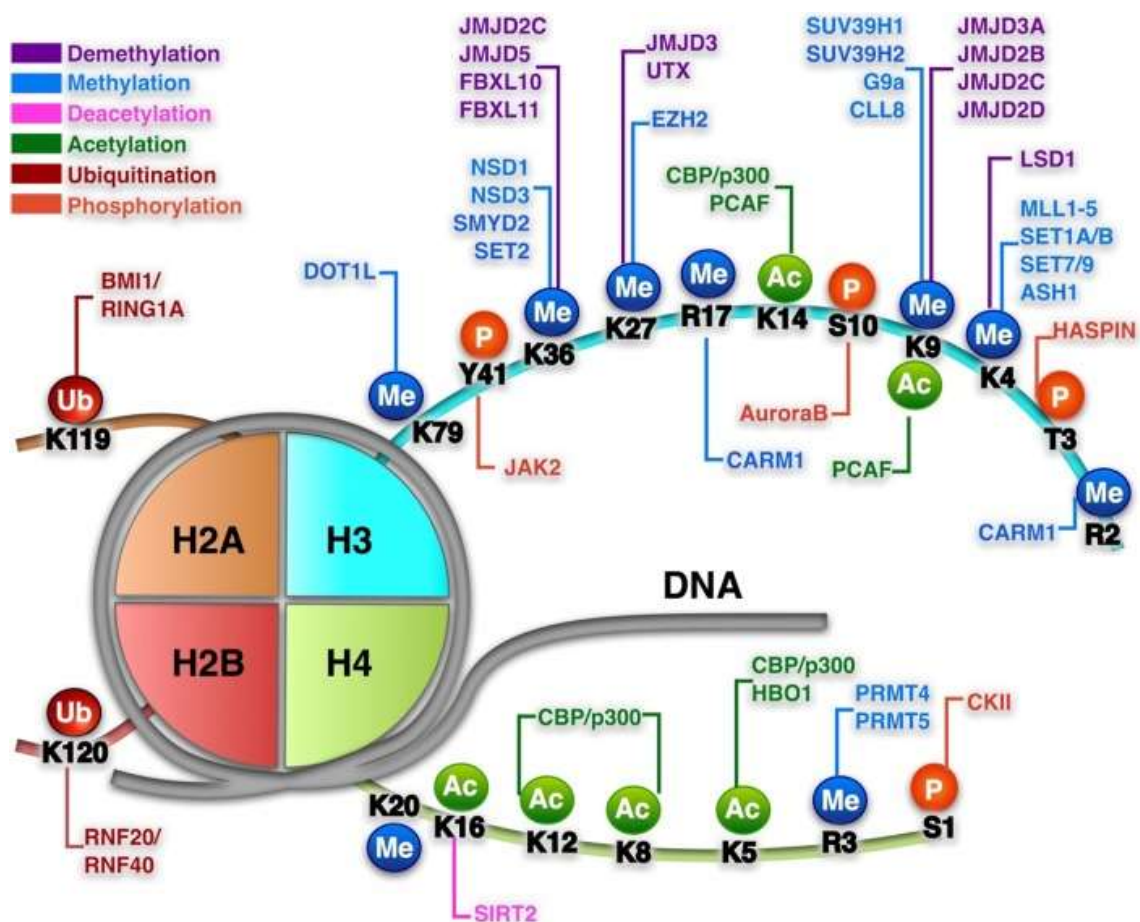


Fig. 1.4: Histone modifying enzymes. The histone octamer is assembled from a histone H3:H4 tetramer and two H2A:H2B dimers. The histone tails of all four core histones are subject to a variety of post-translational modifications, including methylation (Me), acetylation (Ac), phosphorylation (P), and ubiquitination (Ub). These modifications are controlled by enzymes such as: histone methyltransferases (HMTs) (dark blue), HDMs (purple), HATs (dark green), HDACs (pink), kinases (orange), and ubiquitin-conjugating enzymes (dark red) [92].

2. HISTONE POSTTRANSLATIONAL MODIFICATIONS (PTMs)

2.1 Histone Methylation

Methylation of histones was first described in 1964 [93]. Direct evidence linking methylation and transcription was only found some 35 years later, when the histone H3 arginine-specific histone methyltransferase (HMT) CARM1 was shown to interact and cooperate with the steroid-hormone-receptor coactivator GRIP-1 in transcriptional activation [94]. Histone methylation occurs on all basic residues: arginines, lysines and histidines. Lysines can be mono-, di- or trimethylated on their ϵ -amine group [93, 95], arginines can be monomethylated, symmetrically dimethylated or asymmetrically dimethylated on their guanidinyll group, and histidines have been reported to be monomethylated, although this methylation appears to be rare and has not been further characterized [96-97]. Initial studies of histone modifications have indicated that histones H3 (lysines 4, 9 and 27) and H4 (lysine 20) are frequently preferentially methylated [98]. Whereas, Arginine methylation takes place within the tails of histone H3 at R2, R17, R26 and histone H4 at R3. Furthermore, the N-terminus of H1 is methylated at lysine residues [99] and the methylation of nonhistone proteins has been documented as well [100-101]. However, many other basic residues beside the histone proteins H1, H2A, H2B, H3 and H4 have also recently been identified as methylated by mass spectrometry and quantitative proteomic analyses. The number of targetable histone lysine residues and the degree of methylation on each methylation site give rise to a highly complex repertoire of potential functional outputs. Histone methylation marks do not working in isolation but rather in cooperation with other histone modifications [102]. While some lysine methylation marks are preferentially associated with euchromatin and hence gene activation (like H3K4, H3K36, and H3K79) or with heterochromatin and gene silencing (H3K9, H3K27, and H4K20) [103], more often the final effect on chromatin is influenced by the interplay of several histone modifications together ("histone crosstalk") [104]. An aberrant covalent histone modification profile, leading to a dysregulated expression of oncogenes and tumor suppressor genes, is often associated with cancer [102]. Fraga et al. demonstrated, for example, that the reduction of Lys16 acetylation and Lys20 trimethylation at histone 4 constitutes a typical "cancer signature" [105]. Furthermore, aberrant histone methylation has been related not only with cancer but also with mental retardation and aging [106-108].

Histone methylation is a stable epigenetic mark that does not alter the overall charge of the histone tails. However, with increasing methylation [109] comes an increase in basicity, hydrophobicity, and an influence on the affinity for anionic molecules like DNA [110-111]. HMTs display remarkable specificity in the level of methylation they catalyze, and the latest findings suggest that this could have functional significance in transcription [112].

Similar to other histone modifications, histone methylation can modulate histone interaction with DNA and chromatin associated proteins, which results in an alteration of nucleosomal structures and functions, and ultimately contributes to different biological processes [113]. Two super-families of enzyme control histone lysine methylation states: lysine methyltransferases (KMTs) and demethylases (KDMs).

2.1.1 Histone Methyltransferases

Histone lysine methyltransferases (termed protein lysine methyltransferases, PKMTs, because of their histone and non-histone substrates) and histone arginine methyltransferases (termed protein arginine methyltransferases, PRMTs) [114] catalyze the transfer of a methyl group from S-adenosyl-L-methionine (Ado-Met) to *N*-terminal histone lysines (producing mono, di-, and trimethylate) and arginines (producing mono- or dimethylate in a symmetric or asymmetric manner), respectively, with release of S-adenosyl-L-homocysteine (Ado-Hyc) (Fig. 2.1). A range of 60–96 HMTs have been identified in the human genome through phylogenetic analysis, though not all putative HMTs have been shown to methylate histones [23, 114]. There are two different families of lysine methyltransferases divided on the basis of their catalytic domain sequence: the DOT1-like proteins and the SET domain-containing proteins. The acronym SET came from the *Drosophila* polycomb proteins in which this domain was originally found, namely Suppressor of variegation 3–9 (Su(var)3–9), Enhancer of zeste (E(z)), and Trithorax (Trx) [115-117].

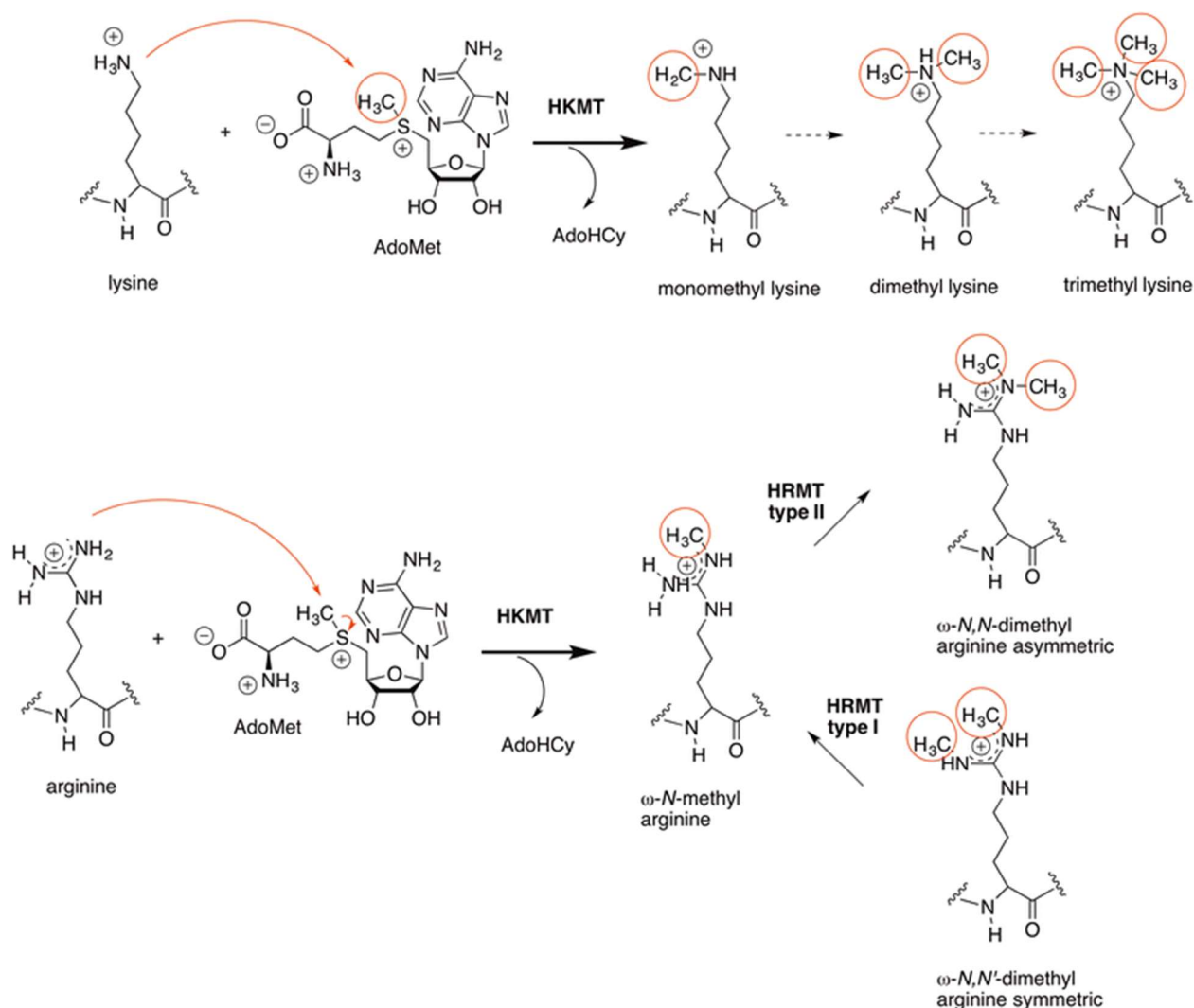


Fig. 2.1: (top) Mechanism of methylation of histone lysine residues catalyzed by KMTs and (bottom) of arginine residues catalyzed by PRMTs [57].

To date, over 300 proteins have been identified that contain SET domains[118], and which can be grouped into four major classes: SET1, SET2, SUV39 and RIZ-SET. Their classification is based foremost on sequence similarity between the SET domains and secondarily on their relationship to SET domains in the yeast *S. cerevisiae* [119-120]. Furthermore, each enzyme family shows other common structural features, such as bromo-, chromo-, PRE-SET- and POST-SET domains; it appears that all of them have the same substrate specificity [119, 121-122].

The SET methyltransferase represents the catalytic domain, while the accessory proteins control the selectivity and the activity of the complex. The SET1 family is characterized by the presence of the SET domain usually followed by a post-SET domain, even if the two most studied members of this family, EZH1 and EZH2, do not harbor this region. The members of

the SET2 class have a SET domain that is always between a post-SET and an AWS domain, rich in cysteines. In this family, we find the nuclear receptor binding SET domain-containing proteins NSD1-3, the SETD2 and the SMYD family proteins. The SUV39 family members all present a pre-SET domain, essential for enzymatic activity [115]. SUV39H1, SUV39H2, G9a, GLP, ESET, and CLLL8 belong to this class. Finally, the RIZ family members, bearing the SET domain at the amino terminus, are RIZ1, BLIMP1, and PFM1. To date, no known RIZ proteins possess methyltransferase activity. There are examples of SET domain HKMTs that monomethylate only (SET7/9) and that mono-, di-, and trimethylate (G9a, EZH2) histone lysines. PKMT-catalyzed trimethylation has been found to proceed by both processive (G9a) and distributive (EZH2) biochemical mechanisms [123-125].

In 2002, the first non-SET HKMT was identified, termed Dot1. It exhibits specificity for H3-K79 [116]. For this reason, HKMTs should not be classified by sequence homology, but instead on the basis of epigenetic criteria regarding their histone specificity. At this point it is not known how different HKMTs control their catalysis of mono-, di-, and trimethylation, and in which way this varied substitution pattern correlates with transcription [126].

Mammalian PRMTs methylate the terminal guanidino side chain of Arg to one of three species: (1) monomethyl arginine, (2) asymmetric dimethylarginine, and (3) symmetric dimethylarginine (Fig. 2.1) [127-128]. There are nine mammalian PRMTs, all of which catalyze the formation of monomethyl arginine. Among these, type I PRMTs also catalyze the formation of asymmetric dimethylarginine (PRMT1-4, -6, and -8), and type II PRMTs also catalyze the formation of symmetric dimethylarginine (PRMT5) [128-129]. PRMT7 catalyzes only monomethyl arginine formation, and PRMT9 is active but has not yet been characterized. Enzyme and structural studies indicate that PRMT-catalyzed reactions proceed via an ordered sequential bi-bi kinetic mechanism with Ado-Met, as the methyl donor, binding followed by binding of the arginine-containing protein [130]. Similar to that of PKMTs, PRMT-catalyzed methyl transfer likely proceeds through an SN2 mechanism, and data indicate that the reaction is processive from arginine to dimethylarginine (Fig. 2.1) [114, 131].

2.1.2 Histone Demethylases

For many years after the discovery and characterization of histone methylation, it was proposed that this PTM is highly stable [111, 132] and that only nonenzymatic mechanisms, such as histone protein exchange, are responsible for histone demethylation [133-134]. Only

a decade ago was this disproven by Shi and colleagues with the first report of a histone demethylase, lysine-specific demethylase 1 (LSD1) [115].

Up to date, two classes of KDM have been described: the amine-oxidase type lysine-specific demethylases 1 and 2 (LSD1 and 2; also known as KDM1A and B, respectively) and the JumonjiC (JMJC) domain-containing histone demethylases (Table 2.1). The latter consist of a group which contains over 30 members and can be divided, based on the JMJC-domain homology, into seven subfamilies (KDM2-8) [115, 135-136]. These two classes of demethylases possess different catalytic mechanism. LSD1 and LSD2 are flavin adenine dinucleotide (FAD)-dependent amine oxidases that catalyze a two-electron oxidation of methylated lysine, generating FADH₂ and H₂O₂, to form an imine that reduces upon addition of water to form demethylated lysine and formaldehyde (Fig. 2.2). The catalytic mechanism relies on a lone electron pair on the lysine ε-nitrogen atom, and for this reason the LSD enzymes can demethylate mono- and dimethylated lysines but not trimethylated lysines [137]. Whereas the Jumonji domain-containing demethylases are iron and α-ketoglutarate (2-oxoglutarate (2-OG))-dependent enzymes and are able to remove methyl groups from all three methyl lysine states, with concomitant production of succinate, carbon dioxide, and the demethylated lysine and formaldehyde (Fig. 2.3) [136, 138]. The target specificity of KDMs is regulated by their participation in different complexes. KDMs are implicated in different diseases, such as leukemia, prostate and breast cancer, esophageal squamous carcinoma, and as mental retardation [102, 139-140].

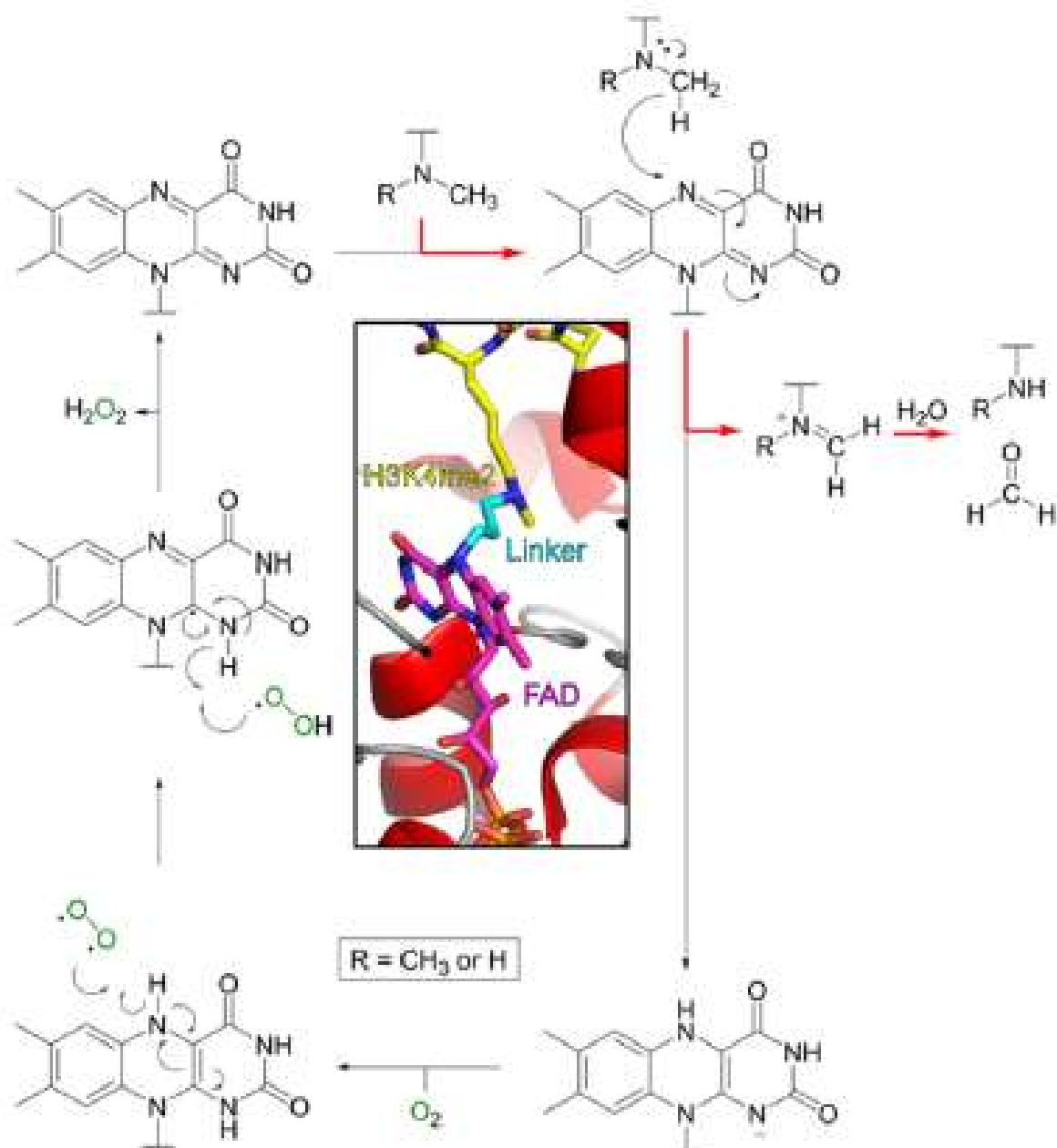


Fig. 2.2: Outline of the demethylation mechanisms for the KDM1 (LSD). The KDM1 enzymes (KDM1A and KDM1B) are members of the amine oxidase superfamily that couple oxidation of the methyl group to reduction of the co-substrate flavin adenine dinucleotide (FAD), likely via transfer of hydride. The resultant iminium ion intermediate is unstable and reacts with water to give the demethylated product and formaldehyde. The reduced FAD is reoxidized by molecular oxygen, forming hydrogen peroxide. The inset shows a view from a crystal structure of KDM1A (PDB 2UXN).

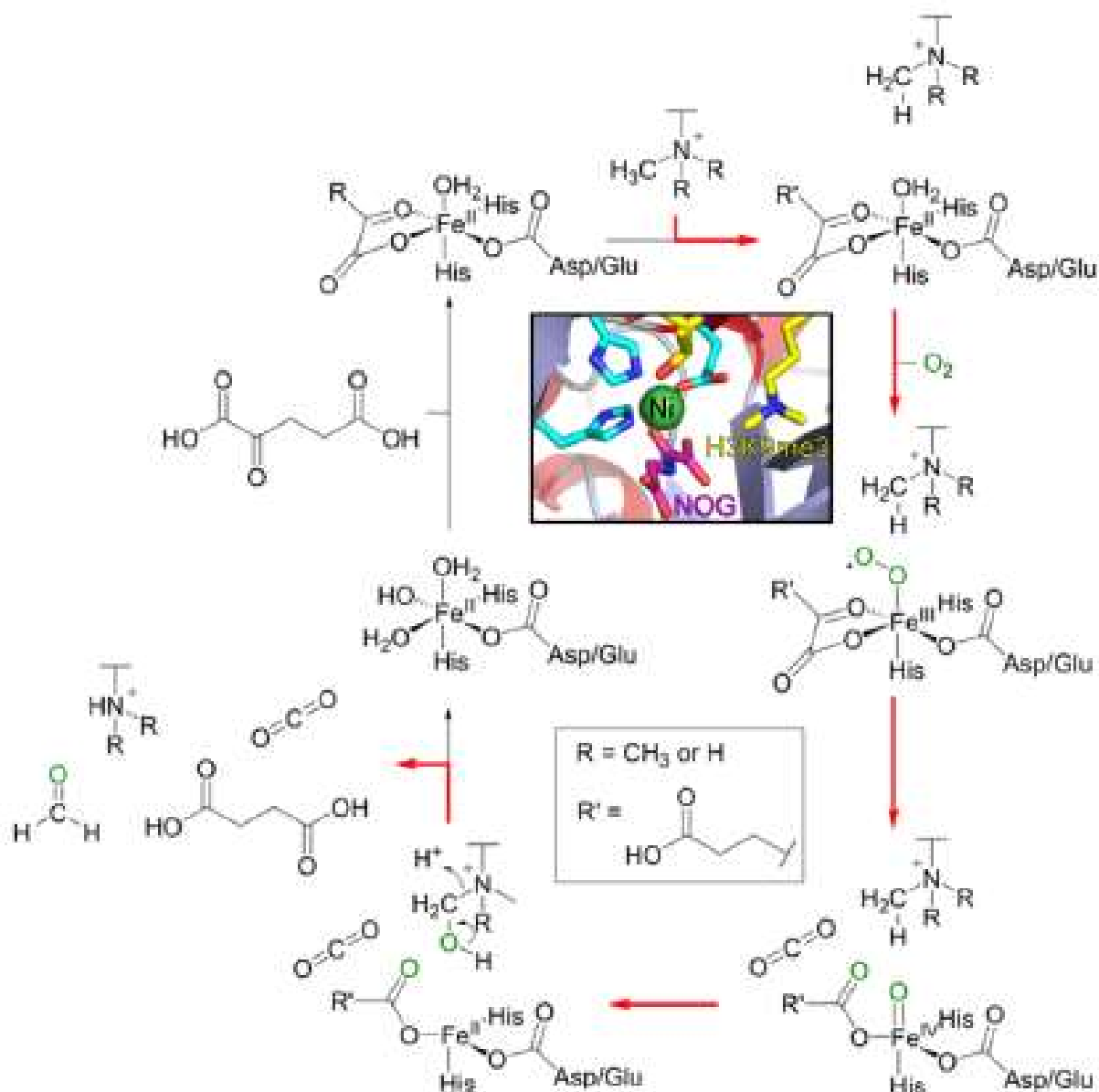


Fig. 2.3: Outline of the demethylation mechanisms for the JmjC KDM. JmjC KDM catalysis proceeds via oxidative decarboxylation of 2-oxoglutarate to give succinate, carbon dioxide and a Fe(IV) = O species, which catalyzes methyl group oxidation to give a hemiaminal which fragments to give the demethylated product and formaldehyde. The inset shows a view from a crystal structure of KDM4A complexed with H3K9me3, N-oxalylglycine substituting for 2-oxoglutarate, and nickel for iron (PDB 2OQ6).

Table 2.1: Classification of histone demethylases

Histone demethylase	Other names	Histone Substrates	Phenotype	Association with human disease
LSD1	KDM1A, AOF2, BHC110	H3K4me2/1 H3K9me2/1	Embryonic lethality around E5.5	Overexpression in prostate cancer, undifferentiated malignant neuroblastoma, oestrogen-receptor-negative breast cancer, bladder cancer, lung and colorectal

				carcinoma and silencing/downregulation in breast cancer
LSD2	KDM1B, AOF1	H3K4me2/1	Maternal effect lethality	Amplification and overexpression in urothelial carcinoma
JMJD5	KDM8	H3K36me2	Embryonic lethality around E11	N.D.
JMJD6	N.D.	H3R2, H4R3	Perinatal lethality and various developmental defects	Overexpression in chronic pancreatitis
FBXL11	KDM2A, JHDM1A	H3K36me2/1	N.D.	N.D.
FBXL10	KDM2B, JHDM1B	H3K36me2/1 H3K4me3	Partial peri- or postnatal lethality, neural tube closure defects, exencephaly and reduced sperm count	Overexpression in various leukaemias and bladder carcinoma
KIAA1718	KDM7A, JHDM1D	H3K9me2/1 H3K27me2/1	N.D.	N.D.
PHF2	JHDM1E	H3K9me2	N.D.	Mutation or silencing/downregulation in breast carcinoma and head and neck squamous cell carcinoma
PHF8	JHDM1F	H3K9me2/1 H4K20me1	N.D.	Mutation and deletion associated with X-linked mental retardation and cleft lip/palate
JMJD1A	KDM3A, JHDM2A, TSGA	H3K9me2/me1	Male infertility and adult onset obesity	Overexpression in malignant colorectal cancer, metastasized prostate adenocarcinoma, renal cell carcinoma and hepatocellular carcinoma
UTX	KDM6A	H3K27me2, H3K27me3	Neural tube defects at E9.5, female embryonic lethality at E10.5, partial male embryonic lethality, defects in cardiac development	Mutation in multiple tumour types including multiple myeloma, oesophageal squamous cell carcinoma, renal clear cell carcinoma, transitional cell carcinoma, chronic myelomonocytic leukaemia, overexpression in breast cancer and deletion in Kabuki syndrome

			and increased tumour formation	
JMJD3	KDM6B	H3K27me3/me2	Perinatal lethality and premature lung development	Overexpression in various cancers including lung and liver carcinomas and several haematological malignancies, in neutrophils of patients with ANCA vasculitis and in primary Hodgkin's lymphoma
JMJD2A	KDM4A, JHDM3A	H3K9me3/2 H3K36me3/2 H1.4K26me3/2	Altered response to cardiac stress	Silencing/downregulation in bladder cancer and overexpression in breast cancer
JMJD2B	KDM4B, JHDM3B	H3K9me3/me2 H3K36 me3/me2 H1.4K26, me3/me2	N.D.	Overexpression in malignant peripheral nerve sheath tumour
JMJD2C	KDM4C, JHDM3C, GASC1	H3K9me3/me2 H3K36me3/me2 H1.4K26me3/me2	N.D.	Amplification in oesophageal cancer, breast cancer, medulloblastoma and translocation in lymphoma
RBP2	KDM5A, JARID1A,	H3K4me3/2	Aberrant behaviour when held by the tail and haematological abnormalities	Silencing/downregulation or deletion in melanoma, translocation in acute leukaemia and mutation in ankylosing spondylitis
JARID1B	KDM5B, PLU1	H3K4me3/2	Embryonic lethality before E7.5	Overexpression in bladder cancer, prostate cancer and breast cancer
JARID1C	KDM5C, SMCX	H3K4me3/2	Neurulation and cardiac looping defects	Mutation in mental retardation, in autism and in renal carcinoma
JARID1D	KDM5D, SMCY	H3K4me3/2	N.D.	Deletion in prostate cancer
JARID2			Embryonic lethality before E15.5	Mutation associated with non-syndromic cleft lip, spina bifida and congenital heart defects
NO66	N.D.	H3K4me3/2 H3K36me3/2	N.D.	Overexpression in non-small cell lung cancer

2.1.2.1 Lysine Specific Demethylase-1 (LSD1)

Human lysine demethylase 1 (KDM1 or LSD1) was originally identified as a component of a transcriptional corepressor complex that also contained the REST corepressor (CoREST) and HDAC1/2. This transcriptional corepressor complex could be recruited to RE1 element-

containing gene promoters by REST and repressed the transcription of neuron-specific genes in nonneuronal cells [141-144].

Analysis of the LSD1 structure has led to significantly greater insight into its function. Overall, the structure of LSD1 consists of an N-terminal SWIRM domain [145], and an amine oxidase domain split into two halves, consisting of a substrate-binding half and an FAD-binding half, which come together to form a globular domain (Fig. 2.4). The active site of the enzyme is located in between these two halves. Two long, antiparallel α -helices divide and project away from the globular halves of the amine oxidase active site. This so-called tower domain serves as the binding interface between LSD1 and its protein cofactor, CoREST, and distinguishes it from other amine oxidases [146-147]. The Tower domain of LSD1 is essential for the interaction with other proteins, such as a transcriptional corepressor protein (CoREST) and histone deacetylase (HDAC) 1 or 2, together with them it forms a stable core subcomplex recruited by many chromatin remodeling multiprotein complexes [148].

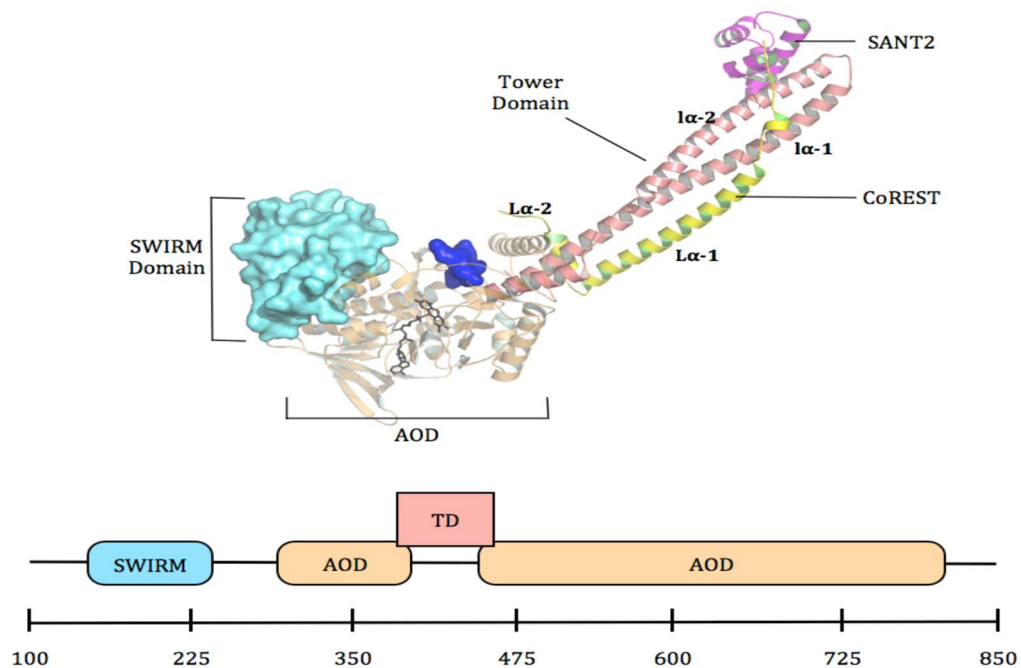


Fig. 2.4: LSD1 structure interacting with CoREST (PDB code 2UXN). The SWIRM domain is represented as cyan protein surface. AOL domain is represented as orange cartoon, while the tower domain is represented as salmon cartoon. FAD is shown as black sticks while the substrate is represented as blue surface. CoREST is represented as yellow cartoon, while SANT2 domain is shown as purple cartoon. There is a schematic representation of the LSD1 domains according to residues enumeration at the bottom [148-149].

In corepressor complexes, LSD1 binds to the C-terminal portion of CoREST, forming a biochemically stable complex that renders LSD1 less prone to proteasomal degradation [150-151]. In addition to its function as an adaptor, CoREST binding is required for LSD1 to catalyze H3K4 demethylation on intact nucleosomal particles [150, 152]. Although nucleosomal

substrates are refractory to recombinant LSD1, addition of recombinant CoREST endows nucleosomal demethylation by LSD1, indicating that the primary function of CoREST is to enable LSD1 demethylation of nucleosomal substrates [150, 152]. Consistently, mutations that inhibit the ability of CoREST to bind to DNA inhibit the ability of the complex to demethylate nucleosomes [147].

Without these binding proteins LSD1 is able to demethylate H3K4me1/me2 in peptide or bulk histones but not in nucleosomes. The crystal structure of the LSD1-CoREST-histone peptide ternary complex reveals that the peptide binds to the amine oxidase domain [153] adopting a folded conformation that enables the binding site to accommodate the relatively long stretch of the N-terminal H3 tail (Fig. 2.4). The H3-histone N-terminal tail peptide binding of LSD1 performs as an allosteric modulator by repressing the turning of the amine oxidase (AO) domain regarding the tower domain [154-155].

Modulation of LSD1 specificity can also be altered by association with other specific cofactors. Metzger *et al.* demonstrated that LSD1 can change specificity from H3K4 to H3K9 when it is associated with the androgen receptor. This presents a strategy by which LSD1 can enhance its substrate repertoire by associating with different regulatory proteins [156-157]. The structural basis of this protein cofactor-dependent switch in LSD1 substrate specificity is not known.

Indeed, as well as site of action, the protein complex partners LSD1 takes have a major influence on its downstream effects on gene expression. In vitro LSD1 is able to directly demethylate isolated histones but not when they are organized in the context of intact nucleosomes, as they exist in vivo [137]. Interactions with various protein complexes via the Tower domain release its catalytic activity, but also dictate the genetic loci at which this activity can occur. LSD1 has most commonly been found in association with transcription-repressive complexes, such as the CoREST-containing chromatin regulatory complex, which itself associates with certain HDACs and other proteins with transcription-repressive activity. Its core component, RCOR1, has been found to be critical in allowing LSD1 to demethylate histone lysines on nucleosome complexes. Yang *et al.* showed that this complex interacts in a bidentate manner, with recognition of the H3 tail by a shallow groove on the surface of LSD1 [147], and interactions with DNA on the chromatin via a SANT2 domain bound to the Tower domain of LSD1 [158]. This additional interaction has been observed both to increase the catalytic rate and decrease proteasomal degradation of LSD1, thereby permitting CoREST to

direct its demethylation of H3K4 and so act to repress gene expression [151]. LSD1 has also been found in association with other repressive complexes, including the NuRD and the CtBP chromatin modifying complexes [159-160].

In contrast, LSD1 is also found in complexes that activate transcription, most notably through interaction with the androgen and estrogen receptors, in which context its substrate specificity and demethylase activity is alternatively directed against H3K9, resulting in activated gene expression [156].

Several data have shown that LSD1 is highly expressed in different types of cancer, including bladder and colorectal cancer, oestrogen-receptor-negative breast cancer and prostate cancer [161-163]. Recent demonstrations have suggested that inhibiting LSD1 activity may have therapeutic potential in cancer; examples include the finding that LSD1 is required for the maintenance of acute myeloid leukaemia (AML)-containing MLL translocations [164], and that its inhibition can reactivate the all-*trans* retinoic acid (ATRA) differentiation pathway in AML [165]. In addition to providing genetic evidence for a role of LSD1 in a mouse model of MLL–AF9-induced leukaemia, Harris *et al.* showed that the monoamine oxidase (MAO) inhibitor tranylcypromine (also known as trans-2-phenylcyclopropylamine; 2-PCPA) significantly inhibited the colony-forming ability of AML cells [164]. This proof-of-concept study was further extended using two analogues of tranylcypromine that have been reported to be more potent and more selective inhibitors of LSD1 [164]. These tranylcypromine analogues exhibited 23- and 57-fold higher biological potencies than tranylcypromine in a similar setting, thus underlining the feasibility of LSD1 inhibition for the treatment of AML.

There are very few reports that link histone demethylases to diseases other than cancer. LSD1 is involved in the ‘hyperglycemic memory’ of cells, a series of mechanisms that causes negative effects of hyperglycemia to persist for an extended period of time after return to normoglycemia. LSD1 shows enhanced recruitment to monomethylated H3K9 in hyperglycemic cells and thus contributes to an increased expression of pro-inflammatory genes such as NFκB. The expression of these genes is elevated in mice during and after periods of transient hyperglycemia [166-167].

2.1.2.2 Lysine Specific Demethylase-2 (LSD2)

In 2009, the second FAD-dependent demethylase, AOF1/LSD2/KDM1B, was identified in mammals [135]. Similar to LSD1, LSD2 contains a conserved SWIRM domain required for its

catalytic activity and specifically demethylates H3K4me1 and H3K4me2; nevertheless, its repressing activity seems to be unrelated to the demethylase function [168]. LSD2 shared less than 31% sequence similarity with LSD1. Different from LSD1, LSD2 lacks the Tower domain and thus it is not able to bind CoREST (Fig. 2.5); it forms active complexes with euchromatic histone methyltransferases such as G9a and NSD3 as well as cellular factors involved in transcription elongation rather than with HDACs, and it is localized at the gene body level rather than at the promoters [169]. With respect to LSD1, LSD2 has a more restricted expression pattern, it being abundant essentially in growing oocytes and being required for *de novo* DNA methylation of some imprinted genes [170]. Thus, considering the involvement of both the 2 flavin-containing amino oxidases LSD1 and LSD2 with DNMTs and *de novo* DNA methylation, it seems feasible that a real functional link between DNA methylation and histone demethylation would exist. LSD2 has been reported to promote H3K9me2 in addition to H3K4me2 demethylation, leading to control of stimulus-induced recruitment of NF-κB to the *MDC* and *IL12B* promoters and activation of these inflammatory genes [171].

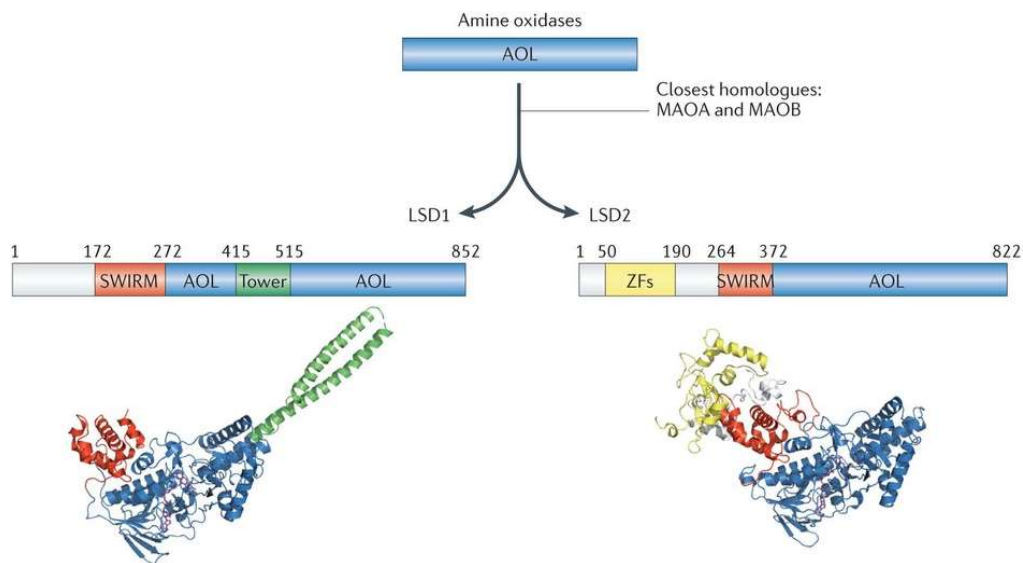


Fig. 2.5: Lysine-specific demethylase 1 (LSD1) and LSD2 have an amine oxidase-like (AOL) domain shared by a large family of oxidases, and uniquely among these they also have the chromatin factor-associated SWIRM (SWI3, RSC8 and Moira) domain. The Tower domain of LSD1 and the zinc finger (ZFs) domain of LSD2 distinguish the two proteins from each other. PDB ID for LSD1: 2H94; PDB ID for LSD2: 4GU1.

2.1.2.3 JmjC Histone Demethylase

The JmjC domain-containing KDMs (KDM2-7 subfamilies; JmjC KDMs) represent the larger KDM class, comprising about 20 human enzymes which are grouped into five subfamilies (KDM2/7, KDM3, KDM4, KDM5, and KDM6) [172]. These enzymes belong to a much larger enzyme superfamily, the 2-OG oxygenases, whose members (about 70-80 genes

in the human genome) catalyse a diverse range of oxidation reactions, using 2-OG, molecular oxygen, and Fe^{2+} as co-substrates/co-factors [173]. In particular, the 2-OG-dependent histone lysine demethylases are members of the Jumonji family of 2-OG oxygenases, which have common structural features (e.g., with respect to 2-OG binding residues) and comprise nonhistone modifying enzymes such as factor inhibiting HIF (FIH) [174]. The name Jumonji, Japanese for 'cruciform', originates from the first reported Jmj family study [175], which detailed the formation of a cross-like shape upon neural groove development in jmj knockout mice. Among the 30 JmjC domain-containing proteins identified so far within the human genome, about 20 have been published to demethylate specific lysines in the histone proteins [176-177].

The enzymatic mechanism involves two cofactors, Fe(II) and 2-oxoglutarate, which are bound in the JMJC domain; they react with dioxygen to form a highly reactive oxo-ferryl (Fe(IV)=O) intermediate that hydroxylates the N^{ϵ} -methyl groups of the methylated lysine substrate. The resulting, hemiaminal intermediate, is highly reactive and spontaneously gives formaldehyde and lysine residue lacking one methyl group, while oxidative decarboxylation α -ketoglutarate gives succinate and CO_2 (Fig. 2.3) [173, 178-179]. Unlike LSD1, the hydroxylation-based mechanism of the JmjC KDMs does not require a protonatable lysine ϵ -amine group, enabling these enzymes to demethylate all 3 lysine methylation states (tri-, di- and monomethylation) at H3K4, H3K9, H3K27, and H3K36, as well as H1K26 [180].

Six different subfamilies (JMJD1s, JMJD2s, JARID1s, UTX/Y-JMJD3, PHFs, and FBXLs) of JmjC histone demethylases have been identified, which have different histone sequence and methylation state selectivity [180-181]. For instance, KDMs of the JmjC domain-containing 2 (JMJD2) subfamily are selective for the demethylation of the tri- and di- N^{ϵ} -methylation states of specific lysines on histone H3, whereas other subfamilies (e.g., the PHF and FBXL subfamilies) are selective for the di- and mono- N^{ϵ} -methylated states and do not accept the trimethylated state [182].

The JmjC domain is a double-stranded β -helical (DSBH) fold also called the jelly-roll fold or double Greek motif. The DSBH fold is composed of eight β -strands that form a β -sandwich structure comprised of two four-stranded antiparallel β -sheets. The active center is buried in the interior of the JmjC domain, where Fe^{2+} is coordinated by three conserved residues (HxE/DxH iron binding motif comprising one aspartyl/glutamyl and two histidyl residues) and further stabilized by the 2OG cofactor (Fig. 2.6). The substrate is bound unusual by hydrogen

bonds, which is formed between one methyl group of methylated lysine and the oxygen atoms from active-site residues [172, 182-185]. In addition to the core structure of the JmjC domain, most JmjC-dependent demethylases contain auxiliary functional domains that maintain the overall structural stability and contribute to substrate recognition, recruitment and catalysis. These auxiliary domains include PHD, Tudor, CXXC, FBOX, ARID, LRR, JmjN, and Zn²⁺ finger domains, which are likely to contribute to substrate selectivity [172, 186-188]. For example, the JmjN domain, which is formed by three short helices and two β -strands, is essential for the demethylation activity of JHDM3/JMJD2 [189].

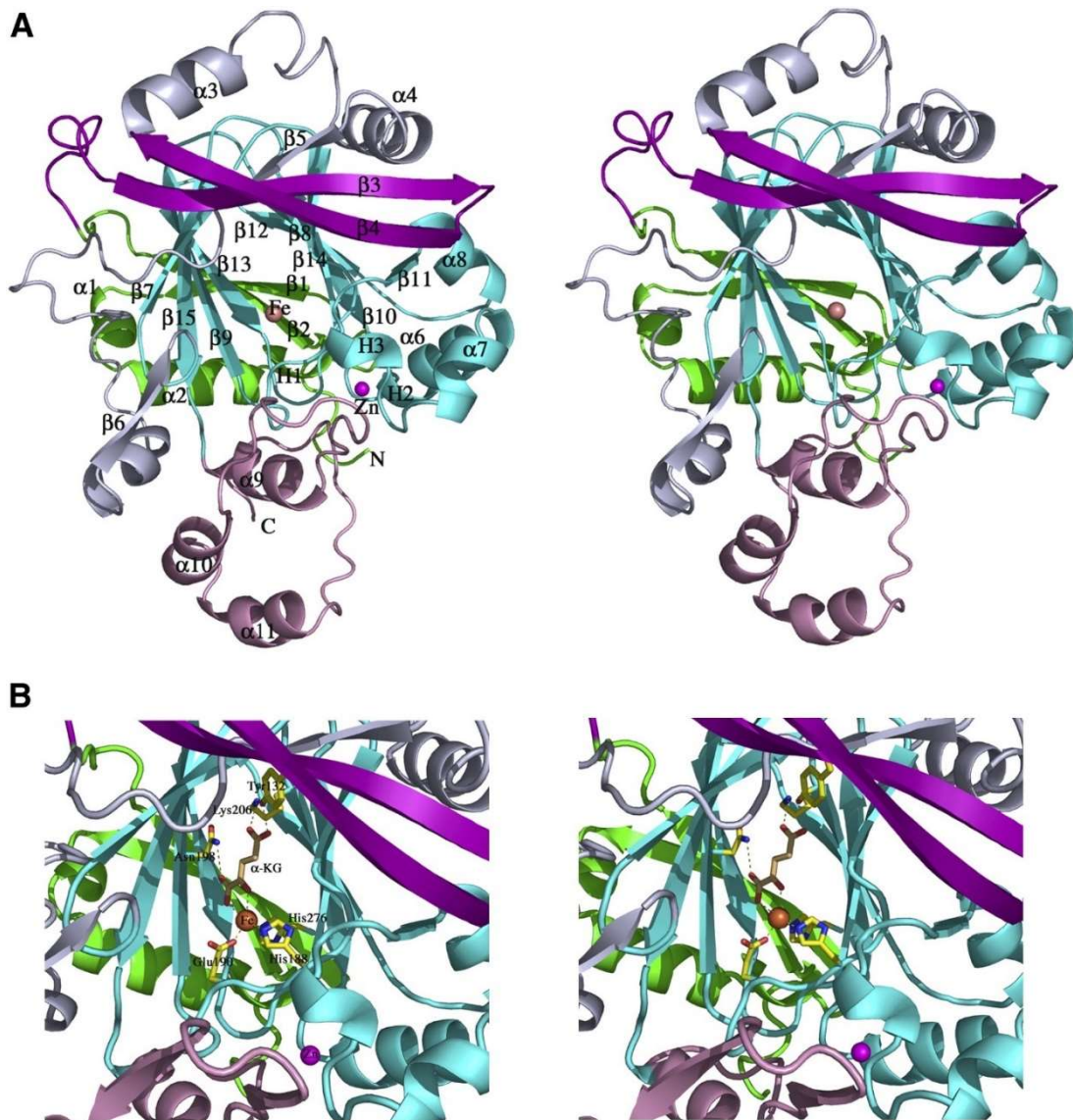


Fig. 2.6: The Overall Structures of c-JMJD2A with and without α -KG. (A) The structure of c-JMJD2A in the presence of Fe²⁺ and Zn. The domains include the JmjN domain (residues 14 to 56, green), the long β hairpin (residues 65 to 94, red), the mixed structural motif (residues 95 to 171, gray), the JmjC domain (residues 171 to 293, light blue), and the C-terminal domain (residues 294 to 350, pink). The Fe and Zn ions are coloured brown and purple, respectively. (B) The structure of c-JMJD2A with Fe²⁺ and α -KG. The colour coding is the same as in (A). α -KG is coloured yellow with the oxygen atoms shown in red. Residues involved in α -KG binding and Fe chelating are labelled.

Despite the functional characterization of many JmJC histone demethylases being still at a relatively early stage, recent evidence suggests for these enzymes many important biological roles ranging from the regulation of cellular differentiation and development to the control of neuronal function. Notably, dysregulation of JmJC demethylases can lead to aberrant histone methylation states and is associated with a number of diseases, including cancer and neurological disorders such as autism and X-linked mental retardation [190-192] (Table 2.1). An additional mechanism by which KDMs are overexpressed in various cancers is via their induction under hypoxic conditions. Inadequate or inefficient vascularization of rapidly growing tumors results in reduced oxygen tension, which activates the hypoxia-inducible factor (HIF) transcription factor [102].

2.2 Histone Acetylation

One of the most widely studied histone PTM is acetylation [193]. Histones are covalently modified at the ϵ -amino group of lysines by histone acetyltransferases (HATs), thereby neutralizing the positive charge and thus interfering with the histone–DNA interaction essential for nucleosome stability [194]. Since Allfrey’s discovery of histone acetylation in 1964 [195], it is now understood that the interplay of acetylation and deacetylation of chromatin plays a critical role in transcription [193]. The transfer or removal of acetyl groups to ϵ -amino group of lysine residues is mediated by two classes of enzymes. HATs catalyze the covalent attachment of acetyl groups to lysine residues of histones and other proteins by using acetyl-coenzyme A (acetyl-CoA) as a cofactor. Histone deacetylases (HDACs) conversely catalyze the amide hydrolysis of acetylated lysine. The attachment of acetyl groups to lysine residues goes along with two functional consequences. First, the positive charge of physiologically protonated ϵ -amino groups is abolished, resulting in altered electrostatic as well as steric properties of the affected protein region. Second, acetylation serves as a mark for distinct “reader” domains, which comprise specialized tertiary structures in proteins that undergo a selective interaction with acetylated lysines [196-197]. Key to this process is the ability of “readers” to recognize specific PTMs that ultimately determine the functional outcome of the PTM [77, 198]. Three readers (bromodomain [199-200], double PHD finger [201-202], and pleckstrin homology domain) [203] that recognize acetylated lysine (KAc) have been identified and the bromodomain is the most thoroughly characterized of the three [204].

ϵ -N-acetylation of lysine residues on the amino-terminal tails of histones has been generally associated with open chromatin architecture as well as transcriptional activation [205]. Upon acetylation, local affinity of the modified histone protein to negatively charged DNA is decreased, resulting in a less condensed chromatin structure and in exposure of promoter sites. As a consequence of the increased accessibility, the DNA globally becomes more prone to access of the transcriptional machinery [131]. In addition, transcription factors and other regulatory elements are recruited in a modification-specific manner to the relaxed promoter locus by interaction of specialized reader domains with acetyl lysine moieties [197, 206]. Thus, HATs and histone acetylation are functionally linked with the control of transcription activation, replication, and DNA damage repair [207].

2.2.1 Histone Acetyltransferases (HATs)

HATs catalyze the acetylation of lysine residues, which has been accepted as an important epigenetic marker. Acetylation occurs on both histone and nonhistone proteins, with an estimated 2,000–4,000 acetylated proteins and 15,000 acetylation sites in animal tissues [208]. HATs catalyze the transfer of acetyl groups to lysine residues using acetyl-CoA as donor. Fig. 2.7 depicts the transfer of the acetyl group to the lysine ϵ -amino residues in histones on a ternary complex with the lysine substrate bound to a hydrophobic pocket located close to the acetyl group of the acetyl-CoA binding site, which is one of the mechanisms proposed based on crystal structures [209].

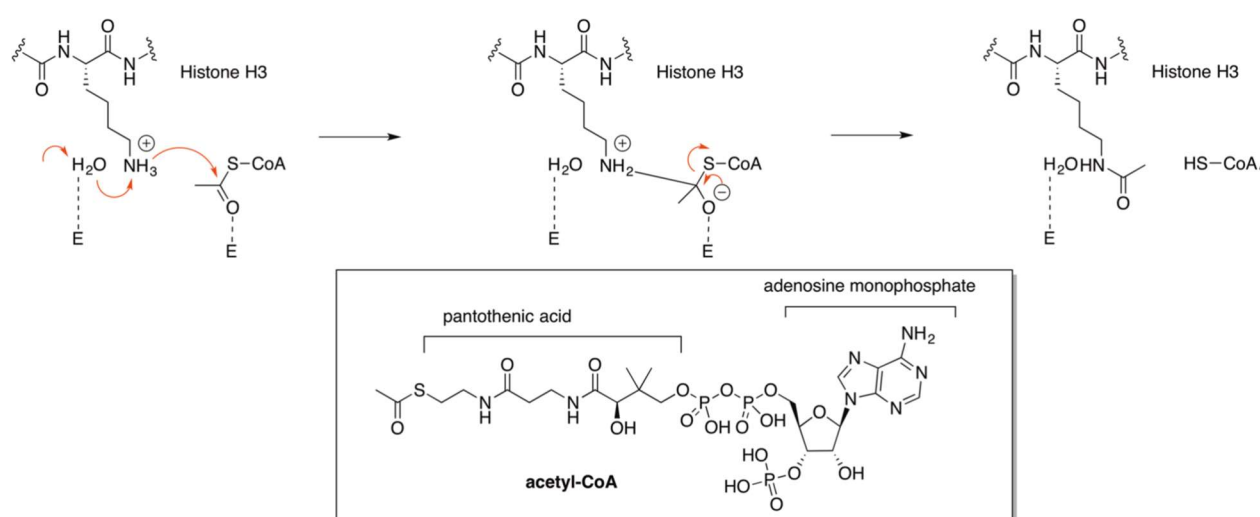


Fig. 2.7: Mechanism of acetyl transfer in the ternary complex containing the HAT, acetyl-CoA (insert), and a fragment of H3 [209]

Since the isolation of the Gcn5 HAT from *Tetrahymena* by Allis and coworkers [210], and the identification of HAT1 by Sternglanz and coworkers [211] and Gottschling and coworkers

[212] just more than a decade ago, many other HATs have been identified from yeast to man. Some of these HATs (e.g., PCAF and HAT1) show sequence conservation with Gcn5 within their catalytic domain, leading to their classification as Gcn5-related histone *N*-acetyltransferases (GNATs) [213]. Many other HATs, like CBP/p300, Rtt109, and the MYST proteins have extremely limited sequence conservation. Based on this sequence divergence within the HAT domain, HATs can be grouped into at least five different subfamilies (Table 2.2). This includes HAT1 (named histone acetyltransferase 1 as the founding member of the superfamily or KAT1) [214], Gcn5/PCAF (named for its founding member yeast Gcn5 and its human ortholog, PCAF, or KAT2a/KAT2B according to the alternative nomenclature), MYST (named for the founding members MOZ, Ybf2/ Sas3, Sas2, and TIP60, or KAT5), p300/CBP (named for the two human paralogs p300 and CBP, or KAT3B/KAT3A), and Rtt109 (named for its initial identification as a regulator of Ty1 transposition gene product 109, also referred to as KAT11). Although the Gcn5/PCAF, HAT1, and MYST subfamilies have homologs from yeast to man, p300/CBP is metazoan specific, and Rtt109 is fungal specific [206]. Although other nuclear HAT subfamilies have been identified, such as the steroid receptor coactivators (ACTR/AIB1, SRC1) [215], TAF250 [216], ATF-2 [217], and CLOCK [218], their HAT activities have not been studied as extensively as the five major HAT classes.

Table 2.2: The five major HAT families.

Major subfamilies	HAT	Prominent members	Key structural and biochemical properties
HAT1		yHat1	Member of the GNAT family, Amino- and carboxy-terminal segments used for histone substrate binding, Requires the yHat2 regulatory subunit for maximal catalytic activity
Gcn5/PCAF		yGcn5 hGCN5 hPCAF	Member of the GNAT family, Uses a ternary complex catalytic mechanism, Amino- and carboxy-terminal segments used for histone substrate binding
MYST		yEsa1 ySas2 ySas3 hMOZ dMof hMOF hTIP60 hHBO1	Uses a ping-pong catalytic mechanism, Requires autoacetylation of a specific lysine at the active site for cognate histone acetylation
p300/CBP		hp300 hCBP	Metazoan-specific, but shows structural homology with yRtt109 Uses a ternary Theorell–Chance (hit-and-run) catalytic

		mechanism, Contains a substrate-binding loop that participates in AcCoA and lysine binding Contains an autoacetylation loop that requires lysine autoacetylation for maximal catalytic activity
Rtt109	yR11109	Fungal-specific, but shows structural homology with p300 Contains a substrate-binding loop that participates in AcCoA and probably also lysine binding, Requires autoacetylation of a lysine residue near the active site for maximal catalytic activity, Requires one of two histone chaperone cofactors (Asf1 or Vps75) for maximal catalytic activity and histone substrate specificity

y, yeast; h, human; GNAT, Gcn5-related *N*-acetyltransferase.

HATs mediate many different biological processes including cell-cycle progression, dosage compensation, repair of DNA damage, and hormone signaling. Aberrant HAT function is correlated with several human diseases including solid tumors, leukemias, inflammatory lung disease, viral infection, diabetes, fungal infection, and drug addiction [219-220]. Deregulated HAT activity is particularly linked to cancer formation and progression [23, 221-223]. Certain types of leukemia are characterized by the occurrence of fusion proteins with increased HAT activity [224]. Furthermore, lysine acetylation of the oncogenic fusion protein AML1-ETO by the HAT p300 has been demonstrated in patient blasts using western blotting and is required for leukemic transformation in mouse models as shown by mutation studies. In addition, the p300 inhibitor C646 increased survival in a mouse model of leukemia [225]. An impaired acetylation equilibrium is also observed in several solid tumors [221, 226] including prostate [227-228], colon [229] and breast [230] cancers with evidences for both HATs and deacetylases as potential drug targets. The activities of HATs and HDACs are also changed in asthma and chronic obstructive pulmonary disease because bronchial biopsies and alveolar macrophages from asthmatic patients show increased HAT and reduced HDAC activity [231]. p300-mediated acetylation of the HIV-1 viral protein, integrase, increases its activity in integrating the HIV-1 virus into the human genome [232]. The leading diabetes drug, Metformin, was shown to act through p300/CBP inhibition, and heterozygous CBP knockout mice are noticeably lean with increased insulin sensitivity [233]. The Rtt109 HAT was also reported to be required for the pathogenesis of *Candida albicans*, the most prevalent cause of hospital-acquired fungal infections [234]. Studies in drug addiction and the related disease

of depression using animal models have also uncovered interesting correlations between stages of drug addiction and histone acetylation status [220].

2.2.2 Histone Deacetylases

HDACs catalyse the removal of acetyl groups from the amino-terminal lysine residues of histone and non-histone proteins, such as transcription factors (TFs), hormone receptors, signaling proteins, chaperones, and DNA damage response proteins [235-238]. There are 18 different mammalian HDACs which are categorized into 2 families and 4 classes. First identified zinc dependent Rpd3/Hda1 family (class I, II, and IV) is referred as 'classical' HDACs, while the NAD⁺-dependent sirtuin family or Sir2 proteins (SIRT1–7) are divided into class III HDACs [13, 236, 239-240]. HDAC1, 2, 3, and 8 belong to class I and are localized in the nucleus, presenting similarity to the yeast Rpd3 [236]. Class II HDACs [241] are present in both the cytoplasm and nucleus, and they shuttle between these compartments [242-245]. Class II HDACs (grouped for homology to Hda1 in yeast) are divided into two subclasses: class IIa (HDAC4, 5, 7, and 9) and class IIb (HDAC6, 10). Class IV HDACs includes one member (HDAC11) [246-247], which can be considered a "hybrid" sharing similarities to both class I and II HDACs. Sirtuins, related to Sir2 in yeast [248], have also been categorized as class III HDACs [249] (Fig. 2.8, lower part) and grouped as SIRT1-7 [250]. These enzymes display an NAD function that is associated to a nuclear, mitochondrial, and cytoplasmic localization [251-252].

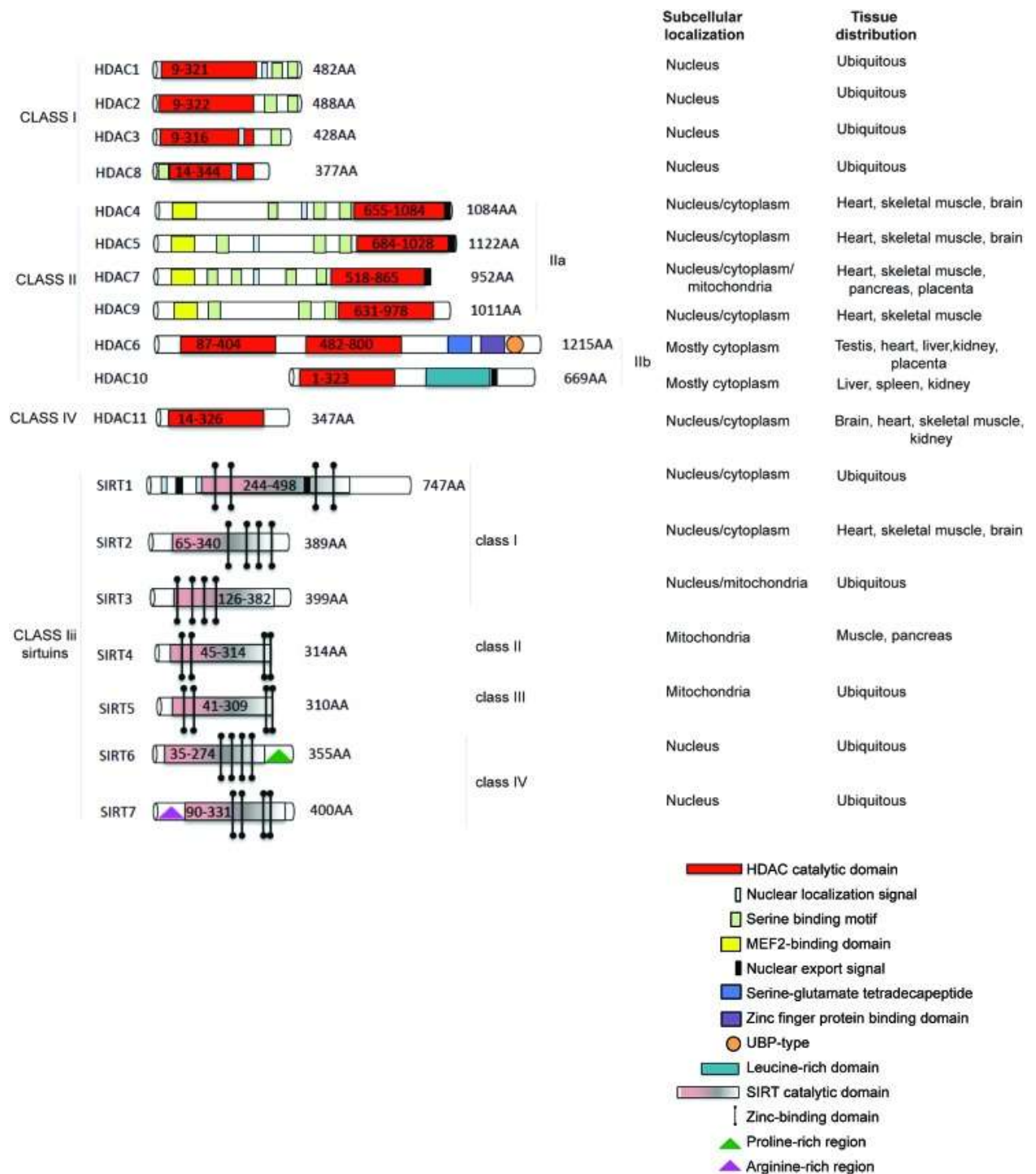


Fig. 2.8: HDAC and SIRT classification. Enzymes are divided into classes and sub-classes; subcellular localization and tissue distribution is reported for each member.

2.2.2.1 HDACs

HDACs are heterogeneous in length, varying from 347 amino acids for the shortest (HDAC11) to 1215 amino acids for the longest (HDAC6) (Fig. 2.8) [235, 253]. All HDACs have a highly conserved deacetylase domain. Based on the ligand-bound crystal structures, the mechanism of deacetylation (Fig. 2.9) was recognized to involve the activation of the

acetamide carbonyl group by the Zn^{2+} ion and its hydrolysis with formation of a tetrahedral intermediate facilitated by a “charge-relay” system. Several variants of the deacetylation mechanism have been proposed [254-257]. Upon activation, the N-acetyl group is attacked by a water molecule, producing an N-3 free lysine and acetic acid. The major residues differences are found at the entry of the active site. The most recent computations support the involvement of two charge-relay systems, the recognition of the H142/D176 dyad as the general base of the reaction, the stabilization of the intermediate by Y306, and the inhibitory effect of K^+ .

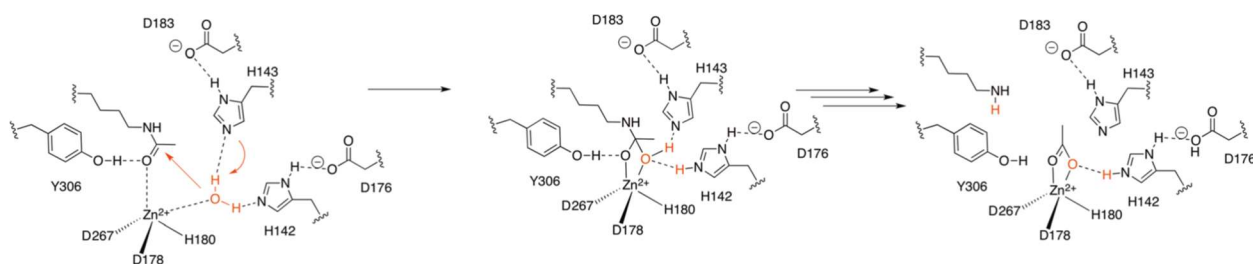


Fig. 2.9: Simplified mechanism for HDAC-8 catalyzed deacetylation reactions [257]

Histone deacetylation gives a tag for epigenetic repression and plays an important role in transcriptional regulation, cell cycle progression and developmental events. The classical HDACs are emerging targets for metabolic disease [258], cancer [259], and neurodegeneration [260]. HDACs are also involved in inflammation and infection. Class I HDACs have a role in innate immunity through inflammatory cytokine production and class IIa HDACs are involved in adaptive immunity through the regulation of antigen presentation [16].

2.2.2.2 HDAC Inhibitors

HDAC inhibitors (HDACi) have set a paradigm to reverse abnormal epigenetic changes related to cancer. HDACi are mostly studied as anticancer agents, but there is a growing body of literature ascribing these enzymes to play a crucial role in other diseases such as neurological disorders, inflammatory processes and infectious diseases [261-264]. With emphasis on their structural diversity, the different classes of HDAC inhibitors include hydroxamic acids, benzamides, short chain fatty acids, macrocyclic peptides and others. These Zn^{2+} dependent HDAC inhibitors share three pharmacophoric motifs, a cap group or a surface recognition unit (usually a hydrophobic and aromatic group interacting with the rim of the binding pocket), a Zn^{2+} binding domain (ZBD) or chelating group (hydroxamic acid, carboxylic acid or benzamide groups), that coordinates with Zn^{2+} ion and a saturated or

unsaturated linker with linear or cyclic structure, joining the cap group to the ZBD (Fig. 2.10). Alterations in any or all three motifs have variably affected the potency and selectivity of the HDAC inhibitors [265-270].

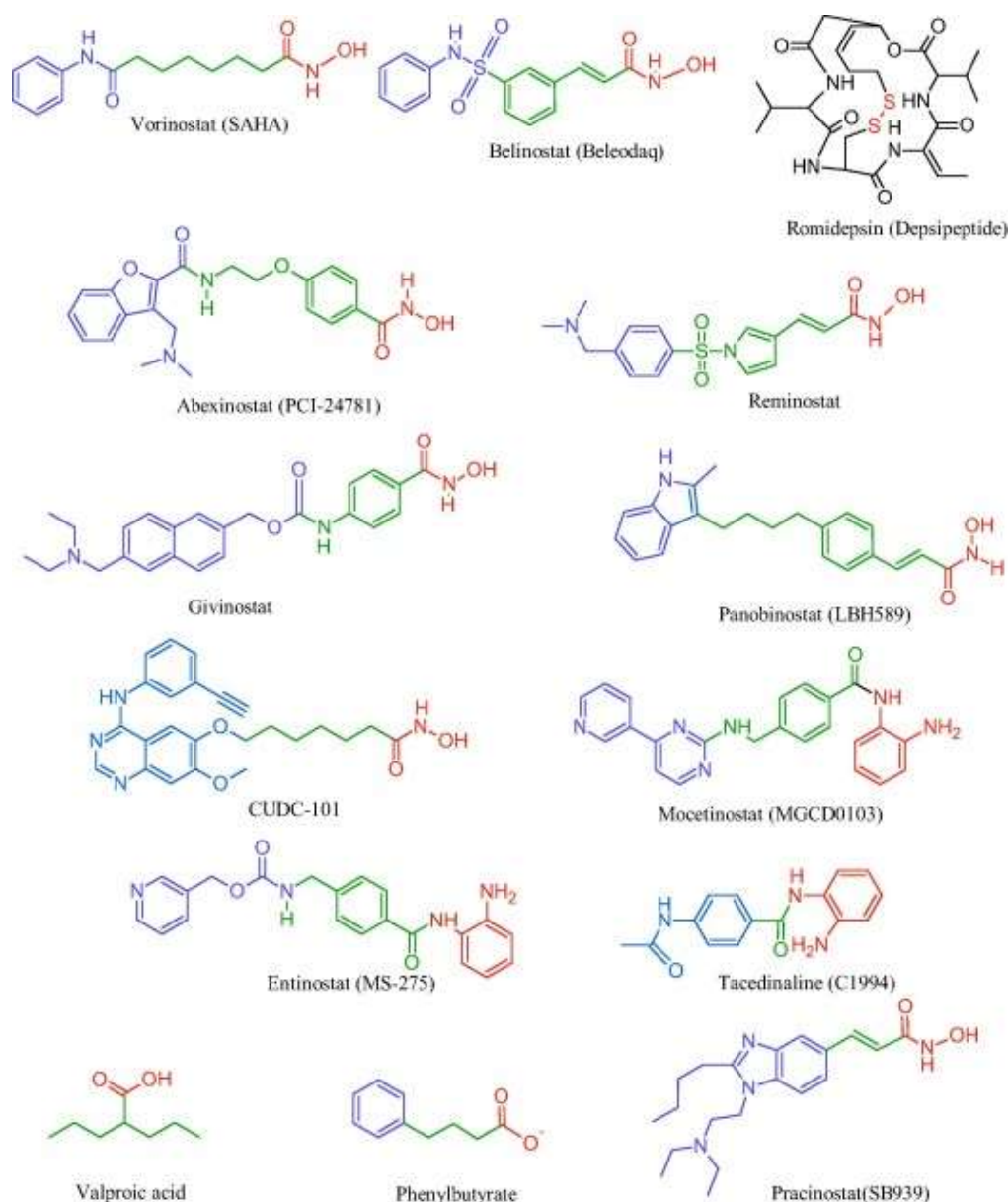


Fig. 2.10: Approved HDAC inhibitors in clinical trials with their pharmacophores. The cap, linker and the Zn²⁺ binding group are represented in blue, green and red, respectively [263].

In 2006, the hydroxamic acid SAHA (suberoylanilide hydroxamic acid, INN: Vorinostat, Fig. 2.10) was the first KDAC inhibitor that was approved for the treatment of cutaneous T-cell lymphoma (CTCL) [271]. Romidepsin, belinostat, and chidamide followed with similar indications (Fig. 2.10). While romidepsin is approved for the treatment of CTCL and peripheral T-cell lymphoma (PTCL) [272], the use of belinostat and chidamide is restricted to PTCL [273-274]. Panobinostat (Fig. 2.10) is approved for the treatment of multiple myeloma [275].

Currently, there are numerous HDACi under clinical development (Table 2.3), which can be divided into three groups based on their specificity: (1) nonselective HDACi, such as vorinostat, belinostat, and panobinostat; (2) selective HDACi, such as class I HDACi (romidepsin and entinostat) and HDAC6 inhibitor (ricolinostat); and (3) multipharmacological HDACi, such as CUDC-101 and CUDC-907 [276].

Table 2.3: HDAC inhibitors currently under clinical investigations

HDACi	Specificity	Cancer types	Clinical trial	Ref
Hydroxamic acid				
Vorinostat (SAHA)	Classes I, II, and IV	CTCL	FDA approved in 2006	[277]
Belinostat (Beleodaq/PXD101)	Classes I, II, and IV	PTCL	FDA approved in 2014	[278]
Panobinostat (LBH-589)	Classes I, II, and IV	MM	FDA approved in 2015	[279]
Resminostat (4SC-201)	Classes I and II	Advanced colorectal and hepatocellular carcinoma; HL	Phase II trial	[280-281]
Givinostat (ITF2357)	Classes I and II	CLL; MM; HL	Phase II trial	[282-283]
Pracinostat (SB939)	Classes I, II, and IV	AML	Phase II trial	[284]
Abexinostat (PCI-24781)	Classes I and II	Metastatic solid tumors; HL; non-HL; CLL	Phase I trial	[285-286]
Quisinostat (JNJ-26481585)	Class I and II HDACs	Advanced solid tumor; lymphoma; CTCL	Phase I and II trial	[287]
MPT0E028	HDAC1, 2, 6	Advanced solid tumor	Phase I trial	[288]
CHR-3996	Class I	Solid tumor	Phase I trial	[289]
CUDC-101	Classes I and II HDAC, EGFR, HER2	Solid tumor	Phase I trial	[290]
CUDC-907	Classes I and II HDAC, PI3K	MM; lymphoma; solid tumor	Phase I trial	[291]
Benzamides				
Entinostat (MS-275)	Class I	Solid and hematological malignancies	Phase I and II trial	[292]
Mocetinostat (MGCD0103)	Class I and IV	Solid and hematological malignancies	Phase I and II trial	[293]
Tacedinaline (CI-994)	Class I	MM; lung and pancreatic cancer	Phase II and III trial	[294]
Ricolinostat (ACY-1215)	HDAC6	MM; lymphoma	Phase I and II trial	[295]
Chidamide (CS055/HBI-8000)	HDAC1, 2, 3, and 10	PTCL	Chinese FDA approved in 2015	[273, 296]
Cyclic peptides				

Romidepsin (Depsipeptide/FK228)	Class I	CTCL; PTCL	FDA approved in 2009 and 2011	[297]
<i>Aliphatic fatty acids</i>				
Valproic acid (VPA)	Class I and II	Solid and hematological malignancies	Phase I and II trial	[298]
Phenylbutyrate	Classes I and II	Solid and hematological malignancies	Phase I and II trial	[299]
AR-42	Class I and IIb	AML	Phase I trial	[300]
Pivanex (AN-9)	Classes I and II	NSCLC; myeloma; CLL	Phase II trial	[301]

2.2.2.3 Sirtuins

Sirtuins, also referred to as Sir2-like proteins, were discovered in the late 1970s by Klar et al. when studying the yeast gene Sir2 (silent information regulator 2) [302]. Initial investigations on the catalytic activity suggested Sir2 to be primarily a mono-ADP-ribosyltransferase [303]. It took a while until the NAD⁺-dependent deacetylase activity of Sir2 was elucidated by Imai et al. in the year 2000 [304]. Today, more than 200 members of the sirtuin family were identified in bacteria, plants, invertebrates, and vertebrates [305]. In prokaryotes, usually one or two sirtuin isotypes can be found, whereas eukaryotic genomes encode several sirtuin isotypes. The hallmark of this enzyme family is a domain of approximately 260 amino acids with a high degree of sequence homology across the species [249]. In mammals, the sirtuin family comprises seven proteins (SIRT1-SIRT7), which vary in tissue specificity, subcellular localization, enzymatic activity and targets. Sirtuins carry a conserved catalytic domain consisting of about 275 residues. Based on phylogenetic analysis mammalian Sirtuins are grouped into four different classes (I-IV) [306-308]. SIRT1, SIRT2 and SIRT3 belong to class I along with most eukaryotic Sirtuins such as Sir2.1 from *Drosophila melanogaster* and the founding member yeast Sir2, HST1 and 2 from yeast. SIRT4 belongs to class II, SIRT5 to class III, and SIRT6 and SIRT7 are placed in class IV. Additionally, a novel class ("U") has been created to include sirtuins with unique features, such as gram-positive bacteria and *Termoga maritime* sirtuins [308-310].

The subcellular localization of the sirtuin isotypes as well as their different splice variants (isoforms) is actively regulated by their C- and N-termini, which can contain specific localization sequences. For example, Sirt1 and Sirt2 were shown to be able to shuttle between nucleoplasm and cytoplasm in a cell cycle and cell-type-dependent manner [311-312]. Nevertheless, Sirt1 is a primarily nuclear deacetylase, while Sirt2 is the most important

cytosolic sirtuin isotype. The mitochondrial sirtuins are Sirt3–5. However, the existence of a long, unprocessed isoform of Sirt3 (lSirt3) in the nucleus was reported as well [313–314]. After its mitochondrial uptake lSirt3 is cleaved by the mitochondrial matrix processing peptidase (MPP) to sSirt3, which is shorter by 16 kDa [315]. Sirt6 is an exclusively nuclear isotype. The localization of Sirt7 was reported to be restricted to the nucleolus. Recently, a cytosolic isoform of Sirt7 (lSirt7, 47.5 kDa) was identified, which is slightly longer than the known nucleolar isoform (sSirt7, 45 kDa) [316]. SIRTs can catalyze both deacetylation and ADP-ribosylation [251]. Their best characterized activity is NAD⁺-dependent lysine deacetylation, but recent studies demonstrated that some SIRTs also remove other acyl groups such as succinyl, malonyl, glutaryl, and long-chain fatty acyl groups [307, 317] (Table 2.4). Moreover, SIRT4 and SIRT6 possess ADP-ribosyltransferase activity, yet its biological relevance remains to be fully established [303, 318–320]. Together, all these enzymatic activities are essential for mammalian sirtuins to modulate a variety of physiological processes, such as transcriptional regulation, genomic stability, cellular responses to stress, metabolism, inflammation, aging and cancer [321–322].

Table 2.4: Characterization of seven mammalian sirtuins

HDAC III	Sirtuin	Localization	Substrates	Catalytic activity	Function	Phathology
Class I	SIRT1	Cytosol, nucleus	PGC1 α , eNOS, FOXO, MyoD, NF- kB, H3K9ac, H1K26ac, H4K16ac	NAD ⁺ - dependent protein deacetylation	Cell survival, insulin, signaling, inflammation, metabolism regulation oxidative stress response, lifespan regulation.	Neurodegenerat ive diseases. Cancer: AML, colon, prostate, ovarian, glioma, breast, melanoma, lung adenocarcinom a.
	SIRT2	Cytosol, nucleus	H3K56ac, H4K16ac, α - tubulin, Foxo3a, p53, G6PD, MYC	NAD ⁺ - dependent protein deacetylation	Cell cycle regulation, nervous system development.	Neurodegenerat ive diseases. Cancer: brain tissue, glioma.
	SIRT3	Mitochondria , nucleus	AceC2, ShdhA, SOD2, PDMC1a, IDH2, GOT2, FoxO3a	NAD ⁺ - dependent protein deacetylation	Regulation of mitochondrial energetic metabolism.	Neurodegenerat ive diseases. Cancer: B-CLL, mantle cell lymphoma, CLL, breast, gastric.

Class II	SIRT4	Mitochondria	GDH, MCD	Mono- ADP-ribosyltransferase, NAD ⁺ -dependent protein deacetylation	Regulation of mitochondrial energetic metabolism/ lipid metabolism, insulin secretion.	Cancer: breast, colorectal.
Class III	SIRT5	Mitochondria	Histone H4, CPS1, cyt c	NAD ⁺ -dependent Malonyl, succinyl, glutaryl deacetylase	Urea cycle regulation, apoptosis.	Cancer: pancreatic, breast, non-small cell lung carcinoma.
Class IV	SIRT6	Nucleus	H3K9ac H3K56ac, PARP1	NAD ⁺ -dependent protein deacetylation, Mono- ADP-ribosyltransferase, long-chain fatty acyl deacetylase	Genome stability, DNA repair, nutrient-dependent metabolism regulation.	Cancer: breast, colon
	SIRT7	Nucleoli	RNA pol I, p53, histone H3K18ac	NAD ⁺ -dependent protein deacylation	Regulation of rRNA transcription, cell cycle regulation.	Cancer: liver, testis, spleen, thyroid, breast.

All sirtuins share a conserved catalytic core of ~275 amino acids that is flanked by N- and C-terminal extensions. The extensions are variable in length and sequence, and they have been reported to play various roles such as ensuring a proper cellular localization, regulating the oligomerization state, and/or exerting autoregulation mechanisms [315, 323-324]. Whereas other HDAC families activate a water molecule for the hydrolysis reaction by using a zinc cofactor, the unique Sirtuin mechanism is based on the use of NAD⁺ as a co-substrate. Catalytic mechanisms of nucleophilic substitution SN1-type [325-326] or SN2-type [327-329] deacetylation by NAD⁺-dependent class III deacetylases or sirtuins [330] have been proposed with formation of an O-alkylamidate intermediate as shown in Fig. 2.11. A highly dissociative and concerted displacement of nicotinamide has been proposed as first step of the mechanism of deacetylation. The transition state shows a significant oxocarbenium ion character, but the cleavage appears to be facilitated by the nucleophilic assistance of the acetylated lysine, as shown by dynamics simulations [331]. Once the nicotinamide has been

released it can rebind in the C-pocket and react with the intermediate to reform NAD^+ . In this step Phe33 appears to play a role as gatekeeper in the nicotinamide exchange reaction in which it helps to shield the *O*-alkylamidate intermediate from free nicotinamide. After the formation of 1'-*O*-alkylamidate intermediate, the 2'-hydroxyl group of the ribose is activated by a conserved His116 to afford 1', 2'-cyclic intermediate. Then a protonated histidine can act as acid, protonates the amino-acetal and led the deacetylated substrate release. Finally, an activated water molecule attacks the cyclic intermediate to furnish 2'-*O*-acetyl-ADP ribose (might be in equilibrium with its corresponding 3' isomer) [328, 332].

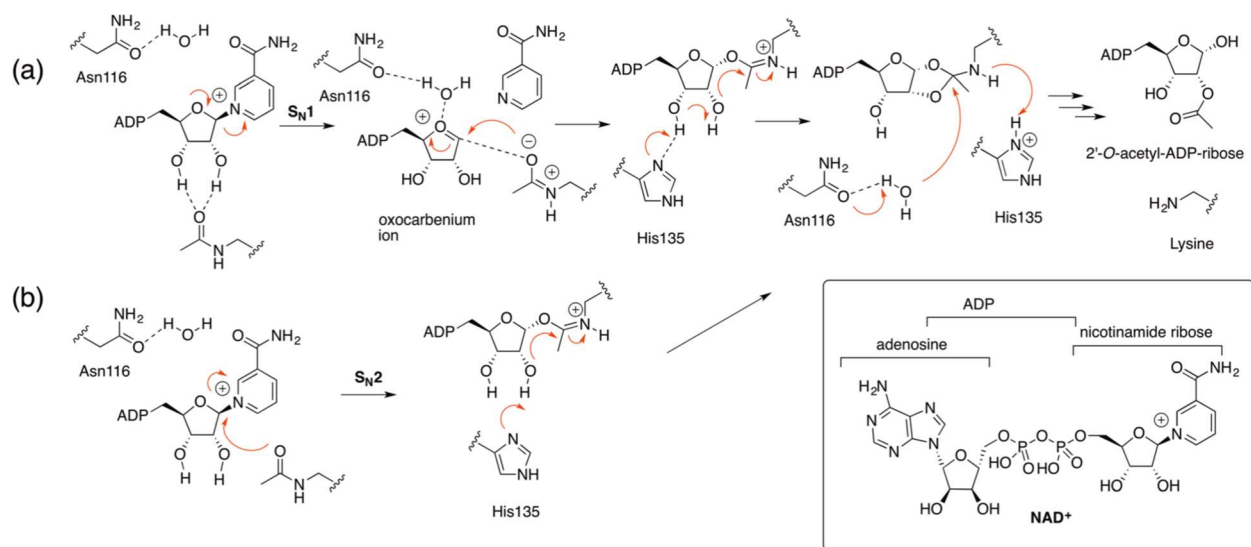


Fig. 2.11: Mechanism of deacetylation of acetylated lysine catalyzed by sirtuins [258, 325-326, 331].

2.2.2.4 Sirtuin Inhibitors

The potential involvement of sirtuins in the pathogenesis of several diseases has driven research groups worldwide to develop small-molecule modulators of sirtuin activity. To identify novel sirtuin modulators various approaches have been applied, for example, high-throughput screening, focused library screening, fragment-based screening, or computer-based screening in combination with in vitro modulation tests. Despite the little structural information toward sirtuin modulation, the use of in silico methods has resulted in the identification of several promising sirtuin modulators. However, in contrast to the small-molecule inhibitors of the Zn^{2+} -dependent KDACs, which are already established drugs in the treatment of certain cancers, the clinical potential of sirtuin inhibitors is mostly unknown. Up to date, only one sirtuin inhibitor, selisistat, reached clinical trials [333-335]. One reason for this is certainly that until recently, most of the developed inhibitors lack either potency, isotype selectivity, or suitable physicochemical properties. In the last few years, however,

several promising inhibitor classes have been developed that fulfill these requirements. Most studies that were launched to discover sirtuin inhibitors focused on the isotypes Sirt1–3 and mainly on the inhibition of their deacetylase activity. Very recently, first studies were published concerning the pharmacological inhibition of isotypes Sirt4–7 as well as the acyl selectivity of sirtuin inhibition. Nonetheless, several small-molecule [336-342] and peptide-based [343-358] Sirtuin inhibitors have been reported in the literature.

2.3 Histone Phosphorylation

Phosphorylation of histones, which is highly dynamic, takes place on serines, threonines and tyrosines, predominantly, but not exclusively, in the N-terminal histone tails [76]. The levels of the modification are controlled by kinases and phosphatases that add and remove the modification, respectively [359]. All of the identified histone kinases transfer a phosphate group from ATP to the hydroxyl group of the target amino-acid side chain. In doing so, the modification adds significant negative charge to the histone that undoubtedly influences the chromatin structure [360].

Histone phosphorylation controls many important cellular processes, including transcription, apoptosis, DNA repair, and chromosome condensation [14, 361-363]. In most cases, phosphorylation of serine and threonine residues of the histone tails appears to be involved in chromatin condensation during mitosis and meiosis; for example, C-terminal phosphorylation of Thr119 in histone H2A is linked to regulation of chromatin structure and function during mitosis [362], and H3 Ser10 (H3S10) phosphorylation is related to chromatin compaction during mitosis. Yet H3S10 phosphorylation has also been shown to play a role in transcriptional activation of NF- κ B pathway genes and immediate early genes like *c-jun* and *c-fos* [14]. With regard to DNA repair, phosphorylation of histone H2AX at Ser139 (γ -H2AX) has been identified as one of the early events after a DNA double-strand break that helps recruit DNA damage repair proteins to the site [364].

2.4 Histone Ubiquitylation

Ubiquitin (Ub) is a highly conserved protein of 76 amino acids. Its name reflects the broad presence of Ub in all eukaryotic cells [365]. The covalent attachment of Ub to other proteins was observed 30 years ago with histones [366]. The exact purpose of this modification is still under investigation. In most cases, ubiquitylation serves as a mark for the proteolytic, ATP-dependent degradation of proteins by the proteasome [367]. In this process, several Ub units are transferred to the target protein by a succession of three enzymatic steps [368].

Histone H2A is the first protein identified to be modified by ubiquitin in cells [369]. We know now H2A and H2B are two of the most abundant ubiquitinated proteins in the nucleus. The dominant form of ubiquitinated histones are monoubiquitinated H2A (H2Aub) and H2B (H2Bub). A single molecule of ubiquitin is added to the highly-conserved lysine residues: Lys-119 for H2A, and Lys-123 in yeast or Lys-120 in vertebrate for H2B [370-372]. Usually histone modifications result in relatively small molecular changes to amino-acid side chains. In contrast, ubiquitylation results in a much larger covalent modification. Ubiquitin itself is a 76-amino acid polypeptide that is attached to histone lysines via the sequential action of three enzymes: ubiquitin-activating enzymes, ubiquitin-conjugating enzymes and ubiquitin ligases [373]. Even though ubiquitylation is such a large modification, it is still a highly dynamic one. The modification is removed via the action of isopeptidases called de-ubiquitinating enzyme (DUBs) and this activity is important for both gene activity and silencing [76].

In addition to H2A & H2B, core histones H3, H4, and linker histone H1 have also been reported to be modified by ubiquitin. For example, H3 & H4 were polyubiquitinated *in vivo* by CUL4–DDB–RBX1 ubiquitin ligase complex after UV irradiation[374-375]. But the biological function of these modifications has not been well elucidated. Besides monoubiquitination, histone H2A and H2B can be modified by ubiquitin chains [376-377]. Ubiquitination of mammalian H2B occurs at K120 and is predominantly regulated by ubiquitin-conjugating enzyme E2A (UBE2A or RAD6A) and the RNF20/RNF40 ubiquitin ligase complex [378]. Altered expression of UBE2A and RNF20/RNF40 may contribute to the development and progression of various tumor types. Recent study shown that the ubiquitination of H2B is involved in DNA double strand break (DSB) repair [371, 379]. Furthermore, cells in which either RNF20 or RNF40 were independently or simultaneously silenced exhibited significant increases in DSBs which strongly links H2Bub1 to DNA DSB repair [380].

2.5 Histone ADP-ribosylation

Histones are known to be mono- and poly-ADP ribosylated on glutamate and arginine residues, but relatively little is known concerning the function of this modification. What we do know is that once again the modification is reversible. For example, poly-ADP-ribosylation of histones is performed by the poly-ADP-ribose polymerase (PARP) family of enzymes and reversed by the PARP family of enzymes. These enzymes function together to control the levels of poly-ADP ribosylated histones that have been correlated with a relatively relaxed chromatin state [381]. Presumably, this is a consequence, at least in part, of the negative

charge that the modification confers to the histone. In addition, though, it has been reported that the activation of PARP-1 leads to elevated levels of core histone acetylation [382]. Moreover, PARP-1-mediated ribosylation of the H3K4me3 demethylase KDM5B inhibits the demethylase and excludes it from chromatin, while simultaneously excluding H1, thereby making target promoters more accessible [383]. Histone mono-ADP-ribosylation is performed by the mono-ADP-ribosyltransferases and has been detected on all 4 core histones, as well as on the linker histone H1. Notably, these modifications significantly increase upon DNA damage implicating the pathway in the DNA damage response [381].

The inclusion of PARP-1 into the group of chromatin modifying enzymes is justified by some similarities to HATs, for example [384]. PARP-1 affects various DNA-based processes like transcription, replication, and DNA repair; it also participates directly in the assembly of transcription complexes at enhancers and promoters [385]. In addition, the PAR modification is part of a synergism that is typical for the histone code: nucleosomes can be modified simultaneously by acetyl groups and PAR residues [386].

2.6 Histone SUMOylation

The abbreviation SUMO (small ubiquitin-like modifier) designates a group of small proteins that are related to Ub through secondary and tertiary structure elements [387]. Their mechanism of attachment to target proteins is also similar to that of Ub. A SUMO-activating enzyme E1 (SAE1/SAE2) binds SUMO with concomitant ATP hydrolysis as a reactive thioester, which is trans-esterified to the SUMO-conjugating enzyme E2 (Ubc9). The last step is likely to be the transfer of the SUMO group from E2 to the ϵ -amino function of a lysine residue by the action of a ligase E3 [388].

Sumoylation is a modification related to ubiquitylation [388], and involves the covalent attachment of small ubiquitin-like modifier molecules to histone lysines via the action of ubiquitin-activating, conjugating and ligases enzymes. Sumoylation has been detected on all four core histones and seems to function by antagonizing acetylation and ubiquitylation that might otherwise occur on the same lysine side chain [389-390]. Consequently, it has mainly been associated with repressive functions, but more work is clearly needed to elucidate the molecular mechanism(s) through which sumoylation exerts its effect on chromatin.

3. EPIGENETIC TARGETS IN MALARIA AND NEGLECTED TROPICAL DISEASES

3.1 Overview of Malaria and Neglected Tropical Diseases

Neglected tropical diseases (NTDs) are defined by WHO as ‘a diverse group of communicable diseases that prevail in tropical and subtropical conditions;’ the official WHO list of NTDs is currently comprised of 17 infectious diseases [391]. NTDs, which though treatable and/or preventable, remain a leading cause of morbidity and mortality among the world’s poorest populations. These diseases further fuel a vicious cycle because they are also big contributors to regression of child development and human productivity [392]. Alongside malaria, these diseases predominantly affect populations living in poverty, under poor living conditions and in close proximity with the vectors of disease-causing agents. Their effects are far-reaching and devastating: over 1 billion people in 149 countries suffer from one or more NTDs with millions of others at risk, and the economic repercussions of these diseases can be just as damaging as their health effects [391-392]. These diseases contribute significantly to child mortality in the developing world and greatly undermine economic development. In 2010, NTDs and malaria were estimated to be the cause of 1.321 million deaths globally, an increase of 9.2% from 1990 and representing 2.5% of all deaths that year [393]. The socioeconomic impact of the NTDs is not trivial. It is projected that 57 million disability adjusted life-years (DALYs) are lost every year due to these diseases, a figure widely believed to be an underestimate [394]. Additionally, diseases such as the trypanosomiasis, which are zoonoses, also affect livestock, contributing to reduced livestock productivity in infected populations and thereby aggravating the economic impact by decreasing agricultural output [391].

Although most, if not all, of the NTDs including malaria can be managed clinically through fairly inexpensive chemotherapeutic and public health interventions, major contributors to their continued prevalence include increasing drug resistance, a limited range of available drug options, and in the case of diseases such as trypanosomiasis and leishmaniasis, the high cost and very significant toxicity of current recommended drug regimens. Most important is the fact that these diseases mainly afflict patients from the poorest populations in the world where costs of healthcare remain largely beyond the reach of many [392].

Altogether, in the absence, with the only exception of RTS,S/AS01 for malaria [395], of approved vaccines targeted to the human parasitic diseases, anti-parasitic drugs, together with focused public health measures, continue to be crucial to addressing the growing health

and economic burdens caused by these diseases. Unfortunately, where the drugs are available, they are old, have unknown mechanisms of action, and quite often have limited efficacy and poor safety profiles. Moreover, the pandemic drug resistance, that has been observed following the treatment of all major parasitic pathologies, put the currently available drugs under an increasing threat of failure. Therefore, huge research efforts are now underway to develop new drugs to treat parasitic diseases and to overcome the growing problem of drug resistance. One extremely promising strategy to face these problems is represented by the so called “piggyback” approach that, focusing on drug targets and associated drug compounds that have been already validated for other human diseases, try to apply them to new indications such as parasitic diseases. Although this “drug repurposing” strategy is quite attractive, since it has the potential to accelerate the drug development process due to lower costs, reduced risk and decreased time to market due to availability of preclinical data, the parasite selectivity remains one of the major obstacles to overcome in moving such compounds into clinical trials as potential novel anti-parasitic drugs [396-397].

By using the “piggyback” approach, small molecule epigenetic modulators, which have been originally targeted for cancer use or other diseases, are now being investigated to target a range of parasitic diseases [397]. This approach holds great promise and can in part mitigate the relative lack of investment in efforts to improve the control and treatment of those malaria and neglected parasitic diseases.

3.2 Malaria Epidemiology and Therapeutics

The word ‘Malaria’ originates from the Italian word *mala aria*, meaning ‘bad air’ which justly reflects how this deadly disease had instilled fear from people in the medieval time [398]. Malaria is a devastating infectious disease that is characterized by intermittent high fevers and, in the case of cerebral malaria, neurological complications such as brain injury and coma. Found in tropical regions throughout sub-Saharan Africa, Southeast Asia, the Pacific Islands, India, and Central and South America, malaria parasites threaten the lives of 3.3 billion and cause 600,000 deaths and there are approximately 200 million clinical cases of infection each year. Africa is still the leading region in terms of malaria burden. This region accounts for majority (80%) of the malaria cases as well as malaria-associated deaths (90%) globally [264, 396]. While pregnant women and children are particularly vulnerable to the threat of malaria, severe disease is also a threat for naïve travelers to malaria endemic regions and immunocompromised people [399]. It is caused by protozoan parasites of the genus

Plasmodium, which are transmitted to humans by the bites of female Anopheles mosquitoes. Four of the more than 100 *Plasmodium* species infect humans and cause distinct disease patterns: *P. falciparum* (malaria tropical), *P. vivax*, *P. ovale* (both malaria tertiana), and *P. malariae* (malaria quartana). *P. falciparum* and *P. vivax* account for 95% of all malaria infections. *P. falciparum* is found throughout tropical Africa, Asia, and Latin America. Nearly all severe and fatal cases are caused by *P. falciparum*. *P. vivax* is more common in India and South America, but is also found worldwide in tropical and some temperate zones. *P. ovale* is mainly confined to tropical West Africa, while the occurrence of *P. malariae* is worldwide, although its distribution is patchy [400-401].

Indeed, a strong relationship exists between poverty and malaria. This relationship is evident in the fact that most malaria endemic countries are also among the poorest countries of the world. Poverty contributes to the malaria burden as it has the ability to affect integral aspects of malaria treatment-seeking behaviors [402], including access to preventive measures and treatment—in relation to affordability, acceptability and availability—[403], and adherence to treatment.

Presently, there have been renewed efforts in the global malaria control with several organizations and non-endemic countries increasingly getting involved in the fight against malaria [404-405]. These efforts have resulted in reduction in the global malaria burden over the last decade [406]. The current achievement is mostly attributed to the increase in malaria research funding, and scale-up of interventions against malaria, including insecticides-treated nets (ITNs), indoor residual spraying (IRS), rapid diagnostic testing (RDT), and importantly, the use of artemisinin-based combination therapy (ACT) [407]. There has been significant improvement in access, availability and affordability of ACT in malaria endemic regions [406].

While substantial funds have been invested in producing a malarial vaccine, to date poor efficacy has been achieved for those that have been trialed clinically, including the leading candidate RTS,S [408-409]. This means that mosquito control and chemotherapy are the main strategies for the prevention and treatment of this disease. ACTs have been adopted as first line treatment for uncomplicated malaria in most endemic countries, while chloroquine is now only used in some countries in the Americas due to widespread drug resistance [396]. In relation to previously used anti-malarial drugs, artemisinin drugs are very effective in parasite clearance and can relieve the malaria symptoms faster [410-411]. Unfortunately, the development of resistance to ACT (which has been confirmed in five countries of Southeast

Asia: Cambodia, Lao PDR, Myanmar, Thailand and Viet Nam] [412-415] poses a major threat to its efficacy and use as first-line treatment. This also threatens the sustainability of the present success in malaria control [416].

Similar to the artemisinin class drugs, the development of resistance to most of the previously used anti-malarial drugs (such as chloroquine, sulfadoxine-pyrimethamine, mefloquine) originated from South East Asia. Nevertheless, the burden and effects of resistance are usually borne more by the African region that accounts for most of the global malaria cases. Considering the quick and widespread of previous cases of resistance to anti-malarial drugs from the SEA to Africa, the African region stands at risk of spread of artemisinin resistance [417-418]. Regrettably, only one drug, primaquine, can completely eliminate *P. vivax* and *P. ovale* and thus provide a radical cure. *P. vivax* and *P. ovale* infections are challenging to treat because they form dormant liver stages (hypnozoites) that are refractory to most drugs. Primaquine, an 8- aminoquinoline, requires repeated dosing (up to 15 days) and is toxic to individuals with glucose-6-phosphate dehydrogenase deficiency [419] a common condition in malaria endemic regions. This limits the use of primaquine by the billions of people at risk for *P. vivax* infection in Central and Southeast Asia, and in Central and South America [420]. Therefore, new drugs with activity against all stages of the parasite life cycle and with new mechanisms of action are needed to help fulfill the ultimate goal of elimination. This is pushing research efforts into development and discovery of new antimalarial drugs endowed with new mechanisms of action on novel targets in the parasite.

3.3 Malaria Life Cycle

Malaria parasites have a complex life cycle that use a multi-stage developmental program to transition between their mammalian host and mosquito vector: while replicative stages in the host are strictly haploid and intracellular, cell division in the vector occurs in an extracellular milieu, within a cyst-like structure. Each developmental stage (Fig. 3.1) has a distinct morphology and physiology that is determined by its gene expression profile, as revealed by stage-specific transcriptomic and proteomic analyses of human and rodent malaria parasites [421-427]. Human infection starts with the bite of an infected female *Anopheles* mosquito, resulting in the transfer of sporozoites, motile cell forms that enter the bloodstream soon after the insect's bite, that quickly migrate to the liver [428-433]. Inside liver cells (hepatocytes), these sporozoites multiply extensively over a period of approximately two weeks and are then released into the vasculature in the form of thousands

of merozoites to infect red blood cells. *P. vivax* and *P. ovale* can remain dormant in the liver as hypnozoites, but can re-emerge and begin a blood-stage infection month to years after initial infection (relapsing malaria). During this intra-erythrocytic developmental cycle (IDC), the parasite progresses through three distinct stages, termed ring, trophozoite, and schizont. The ring stage is characterized by remodeling of the host cell to establish the supply of hemoglobin as an energy source, as well as to ensure evasion of the human immune system. During the trophozoite stage, the parasite becomes highly transcriptionally and metabolically active, in preparation for cell division. Finally, the parasite multiplies into 16–32 daughter parasites using a process of asexual replication called schizogony. During schizogony, the nucleus undergoes multiple rounds of division, which is followed by cytokinesis to subdivide the multinucleated parasite into identical daughter cells. Approximately 48 h after invasion of the red blood cell, these daughter parasites burst out of the host cell, ready to invade new red blood cells [432-433].

In a process that is not completely understood, a small fraction of the haploid asexual parasites differentiate into male and females gametocytes within the red blood cell [434]. It is possible that secreted parasite factors induce this differentiation [435-436]. These asymptomatic, non-replicating forms can persist for weeks and are responsible for malaria transmission. The uptake of mature gametocytes by a feeding mosquito followed by sexual replication in the mosquito midgut [437] and further develop into the salivary gland sporozoites that can be transmitted to a new human host.

The asexual replication cycle is responsible for symptomatic disease and for the complications that are associated with severe malaria, such as anemia due to rupturing of red blood cells. In addition, severe disease can result from cytoadherence, the attachment of *P. falciparum*-infected erythrocytes to the smallest blood vessels, preventing clearance by the spleen and causing organ dysfunction. This cytoadherence is mediated by a family of parasite virulence proteins that are expressed on the erythrocyte surface: *Plasmodium falciparum* Erythrocyte Membrane Protein 1 (*PfEMP1*) [438-440]. Each *P. falciparum* parasite has approximately 60 different *PfEMP1* variants encoded by *var* genes, only one of which is expressed at any time. Switching *var* gene expression enables the parasite to escape from host immune responses [441-442]. This process of antigenic variation is one example of the excellent adaptation of the parasite to survive in the human host. For these reasons, this parasite species and this stage of the parasite life cycle have been most extensively studied.

Consequently, most of our knowledge concerning epigenetic regulation of gene expression in the parasite is restricted to the *P. falciparum* IDC, while little is known about epigenetic profiles in sporozoites, the liver stage, the mosquito stages, or in other *Plasmodium* species.

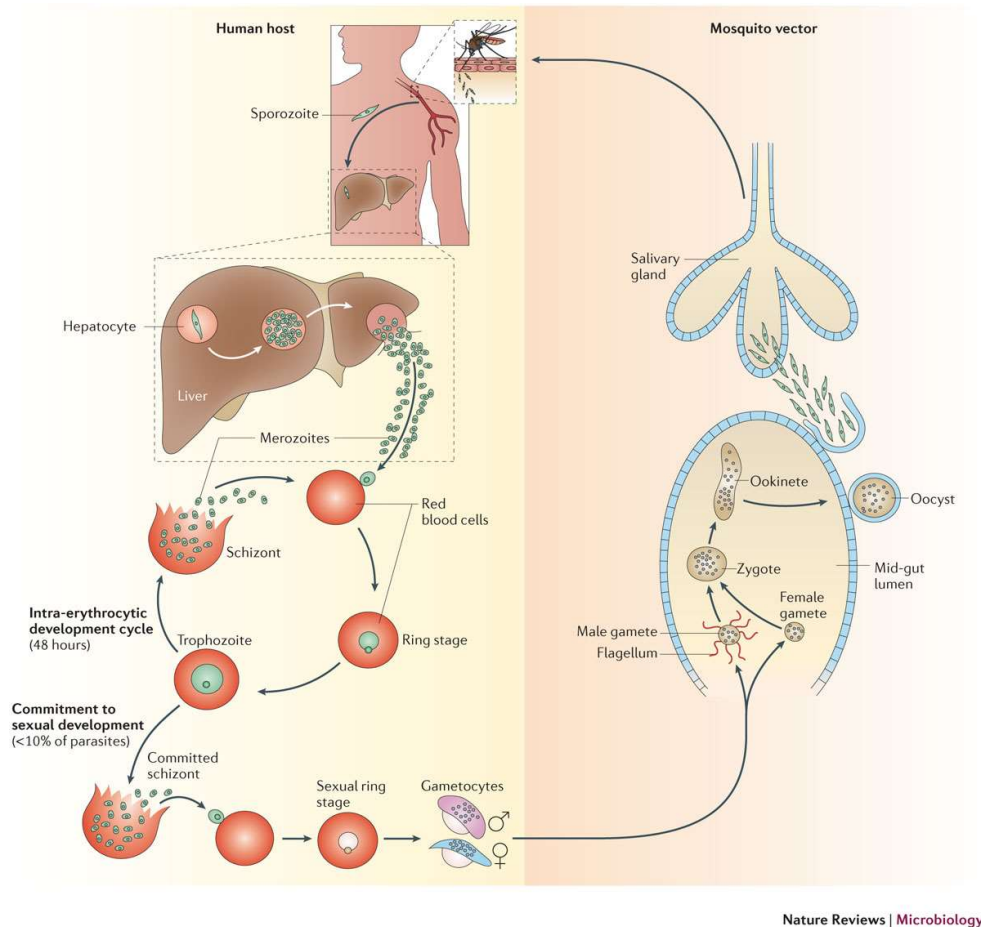


Fig. 3.1: Life cycle of malaria [431].

3.4 The Epidemiology and Distribution of Human Schistosomiasis

Schistosomiasis is one of the major neglected parasitic diseases which still represents a serious public health problem in tropical regions of the world [443-444]; where infections are mediated through contact with infected fresh water snails that serve as intermediate vectors between human hosts. However, recently *S. haematobium* was reported in the Mediterranean area, particularly in the island of Corsica, a French territory [445-447]. This finding, together with a decade of native cases around Europe, raised concerns regarding the presence of schistosomiasis in Europe. Three epidemiological conditions were argued [446] to be of special relevance in further assessing the risk of schistosomiasis in Mediterranean Europe: (i) this area is ecologically favorable to snails of the genus *Bulinus* which are the intermediate hosts of human and animal schistosomes [448], (ii) climate warming creates favorable conditions for local transmission of *Schistosoma* spp. [449], and (iii) movement of

people which brings infected individuals from endemic regions to the European region allowing, given the conditions, the establishment of transmission chains in these areas.

The disease is endemic in 76 countries globally; mainly in South America, southeast Asia, but mostly Africa where more than 90% of the estimated 41 000 deaths and approximately 1.7 million DALYs lost occur every year. It is also estimated that the disease has a prevalence of 230 million cases annually worldwide [450]. It also affects almost 259 million people worldwide [451] causing an annual death toll of 280,000 [452] and millions of people suffering from long-term morbidity due to chronic schistosomiasis. Eight species of *Schistosoma* have been reported infecting humans (Table 3.1). Definitive vertebrate host species, other than human, may contribute to *Schistosoma* epidemiology and persistence in nature (Table 3.1).

Table 3.1: The eight species of schistosome reported in humans [453].

<i>Schistosoma</i> species	Distribution	Natural definitive host species (excluding humans)	Human public health importance
<i>S. mansoni</i>	Africa, Middle East, South America, Caribbean	Non-human primates (including apes), rodents, insectivores, artiodactylids (waterbuck), procyonids (raccoon)	High
<i>S. haematobium</i>	Africa, Middle East	Non-human primates (not apes)	High
<i>S. intercalatum</i>	Central Africa (D.R. Congo only)	Possibly rodents	Low
<i>S. guineensis</i>	West Africa (Lower Guinea)	Possibly rodents	Low
<i>S. mattheei</i>	Southern Africa	Non-human primates (not apes), artiodactylids (cattle, antelope)	Low
<i>S. japonicum</i>	East Asia (China, Philippines, Indonesia)	Non-human primates, artiodactylids (water buffalos in particular), carnivores, rodents, perissodactylids (horses)	High
<i>S. mekongi</i>	SE Asia (Vietnam, Cambodia, Laos, Thailand)	Carnivores (dogs), artiodactylids (pigs)	Moderate
<i>S. malayensis</i>	Malayan penisular	Rodents (van Mueller's rat)	Low

3.5 *Schistosoma mansoni* Life Cycle

Schistosomiasis is caused by the platyhelminth worms of the genus *Schistosoma*, trematodes that live in the bloodstream of humans and animals. Three species (*Schistosoma mansoni*, *Schistosoma haematobium* and *Schistosoma japonicum*) account for the majority of human infections [454]. Schistosomes are digenean parasites that successively infect fresh water snails (the intermediate host) and the vertebrate definitive host. They reproduce both

asexually (within the snail host) and sexually (vertebrate host) and their life-cycle includes four distinct morphological forms and separate sexes at the adult worm stage (Fig. 3.2) [455]. Cercariae break out of the snail tissues into the water, swimming actively till dying or penetrating the unbroken skin of humans or animals, the definitive host, where they lose their bifurcated tail and become schistosomula. During the first 24 h after infection, nearly 90% of *S. mansoni* and *S. haematobium* schistosomula are present only in the blood-free, lymph-free epidermis. Majority of schistosomula are found in the dermis only after 48 h, and they appear to reach the dermal vessels around 72 h after infection [456-458]. Once in the blood capillaries, the schistosomula are carried passively by the blood flow till reaching the right heart and then the lungs. Depending on the species, schistosomula stay inside the pulmonary capillaries from 3 to 16 days, where they change into much longer and slender organisms, such a shape that enables them to traverse the thin pulmonary capillaries to the left heart and the systemic circulation [459].

Following this period, schistosomula migrate from the lungs to the hepatic portal system via the blood stream and transform into adult worms. Male and female worms pair in the hepatic portal system and migrate to the mesenteric veins (except *S. haematobium*, which migrates to the urogenital system) to lay nearly 300 eggs per day. These eggs either pass into the gut lumen to be voided in the faeces and continue the life cycle or pass through the mesenteric veins and lodge in the liver, where they can cause granulomatous changes and fibrosis, both of which are key contributors to schistosomiasis [456, 460]. The morbidity associated with schistosomiasis results from the immunologic reactions to egg-derived antigens, beside the mechanical and toxic irritation caused by eggs trapped in the wall of blood vessels. Some of the most common pathological changes seen in chronic schistosomiasis infections include bleeding into the intestine or urinary system, liver and spleen enlargement, and periportal fibrosis [460-462].

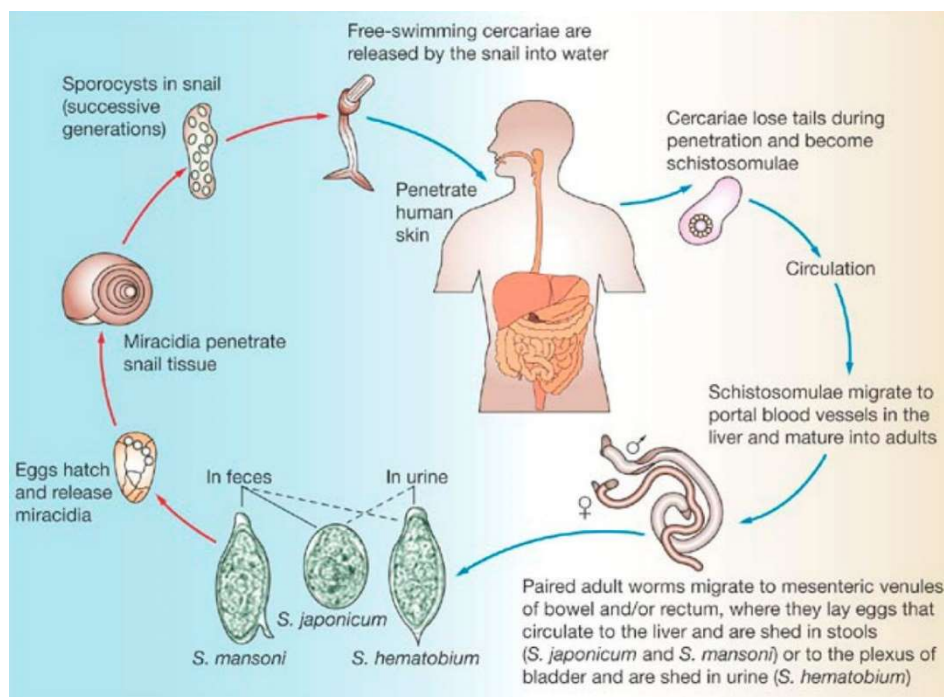


Fig. 3.2: Lifecycle of *Schistosoma* [392].

3.6 Control of Schistosomiasis, the Lack of Alternative Therapeutics

Despite its introduction in the mid-1970s, praziquantel still remains the only drug of choice for the treatment of schistosomiasis [463-464]. Praziquantel is a low-cost and highly effective antischistosomal agent, which is active against all *Schistosoma* species, albeit its exact mechanism of action is still not fully understood [465-466]. It is administered orally as a single dose, showing no notable side effects [467]. The long-term use of praziquantel as a sole antischistosomal treatment alongside its implementation in mass drug administration campaigns has raised deep concerns over the potential for emergence of drug-resistance [465-466, 468-470]. Indeed, incidences of a reduced efficacy of praziquantel against some *Schistosoma* species [471-473] and the induction of drug-resistance in laboratory strains [474-476] have already been reported. Evidently, a diminished efficacy of praziquantel would have a serious impact on the ongoing efforts to combat the disease, highlighting the need to develop new antischistosomal agents.

4. MALARIA EPIGENETICS

4.1 Epigenetic Mechanisms as Drug Targets for *P. falciparum*

Throughout the *Plasmodium* lifecycle, regulation of gene expression is orchestrated by a variety of mechanisms, including epigenetic, transcriptional, posttranscriptional, and translational control of gene expression. Owing to the absence of most canonical eukaryotic transcription factors in the *Plasmodium* genome [477], epigenetic control has long been recognized to play an important role in gene expression regulation.

The epigenome of *P. falciparum* mainly consists of histone PTMs, histone variants, chromatin remodelers, histone modifying enzymes and non-coding RNAs (ncRNAs) [429, 431, 478-485]. DNA methylation, although not well characterized in *P. falciparum* and which previously could not be detected [486], has recently been identified [487-488]. Still, the overall epigenetic makeup of *Plasmodium* is unique and differs from other eukaryotic organisms in many ways. Unlike the other eukaryotes, the *Plasmodium* epigenome is mainly euchromatic [489-490] and lacks the linker histone H1 [491]. Absence of a functional RNA interference system [492] also suggests an involvement of alternative regulators of epigenetic processes compared with other eukaryotes.

In malaria parasites, epigenetic regulation of gene expression has been extensively studied only in *Plasmodium falciparum*. For many years, studying epigenetics in this parasite was almost synonymous to studying the regulation of *var* genes, which are important for antigenic variation and virulence [493]. However, recent findings have revealed a more general role for epigenetics in malaria parasite biology, including processes as diverse as erythrocyte invasion, solute transport, or formation of sexual forms necessary for human-to-mosquito transmission. The contribution of epigenetic regulation of gene expression to these processes stems from the clonally variant expression of some of the genes involved. Silencing of clonally variant genes, which is a process truly controlled at the epigenetic level [494], generally depends on histone modifications that result in reversible formation of repressive chromatin structures (heterochromatin), but several additional layers of regulation operate specifically on particular gene families such as *var* genes.

In *Plasmodium*, the epigenetic mechanism of regulation of gene expression can be divided broadly into three distinct areas based on parasite development [495].

Firstly, during asexual intra-erythrocytic developmental stages where differential gene expression occurs which are responsible for all clinical symptoms of malaria. *Plasmodium*

falciparum shows unusual mode of gene expression during its 48 h developmental process within the erythrocyte, implying tight and integrated genome-wide regulation of transcription [496-498]. Recently, a battery of proteins like Api-AP2, HP1, histone deacetylases, and histone methylases have been shown to be involved in gene regulation [499-501]. Two nucleosome assembly proteins, *PfNapS* and *PfNapL*, have been also identified [502] and *PfNapS* was shown to be essential for the parasite's survival [503]. These observations suggest the role of epigenetic mechanism in transcriptional regulation in *Plasmodium*.

Secondly, epigenetics likely play role during sexual and morphological differentiation for the rest of the life cycle. The blood stage parasites differentiate into gametocytes. These gametocytes mate to form ookinetes followed by formation of sporozoites in the mosquito, leading to the subsequent transmission and development in the human hepatocytes before the release of the merozoites in the asexual erythrocytic cycle. Distinct transcriptional profiling has been reported in gametocytes, ookinetes, oocyst sporozoites, salivary gland sporozoites hepatocyte stage and erythrocyte stage [424, 504-508]. All these observations may suggest epigenetic control over life cycle transition and stage differentiation. The AP2 transcription factor, *pfap2-g*, located on chromosome 12, is one of the master regulators of gametocyte differentiation [509-510]. In asexual parasites, the locus containing *pfap2-g* is localized to the nuclear periphery and silenced by H3K9me3 and PfHP1 (Fig. 4.1C) [489, 511]. *In vitro* studies show that downregulation of PfHDA2 activates *pfap2-g* and induces the formation of gametocytes [512]. Similarly, depletion of PfHP1 activates *pfap2-g* and increases the rate of gametocyte production [513]. These results raised the idea that sexual conversion is regulated at the epigenetic level, a view that was later corroborated by studies in which specific epigenetic factors were depleted [512-513]. The ortholog of *pfap2-g* in the distantly related murine malaria parasite *P. berghei*, *pbap2-g*, also plays a key role in gametocyte formation [510]. This observation suggests that *ap2-g* is a conserved regulator of sexual conversion in malaria parasites; whether or not epigenetic control of the process is a conserved feature in all *Plasmodium* species awaits experimental confirmation.

Moreover, invasion proteins present in *P. falciparum*, responsible for new erythrocyte invasion are also regulated epigenetically. Invasion of a new erythrocyte by the malaria parasite involves binding of parasite ligands to specific recognition surface receptors on the red blood cell [514]. *Eba*, *rhoph1/clag*, *acbp*, and *PfRH* are among some of the gene families involved in the invasion process, but are not essential for parasite survival. The genes in these

families are thought to be partially regulated through epigenetic mechanisms and show differential expression patterns in different parasite lines, as they can be in either active or inactive states (Fig. 4.1B) [515]. According to a more recent study exploring the parasite-specific bromodomain protein *PfBDP1* using *in vitro* culture, invasion genes are regulated in a more 'classical' manner by transcription factors interacting with specific promoters [516]. In schizonts, an enrichment of *PfBDP1* was observed at the transcription start sites of invasion genes. *PfBDP1* was shown to positively regulate transcription of invasion genes by binding to acetylated histone H3. Additionally, conditional knockdown of *PfBDP1* resulted in erythrocyte invasion defects and parasite growth inhibition, further confirming the essentiality of this bromodomain protein for the coordinated expression of invasion genes in *P. falciparum*.

Thirdly and most importantly, epigenetic control is involved in the mutually exclusive expression of individual *var* genes involved in the virulence processes such as cytoadherence and variant erythrocyte invasion. The best characterized family of antigen coding gene is the *var* family in *P. falciparum*. This gene family encodes ~ 60 variants of *PfEMP1*, expressed on infected erythrocytes. *PfEMP1* is responsible for the attachment of the infected erythrocytes with the vascular endothelial cells thereby preventing the clearance from the circulatory system. Most of the *var* genes are generally silenced, with only one or a few being expressed at any given time [495, 497, 517-520]. Silent *var* genes are clustered to one or more repressive regions at the nuclear periphery, marked by H3K9me3 and *PfHP1* (Fig. 4.1A) [489-490, 511, 521-524]. Absence of *PfHP1* in the parasite has also been shown to result in loss of monoallelic *var* gene expression as well as result in parasite growth arrest [513], which indicates that *PfHP1* plays an essential role in maintaining repressive heterochromatin. The variegated expression of these genes has been shown to correlate with alterations in histone modifications and these chromatin states can be epigenetically inherited [489, 525-526]. HDACs, in particular NAD⁺-dependent class III HDAC proteins *PfSIR2A* and *PfSIR2B* and class II HDAC protein *PfHDA2*, play a role in regulating the repressive clusters containing silent *var* genes, as manipulated parasite lines lacking these proteins show loss of monoallelic *var* gene expression [489, 512, 527-528]. *PfSET2* is an HKMT that specifically marks *var* genes, and the disruption of *PfSET2* results in the de-repression of the silenced *var* gene cluster(s) [529-530]. The active *var* gene, transcribed at the ring stage, is distinguished by the presence of H3K4me3 and H3K9ac marks and resides in a region of the nucleus away from the repressive heterochromatin cluster(s) [489, 526-527]. At the later

trophozoite and schizont stages, the active *var* gene is controlled by the HKMT *Pf*SET10, which is suggested to play a role in maintaining epigenetic memory of *var* gene expression [531]. Recent evidence suggests that sense and anti-sense long ncRNAs can also regulate *var* gene expression [532-534]. Collectively, these results highlight the relationship between proper chromatin assembly and regulation of antigenic variation in the parasite.

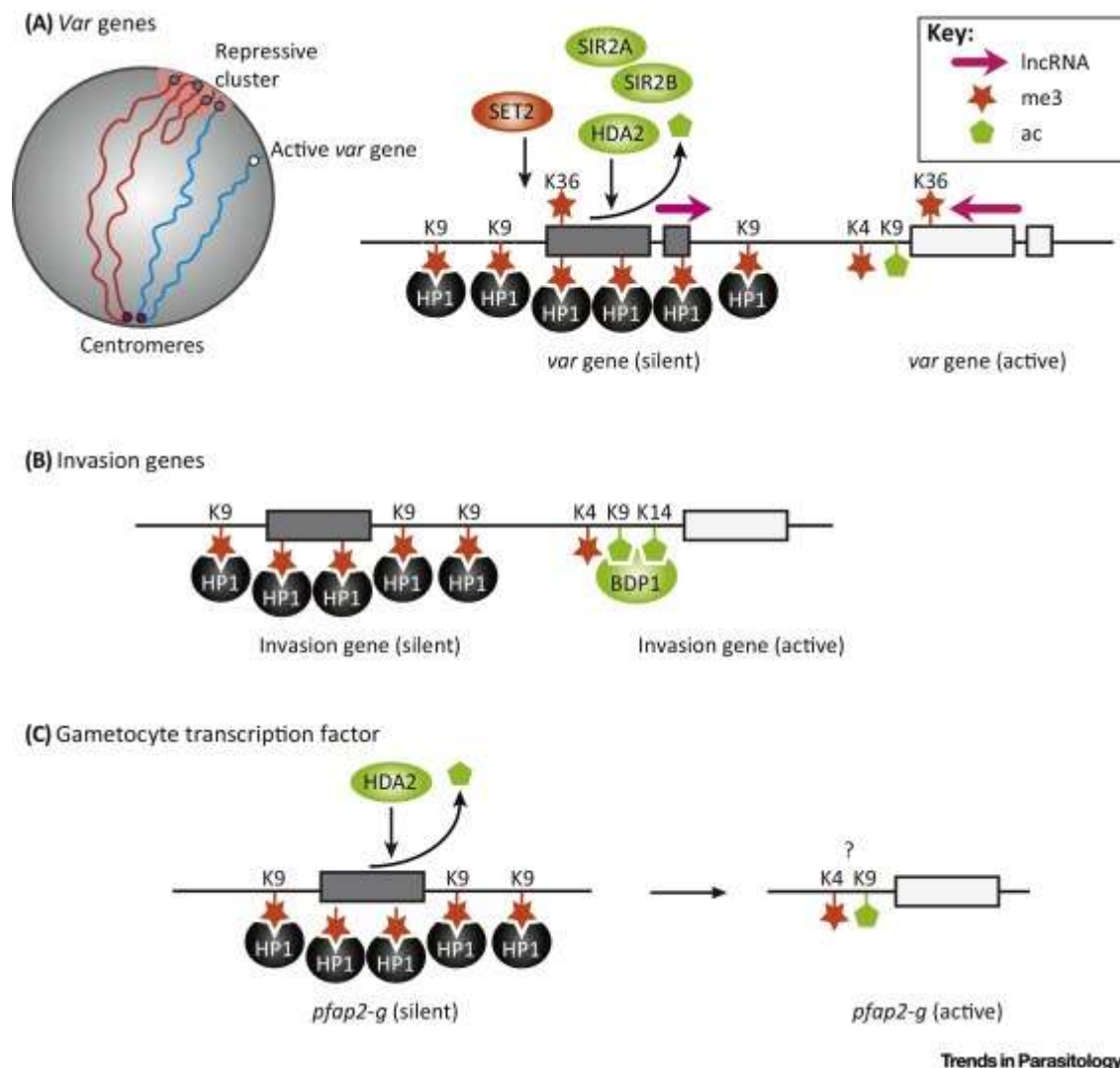


Fig. 4.1: Epigenetic Regulation of Specific Genes and Gene Families in *Plasmodium falciparum*. (A) The family of *var* genes is controlled by clustering of silent *var* genes at the nuclear periphery and the deposition of repressive H3K9me3 marks, which recruits PfHP1 and results in the formation of heterochromatin. The single active *var* gene is isolated from all other *var* genes, marked by H3K4me3 and H3K9ac, and localized in a euchromatic environment. lncRNAs transcribed from a bidirectional promoter in the *var* introns also contribute to regulation of *var* gene expression. (B) Several families of invasion genes are epigenetically regulated through repressive and active histone marks that recruit heterochromatin marker PfHP1 and gene activator PfBDP1, respectively. (C) During the IDC, gametocyte-specific TF *pfap2-g* localizes to the nuclear periphery and is silenced by repressive histone marks, including H3K9me3 and PfHP1 [483].

4.2 *Plasmodium falciparum* Chromatin Organization and Histone PTMs

The malaria parasite chromosomes have a typical nucleosomal organization consisting of 155 bp of DNA [535]. This is complemented by the absence of linker histone H1 [536], indicating “looser” chromosome packaging and/or an absence of higher order compaction of *P. falciparum* DNA. The low level of chromosome compaction likely underlines the transcriptionally active euchromatin that persists throughout the IDC. The four core histones H2A, H2B, H3, and H4, as well as four *P. falciparum* variant histones H2A.Z, H2Bv (or H2B.Z), H3.3 and H3Cen (H3 centromeric), have been identified in *P. falciparum* parasites [491, 537]. The *P. falciparum* H3 and H3.3 protein sequences are 94% identical. PfCenH3 protein shares 61% amino acids identity with H3 and H3.3 (Table 4.1) [479].

Table 4.1: Histones and their different modifications in *P. falciparum*

Sr. No.	Histones	Gene ID	Chromosome	Length (aa)	PTM(s)
1.	H2A	PFF0860c	11	132	N-term-ac, K3ac, K5ac
2.	H2A.Z	PFC0920w	3	158	N-term-ac, K11ac, K15ac, K19ac, K25ac, K28ac, K30ac, K35ac
3.	H2B	PF11_0062	11	117	K112ub
4.	H2Bv	Pf07_0054	7	123	N-term-ac, K3ac, K8ac, K13ac, K14ac, K18ac, T85ph
5.	H3	PFF0510w	6	136	K4me, K4me2, K4me3, K9ac, K9me, K9me3, K14ac, K14me, R17me, R17me2, K18ac, K23ac, K27ac, K36me3, K56ac, K79me3
6.	H3.3	PFF0865w	6	136	K4me, K4me2, K4me3, K9ac, K14ac, R17me, R7me2, K18ac, K23ac, K27ac
7.	H4	PF11_0061	11	103	N-term-ac, R3me, R3me2, K5me, K5ac, K8ac, K12ac, K12me, K16ac, R17me, K20me, K20me2, K20me3
8.	CenH3	Pf13_0185	13	170	

Epigenetics lies at the very heart of gene expression, regulating access of the transcriptional machinery to chromatin [482, 538] via (1) PTMs of histones, (2) nucleosome occupancy, and (3) global chromatin architecture. In the past decade, various histone PTMs have been identified throughout the *Plasmodium* lifecycle. Although the histones are well conserved amongst the eukaryotes, *P. falciparum* histone variants H2A.Z and H2Bv carry more PTMs including several unique acetylations [537]. At least 50 different histone PTMs (Table 4.2) have been identified in *P. falciparum*, including acetylations, methylations,

phosphorylations, ubiquitylations, and sumoylations [491, 537, 539-540]. PTMs involve multiple acetylation sites on H2A, H2A.Z and H2Bv, one phosphorylation site on H2Bv, one ubiquitination site on H2B, and many acetylation and methylation sites on H3, H3.3 and H4. An additional in-depth analysis revealed the presence of 14 phosphorylation sites at the N-terminal tails of all histones in *P. falciparum* that are frequently adjacent to acetylation sites [541]. Moreover, H4 and H2A.Z were identified as small ubiquitin modifier (SUMO) substrates with at least six independent SUMOylation sites [542]. It is, however, important to mention that a majority of the parasite genome carries a large proportion of activating histone marks (H3K9ac and H3K4me3) compared to silencing marks (H3K9me3 and H3K36me3). This contrasts with what has been identified in multicellular eukaryotes [543], but validates further the transcriptionally permissive euchromatic state of the parasite genome. In mammalian genomes, H3K9ac and H3K4me3 strictly localize to active promoters [103, 544-547], while in *P. falciparum* these modifications not only mark promoters and 5' coding regions of genes that are highly transcribed [548-549], but are also found in intergenic regions and 'silenced' promoters [490, 537, 548].

Repressive histone marks are mostly limited to regions of the genome harboring the clonally expressed variant surface antigen gene families (*var*, *rifin*, *stevor*, and *pfmc-2tm*) and invasion gene families (*eba* and *clag*), as well as some additional loci, such as the gametocyte-specific transcription factor *pfap2-g*. These regions are organized into transcriptionally silent heterochromatin marked by H3K9me3 [489-490, 523, 525, 550]. In addition, silent *var* genes and to a lesser extent *rifin* and *stevor* genes carry H3K36me3 [49]. The single active *var* gene is physically separated from this repressive heterochromatin and is enriched in H3K4me3 and H3K9ac, in particular around its TSS [526].

The extensive ability of *P. falciparum* to evade the host's immune system has been traditionally attributed to the high sequence variability and the mutually exclusive pattern of the *var* gene family expression. However, transcriptional switching is also one of the main factors of *var*-driven immune evasion of *P. falciparum* and it is now clear that epigenetic mechanisms play a central role in silencing of the *var* genes and possibly other heterochromatin-linked genes in *P. falciparum*. Indeed, the canonical heterochromatin marker, H3K9me3, helps in maintaining the silenced state of the *var* genes [489]. Their activation is then restored by replacement of H3K9me3 at their 5'flanking regions by H3K9ac [525-526]. Hence epigenetic memory plays a role in antigenic switching of the *var* genes as

well as other transcriptional heterogeneity amongst isogenic parasite lines [551-553]. Similar to *var* genes, factors involved in red blood cell invasion and genes implicated in nutrient import across the infected red blood cell plasma membrane are also regulated through epigenetic mechanisms; some in a mutually exclusive manner [515, 554]. There is a general association between heterochromatin marks and clonally variant gene expression of essentially all differentially expressed gene families [553, 555]. These results suggest that phenotypic variations of parasite populations are (at least partially) governed by H3K9me3 linked heterochromatin.

H3K36me3 is also enriched at the transcription start sites (TSSs) of silent *var* genes and at the coding regions of both active and repressed members [529]. Moreover, H3K36me2 serves as another global repressive mark in *P. falciparum* and gene expression is regulated by altering the ratio of activation marks to H3K36me2 [556]. Interestingly, the highly conserved heterochromatic marker, H3K27me3, has not been detected in *Plasmodium* [537]. H4K20 methylations also mark silent heterochromatic domains in *P. falciparum* and *Toxoplasma gondii* [557] but their distribution and role are still not conclusive. In particular, H4K20me3 that is enriched at heterochromatin in most eukaryotes [558-559], has a broad chromosomal distribution in *P. falciparum* [489]. In fact, H4K20me3 marks euchromatic as well as heterochromatic domains but its transcription associated occupancy is restricted mainly to the *var* genes [560]. These observations tempt us to speculate that the mutually exclusive expression of *var* genes and epigenetic memory are maintained by multiple histone PTMs including H3K9ac, H4K20me3, H3K36me2 and possibly others.

In addition to histone PTMs, nucleosome organization plays a critical role in gene expression regulation in *Plasmodium*. In general, heterochromatin is substantially enriched in nucleosomes compared with euchromatin [561] and active promoters and intergenic regions in Pf show markedly reduced nucleosome occupancy [562]. In addition, common transcript features such as TSSs, transcription termination sites, and splice donor/ acceptor sites show clearly distinguishable nucleosome positioning in *P. falciparum* [563], but previously described dynamic changes in nucleosome positioning [561] appeared to be mostly restricted to TSSs during the IDC [563]. Uniquely in *Plasmodium* spp., canonical histones in intergenic regions are replaced by histone variant H2A.Z [548], which, in concert with the apicomplexan-specific H2B.Z, establishes a H2A.Z/H2B.Z double-variant nucleosome subtype enriched at AT-

rich promoter regions and correlates with open chromatin and active gene transcription [564].

Table 4.2: List of putative epigenetic factors involved in controlling chromatin structure and epigenetic regulation in *P. falciparum*

Histone methyltransferases		Proposed function
Protein name	Gene ID (previous ID)	
PfSET1	PF3D7_0629700 (PFF1440w)	Involved in the deposition of the epigenetic mark H3K4me3
PfSET2 (PfSETvs)	PF3D7_1322100 (MAL13P1.122)	Involved in the deposition of the epigenetic mark H3K36me2/3, participates in var regulation
PfSET3 (PfKMT1)	PF3D7_0827800 (PF08_0012)	Involved in the deposition of the epigenetic mark H3K9me2/3
PfSET4	PF3D7_0910000 (PFI0485c)	Involved in the deposition of epigenetic marks on H3K4
PfSET5	PF3D7_1214200 (PFL0690c)	Involved in the deposition of unknown epigenetic marks; mitochondrial localization also reported
PfSET6	PF3D7_1355300 (PF13_0293)	Involved in the deposition of epigenetic marks on H3K4
PfSET7	PF3D7_1115200 (PF11_0160)	In vitro data suggest methylation of H3K4 and H3K9
PfSET8	PF3D7_0403900 (PFD0190w)	Involved in the deposition of the epigenetic mark H4K20me1/2/3
PfSET9	PF3D7_0508100 (PFE0400w)	Involved in the deposition of unknown epigenetic marks
PfSET10	PF3D7_1221000 (PFL1010c)	Involved in the deposition of the epigenetic mark H3K4me3, localized to the var expression site
Protein Arginine transferase (PRMT)		
PfRMT1	PF14_0242	
PfRMT4/PfCAR M1	PF08_0092	
PfRMT5	PF13_0323	
Histone demethylases		
JmjC1	PF3D7_0809900 (MAL8P1.111)	Involved in the removal of epigenetic marks from H3K9 and H3K36
JmjC2	PF3D7_0602800 (PFF0135w)	Involved in the removal of unknown epigenetic marks
LSD1	PF3D7_1211600 (PFL0575w)	Involved in the removal of unknown epigenetic marks
Histone acetyltransferases		
PfGCN5	PF3D7_0823300 (PF08_0034)	Involved in the deposition of the epigenetic marks H3K9ac and H3K14ac
PfHAT1	PF3D7_0416400 (PFD0795w)	Probable ortholog to HAT1 in higher eukaryotes
PfMYST	PF3D7_1118600 (PF11_0192)	Member of the MYST family of acetyltransferases, proposed to acetylate H4K5, K8, K12, and K16
Histone deacetylases		
PfSIR2A	PF3D7_1328800	Involved in telomere maintenance and
PfSIR2B	(PF13_0152) PF3D7_1451400	regulation of var gene expression

	(PF14_0489)	
PfHDAC1	PF3D7_0925700 (PFI1260c)	Putative class I histone deacetylase, probable ortholog of Rpd3 from yeast
PfHDAC2	PF3D7_1472200 (PF14_0690)	Putative class II histone deacetylase
PfHDAC3 (PfHda2)	PF3D7_1008000 (PF10_0078)	Putative class II histone deacetylase, linked to var gene silencing and sexual differentiation
Other		
PfBDP1	PF3D7_1033700 (PF10_0328)	Bromodomain protein 1, involved in the regulation of genes linked to erythrocyte invasion
PfHP1	PF3D7_1220900 (PFL1005c)	Heterochromatin protein 1, involved in the maintenance of silenced regions of the genome, linked to var gene silencing and sexual differentiation

Both current 3D7 ID numbers and previous numbers are provided, along with a brief, general description of the predicted function. Many of the listed functions are predicted based on computational analysis and have not been experimentally verified. Several additional uncharacterized putative epigenetic factors have been predicted by in silico analysis [565].

4.3 Malarial Histone-modifying Enzymes

There are several classes of histone-modifying enzymes influencing chromatin structure via histone PTMs that were recently studied in *P. falciparum*. These include (i) modifiers of histone acetylation: HATs and HDAC); and (ii) modifiers of histone methylation: HMTs and HDMs (Table 4.2).

4.3.1 Modifiers of histone acetylation

4.3.1.1 *Plasmodium* HATs

Histone acetylation is usually associated with transcriptionally active genomic regions through direct alterations of physical properties of the chromatin and/or recruitment of specialized protein complexes that regulate transcription directly or indirectly [566]. In particular, acetylation of nucleosomes around the TSSs stabilizes binding of transcription-modulating chromatin remodeling factors at the promoter regions [567]. Histone lysine acetylation is catalyzed by histone acetyltransferase (HATs). At least four HATs are found in malaria parasite genomes: PF08_0034, PF11_0192, PFL1345c and PFD0795w [568]. *Plasmodium falciparum* GCN5 N acetyltransferase 5 (*PfGCN5*), a well characterized member of GNAT family has most homologous region within HAT domain and bromodomain in *Plasmodium* species [500]. *PfGCN5* (PF08_0034), in association with its coactivator ADA2 [569], acetylates H3K9 and H3K14 residues in *P. falciparum* [500, 569], implicating that its

active role in chromatin remodeling and regulation of transcription in *P. falciparum* [569]. By contrast, *PfMYST* exhibits a predilection to acetylate histone H4 at K5, K8, K12 and K16 [531]. Both proteins seem to be essential for asexual intraerythrocytic growth, and *PfGCN5* inhibition leads to the arrest of parasite development, while *PfMYST* overexpression leads to the disruption of cell cycle regulation and DNA repair [531, 570].

4.3.1.2 *Plasmodium* HDACs

In contrast, HDACs mediate removal of acetyl groups that generally leads to tight internucleosomal interactions limiting the access of DNA to transcription factors. The HDAC superfamily is grouped into three classes based on their phylogenetic relationship to the yeast orthologues. Class I (Rpd3) and class II (Hda1) have a zinc-dependent HDAC activity and act on intra-chromosomal domains [571], while class III HDACs (Sir2) are NAD-dependent and mediate gene silencing at the subtelomeres as well as the mating-type and rDNA loci [572-573]). Five HDAC encoding genes have been identified in the *Plasmodium falciparum* genome. Three of these genes encode proteins with homology to class I (*PfHDAC1*) or class-II (*PfHDAC2* and 3) mammalian HDACs, while two genes are class-III HDAC homologues (*PfSir2A* and *PfSir2B*) [264, 397, 512, 574-576].

PfHDAC1 is localized in the parasite nucleus, has up to ~ 55% sequence identity to other eukaryotic class-I HDACs and is expressed/transcribed across multiple lifecycle stages of the parasite (asexual intraerythrocytic parasites, gametocytes, and sporozoites) [397, 422, 574-575, 577]. Despite the *PfHDAC1* functional roles have still to be fully characterized, the consequences of the HDACi treatment of *P. falciparum* parasites have recently begun to be elucidated and confirm that *PfHDAC1* is involved in the post-translational modification of histone and non-histone *Plasmodium* proteins, in the consequent modulation of its gene expression, and seems also important for the parasites survival [550, 574-575, 578-580]. *In silico* homology modeling studies of *PfHDAC1* have shown that the predicted active site tunnel of *PfHDAC1* is highly conserved with that of human HDACs, but displays differences at its entrance that could explain the better *in vitro* growth inhibition of *P. falciparum* compared with mammalian cells that has been observed with several HDACi [264, 397, 574-575] and could also be more efficiently exploited by novel HDACi tailored to be selective for *PfHDAC1* over hHDACs [264, 397, 422, 574-575, 577-579].

The *PfHDAC2* regulates virulence gene expression and frequency of gametocyte conversion [512]. Thus, *PfHDAC2* is part of the epigenetic machinery that controls the

expression of *var* genes and of the master regulator of sexual development — the transcription factor PfAP2G [509, 512]. PfHdA2 is proposed to control histone PTMs within the heterochromatin domain as its knockdown leads to deregulation of the *var* genes and increased conversion to gametocytes. The latter event is likely caused by upregulation of the PfAP2-G transcription factor that resides in a heterochromatin domain and is believed to function as a “master regulator” of the sexual stage commitment. Both PfHDAC2 and PfHDAC3 are predicted to be high molecular weight proteins, that share less than 14 % amino acid identity to each other, and have limited sequence homology with other class II HDACs [422, 512, 576-577]. Recently, by the mean of knock-down experiments, PfHDAC3 has been reported to be essential to the asexual-stage *P. falciparum* parasite growth and survival, and to play a role in *P. falciparum* transcriptional control [512].

4.3.1.3 Plasmodium Sirtuins

Sir2 is an NAD⁺-dependent HDAC (or sirtuin) that was first identified in yeast as important for silencing telomeric genes. Since NAD⁺ is a key cofactor and metabolite, Sir2 may act as a sensor for environmental or nutrient changes. In *Plasmodium*, there are two Sir2 orthologs, PfSir2A and PfSir2B [528] that work in concert to regulate *var* silencing. Plasmodium parasites that lack PfSir2A and B are unable to effectively silence undesired *var* genes, and transcript levels of *var* genes are generally elevated [528, 581].

PfSir2A and PfSir2B have been assigned as type III and IV sirtuins since they have 30% and 38% sequence identity to an *Archaeoglobus fulgidus* class-III HDAC and group IV sirtuins, respectively [528, 582]. In addition to both histone deacetylase and ADP-ribosyltransferase activity [582-583], PfSir2A is also able to effectively remove medium and long chain fatty acyl groups from lysine residues [584]. PfSir2A has a role in maintaining *P. falciparum* telomere length, in establishing heterochromatin in subtelomeric genomic regions, and in the regulation of a subset of *P. falciparum* virulence genes involved in antigenic variation and cytoadhesion/pathogenesis [528, 550]. Recently, a new role has been reported for PfSir2A in modulating rRNA transcription [585]. Using a parasite line in which PfSir2A has been disrupted, it was observed that histones near the transcription start sites of all rRNA genes are hyperacetylated and that transcription of rRNA genes is upregulated, which are linked to higher numbers of daughter merozoites and increased parasite multiplication rate. More in detail, both PfSir2A and PfSir2B are involved in the mutually exclusive silencing (or expression) of different telomeric-associated *var* gene subsets, with distinct promoter types, that encode

for the parasite-derived *P. falciparum* erythrocyte membrane protein 1 (PfEMP1) molecules that are displayed on the erythrocyte surface [528, 550]. The resulting antigenic variation of PfEMP1 accounts for the ability of *P. falciparum* to evade the host immune surveillance during infection.⁷⁶ Apart from virulence genes, PfSir2A also deacetylates rRNA genes and regulates the multiplication rate in *P. falciparum* [585]. Moreover, PfSir2B has been also found to have a role in the telomeric end protection [528]. Knock-out of the two *P. falciparum* Sir2 genes has shown that the absence of either one of them is not lethal to the parasite, and also established their functional redundancy in the parasite [528]. However, to the best of our knowledge, the effect of a simultaneous knock-out of both PfSir2 genes has not been examined yet. Despite both PfSir2A and PfSir2B seem to dispensable for the *in vitro* growth and development of *P. falciparum* [550, 576], both of them, for their crucial role in regulating *var* genes expression, are thought to be essential for the persistence parasite survival *in vivo* (or inside a host), and have been proposed as potential targets for antimalarial therapies, for example by interfering with infected erythrocyte cytoadhesion to host cell receptors that mediate severe forms of the diseases and/or by blocking the malarial parasite's evasion from the host innate immune system [528, 550]. In other *Plasmodium* species, even though no *var* genes have been identified, other sub-telomeric gene families able to undergo antigenic switching have been disclosed, suggesting the possible involvement of their sirtuins (Sir2A and Sir2B) in the mutually exclusive silencing (or expression) of these sub-telomeric genes [528].

4.3.2 Modifiers of Histone Methylation

Histone methylation, either in lysine or arginine residues, mediated by histone lysine methyltransferases (HKMT) or protein arginine methyltransferases (PRMT), is involved in both transcriptional activation and silencing [586]. Bioinformatics analysis of *P. falciparum* genome reveals at least ten members of histone methyltransferases (HMTs) containing a SET [Su(var), E(z), Trithorax] domain, characteristic of histone lysine methyl transferases and five putative PRMTs [587]. During the IDC, PfSET1, PfSET2, PfSET3 and PfSET8 mediate methylations at H3K4, H3K36, H3K9 and H4K20, respectively [557, 588]. An unusual function has been revealed for PfSET2, which methylates H3K36 and is associated with repressive chromatin of the *var* multigene family (in other eukaryotes, SET2 is associated with RNA polymerase II function) [529]. PfSET8 displays conserved activity to confer H4K20 mono-, di-, and trimethylation [557, 588]. The H3K9 methylase PfSET3 (PF08_0012) is encoded by an essential

gene and is localized to the heterochromatic nuclear periphery marked by CenH3, and H3K9me3-enriched genes also reside in this compartment [489, 589]. PfSET7 methylates H3K4 and H3K9, and localizes to distinct foci outside of the parasite nucleus in erythrocytic and liver stages, and throughout the cytoplasm in sporozoites [590]. This cytoplasmic localization hints that pfSET7 might be acting on newly synthesized histones and/or additional non-histone substrates. PfSET7 is presumed to be essential for both the blood and mosquito stages of parasite development and thus may be amenable as a potent drug target. PfSET10, which methylates H3K4, colocalizes with the active var gene in post-ring stages, suggesting a role for PfSET10 in maintaining the active var gene in a poised state during mature stage 55. In contrast, Dot1, the HKMT without a SET domain, is absent in apicomplexans. The presence of corresponding epigenetic mark H3K79 methylation in *P. falciparum* is controversial as it was not seen by mass spectrometry [537, 588], but it has been shown to be localized to the nuclear periphery [591]. The SET subfamily E(z) and the corresponding mark H3K27me are also not reported in *P. falciparum* [537, 588]. Among, the PRMTs, only PfPRMT1/ PfCARM1 has been characterized. PfPRMT1 localizes to the nucleus and cytoplasm of intraerythrocytic parasites and catalyzes mono- and di-methylation of R3 of histone H4, as well as non-histone protein substrates [587].

The malaria parasite genome also contains two types of histone demethylases (HDMs), the lysine specific demethylases (LSD1) and JmjC (jumionji C) domain containing histone demethylases (JHDMs). There are at least one LSD1 (PFL0575w) and two JHDMs (MAL8P1.111 and PFF0135w) in *Plasmodium* [592]. Knockout of the corresponding genes showed that these genes are not essential in blood-stage parasites [529]. The role of histone methylation in gene regulation and maintenance of the subtelomeric heterochromatin needs to be explored further in *P. falciparum*.

4.3.3 Consequences of Histone Modifications: “Histone Readers” in Malaria

It is now clear that both heterochromatin and euchromatin carry multiple types of epigenetic “modules” that are characterized by distinct combinations of histone PTMs. For transcriptional regulation, these must be interpreted by downstream factors known as “histone readers” [565, 593]. Many histone PTMs exert their function by recruiting specific proteins called histone readers, which contain functional domains that bind to acetylated lysine residues (bromodomains), methylated lysine residues (chromodomains and plant homeodomains (PHDs)) or phosphorylated serine and threonine residues (14-3-3 proteins)

(Fig. 4.2) [120, 199, 429, 480, 593-594]. *P. falciparum* has more than 15 predicted proteins containing such binding domains [479, 565, 589], and two of them have been validated as specific histone readers: the structural protein heterochromatin protein 1 (PfHP1) and a 14-3-3 protein. Specifically, PfGCN5 (HAT) and PfSET1 (HKMT) carry a single bromodomain, and PfMYST and heterochromatin protein 1 (PfHP1) possess one chromodomain. In addition to bromodomain, PfSET1 also possesses four PHD domains, suggesting that PfSET1 is targeting the euchromatic regions that are marked with histone acetylations and H3K4 methylations [588]. Despite the great number of potential histone PTM-binding modules in *Plasmodium*, only PfHP1 has been characterized [511, 524]. PfHP1 contains a chromodomain and a chromo-shadow domain, which are involved in H3K9me3 binding and dimerization, respectively. Inducible PfHP1 depletion leads to *var* gene derepression and gametocyte production, showing that the same histone modification controls monoallelic *var* gene expression and switch to sexual commitment [513], which is similar to the dual effects mediated by the deacetylase PfHDAC2 [512]. PfSIP2, a member of the ApiAP2 family of transcription factors, is associated with PfHP1 [499, 595-596]. A parasite-specific bromodomain protein, PfBDP1, binds at TSSs of invasion-related genes and positively controls their expression [516]. PfBDP1 also binds to acetylated histone H3 and another bromodomain protein, PfBDP2, suggesting a critical coordination during the expression of the invasion genes. PfHP1 is essential for IDC, and overexpression of PfHP1 leads to enhancement of variegated gene expression [511]. The ability of this protein to dimerize is probably responsible for aggregating nucleosomes in the subtelomeric regions and thus for the formation of the subtelomeric heterochromatin.

In addition to the canonical histone readers, *P. falciparum* protein Pf14-3-3I binds selectively to histone H3 phosphorylated on Ser28, suggesting its role in chromatin binding [541]. Taken together, *P. falciparum* contains a number of well conserved as well as unique chromatin binding proteins that are capable of interpreting the histone PTM modules in both heterochromatin and euchromatin. Given the unique character of the *P. falciparum* epigenome, it is feasible to speculate that these proteins evolved to adjust to the highly dynamic character of the unique histone PTM combinations.

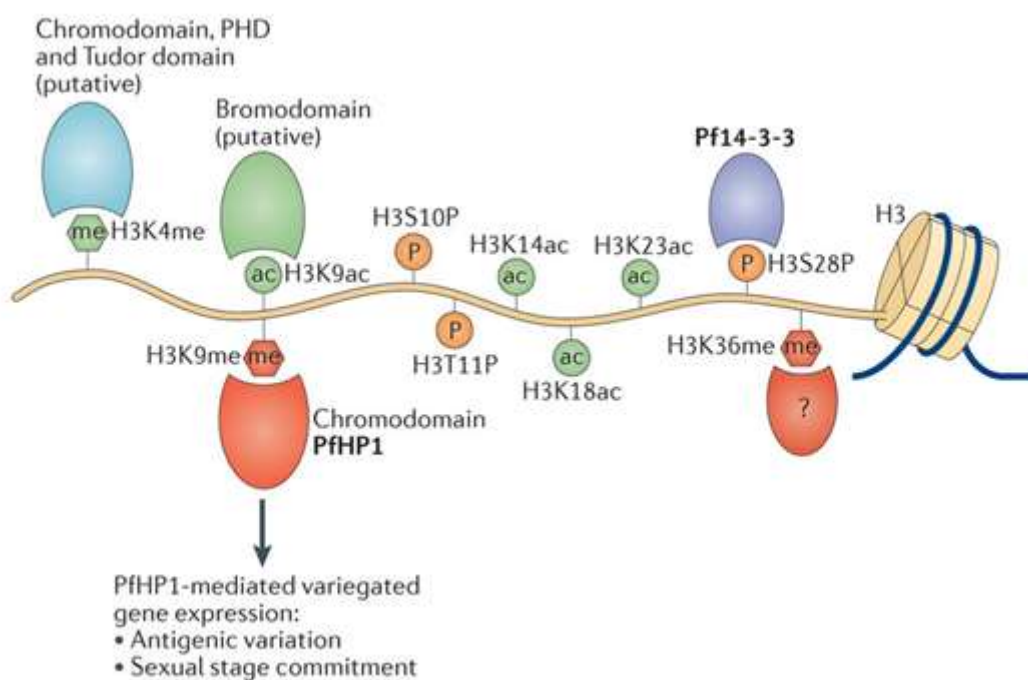


Fig. 4.2: Post-translational modifications (PTMs) and their writers and readers observed in the amino-terminal region of histone H3 of *Plasmodium falciparum* — including methylation (me; on lysine 4 (K4), K9 and K36), acetylation (ac; on K9, K14, K18 and K23) and phosphorylation (P; on serine 10 (S10), threonine 11 (T11) and S28) — are illustrated.

4.4 Antimalarial Epi-drugs

The emergence and spread of malaria drug resistance presents a worrisome situation impacting disease control programs. It is now becoming clear that the (possibly near) future of malaria control will require the introduction of new chemotherapies to overcome this situation. In fact, in the search for promising drugs to combat malaria, inhibitors of chromatin modifying factors have started to obtain attention. The first obvious targets for antimalarial “epidrug” development are the enzymes that add or remove acetyl or methyl groups from histone tails (Table 4.2). Importantly, inhibitors of this type of enzymes have been developed for the fight against other diseases such as cancer, providing a large number of chemical starting points and a wealth of knowledge that could be used for the development of malaria-specific epigenetic inhibitors. Several compounds that were identified as inhibitors of HDACs or HATs in other eukaryotes inhibit *P. falciparum* growth, and some of them have a more potent effect on malaria parasites than on human cells [264, 481, 574, 583, 588, 597]. Inhibitors of *P. falciparum* KMTs have also been identified and shown to effectively kill malaria parasites of different species and at different stages of development [598-599]. In any case, new antimalarial drugs with desirable properties, such as being effective against all parasite stages or requiring a single dose, if available, would certainly facilitate the task. In this regard,

epigenetic regulators are considered a promising new class of drug targets, with some attractive characteristics described below.

4.4.1 Antimalarial HAT Inhibitors

Histone acetylation in the parasite has been shown to regulate the monoallelic expression of the *var* genes, which mediates the antigenic switching and virulence of the parasite [527, 550]. Variegated expression of genes essential for erythrocyte invasion in different parasite clones are under epigenetic control suggesting conserved epigenetic mechanism for transcriptional regulation in malaria parasites [515]. The H3 acetylation by GCN5 plays important role in the parasite gene activation and inactivation of histone acetylation compromises the parasite development suggesting its role for viable drug targets [500, 549, 569]. Parasite growth has been shown to be inhibited by *PfGCN5* HAT inhibitors curcumin (Fig. 4.3) [570]. Reversible and noncompetitive inhibition of *PfGCN5* by Anacardic acid (**1**) treatment induced hypoacetylation at H3K9 and H3K14, causing down-regulation of 207 genes in late trophozoite state [600]. Treatment with Anacardic acid for 12 h induced two-fold or greater changes in the expression of ~5% of genes in *P. falciparum* trophozoites, among which 76% were downregulated [600]. Both curcumin (**2**) and Anacardic acid inhibited the growth of chloroquine resistant and susceptible strains of *P. falciparum* either by generating reactive oxygen species or by down-regulating the HAT activity of *PfGCN5* which introduced disturbances in the regulation of transcription in the parasite [600] [570]. Embelin (**3**) (Fig. 4.3), a HAT inhibitor showed down-regulation of *var* gene expression with hypoacetylation at H3K9 around *var* gene promoters suggesting interplay among histone acetylation status, as well as subnuclear compartmentalization of different genes and their activation in *P. falciparum* [601]. Competitive methylation and acetylation marks at H3K9 in *var* 5' flanking region is reported to epigenetically regulate mono-allelic expression pattern of *var* genes during parasite proliferation through activation or repression [602]. Kumar et al. elucidated, through comparative sequence and structural analysis, differences in the catalytic pocket of *PfGCN5* which can be exploited to design selective inhibitors specific to *PfGCN5* over HsGCN5 [603]. This study reports 20 potential inhibitors of *PfGCN5*, in which 11 were found to be selective to *PfGCN5* over HsGCN5. Compound C14 (**4**) (Fig. 4.3) was validated for its inhibitory action against *PfGCN5* experimentally. *In vitro* parasite growth assay in the presence of C14 showed significantly lower IC₅₀ (225 nM) than the previously known HAT inhibitor like Curcumin, Anacardic acid and Embelin (20 µM, 30 µM and 25 µM, respectively)

in *P. falciparum*, but, no effect in mammalian fibroblast cells was observed for C14 (up to 20 μ M). The authors suggested that C14 could be used as hit to study the effect of GCN5 mediated acetylation in gene expression of *P. falciparum*.

Therefore, the effect of these inhibitors in histone hypoacetylation and downregulation of developmentally regulated genes in the parasite may have great potential for parasite survival and growth.

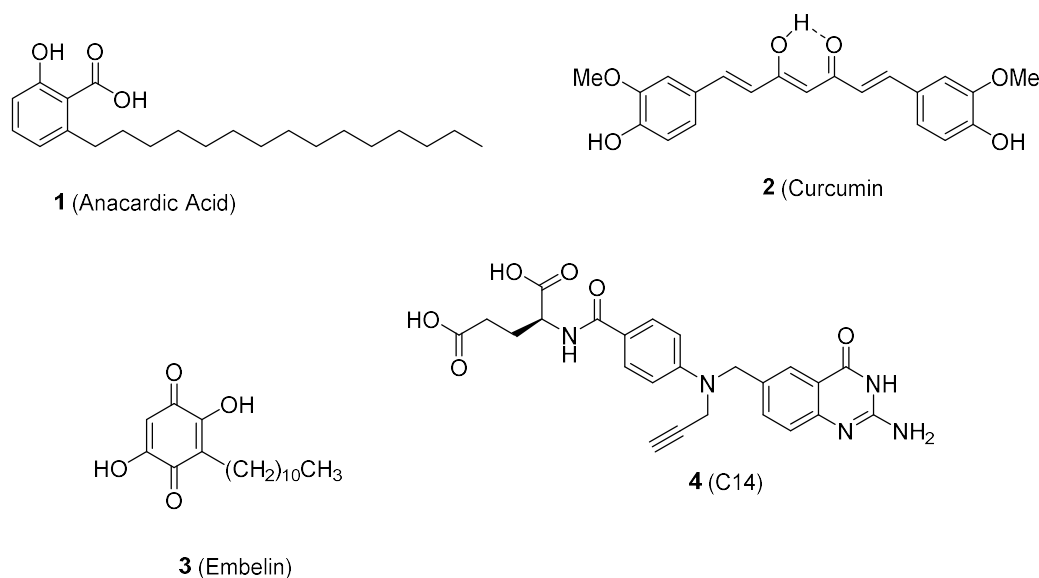


Fig. 4.3: HAT inhibitors potentially active against *Plasmodium falciparum*

4.4.2 Antimalarial HDAC Inhibitors

The potential utility of HDACi as antimalarial agents was first reported two decades ago when the cyclic tetrapeptide **5** (apicidin) was found to potentially target *Plasmodium* and other Apicomplexan parasites [604]. Since then a growing number of studies have focused on the antimalarial activity of HDACi belonging to various structural classes, highlighting the potential of these epigenetic modulators for anti-parasitic intervention.

4.4.2.1 Cyclic Tetrapeptide HDAC Inhibitors

In a pioneering study in 1996, Darkin-Ratray *et al.* disclosed that the natural cyclic tetrapeptide **5** (Table 4.3) is endowed with a potent *in vitro* activity against *P. falciparum* (IC_{50} = 200 nM) and a panel of Apicomplexan parasites (*T. gondii*, *Cr. parvum*, *N. caninum*, *B. jellisoni*, *E. tenella*, etc.) [604]. Subsequent studies showed that **5** is able to induce substantial changes to the *P. falciparum* intra-erythrocytic developmental cycle transcriptional cascade, with ~ 30-60% of the genes showing altered expression [605-606], so resembling the effects of many HDACi, including **5** itself, on higher eukaryotic cells [607-608]. Indeed, **5** causes *in situ* hyperacetylation of *P. falciparum* histones [604] and inhibits the activity of recombinant

PfHDAC1 enzyme in the low nanomolar range ($IC_{50} \sim 1$ nM) [580]. Despite orally (2-20 mg/kg for 3 days) active *in vivo* in a lethal *P. berghei* mouse model of malaria [609], **5** for its poor bioavailability and a substantial lack of selectivity for *P. falciparum*-infected erythrocytes versus mammalian cell lines (Table 4.3) has never been considered suitable for clinical applications. While the structural similarities between one of the side chains of **5** called Aoda (2-amino-8-oxodecanoic acid) and the acetylated histone lysines enable the chelation of the zinc ion at the bottom of the HDAC catalytic tunnel, the other components of the cyclic peptide presumably do not distinguish the flanking amino acid residues that characterize the different entrances to the catalytic active site of the different HDAC isoforms so providing a possible explanation for its inability to selectively inhibit *P. falciparum* over human HDACs [604, 609]. To address the selectivity issue, many analogues of **5** were prepared over the years by Merck Research Laboratories by modifying either its Aoda side chain or its tryptophan moiety, and it was found that the replacement of tryptophan with quinolone/quinoline nuclei led to analogues of **5** showing 50- to >230-fold parasite selectivity over mammalian cells (*e.g.* compound **6**, Table 4.3) [609-612]. Together with a series of synthetic analogues, **5** was also comparatively investigated for inhibitory activity against two *Trypanosoma* species (*T. cruzi* and *T. brucei*), *P. falciparum* and *L. donovani*. Both **5** and its analogues showed potent and nonselective activity toward *T. brucei*, similarly to *P. falciparum*, but revealed to be toxic against *T. cruzi* and *L. donovani* [612]. Recently, the cyclic depsipeptide **7** (romidepsin, also called FK228 in Table 4.3), together with the other three HDACi to date clinically approved as anticancer drugs (see below in the text), was assessed for its *in vitro* activity against drug sensitive (3D7) and drug resistant (Dd2) asexual *P. falciparum* parasites and the bloodstream forms of *T. b brucei*. Parasites [613]. Compound **7** displayed activity in the low nanomolar range against all parasite lines, caused hyperacetylation of both histone and non-histone proteins in *P. falciparum*, and inhibited deacetylase activity of parasite nuclear extracts and recombinant PfHDAC1, but unfortunately exhibited no selectivity over mammalian cells (NFF and HEK293) for both parasites ($SI < 1$) [613].

4.4.2.2 Short-chain Fatty Acid HDAC Inhibitors

Short-chain fatty acid-type HDACi, such as **8** (VPA, Table 4.3), sodium butyrate, 4-phenylbutyrate and related derivatives, despite weak inhibitors of mammalian HDACs, are pretty safe molecules, in one case already approved for some therapeutic indications (*e.g.* **8** is still widely used as antiepileptic and mood-stabilizing drug), that are now undergoing

several trials for HDAC-related diseases, and could be intriguing for repurposing in parasitic diseases [614]. These compounds are active *in vitro* in the (sub)millimolar range against different parasites such as *P. falciparum*, *T. gondii* and *S. mansoni* and suffer from poor selectivity for parasites (especially *P. falciparum*) over mammalian cells [615-617]. To best of our knowledge, compound **8**, despite its anti-parasitic activity *in vitro* falls within the therapeutic range of the compound for its primary use as mood-stabilizing drug, has still to be tested *in vivo* in animal models of any of these parasitic diseases.

4.4.2.3 Hydroxamate-Based HDAC Inhibitors

As in other human diseases such as cancer, HDACi bearing a hydroxamic acid warhead as zinc-binding group (ZBG) are the best studied anti-parasitic HDACi and have shown promising *in vitro* activity profiles against *P. falciparum* and other parasites. Several studies have been devoted to investigate the antimalarial potential of a number of natural and synthetic class-I/II HDACi such as **9** (TSA) [618], suberoylanilide hydroxamic acid **10** (SAHA) [613], suberic bishydroxamate **11** (SBHA) [618], **12** (MW2796) [618] and aroyl-pyrrolylhydroxyamides (APHAs, e.g. **13**), [619] which were among the first hydroxamate-based HDACi tested against several parasites, including *P. falciparum* (Table 4.3) [618] [397, 574-575, 580, 619-620]. These compounds showed inhibitory activities against *P. falciparum* in the range of low/sub micromolar (**10**, **12**, **13**, etc.) to nanomolar (**9**) concentrations, but almost all suffered, despite to a different extent, of poor selectivity versus host cells, with the only exception of **11**, which displayed somewhat better selectivity for the parasite based on mammalian cytotoxicity data. More in detail, the extremely potent compound **9**, despite not suitable for clinical progression for its lack of selectivity, has resulted a highly useful tool to understand how HDAC inhibition affects malarial parasite's growth, development and gene transcription [580, 605, 621]. Indeed, **9** inhibited PfHDAC1 activity in the subnanomolar range ($IC_{50} \sim 0.6$ nM) [580] and, like **5**, caused hyperacetylation of *P. falciparum* histones and large scale genome-wide transcriptional changes in the parasite [605]. Compound **10**, the first HDACi approved for the clinical treatment of cutaneous T-cell lymphoma in humans with the name of vorinostat in 2006, is less potent than **9** against *P. falciparum* parasites *in vitro* (IC_{50} values in the submicromolar range), but displays a somewhat improved parasite selectivity (up to ~ 200 -fold, Table 4.3) [397, 574, 620]. Despite its clinical utility for cancer, the *in vivo* efficacy of **10** against *Plasmodium* parasites in mice models of malaria has still to be evaluated. In contrast, compound **11**, endowed with lower

in vitro potency than **10** against *P. falciparum*, but, depending on the specific cell lines examined, better selectivity for the parasite versus mammalian cells (Table 4.3), has been examined *in vivo* in *P. berghei*-infected BALB/c mice (200 mg/kg, twice daily intra-peritoneally for 3 days) where it showed a cytostatic effect by significantly inhibiting peripheral parasitemia [618]. Despite no mice recovery was observed, these early data about compound **11** suggested that hydroxamate-based HDACi deserved further investigation as potential antimalarial agents [397, 574, 618].

Inspired by the promising initial results, a number of HDACi with better *in vitro* potency against *P. falciparum* parasites than **10** or **11**, and with varying improvements on selectivity, were identified in the subsequent years by screening compounds that, keeping intact the hydroxamic acid as ZBG, showed variations into the three other structural motifs of the general pharmacophoric model for HDAC inhibition: the CAP group that, acting as an enzyme surface recognition moiety, interacts at the entrance of the catalytic tunnel; the linker region that connecting the CAP with the ZBG fits the narrow, hydrophobic, tubular enzyme cavity; and the dispensable polar connection unit (CU) between the CAP and the linker [397, 574-575, 622]. Among them, supported by *in silico* molecular modeling of PfHDAC1 and docking studies, the Fairlie's group reported some *L*-cysteine-based (thioether in the linker region, e.g. **45**) and 2-aminosuberic acid (2-ASA)-based (only methylene groups in the linker region) hydroxamates that showed similar *in vitro* anti-parasitic potency (IC₅₀s in the low nanomolar range) against both CQ-sensitive (3D7) and CQ-resistant (Dd2) *P. falciparum* strains, with the better selectivity generally observed for the 2-ASA compounds (Table 4.3). Among these latter, **15** (2-ASA-9) and **16** (2-ASA-14), in addition to cause a marked hyperacetylation of *P. falciparum* histones, showed the interesting capability to inhibit the *P. falciparum* growth in erythrocytes at both early and late stages of the parasite's life cycle [579]. In one study, **9**, **10** and **15** were profiled for their effects on gene expression in *P. falciparum* parasites. Each compound caused genome-wide transcriptional changes (up to 2-21%), consistent with inhibition of HDAC activity in the parasite. Though the three inhibitors had very different overall effects on gene expression profiles, α -tubulin II was found to be one of the small set of genes up-regulated by all three HDACi and its identification as transcriptional marker induced by structurally different HDACi in *P. falciparum* has been proposed as an important finding since this marker might be utilized for developing HDACi as "specific" antimalarial agents [597]. The ASA compounds **15** and **16**, as well as **10**, were also the first HDACi to be

tested against *P. vivax*, that is the second most important human infecting malaria parasite because, despite not generally responsible of death, is the cause of significant malaria-related morbidity and relapses due to parasite stages that can remain dormant in the liver. All three hydroxamates were able to inhibit the *ex vivo* growth of multi-drug resistant *P. falciparum* and *P. vivax* isolates obtained directly from infected patients [623]. The similar activity profiles obtained for **10**, **15** and **16** against both *P. falciparum* (IC₅₀ 310, 533, and 266 nM, respectively) and *P. vivax* (IC₅₀ 170, 503, and 278 nM, respectively), despite somewhat higher than those reported *in vitro* against laboratory strains, provided the first examples of HDACi targeting multiple human-infecting malaria parasite species, which is nowadays thought to be highly beneficial for clinical applications. Several series of 2-ASA compounds, such as the one containing typical non-steroidal anti-inflammatory (NSAID) components in the CAP region (e.g. **17**, Table 4.3) were tested over the years for their inhibitory activity against *P. falciparum*, but although many compounds displayed an extremely potent activity against *P. falciparum* (IC₅₀s in the low nanomolar range), it was substantially impossible to get significant improvements of parasite selectivity in comparison to **15** (Table 4.3) [624].

In 2009, Patel *et al.* screened in a high-throughput viability assay the antimalarial efficacy of a library of ~ 2000 HDACi characterized by an acyl hydrazone moiety as CU and with chemical diversity in the recognition CAP, the ZBG, and the hydrophobic linker length (4-6 methylene units). Although many compounds potently inhibited *P. falciparum* parasite growth and recombinant PfHDAC1 activity, only 17 derivatives demonstrated anti-parasitic activity in the low nanomolar range coupled with minimum perturbation of mammalian cell (human myeloma MM.1S cells) histone acetylation, that was used as an indicator of selectivity. Within this series, the selective inhibition of *P. falciparum* proliferation was highly favored by the presence of *ortho*-substituents (mainly bromine and hydroxyl) in the CAP aromatic group, of a hydroxamic acid as metal chelator, and of a linker of five methylene units (e.g **18**, Table 4.3) [580].

In the same period, Kozikowski and collaborators reported two series of suberoylamide hydroxamates bearing substituted triazolyphenyl and phenylthiazolyl (WR compounds) moieties as CAP groups. Among the triazolyphenyl-based HDACi, compound **19**, endowed with an activity in the low nanomolar range (Table 4.3), resulted one order-fold more potent than most of the other congeners and more active than mefloquine and chloroquine against the multiple drug-resistant *P. falciparum* strains C235 and C2A, but in the best case was only

~ 23 fold more selective for C235 over mammalian cells [625]. Interestingly, in a panel of 50 phenylthiazolyl hydroxamate-based HDACi, were identified three very potent compounds ($IC_{50} < 3$ nM) with more than 600-fold selectivity toward *P. falciparum* compared to human cells. The most promising HDACi from this set resulted the derivative **20** (WR301801), that exhibited IC_{50} values in the (sub)nanomolar range against several drug-resistant strains (D6, W2, C235 and C2A) of *P. falciparum* (Table 4.3), with a significant inhibition of HDAC activity in *P. falciparum* nuclear extracts ($IC_{50} \sim 10$ nM), and a strong hyperacetylation of parasite histones *in situ* [620]. In one study, **20** caused a significant suppression of parasitemia but did not cure *P. berghei*-infected mice when administered orally as monotherapy at doses of up to 640 mg/kg, while some, but not all, mice were cured when it was combined with sub-curative doses of CQ (52 mg/kg of **20** plus 64 mg/kg of CQ) [620]. Likewise, oral administration of **20** (32 mg/kg/day for 3 days) to *P. falciparum*-infected *Aotus* monkeys resulted in parasite suppression but not eradication [620]. In another study, **20** improved survival and completely and irreversibly suppressed parasitemia in *P. berghei*-infected mice when given by intra-peritoneal injection at a dose of 50 mg/kg/day for 4 days, with an experimental follow up period of 6 weeks [626]. Despite the optimization of the pharmacokinetic properties of **20** seems highly desirable since it is rapidly hydrolyzed both *in vitro* and *in vivo* to its corresponding inactive carboxylic acid, these findings clearly demonstrate the potential of HDACi in mono- and/or combination therapy for the treatment of malaria [620, 626].

In 2010, a series of aryltriazolyl hydroxamate-based HDACi was tested by Oyeleré's team for their inhibitory activity against promastigote stages of *L. donovani* and asexual *P. falciparum* blood-stage parasites [627]. Under the tested conditions, several compounds achieved better inhibitory activity (IC_{50} s in the nanomolar range) and selectivity than **10** against *P. falciparum* growth (D6 and W2 strains). Despite less active than against *P. falciparum*, some compounds possessed also modest inhibitory potency versus *L. donovani*, with IC_{50} values from 2- to 4-fold better than those of compound **10** and comparable to miltefosine, the standard oral drug for the treatment of visceral leishmaniasis. Notably, the anti-parasitic activity was dependent on the length of polymethylene linker and the nature of the CAP group. For any given CAP moiety, the activity against both parasites was maximal in analogues with 5 or 6 methylene units in the spacer region between the CAP and the ZBG. Indeed, compounds **21** and **22** (Table 4.3), characterized by a 3'-biphenyltriazolyl moiety as CAP and by a 6 and 5 methylene units linker, respectively, displayed the best activity and

selectivity against *P. falciparum*, with **22** that resulted also the most active against *L. donovani* ($IC_{50} \sim 32 \mu M$) [627]. Oyelere and collaborators also investigated the antimalarial and antileishmanial activity of five tricyclic ketolide-based phenyltriazolyl HDACi [628]. Under the tested conditions, the optimal length of the linker between the CAP and the hydroxamic acid was of 6 methylene units for the best antimalarial activity that also mirrored the most potent PfHDAC1 inhibition (**23a**), while of 9 methylene units for the best antileishmanial activity that did not correlate with the PfHDAC1 inhibition (**23b**) [628]. More in detail, compound **23a** showed IC_{50} values against both CQ-sensitive (D6) and CQ-resistant (W2) *P. falciparum* strains from 7- to 10-fold lower than those of compound **10**, resulted up to 10-fold more selective over mammalian cells (Vero) compared to it (Table 4.3), and was devoid of antileishmanial activity, while compound **23b** showed an activity against *L. donovani* ($IC_{50} \sim 5 \mu M$) 16-fold stronger than **10** ($IC_{50} \sim 81 \mu M$) together with modest antimalarial effects (Table 4.3) [628]. The same group also reported the antimalarial and antileishmanial activities of HDACi characterized by nonpeptide macrocyclic skeletons derived from 14- and 15-membered macrolides linked to a phenyltriazolyl moiety as large recognition CAP groups. All compounds inhibited the proliferation of both CQ-sensitive (D6 clone) and CQ-resistant (W2 clone) strains of *P. falciparum* with IC_{50} values in the (sub)micromolar range [629]. For both macrolide skeletons, the maximum activity and selectivity against *P. falciparum* was achieved with 6 methylene units in the linker group separating the triazole ring of the CAP group from the active-site zinc binding hydroxamate, accordingly to previous reports [627-628]. The best among these compounds resulted the derivative **24** (Table 4.3), that is characterized by a 15-membered macrolide skeleton, showed the highest anti PfHDAC1 activity ($IC_{50} = 29 nM$) and exhibited up to 11-fold more potent antiplasmodial activity and up to 14-fold increased selectivity over mammalian cells (Vero) in comparison to **10**. Interestingly, for both macrolide skeletons, compounds with 5 to 7 methylene units at the linker group were devoid of activity against the promastigote stage of *L. donovani*, while maximum activity was obtained for those compounds having either 8 or 9 methylene units [629], as in the case of ketolide-based HDACi [628], but differently from SAR observed in aryltriazolyl hydroxamates [627]. In particular, compound **25** (Table 4.3), that contains a 14-membered macrolide skeleton and a 9 methylene units linker, was up to 25-fold more active than **10** ($IC_{50} \sim 81 \mu M$), displaying the

maximum antileishmanial activity with IC₅₀ values of 3.2 and 4.7 μ M against the promastigote and amastigote stages of the parasite, respectively [629].

In 2012, Andrews and coworkers reported the *in vitro* and *in vivo* antiparasmodial activities of the orally active anticancer HDACi **26** (pracinostat, also indicated as SB939). Compound **26** potently inhibited the growth of *P. falciparum* asexual-stage parasites in human erythrocytes *in vitro* (IC₅₀s in the nanomolar range), causing hyperacetylation of parasite histone and non-histone proteins and showing selectivity indexes over mammalian cells ranging from 4 to > 1250, depending on the different tested cell lines (Table 4.3) [630]. In addition to a promising additive effect *in vitro* in combination with the antimalarial protease inhibitor lopinavir, **26** offered the first evidence of HDACi as liver-stage antimalarial drug leads. Indeed, **26**, as well as **10**, displayed a potent inhibition of the *in vitro* growth of exo-erythrocytic-stage *P. berghei* ANKA mouse malaria parasites within HepG2 human hepatocytes (IC₅₀ ~ 150 nM) [630]. Finally, orally administrated compound **26** was found to be effective *in vivo* by reducing both peripheral parasitemia and total parasite burden at doses of up to 100mg/kg/day in the *P. berghei* ANKA mouse model of malaria. Despite mice were not cured, treatment with **26** prevented the development of experimental cerebral malaria-like symptoms, and mice did not develop hyperparasitemia until 2-3 weeks after the interruption of the treatment.

Subsequently, a panel of 21 HDACi characterized by a pentyloxyamide connection unit/linker moiety and by a substituted benzene ring as CAP were tested by the same group *in vitro* for their effects against different *Plasmodium* life cycle stages: asexual blood stage of *P. falciparum* (3D7 line); tissue schizontocidal stage of *P. berghei* (exo-erythrocytic forms cultured in HepG2 human liver cells); and late stage (IV and V) *P. falciparum* gametocytes. All compounds displayed activity (IC₅₀ values in the range of 0.09-1.12 μ M) against the asexual form of *P. falciparum*, with the potency and selectivity increasing along with the bulkiness of the alkyl/alkoxy substituents at the *para* position of the phenyl ring, as exemplified by the most active compound **27a** (Table 4.3). Three derivatives revealed nanomolar activity against all three life cycle stages (e.g. **27b**, Table 4.3), and several compounds showed an improved parasite selectivity compared to **11** for at least the asexual and exo-erythrocytic life cycle stages (e.g. **27c**, Table 4.3) [631]. The same team also reported the antimalarial activity and a structure-activity relationship investigation of a series of related alkoxyurea-based HDACi [632-633]. Several compounds were active at (sub)micromolar level against the 3D7 line of *P. falciparum* [632], and some of them also displayed early/late stage gametocytocidal activity

in the single digit micromolar range (IC_{50} = 1.68-6.65 μ M) [632-633]. The SAR studies revealed that the hydroxamic acid as ZBG and a linker of 5 methylene units were crucial for the antiplasmodial activity. Indeed, alternative ZBGs such as *N*-methylhydroxamic acid, *o*-hydroxyanilide and *o*-aminoanilide were inactive, and chain-shortened analogues (less than 5 methylene units at the linker) exhibited lower potency. Also in this series, bulky alkyl/alkoxy substituents at the 4-position of the phenyl CAP group, and its replacement with bulky aromatic rings led to the most potent and selective compounds against both asexual and gametocyte *P. falciparum* forms, as exemplified by the 4-*tert*-butyl derivative **28** and the 1-naphthyl derivative **29**, that anyway both resulted not better than **10** in terms of potency while, under the tested conditions, compound **29** was more parasite selective than **10** in its asexual stage and late-stage gametocyte killing activity (Table 4.3).

In 2015, Giannini *et al.* assessed the potential anti-parasitic (*P. falciparum*, *L. donovani*, *T. cruzi*, *T. brucei*, *G. lamblia*) efficacy and SAR of a few **10** analogues characterized by the substitution with β/γ lactam-carboxamides at the position α of the anilide CU and with (trifluoro)methyl groups in the *meta* position of the phenyl ring CAP, as well as by an hydroxamic acid or a thiol function as ZBG [634]. Remarkably, all hydroxamates showed a potency comparable with CQ (3-23 versus 6 nM) and slightly better than **10** (3-23 versus 25 nM) against *P. falciparum*, the most sensitive parasite, and were highly selective for *P. falciparum* over mammalian L6 cells (SIs = 205-3953), while the thio derivatives, both the free and the pro-drug, exhibited poor anti-parasitic activity. It can be pointed out that a hydroxamate as ZBG, a γ -lactam carboxamide in α to the anilide CU, and a methyl or trifluoromethyl substituent in the *meta* phenyl ring position associate with an enhanced anti-parasitic activity (at least toward *P. falciparum* and, to a lesser extent, *T. cruzi* and *brucei* species), though the phenyl modifications are also responsible of an increased cytotoxicity and reduced selectivity over mammalian cells [634]. Indeed, in a preliminary test *in vivo* the best results in a *P. berghei* mouse model of malaria were obtained with the unsubstituted phenyl derivative **30**, that was the most selective *in vitro* (Table 4.3) and that inhibited ~ 88% of the *Plasmodium* development versus 99.8% of dihydroartemisinin.

In 2015, as already above mentioned, Andrews and coworkers reported the *in vitro* activity against *P. falciparum* (Table 4.3) and *T. b. brucei* parasites of all four HDACi clinically approved for the treatment of cancer [**7**, **10**, **31** (belinostat), and **32** (panobinostat)] up to now [613]. All compounds inhibited the growth of asexual-stage *P. falciparum* parasites with

nanomolar potencies (Table 4.3), while only **7** was active at nanomolar level against the bloodstream form *T. b. brucei* ($IC_{50} = 35$ nM), despite devoid of any selectivity over mammalian cells. The four HDACi also inhibited the deacetylase activity of *P. falciparum* nuclear extracts and of recombinant PfHDAC1 and caused hyperacetylation of (non)histone proteins, differentially affecting the acetylation profiles of histones H3 and H4, but no one, with the exception of **10** and, to a lesser extent, of **31**, displayed some selectivity for malaria parasites over mammalian cells (NFF and HEK293) [613].

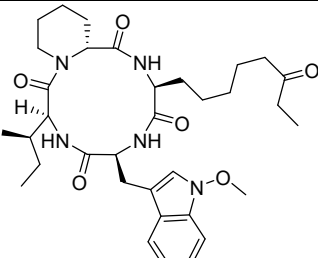
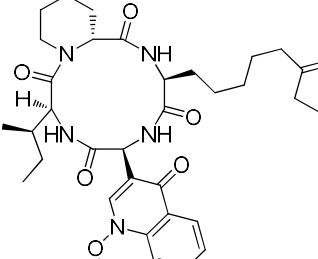
4.4.2.4 Thiol-based HDAC Inhibitors

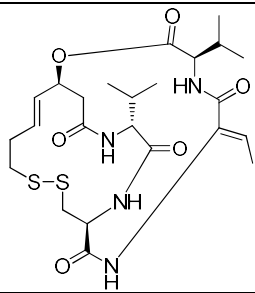
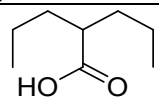
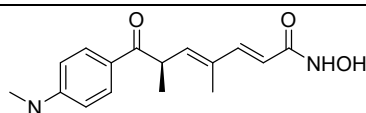
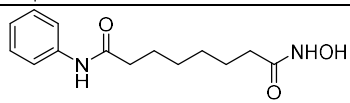
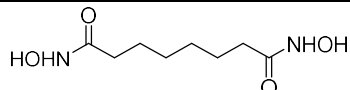
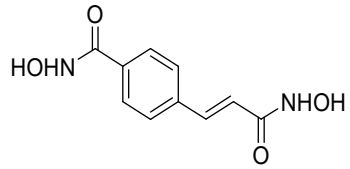
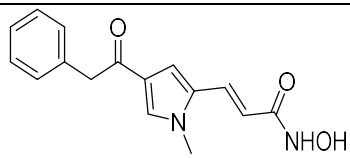
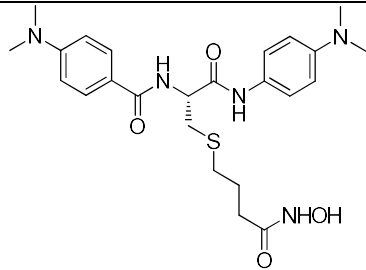
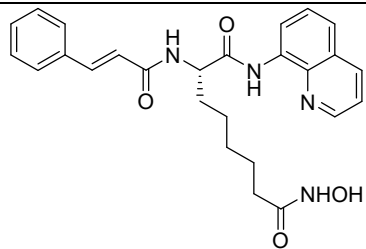
The thiol-based HDAC6 (class IIb) selective inhibitor **33** [635], when tested against CQ-sensitive (3D7) and CQ-resistant (Dd2) *P. falciparum* strains, resulted only poorly active (IC_{50} s in the micromolar range) in inhibiting the proliferation of the parasite (Table 4.3), so providing a further evidence of the necessity to focus on hydroxamate-based and likely on pan-HDACi as potential antimalarial agents [579].

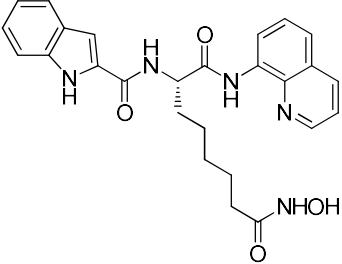
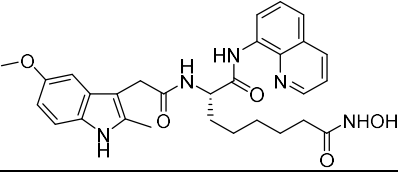
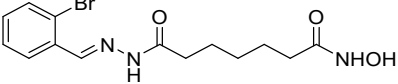
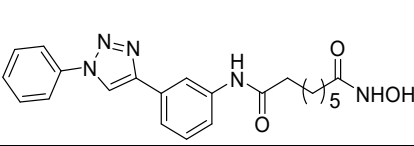
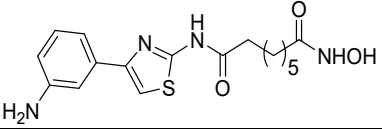
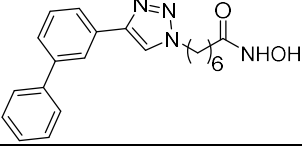
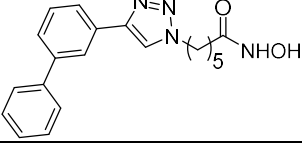
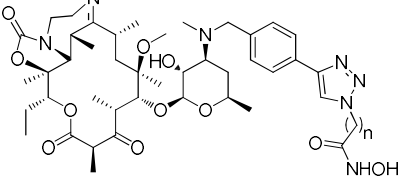
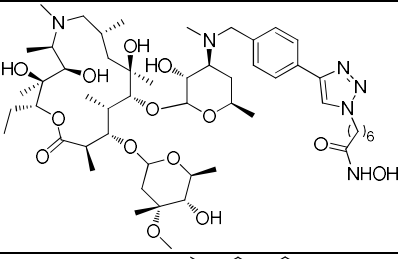
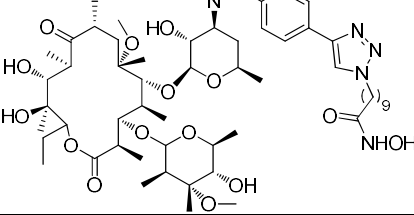
4.4.2.5 Ortho-Amino-Anilides HDAC Inhibitors

The same conclusions can be drawn by considering the series of HDACi containing an *ortho*-aminoanilide moiety as ZBG. The prototype of these HDACi is the class-I HDAC selective inhibitor **34** (MS275, entinostat) [622, 636-637], that in multiple screening over the years has always resulted a modest inhibitor of both PfHDAC1 and parasite proliferation with IC_{50} values of 0.94 μ M and ~ 8 μ M, respectively [264, 397, 574-575, 579-580].

Table 4.3: *In vitro* Antimalarial Activity of Selected Class-I/II HDAC Inhibitors

Class/ Inhibitor	Structure	Nuclear extract [rPfHDAC1] ^a IC_{50} (nM)	<i>P. falciparum</i> IC_{50} (μ M)	Mammalia n cells IC_{50} (μ M)	SI ^b
5 (Apicidin)		NA [1 \pm 0.1]	0.200	0.05-0.1	0.2- 0.5
6		NA	0.063	>15	>238

7 (Romidepsin, FK228)		0.9±0.8 [48±39% @1μM]	0.09-0.13	0.001- <0.005	<1
Short-Chain Fatty Acids					
8 (Valproic acid, VPA)		NA	>100	1350	NA
Hydroxamic Acids					
9 (TSA)		NA [0.6±0.1]	0.008-0.120	0.2-0.3	2-38
10 (SAHA, Vorinostat)		NA [59±6]	0.025-2.2	0.26-20	0-200
11 (SBHA)		NA	0.8-2.3	50-300	22-375
12 (MW2796)		NA	0.9-1.1	NA	NA
13 (APHA-7)		NA	1.2-4	>20	5-17
14		NA	0.048	0.6	12
15 (2-ASA-9)		NA	0.015-0.039	1.24	30-83

16 (2-ASA-14)		NA	0.013-0.033	0.34	10-26
17		NA	0.013	0.26	20
18		NA [37]	0.015	NA	NA
19		NA	0.017-0.035	0.02-0.8	0.6- 22.8
20 (WR301801)		1-10 [NA]	0.0006-0.0016	0.6	400- 1016
21		NA	0.069	NC	>190. 4
22		NA	0.074-0.107	NC	>127 (>183)
23a (n=6)		NA [10±0.5]	0.144-0.148	>5.2	>36 (>35)
23b (n=9)		NA [304±17]	0.93-1.24	>5	>5.4 (>4)
24		NA [29±0.9]	0.094-0.226	NC	>20.7 (>47.6)
25		NA [401±19.7]	0.76-1.32	NC	>3.4 (>6)

26 (Pracinostat, SB939)		NA	0.08-0.15	0.8->100	4- >1250
27	<div> </div> <div> <p>a. R = 4-<i>t</i>-Bu-Ph [68.6±1.2% @1μM]</p> <p>b. R = 3,4-CH₃-Ph [82.6±4.2% @1μM]</p> <p>c. R = 4-BuO-Ph [72.1±5% @1μM]</p> </div>				
28		NA	0.16 (3.45) ^c	4.9	31 (2) ^c
29		NA	0.25-0.32 (2.12-2.25) ^c	19.5	36-78 (9) ^c
30		NA	0.019	75.1	>3950
31 (Belinostat)		214.7±15.3 [78.5±4.7% @1μM]	0.06-0.13	1.4-2.4	11-40
32 (Panobinostat)		3.3±0.7 [100±0% @1μM]	0.01-0.03	0.07-0.18	2-18
33		NA	15.2-19.9	NA	NA
34 (MS275, Entinostat)		NA [940±90]	7.8-8.3	>20	~2.5

^a Deacetylase activity tested using either *P. falciparum* nuclear lysates (no brackets) or recombinant PfHDAC1[brackets]; ^bSI: Selectivity Index - fold difference between mammalian cell and *P. falciparum* IC₅₀ values (IC₅₀ mammalian cells/IC₅₀ *P. falciparum*); ^c Relative to gametocytocidal activity; NA: data not available; NC: no cytotoxicity at the maximum tested concentration.

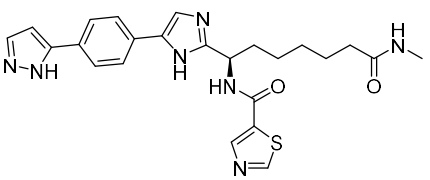
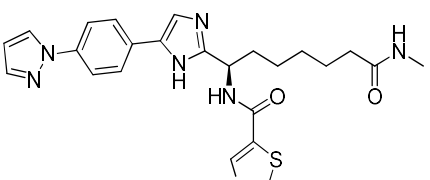
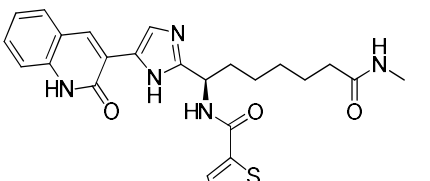
4.4.2.6 Other Amides as HDAC Inhibitors

Very recently, Ontoria *et al.*, in addition to cast doubts on PfHDAC1 inhibition data reported in literature so far, described an innovative screening approach that led to the identification of a novel series of *P. falciparum* growth inhibitors claimed as selective PfHDACi

and characterized by a secondary amide as ZBG, an examethylene chain as linker and two groups such as an (hetero)aryl substituted imidazole ring and a 2-thiazolylcarboxamide as surface contact CAP moieties. Some derivatives in the series showed submicromolar inhibition of *P. falciparum* proliferation ($EC_{50} < 500$ nM) with only a modest inhibition of human class I HDACs in HeLa cells (IC_{50} values in the micromolar range), used as an indicator of selectivity [638]. Both activity and selectivity were strongly influenced by the nature of the (hetero)aryl substituent attached to the imidazole core. Although clear SAR trends were difficult to identify, compounds based on phenyl-/ biphenyl-/ benzimidazole- or benzotriazole- substituted imidazoles were either weak or poorly selective inhibitors of parasite growth. Conversely, analogues bearing indole-, indazole-, isoquinoline- and mainly pyrazolylphenyl- (**35** and **36**) or quinoline-substituted (**37**) imidazoles turned out to show the best activity and selectivity for the parasite (Table 4.4) [638]. Support for the selective PfHDACs inhibition as the mechanism of action of these compounds was provided by the evidence that compound **35**, one the most potent and selective ($SI = 37$) of the series, induced the hyperacetylation of the histone H4K8 in parasite cells at a concentration ($EC_{50} = 350$ nM) quite close to the potency measured in the parasite growth inhibition assay ($EC_{50} = 450$ nM) and quite far from the concentration necessary to inhibit recombinant ($EC_{50} > 5$ μ M) and cellular ($EC_{50} = 16.7$ μ M) hHDACs and to promote the same extent of histone H4 hyperacetylation in human HeLa cells ($EC_{50} > 25$ μ M). In summary, the two step screening strategy [(i) comparison of parasite growth inhibition in erythrocytes with hHDAC inhibition in HeLa cells as preliminary readout of selectivity; (ii) conclusive validation of the parasite selectivity of the most promising compounds by measurements of nuclear histone hyperacetylation in both human and parasite treated cells] proposed by Ontoria *et al.* for evaluating the parasite selectivity of new potential antimalarial agents seems quite attractive because it allows to avoid the problems of the common PfHDAC preparations that are likely inactive without endogenous cofactors and are endowed with low *in vitro* activities just because contaminated by co-purified host HDACs coming from the cellular expression vectors, and therefore are not reliable for inhibition studies.

Table 4.4: *In vitro* Antimalarial Activity of *N*-Methyl Carboxamides as HDAC Inhibitors.

Class/ Inhibitor	Structure	Nuclear extract [rPfHDAC1] ^a IC_{50} (nM)	<i>P. falciparum</i> EC_{50} (μ M)	Class I hHDACs in HeLa cells IC_{50} (μ M)	SI ^b
---------------------	-----------	-----------------------------------------------------------------	----------------------------------------------	------------------------------------------------------------	-----------------

35		NA	0.45	16.6	37
36		NA	0.90	20.5	23
37		NA	0.5	>25	54

^a Deacetylase activity tested using either *P. falciparum* nuclear lysates (no brackets) or recombinant PfHDAC1[brackets]; ^b SI: Selectivity Index [HeLa class I HDACs IC₅₀ (μM) / *Pf*growth EC₅₀ (μM)]; NA: data not available.

4.4.3 Antimalarial Sirtuin Inhibitors

Despite less studied than class I/II/IV HDACi, a certain number of SIRTi have been tested *in vitro* for anti-proliferative activity against *P. falciparum*-infected erythrocytes and for inhibition of the recombinant PfSir2A protein [264, 397, 574]. Known natural and synthetic SIRTi that have been examined over the years for *P. falciparum* growth inhibition comprise **38** (IC₅₀ ~ 9-13 μM) [582-583], **39** (splitomycin, IC₅₀ > 10 μM) [580, 582-583], **40** (surfactin, IC₅₀ ~ 9 μM) [582], and **41** (hyperforin, IC₅₀ ~ 1.5-2 μM) [639-640] (Fig. 4.4). Compound **42** (nicotinamide), the physiological product of the Sir2-catalyzed NAD⁺-dependent deacetylation reaction, was found to be significantly less active at whole cell level (IC₅₀ ~ 9.9 mM), with a delayed parasite growth inhibitory effect observed (Fig. 4.4) [582-583, 641].

The depsipeptide **40** and, to a lesser extent, **42** are more potent inhibitors of PfSir2A (IC₅₀ = 35 and 51 μM, respectively) than hSIRT1 (IC₅₀ > 600 and = 88-250 μM, respectively), while **38** and **39** are less active than them versus PfSir2A (IC₅₀ > 50 and > 400 μM, respectively). In 2009, Chakrabarty *et al.* applied a click chemistry approach to synthesize lysine-based tripeptide analogues designed to target PfSir2A through competition with the peptide binding pocket [642]. Despite three of four tested analogues had similar or better potency (IC₅₀s = 23-

34 μ M) against PfSir2A compared with **40** and **42**, all of them were devoid of selectivity for the parasite Sir2 over human SIRT1. The most active compound **43** versus PfSir2A was also tested *in vitro* against *P. falciparum*-infected erythrocytes where it was as potent as **38** and **40** in inhibiting the growth of the parasite ($IC_{50} = 9.8 \mu$ M) [582]. The natural hSIRT1 activator resveratrol [308], able to modestly inhibit *in vitro* the growth of *P. falciparum* ($IC_{50} \sim 60 \mu$ M), was also tested against recombinant PfSir2A, but no enzyme activation or inhibition was detected [583].

Overall, the *in vitro* activity of the SIRTi tested so far against *P. falciparum* parasite growth is modest, but this is not surprising in the light of the aforementioned experimental evidences that seem to indicate PfSir2A and PfSir2B as not essential for the *in vitro* parasite growth and development, and anyway considering the low sequence homology observed between the PfSir2 and other eukaryotic Sir2 proteins [527-528]. Moreover, the somewhat low consistency between the PfSir2A inhibitory potencies and the *in vitro* antiproliferative effects promoted by some compounds (*e.g.* **38**, **39**, **42** and, to a lesser extent, **40**) and the pleiotropic nature of some of them (*e.g.* **38** and **42**), do not allow to exclude additional mechanisms involved in their *P. falciparum* growth inhibitory activity. For these reasons, it is presently highly desirable to identify/develop inhibitors with significantly increased potency against PfSir2 enzymes and selectivity over human sirtuins, that could be useful as tools for studying the biology of *P. falciparum* sirtuins and potentially for their pharmacological validation as targets of drugs exerting a direct or an indirect (by blocking the parasite evasion from the host innate immune surveillance) anti-parasitic activity (see above in text) [527-528].

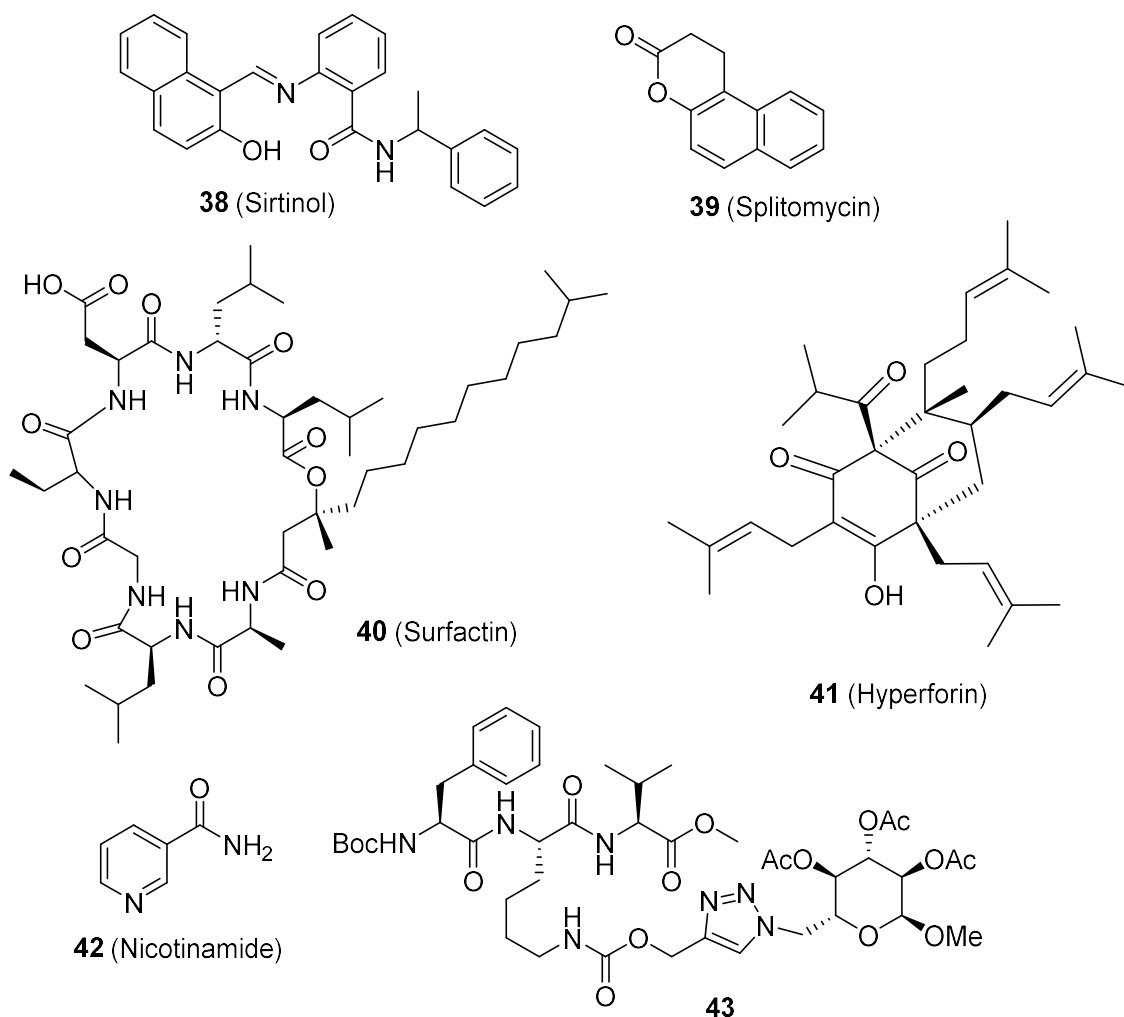


Fig. 4.4: Chemical structures of antimalarial class-III HDAC (SIRT) inhibitors.

4.4.4 Antimalarial HKMT Inhibitors

Plasmodium falciparum HKMTs (*Pf*HKMTs) play key role in controlling *Plasmodium* gene expression through epigenetic pathways [560, 643]. *Pf*HKMTs were found to be essential in the asexual blood-stages of the parasite, in particular, knockout of *Pf*SET2 was found to reverse the silencing of the *var* gene family, which is centrally involved in the immune evasion mechanism by which *Plasmodium* avoids the host antibody response [529, 643], and thus may represent good drug targets [529, 531]. Despite this potential, production of enzymatically active *Pf*HKMTs has proved to be challenging, with only a few successful reports in the literature [531, 590], thus hindering the prospect of *Pf*HKMT inhibitor discovery. Indeed, by modifying the amino side chains of this scaffold, diaminoquinazoline inhibitors have been reported exhibiting human SETD8 [644-645] and EZH2 [646] activity. Given this broad HKMT activity, Malmquist *et al.* [598] suggested that ‘repurposing’ the diaminoquinazoline scaffold as inhibitors of the homologous *Pf*HKMTs as a potential new antimalarial targets. Two compounds, **44** (BIX-01294) and its derivative **45** (TM2-

115) (Fig. 4.5), inhibited *P. falciparum* 3D7 parasites in culture with IC₅₀ values of ~100 nM, values at least 22-fold more potent than their apparent IC₅₀ toward two human cell lines and one mouse cell line. These compounds irreversibly arrested parasite growth at all stages of the intraerythrocytic life cycle. Decrease in parasite viability (>40%) was seen after a 3-h incubation with 1 μ M BIX-01294 and resulted in complete parasite killing after a 12-h incubation. Additionally, mice with patent *Plasmodium berghei* ANKA strain infection treated with a single dose (40 mg/kg) of TM2-115 had 18-fold reduced parasitemia the following day. A dose-dependent reduction in histone methylation (H3K4 and, to a lesser extent H3K9) was observed in parasites upon treatment (Western analysis), suggesting on-target *Pf*HKMT activity [598], and that the broad ranging effects of these compounds is likely due to their target. Highly promising effects were also observed for other life cycle stages, with mature gametocyte progression to gamete formation inhibited at submicromolar concentrations [599], and both compounds were shown to activate dormant liver forms called hypnozoites [647], which are produced by some malaria parasite species including *P. vivax* and are considered one of the less accessible malaria infection reservoirs. This observation raises the intriguing possibility that hypnozoite activation may be regulated at the epigenetic level and suggesting that it may be possible to target these highly resilient forms with epigenetic drugs.

A preliminary SAR study on our diaminoquinazoline series revealed that some pharmacophoric features might be conserved for both parasite-killing and G9a inhibition, thereby suggesting potential similarities between G9a and the yet unidentified *Pf*HKMT target(s) responsible for the anti-parasitic activity [648]. As a result, a variety of analogues, based on BIX-01294 and TM2-115, were designed by substituting the 2 and 4 positions of the quinazoline core and these molecules were tested against *Plasmodium falciparum* (3D7 strain). The resulting derivatives were assessed for cytotoxicity against the human HepG2 hepatocarcinoma cell line as a measure of parasite versus human selectivity. Several analogues with IC₅₀ values as low as 18.5 nM and with low mammalian cell toxicity (HepG2) were identified [648]. Promisingly, four lead compounds, BIX-01294, TM2-115 and two new compounds (**46** and **47**) (Fig. 4.5) were found to not only be highly potent against *Pf*3D7, but also highly selective for parasite versus host cell killing [599]. All four compounds were found to be 110-388-fold more active on *Pf*3D7 compared to HepG2 cell viability. Both **46** and **47** revealed a decreased H3K4me3 and H3K9me3 levels and showed similar rapid and erythrocytic stage-independent killing phenotype as previously shown for BIX-01294 and

TM2-115 [598]. More recently, the same authors reported that an extensive study of the SAR of this series against both G9a and *P. falciparum*. From this series, compound **48** and **49** (Fig. 4.5) were employed in analogous phenotypic assays in order to study whether the diaminoquinoline chemotype has a comparable target profile to the diaminoquinazolines [649]. Consequently, both compounds showed similar erythrocytic stage-independent killing phenotype, suggesting a common target profile for the anti-*Plasmodium* activity with that of BIX-01294. Together, this data suggests that while broadly similar, the G9a and potential *Pf*HKMT target(s) binding pockets and/or binding modes of the diaminoquinazoline analogues exhibit clear and exploitable differences. Thus, there remains significant potential in this series to further develop parasite selective analogues. Based on this, we believe this scaffold to have clear potential for development into a novel and much needed, new medicine for malaria.

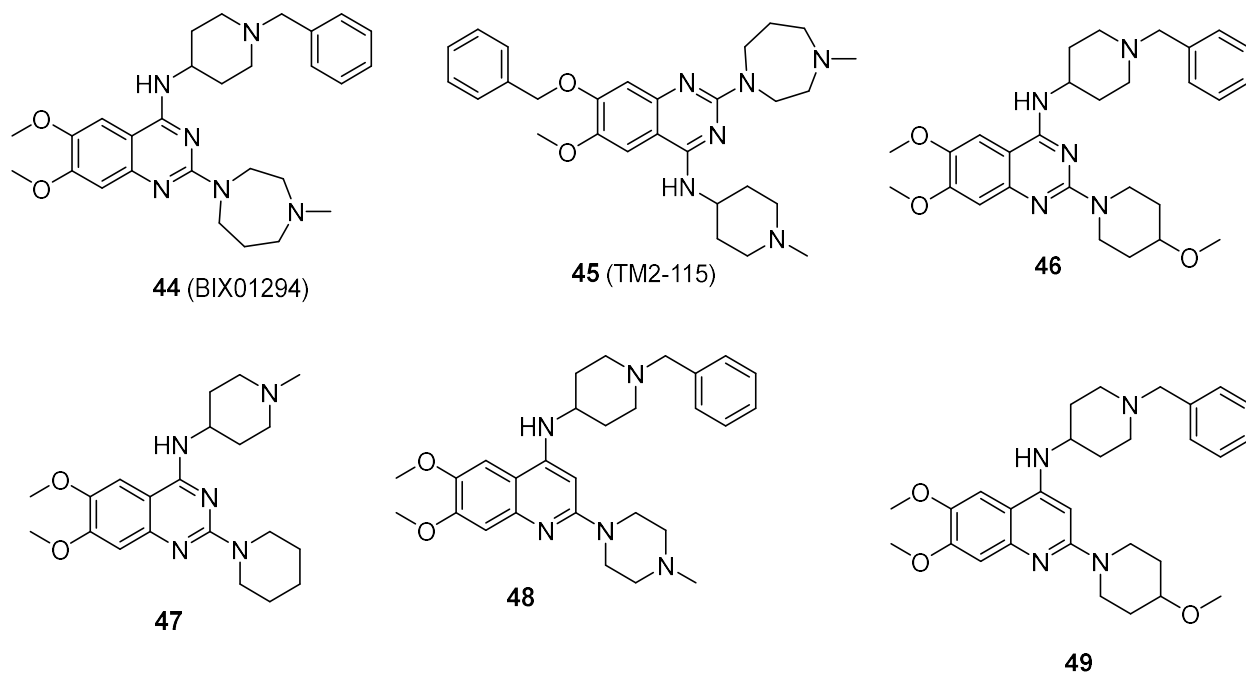


Fig. 4.5: *Pf*HKMT inhibitors

5. EPIGENETIC MECHANISMS AS DRUG TARGETS FOR *SCHISTOSOMA MANSONI*

The term “epigenetics” envelops a variety of heritable changes in gene expression that are linked to structural modifications of the chromatin, without changes to the DNA sequence. These include DNA methylation, reversible post-translational modifications of histones, histone variants, chromatin remodeling factors and non-coding RNAs. The investigation of the role of epigenetic mechanisms in the control of gene transcription in schistosomes, and hence in biological processes like development and reproduction, is in its early stages. Nevertheless, the complexity of schistosome development and differentiation implies a tight control of gene transcription at all stages of the life-cycle and that epigenetic mechanisms are likely to play a crucial role in these processes, suggesting that they are viable drug targets. In this context, the understanding of developmental and reproductive biology of schistosomes is crucial to fight schistosomiasis. Many works have highlighted the responsiveness of the developing *S. mansoni* to the host blood microenvironment and shown that the parasite might exploit endocrine and host immune signals to accomplish its development [650-654]. The mating status (*i.e.* paired vs unpaired) has also been shown to play an essential role for the maturation of both male and female [655-658]. Other molecular studies have highlighted male- or female-biased pathways essential for the development and the reproduction of the parasite [659-661]. Global transcriptomic analyses were carried out on diverse developmental stages [662-663] and sex-biased expressions were explored in adult [663-664] or cercariae [665]. Epigenetic control for gene expression regulation has also been investigated and highlighted sex-specific epigenetic processes with chromatin structural changes occurring on female-specific microsatellite repeats of the W-chromosome during the development of the parasite [666]. Similarly, Picard et al. highlighted that sexual differentiation in *S. mansoni* is accompanied by distinct male and female transcriptional landscapes of known players of the host-parasite crosstalk, genetic determinants and epigenetic regulators [667]. Therefore, the knowledge so far acquired, or inferred from the nature of schistosomes as invertebrate metazoan organisms and from a detailed analysis of the epigenetic actors encoded in their genomes, can be exploited to develop novel therapeutic strategies. Viewed as potential targets, the most readily “druggable” are the enzymes that carry out DNA methylation and histone modifications, and increasingly, micro-RNAs (miRNAs) among the non-coding RNA categories.

5.1 DNA Methylation in Schistosomes

The presence of functional DNA methylation marks in schistosome genomes is controversial. Early work showed no differences in the restriction profiles for adult male or female *S. mansoni* DNA [668]. Moreover, the methyl cytosine-dependent restriction endonuclease McrBC failed to digest *S. mansoni* DNA. However, recently, cytosine methylation was found to be a conserved epigenetic feature throughout the phylum Platyhelminthes, including *Schistosoma haematobium*, *Schistosoma japonicum*, and *S. mansoni* [669]. In addition to cytosine methylation, the arginine methyltransferase PRMT1 homolog was also identified in *S. mansoni* and *S. japonicum* [670-671]. Dnmt 2 has only weak DNA methyltransferase activity but has robust methyltransferase activity toward tRNAAsp and other tRNAs [51]. However, Dnmt2 does retain some cytosine methyltransferase activity [672-673] showed that siRNA knockdown of SmDnmt2 transcripts reduced overall methylcytosine levels in the schistosome genome. These authors have further suggested that cytosine methylation is conserved throughout the phylum Platyhelminthes [669]. Against this, a comprehensive study [674] using whole-genome bisulfite sequencing showed that the *S. mansoni* genome lacked a detectable DNA methylation pattern, even at the “hypermethylated” locus identified by [673]. Some clusters of incompletely converted cytosines were detected outside this region, but were consistent with bisulfite deamination artefacts [675]. However, although these results strongly suggested that the *S. mansoni* genome is in fact unmethylated, the criticism has been levelled that the life-cycle stage analyzed, adult male worms, has the lowest level of DNA methylation measured using an ELISA method [669]. Notwithstanding this controversy, Dnmt inhibitors were found to strongly affect adult worms, particularly in terms of the morphology of the ovaries and *in vitro* egg-laying [673], that indicates Dnmt inhibitors such as 5-azacytidine may provide the basis for developing precursors of novel anti-schistosome drugs.

5.2 Schistosome miRNAs

Early diagnosis of schistosomiasis is critical to control this disease. However, no reliable biomarker exists for early diagnosis of schistosomiasis. Circulating miRNAs, which are present in a stable form in the plasma or serum of an infected host, have been considered ideal biomarkers for the diagnosis of some cancers. It is possible that such circulating miRNAs could also serve as biomarkers for schistosomiasis diagnosis. Because miRNAs act as critical post-transcriptional regulators in many organisms, studies have been conducted to determine the

roles of miRNAs in schistosomes. These miRNAs are likely to play critical roles in schistosome development and gene regulation.

A survey of the available *S. mansoni* EST sequences [676] concluded that 10.3% (21,107 sequences) match the genome but have no protein coding potential and are therefore possible ncRNAs, suggesting that the parasite may use a range of ncRNAs in transcriptional and translational regulation. To the best of our knowledge, miRNAs were first identified in *S. japonicum* [677-678] in two separate studies that demonstrated the existence of a limited number of miRNA that are conserved in other organisms and that the miRNA expression profiles were highly stage-specific. In a more comprehensive study, researchers used a high-throughput sequencing technology to characterize small RNAs populations in *S. japonicum* schistosomula, the early stage in the vertebrate host, which identified 16 schistosome-specific miRNAs [679-680]. In *S. mansoni*, the sequencing of a small-RNA cDNA library yielded 211 novel miRNA candidates of which 11 were further verified by Northern blotting and presented data supporting stage-regulated expression patterns for some of the miRNAs [681].

Thirteen microRNAs exhibit sex-biased expression, 10 of which are more abundant in females than in males [682]. Some miRNAs are associated with the morphological formation of ovaries in female schistosomes in *S. japonicum* [683]. These results demonstrate that during the life cycle of schistosomes, different microRNAs are likely to participate in differentiation/maintenance processes and it is clear that these miRNAs are potential therapeutic targets.

5.3 Schistosome Histone Modifications

The *S. mansoni* genome encodes 55 HMEs involved in protein acetylation/deacetylation or methylation/demethylation (Table 5.1) [684]. Some of these, including the class I HDACs [685] and the sirtuins [686] have been cloned and characterized and preliminary choices of targets can be made based on their degree of sequence conservation. Moreover, histone modifications have been identified in different life stages of schistosomes, and changes in histone modifications appear to be crucial for pathogenesis and thus to be potential therapeutic targets. For example, bivalent histone H3 methylation was observed in cercariae, demethylation of H3K27 and activation of transcription were observed during the transformation into schistosomula (remaining absent in adults), and alterations of H3K9 methylation and acetylation occurred upstream and downstream of the transcriptional start site (TSS) [687]. The modification profiles of four histone modifications (H3K4me3,

H3K27me3, H3K27ac, and H4K20me1) were different between the sympatric host and allopatric host and these histone marks also differ in cercariae and adult [688]. The promoters of the *S. mansoni* mucingene (SmPoMuc), a key component of the compatibility between the schistosome and its snail host, contains the epigenetic marks H3K9Met3 and H3K9Ac, which differ significantly between compatible (C) and incompatible (IC) strains and negatively regulates the expression of SmPoMuc [689]. The structure of the parasite chromatin differentially modifies the transcription of SmPoMuc in the IC strain compared with the C strain [690]. These findings suggest that histone alterations maybe important for the initial steps in the adaptation of pathogens to new hosts and epidrugs can be used to control parasite development. Comparison of H3K27me3 histone modification before (in cercariae) and after (in adults) showed that the H3K27me3 enrichment profile in cercariae differs between the two sexes both upstream and along the transcription unit, whereas in the adult stage, males and females display the same profile after the TSS, while their profile upstream the TSS remains different [667]. These results suggest epigenetic regulators play important roles in the sex determination and sexual differentiation in schistosomes and represent a promising source of therapeutic targets.

Table 5.1: Identity and characteristics of *Schistosoma mansoni* histone modifying enzymes [691].

HME type	Class	Closest human ortholog	Size (aa)	Substrate specificity	Gene Id ^a
HDAC	I	HDAC1	517*		Smp_005210
	I	HDAC3	418*		Smp_093280
	I	HDAC8	440*		Smp_091990
	II	HDAC4	291		Smp_191310
	II	HDAC5	701		Smp_069380
	II	HDAC6	1132		Smp_138770
	III (Sirtuin)	Sirt1	568*	H1 – H3 – H4	Smp_138640
	III (Sirtuin)	Sirt2	337*	H4K16	Smp_084140
	III (Sirtuin)	Sirt5	305*		Smp_055090
	III (Sirtuin)	Sirt6	386*	H3K9 – H3K56	Smp_134630
	III (Sirtuin)	Sirt7	517*		Smp_024670
HAT	GNAT	GCN5 (KAT2A)	899*	H3K9 – H3K14 – H3K18 H2B	Smp_070190
	GNAT	HAT1 (KAT1)	435	H4K5 – H4K12	Smp_178700
	MYST	Tip60 (KAT5)	463	H2AK5 – H3K14 – H4K5 – H4K8 – H4K12 – H4K16	Smp_053140
	MYST	MYST1 (KAT8)	496	H4K16	Smp_194520

	MYST	MYST2 (KAT7)	400	H4K5 – H4K8 – H4K12 – H3	Smp_171700
	MYST	MYST3 (KAT6A)	971	H3K14	Smp_131320
	CBP/p300	CBP/SmCBP1 (KAT3A)	2093*	H2AK5 – H2BK15 – H3K14 – H3K18 – H4K5 – H4K8	Smp_105910
	CBP/p300	CBP/SmCBP2 (KAT3A)	1892	H2AK5 – H2BK15 – H3K14 – H3K18 – H4K5 – H4K8	Smp_127010
	TAFII250	TFIID subunit 1	2241	H3 – H4	Smp_166840
HMT	SET	EZH1	1026	H3K27	Smp_078900
	SET	MLL3 (KMT2C)	399	H3K4	Smp_070210
	SET	MLL3 (KMT2C)	1560	H3K4	Smp_138030
	SET	MLL1/4 (KMT2D)	3002	H3K4	Smp_144180
	SET	MLL5 (KMT2E)	751	H3K4	Smp_161010
	SET	C20orf11/MLL5/Ranbp9	1305		Smp_009980
	SET	NSD2/WHSC1	1746	H3K4 – H4K20	Smp_160700
	SET	NSD1/2 (KMT3B)	1343	H3K36 – H4K44	Smp_137060
	SET	SET8 (KMT5A)	409	H4K20	Smp_055310
	SET	SUV 39H2 (KMT1B)	586	H3K9	Smp_027300
	SET	SUV4-20H1 (KMT5C)	613	H4K20	Smp_062530
	SET	SETD2	1575	H3K36	Smp_133910
	SET	SETD1B	1720/1822	H3K4	Smp_140390
	SET	SETDB	918/1032		Smp_150850
	SET	SETMAR	250	H3K9	Smp_043580
	SET	SET/MYND4	782		Smp_000700
	SET	SET/MYND4	527		Smp_124950
	SET	SET/MYND5	423/429/433		Smp_121610
	DOT1	DOT1L (KMT4)		H3K79	Smp_165000
	PRMT	PRMT1	252/359/334	H4R3	Smp_029240
	PRMT	PRMT3	1564		Smp_127950
	PRMT	PRMT4/CARM1	737	H3R2 – H3R17 – H3R26	Smp_070340
	PRMT	PRMT5	630	H2A – H4	Smp_171150
	PRMT	PRMT7	755		Smp_025550
HDM	KDM1	LSD1A	1043		Smp_150560
	KDM1	LSD1A	916		Smp_160810
	KDM1	LSD1 (KDM1)	1073	H3K4 – H3K9	Smp_162940
	JmjC	JMJD1B (KDM3)	273	H3K9	Smp_161410
	JmjC	JMJD2C (KDM4C)	1136	H3K9 – H3K36	Smp_132170
	JmjC	JMJD4	809		Smp_147870
	JmjC	JMJD6	839		Smp_137240
	JmjC	JHDM1D (KDM7)	653	H3K36	Smp_127230
	JmjC	Jarid (KDM5)	2372	H3K4	Smp_156290
	JmjC	jarid (KDM5)	1639	H3K4	Smp_019170
	JmjC	UTX (KDM6A)	1137	H3K27	Smp_034000

5.3.1 Schistosome Histone Acetyltransferase

Histone acetyltransferase inhibition also has developmental consequences in schistosomes, particularly in egg maturation. The HATs, GCN5, was identified in *S. mansoni*, and specific acetylation at H3K14 was catalyzed by the transcriptional co-activator GCN5 [692-693]. SmCBP/p300 was also identified in *S. mansoni*, and it was expressed during all life cycle stages, interacted functionally with the nuclear receptor SmFtz-F1 and also potentiated the transcriptional activity of this receptor in the CV-1 cell line [694].

The schistosome orthologue of the HAT GCN5 has been shown to acetylate H3 and H2A, and in particular H3K14 [692] and the CBP/P300 orthologue SmCBP1 primarily acetylates H4 [694-695]. Knockdown of either or both of these HATs in adult schistosomes has been shown to markedly reduce the transcription levels of the major egg shell protein p14 and to damage the reproductive system of mature female worms, egg-laying and egg morphology. This result suggests that inhibition of Smp14 expression targeting SmGCN5 and/or SmCBP1 represents a novel and effective strategy to control *S. mansoni* egg development and that HATs can be used as a drug target against schistosomiasis. Moreover, these effects are reproduced by treating adult worm pairs with an HAT inhibitor, PU139 (Fig. 5.1) [696]. After both inhibitor treatment and RNAi to knock down transcripts of the HATs, the phenotypic effects on egg laying and development were correlated with decreased acetylation of H3 and H4, increased methylation at H3K27, a marker of transcriptional repression, on the p14 proximal promoter. More recently, the SmEZH2 methyltransferase PRC2 component was targeted with a new EZH2 inhibitor GSK343 (Fig. 5.1) and showed a synergistic effect with TSA, significantly increasing schistosomula mortality [697]. This paves way to target histone reader genes involved in regulation of the epigenetic program in *S. mansoni* as a starting point to look for possible novel schistosomicidal targets.

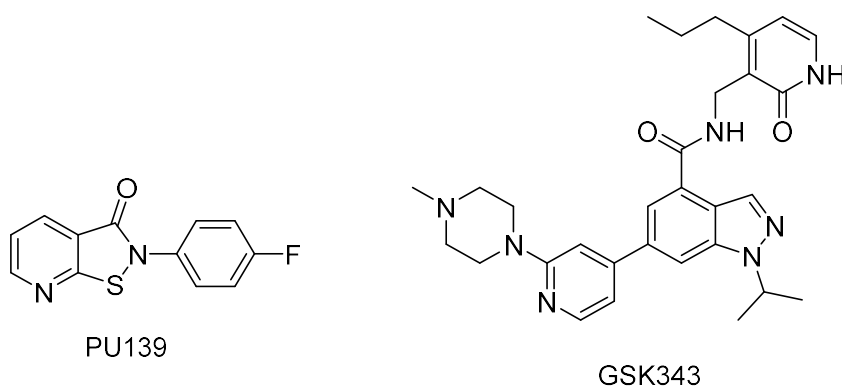


Fig. 5.1: Example of HAT inhibitors active against *Schistosoma mansoni*

5.3.2 Schistosoma HDACs

Studies have shown that class-I HDACs (smHDAC1, 3 and 8) are expressed in all stages of the *Schistosoma* lifecycle, with smHDAC8 being the most abundant [685]. Conversely, the human orthologue HDAC8 was reported to generally show less abundance than HDAC1 and HDAC3 in human cells, except in some tumor cells which show up-regulated levels of HDAC8 [698].

The effects of both HDAC and HAT inhibitors on schistosomes suggest that histone acetylation may be a legitimate therapeutic target and initial studies investigating the effect of pan-HDAC inhibitors demonstrated their ability to induce schistosome mortality; the exact mechanism however is not completely clarified yet [615, 699]. Incubation of schistosomula larvae with trichostatin A (TSA) or valproic acid (VPA) caused parasite mortality *via* an apoptotic mechanism. The results indicated that TSA induces a sustained hyperacetylation of H4 leading to an increased expression of *CASP7*, which is responsible of inducing apoptosis [699]. Another study demonstrated that TSA arrests the transformation of *Schistosoma* miracidia to intramolluskal sporocysts [615]. These experiments shed light on the potential mechanism of HDAC inhibitors-mediated mortality of schistosomes.

Several studies have thus focused on smHDAC8 as a potential therapeutic target for the treatment of schistosomiasis [700-703]. SmHDAC8 was found in *in vivo* studies to play an important role in the homeostasis of the parasite and to be essential for its pathogenicity. Mice infected with smHDAC8 knocked-down schistosomules showed, 35 days post incubation, a reduced number of recovered adult worms and lower egg burden compared to control mice. This indicated the importance of smHDAC8 for the survival and maturation of the parasite in its host [702].

5.3.3 Antischistosomal HDAC Inhibitors

To further investigate and confirm the role of smHDAC8 in schistosome biology, several investigations were dedicated to the development of smHDAC8 small molecule inhibitors and investigate their effect in *in vitro* studies [700-703]. A structure-based virtual screening campaign was successful in finding 25 hydroxamic acid derivatives with an *in vitro* inhibitory potency against smHDAC8. Nine compounds exhibited an activity in the low micromolar range [701]. Among the identified inhibitors, J1075 (Fig. 5.2) was found to induce apoptosis and mortality in schistosomula larvae [702]. Heimbürg *et al.* recently reported on a new proof of concept study, where several benzohydroxamic derivatives were designed as parasite-specific

inhibitors. The developed inhibitors were evaluated for their inhibitory activity against schistosomal and human HDACs (smHDAC8, hHDAC1, hHDAC6 and hHDAC8). Twenty-seven compounds exhibited an inhibitory activity in the nanomolar range in *in vitro* assays. Interestingly, many of the reported compounds showed a notable selectivity for smHDAC8 over the major human HDAC isoforms (HDAC1 and HDAC6), some of which even exhibited a preference for smHDAC8 over human HDAC8 [700]. The obtained crystal structures of smHDAC-inhibitor complexes as well as docking studies show that, besides the expected coordination of the catalytic zinc-ion by the hydroxamate group, two H-bond interactions are formed between the amide linker and the side chains of the protein residues His292 and Lys20. This could partly account for the selectivity of the compound over HDAC1 and HDAC6 (Fig. 5.3). Further phenotypic assays demonstrated that two of the reported compounds caused significant dose-dependent reduction of cultured schistosomula larvae [700], as opposed to praziquantel which is known to be less effective against larval developing stages of the parasite [704]. Moreover, TH65 (Fig. 5.2) caused a noticeable separation of female and male worm pairs and an impairment of egg-laying by adult worms [700]. Further hits from other chemical series, partially including a thiol group as warheads to chelate the catalytic zinc-ion, were also reported to possess *in vitro* inhibitory activity against schistosomula of *S. mansoni* [703].

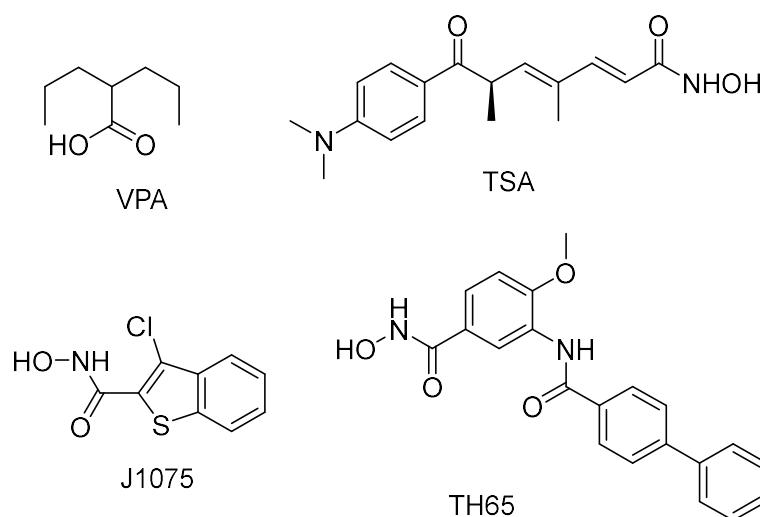


Fig. 5.2: Chemical structures of most relevant antischistosomal HDAC

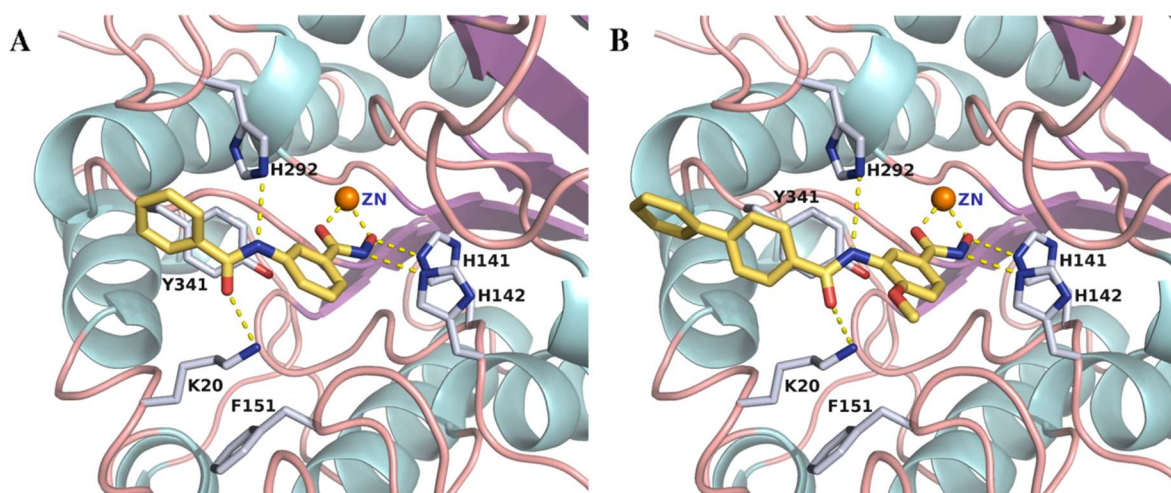


Fig. 5.3: (A) X-ray structure of the inhibitor TH31 in complex with SmHDAC8 (PDB ID 5FUE). (B) Docking pose of the inhibitor TH65 in SmHDAC8. TH31 and **2** are shown in yellow, protein residues involved in the interaction in white, zinc-ion as orange spheres, and H-bond as well as interactions with the metal ion as yellow dashed lines.

5.3.4 Schistosoma Sirtuins

Sirtuins are NAD^+ - dependent lysine deacetylases that are involved in a wide variety of cellular processes including histone deacetylation, and they have been shown to be therapeutic targets in various pathologies including cancer. It has been previously pointed out that several similarities between schistosomes and tumors including the cellular proliferation removed from control by the host, a degree of invisibility to the immune response and energy metabolism based on the consumption of large amounts of glucose and oxidative glycolysis producing lactate as the end-product [684]. It was also pointed out that schistosomes undergo a rapid switch from energy production based on oxidative phosphorylation in cercariae to glycolysis in schistosomula immediately after skin penetration, and this is stimulated by the presence of glucose in the external medium [705]. This metabolic switch is analogous to the Warburg effect noted in numerous tumors. Sirtuins link the control of metabolism and DNA repair to tumorigenesis and it is probable that schistosome sirtuins fulfill similar functions to their human counterparts [706].

Parasitic class I sirtuins, characterized by the GAGXSXXXGIPDFRS, PS/TXXH, TQNID and HG motifs [707] have been extensively and successfully explored as antiparasitic targets. It has been reported that these proteins have vital role in parasite survival by catalyzing the deacetylation reaction of acetylated lysine residues of nuclear histones and other substrates, with NAD^+ as a cofactor [708]. To evaluate schistosomal sirtuins and their potential as therapeutic drug targets, Lancelot et al. identified and characterized 5 sirtuins encoded in the

S. mansoni genome and established their homology relationship to human isoforms. Altogether, five sirtuins were found to be encoded in *S. mansoni* genome, which are orthologues of the human sirtuins SIRT1, SIRT2, SIRT5, SIRT6 and SIRT7. The encoded sirtuins are expressed at all stages of *S. mansoni* life cycle; however, there are wide variations in the levels of transcripts, particularly in the case of the nuclear sirtuins, Sirt6 and Sirt7, which are highly expressed in larval stages, whereas the nucleo-cytosolic sirtuins, Sirt1 and Sirt2 show less variation.

5.3.5 Schistosoma Sirtuin Inhibitors

With the aim of assessing the potential of schistosomal sirtuins as targets for anti-parasitic drug development, several reported mammalian SIRTi were tested in *in vitro* assays to investigate their effects on cultured schistosomula and adult worms. Compound sirtinol, salermide and the thiobarbiturate derivative MS3 (Fig. 5.4) significantly reduced the viability of schistosomula through induction of apoptosis. Moreover, incubation of the aforementioned sirtuin inhibitors with adult worms caused separation of female and male worms and reduction in egg laying. Interestingly, Salermide also caused a remarkable change in the morphology of ovaries and testes [686]. These results suggest that schistosome sirtuins could be potential therapeutic targets and validate screening for selective sirtuin inhibitors as a strategy for the development of new drugs against schistosomiasis.

The molecular features of SmSirt2 as well as its use for the development of new targets for schistosomiasis were explored in some recent studies [709-710]. The schistosome sirtuins, while showing overall conservation of essential catalytic domain residues [686], also show significant differences. The solution of crystal structures of schistosome sirtuins bound to inhibitors would represent a significant advance for the development of selective inhibitors [706].

Nevertheless, the use of high-throughput screening of extensive compound libraries represents a complementary strategy that has recently been used with success to generate inhibitors of human Sirts 1, 2 and 3 that show nanomolar IC₅₀ inhibitory values, although they are not selective [711]. It is to be expected that the application of both high-throughput and structure-based screening strategies will rapidly lead to the identification of both selective and potent sirtuin inhibitors. Indeed, in a recent study, we report the optimization of fluorescence-based assays for *S. mansoni* Sirt2 that allowed a pilot screen with inhibitors

showing IC₅₀ values of <50 μ M and docking studies rationalizing the binding of hits to the target using a homology model of the enzyme [712].

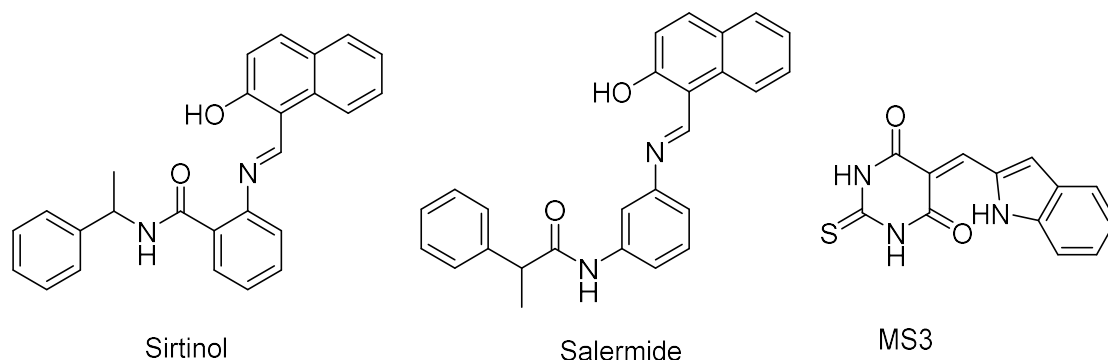


Fig. 5.4: Chemical structures of most relevant antischistosomal HDAC and sirtuin inhibitors.

5.3.6 Histone Methylation and Demethylation

Schistosome genome analysis (Table 5.1) allows to identify 18 lysine methyltransferases and 5 PRMT family proteins [691]. A closer look at the specificity of the orthologues of the schistosome HMT proteins shows that the parasites possess enzymes that could methylate the histone lysine residues involved in transcriptional control: H3K4 (MLL, SETD1B), H3K9 (Suv39H2, SETDB), H3K27 (EZH1), H3K36 (NSD2/WHSC1, SETD2, NSD1/2, SETMAR), H3K79 (DOT1L), H4K20 (NSD2/WHSC1, SET8, NSD1/2, Suv420H1), H3R2 (CARM1) and H4R3 (PRMT1, PRMT5, PRMT7) [713-714]. Putative orthologues are also present of further lysine methyltransferases (Smyd 4 and 5) for which the histone substrates have yet to be defined. On the other hand, of the 11 HDM encoded in the *S. mansoni* genome (Table 5.1), 3 are similar to LSD1 and the remaining 8 are JmjC domain-containing proteins.

In common with the HATs and HDACs, some HMTs have been shown to act on non-histone proteins. For example, schistosomes present an orthologue of PRMT3, which principally methylates the 40S ribosomal protein S2 [715] and the lysine methyltransferase SET8 methylates p53 on lysine-382 [716].

The latter include a putative orthologue of Utx that has H3K27 demethylase activity, but not of JMJD3 that also has this specificity [717].

Overall the lower numbers of both HDMs and HMTs in the schistosome genome compared to the human genome point to a lower degree of functional redundancy for the schistosome enzymes. For example, EZH1 and EZH2 show functional redundancy for the methylation of H3K27 [718] and Utx and JMJD3 are both involved in its demethylation. As the *S. mansoni* genome encodes neither EZH2 nor JMJD3, the EZH1 and Utx orthologues are the

unique enzymes carrying out these tasks and may therefore represent particularly sensitive therapeutic targets [717].

Studies using HMT and HDM inhibitors are less common, but some results have shown that the chloroacetyl derivative, allantodapsone, a PRMT1 (arginine methyltransferase) inhibitor, showed selective inhibition affecting the growth of tumor cells [719]. Recent studies performed, knocked down for PRMT3 and KDMs in schistosomula by RNA interference, show that these enzymes are important for *S. mansoni* reproduction.

6. DESIGN, SYNTHESIS AND BIOLOGICAL VALIDATION OF URACIL-BASED HYDROXAMIDES (HDAC INHIBITORS) AS NEW ANTIMALARIAL AGENTS

6.1 Research Project

The emergence and spread of malaria drug resistance presents a worrisome situation impacting disease control programs [412, 415]. It is now becoming clear that malaria control will require the introduction of new chemotherapies to overcome this situation [720]. One promising strategy to identify new antimalarial agents is the “piggyback” approach, which focuses on drug targets that have been validated for other diseases, try to apply them to new indications such as parasitic diseases [396]. Accumulating evidence indicates that the malaria parasite has a unique histone modification signature that plays a fundamental role in gene expression and virulence [721]. In the search for promising drugs to combat malaria, inhibitors of histone modifying enzymes have started to obtain attention [264]. The factors affecting histone modifications are also suggested to have links between mode of action of artemisinin and its resistance. Earlier studies clearly reported that HAT, Sirtuins and HDAC inhibitors, including apicidin, curcumin and several hydroxamate derivatives as well as the clinically approved HDACi are potent inhibitors of *Plasmodium* growth [264, 397, 429, 582, 599, 722-723]. Specifically, several HDAC inhibitors have been shown to be highly effective blockers of *P. falciparum* growth, which put the HDAC enzymes into the spotlight of this research [264, 397, 574, 579-580, 610, 626, 722, 724] and several of them displaying a significant *in vitro*, *ex vivo* and, in a few cases, *in vivo* activity against malarial parasites. Such findings underscore the potential for PfHDAC inhibitors to be used for malaria therapy [264, 397, 633].

HDAC inhibition is expected to affect chromatin structure and the patterns of gene expression. The transcriptome explorations of the effects of HDAC inhibition have shown that different inhibitors impact differently on the expression of genes highlighting the mechanistic complexity of the control of gene expression in the parasite. Despite some progress in recent years, there are still a number of challenges in the rational development of HDAC inhibitors as antimalarial drug leads. Next generation compounds should retain potent antiplasmodial activity and low host cell toxicity, but they also require improved pharmacokinetic properties relative to current generation compounds.

As in other human diseases such as cancer, HDACi bearing a hydroxamic acid warhead as zinc-binding group (ZBG) are the best studied anti-parasitic HDACi and have shown promising

in vitro activity profiles against *P. falciparum* and other parasites. From a medicinal chemistry point of view, this compound class features fall into a pharmacophoric model widely accepted, which consists of a capping group (CAP), able to interact with the rim of the catalytic tunnel of the enzyme, a zinc binding group (ZBG), able to complex the Zn^{2+} ion at the bottom of the catalytic cavity, and hydrophobic linker connecting the two parts [264, 574, 722]. In this project, we investigated the antimalarial activity of a small library of epi-drugs, including the HDAC inhibitors of the class uracil-based hydroxamides (UBHAs, MC1746 and MC1761), cinnamyl hydroxamates and related compounds (MC1575, MC2780, MC2059), 2'-aminoanilides (MS-275 and MC2392), and Sirtuin inhibitors (MC2141, MC1776) (Fig. 6.1), against *Pf3D7* sensitive strains. These compounds were chosen because having different chemical structures and different selectivity for the various HDAC isoforms. As far as the uracil-based hydroxamides are considered, compounds with a phenyl/benzyl ring at the uracil-C6 position and bearing 4-5 carbon units as well as methylenecinnamyl moiety as a spacer were the most potent inhibitors [725]. Thus, we prepared MC1746 bearing a 2-naphthyl group as a CAP, a uracil moiety as a connecting unit, 4 carbon methylene units as hydrophobic a spacer, and the hydroxamate function to bind the Zn ion. Whereas, MC1761 was characterized by a phenyl group as a CAP, a uracil moiety as a connecting unit, methylenecinnamyl moiety as a spacer, and the hydroxamate function to bind the Zn ion, crucial for the catalytic activity of the enzyme (Fig. 6.1). it would be nice to mention that all biological tests have been performed by Prof. Khalife's group at the 'Institut Pasteur De Lille', Lille, France.

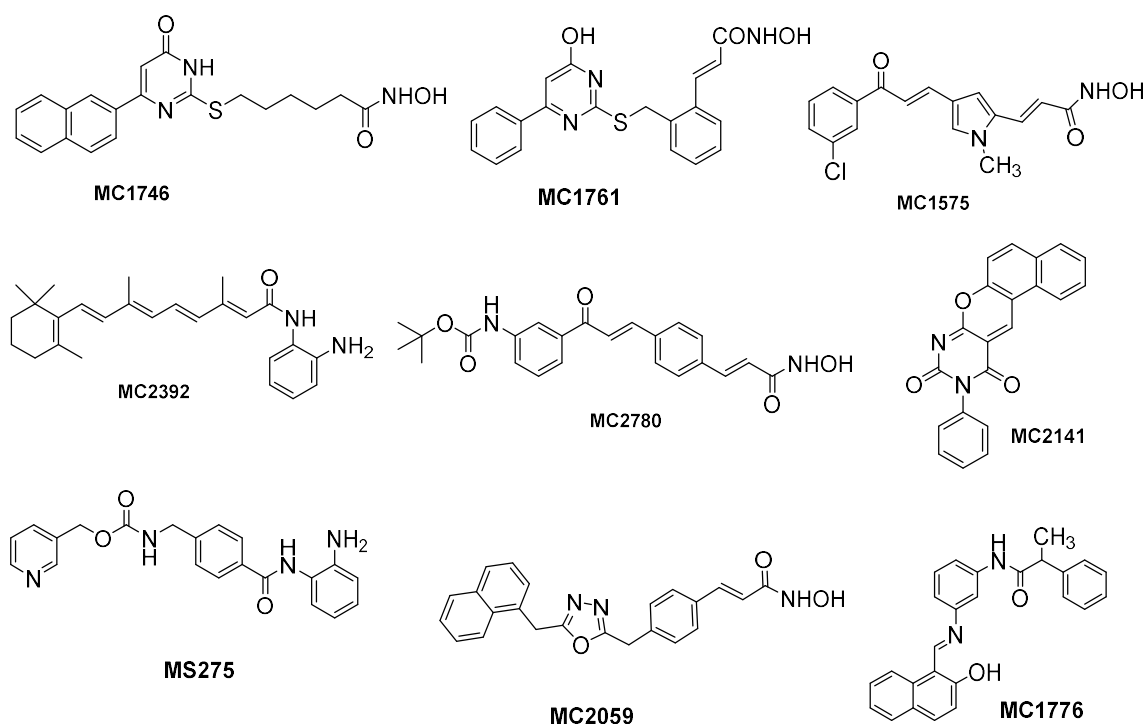


Fig. 6.1: A small library of HDAC and Sirtuin inhibitors tested against *Pf3D7* sensitive and W2 multidrug resistant strains.

The target-based drugs approach using a series of histone modifying enzymes enable us to identify few potent compounds active *in vitro* on *P. falciparum* strains with low toxicity. More specifically, the antiparasitic activity revealed that MC1746, the only HDACi selective towards classes I and IIb of HDACs, as the most potent compound, with IC₅₀ values of 79 nM against *Pf3D7* sensitive strains (Table 6.1).

Table 6.1: Percentage of growth inhibition at 10 μ M and IC₅₀ values on 3D7 of compounds from the primary library. ND: not determined. IC₅₀ values were not determined when the percentage of inhibition at 10 μ M was lower than 50%.

Epi-targets	Compounds	% of inhibition at 10 μ M	IC ₅₀ (nM)
HDACs	MC1746 class I/IIb HDACi	97.44	79.38 \pm 0.73
	MC2392 context-selective class I HDACi	97.09	>1 μ M
	MS-275 HDAC1-3 inhibitor	50.91	>1 μ M
	MC1575 HDAC4-6,8 inhibitor	89.62	>1 μ M
	MC2780 HDAC6-selective inhibitor	100	422.39 \pm 19.44
	MC2059 pan-HDACi	98.00	244.03 \pm 52.18

	MC1761 HDAC8 inhibitor	2.82	ND
Sirtuins	MC2141 Sirt1/2i	80.52	>1 μ M
	MC1776 Sirt1/2i	72.31	>1 μ M

In an effort to improve HDAC inhibitory potency against *P. falciparum*, and however to further generate structure-activity relationships on the core UBHA, we decided to prepare another small group of compounds (Table 6. 2). During this process, we focused our attention on the two portions that, by a HDACi medicinal chemistry point of view, characterize the UBHA template: the CAP group and the hydrophobic spacer (HS) by keeping the hydroxamate as Zn-binding group (ZBG). For what concerning the CAP group (R, Fig. 6.2), first of all, in addition to the phenyl moiety at C6 of the Uracil ring, we also introduced benzyl moiety in which both characterized by variety of substituents at *meta*, or *para* position of the benzene ring of the phenyl/benzyl moiety, including less bulkier aromatic rings (Table 6.2). While pursuing our searches on HS (X, Fig. 6.2), we explored the effect of 4 and 5 methylene units on the anti-plasmodial activity of such compounds. Selected compounds were then examined for their activity against *Pf*3D7 sensitive and W2 multidrug resistant strains (Table 6.3).

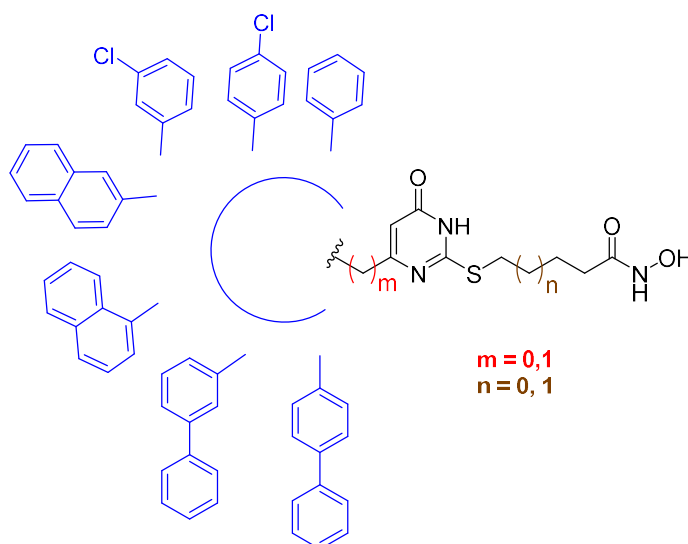


Fig. 6.2: Modifications of the UBHA template

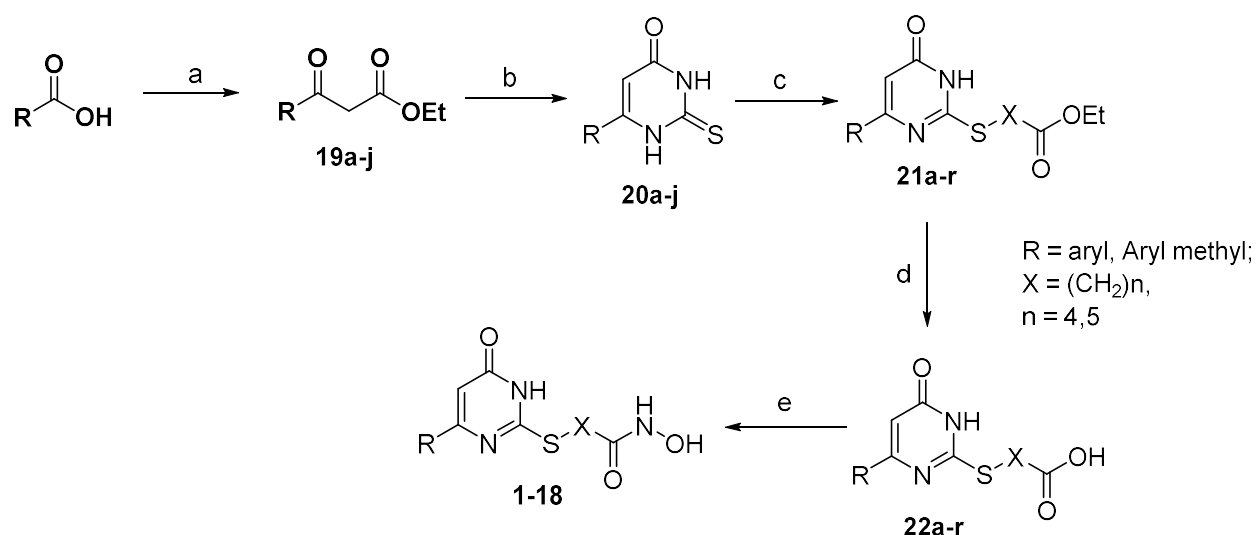
6.2 Chemistry

For the synthesis of the UBHA derivatives bearing linear HSs, the properly 6-substituted 2-thiouracils **20a-j** were treated with various sizes of ethyl ω -bromoalkanoates in the presence of anhydrous potassium carbonate to afford the ethyl esters **21a-r**, which were, in

part, hydrolyzed to the corresponding carboxylic acids **22a-r**. A subsequent treatment of **22a-r** with (i) ethyl chloroformate and triethylamine, (ii) *O*-(2-methoxy-2-propyl)-hydroxylamine [726], and (iii) Amberlyst 15 ion-exchange resin in methanol afforded the related hydroxamates **1-18** (Scheme 1).

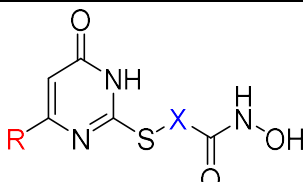
Among the 6-substituted-2-thioxopyrimidin-4-ones **20a-j**, the synthesis of the not commercially available intermediates has been accomplished by condensation of thiourea in alkaline medium with the appropriate ethyl β -ketoesters **19a-j**, previously prepared by reacting potassium monoethylmalonate with chlorides or imidazolides of the corresponding acids in the presence of the magnesium/triethylamine system [727].

Scheme 1^a



^a Reagents and conditions: (a) 1) CDI, CH₃CN, 2) KOOCCH₂COOEt, (Et)₃N, MgCl₂, CH₃CN, rt then reflux, 3) 13% HCl; (b) EtONa, thiourea, EtOH, reflux; (c) Br-X-COOEt, K₂CO₃, DMF, rt; (d) 2N KOH, EtOH, H₂O, rt; (e) 1) ClCOOEt, (Et)₃N, dry THF, 0°C, then NH₂OC(CH₃)₂OCH₃, rt, 2) Amberlyst® 15, MeOH, rt;

Table 6.2. Physical and Chemical Data for Compounds **1-18**.

						
comp d	Lab code	R	X	mp, °C	recryst. solvent ^a	yield, %
1		Ph	(CH ₂) ₄	194-196	b	54
2		Ph	(CH ₂) ₅	144-146	c	57
3	MC1716	3-Cl-Ph	(CH ₂) ₄	196-198	a	61
4		3-Cl-Ph	(CH ₂) ₅	188-192	a	67
5	MC1714	4-Cl-Ph	(CH ₂) ₄	198-200	a	52
6		1-naphthyl	(CH ₂) ₄	182-184	a	48
7		1-naphthyl	(CH ₂) ₅	198-200	a	54

8	MC1745	2-naphthyl	(CH ₂) ₄	188-190	b	51
9	MC1746	2-naphthyl	(CH ₂) ₅	144-146	d	57
10	MC1742	4'-biphenyl	(CH ₂) ₄	202-204	a	57
11	MC1738	4'-biphenyl	(CH ₂) ₅	192-194	a	51
12		3'-biphenyl	(CH ₂) ₅	188-190	a	56
13		3'-biphenyl	(CH ₂) ₄	198-200	a	52
14		PhCH ₂	(CH ₂) ₅	179-181	b	57
15		PhCH ₂	(CH ₂) ₄	104-106	c	49
16		1-naphthylCH ₂	(CH ₂) ₅	172-174	a	51
17		2-naphthylCH ₂	(CH ₂) ₅	160-162	b	52
18		4'-biphenylCH ₂	(CH ₂) ₅	208-210	e	47

^aa: methanol; b: acetonitrile/methanol; c: acetonitrile; d: benzene; e: ethanol.

6.3 Experimental Section

Chemistry. Melting points were determined on a Stuart melting point apparatus SMP10™. ¹H-NMR spectra were recorded at 400 MHz using a Bruker AC 400 spectrometer; chemical shifts are reported in δ (ppm) units relative to the internal reference tetramethylsilane (Me₄Si). Microwave-assisted reactions were performed with a Biotage Initiator™ (Uppsala, Sweden) high frequency microwave synthesizer working at 2.45 GHz, fitted with magnetic stirrer and sample processor; reaction vessels were Biotage microwave glass vials sealed with applicable cap; temperature was controlled through the internal IR sensor of the microwave apparatus Biotage Isolera One™. All compounds were routinely checked by TLC and ¹H-NMR. TLC was performed on aluminum-backed silica gel plates (Merck DC, Alufolien Kieselgel 60 F₂₅₄) with spots visualized by UV light or using a KMnO₄ alkaline solution. All solvents were reagent grade and, when necessary, were purified and dried by standard methods. Concentration of solutions after reactions and extractions involved the use of a rotary evaporator operating at reduced pressure of ~ 20 Torr. Organic solutions were dried over anhydrous sodium sulfate. All chemicals were purchased from Sigma Aldrich s.r.l., Milan (Italy) or from TCI Europe N.V., Zwijndrecht (Belgium), and were of the highest purity. As a rule, samples prepared for physical and biological studies were dried in high vacuum over P₂O₅ for 20 h at temperatures ranging from 25 to 40 °C, depending on the sample melting point.

General Procedure for the Synthesis of *N*-Hydroxy-ω-(3,4-dihydro-4-oxo-6-substituted-2-pyrimidinylthio)alkanamides (1-18). Example 5-((4-([1,1'-Biphenyl]-4-yl)-6-oxo-1,6-dihydropyrimidin-2-yl)thio)-*N*-hydroxypentanamide (10, MC1742). To a 0 °C cooled solution

of 5-((4-([1,1'-biphenyl]-4-yl)-6-oxo-1,6-dihydropyrimidin-2-yl)thio)pentanoic acid (**20j**) (0.53 mmol, 200 mg) in dry tetrahydrofuran (4 mL), ethyl chloroformate (1.3 mmol, 138 mg, 0.12 mL) and triethylamine (1.38 mmol, 140 mg, 0.19 mL) were added and the mixture was stirred for 10 min. The solid was filtered off, and *O*-(2-methoxy-2-propyl)-hydroxylamine (3.18 mmol, 0.24 mL) was added to the filtrate. The resulting mixture was stirred at rt for 1 h then was evaporated under reduced pressure, and the residue was diluted in MeOH (2.5 mL). Amberlyst 15 ion-exchange resin (106 mg) was added to the solution of the *O*-protected hydroxamate, and the mixture was stirred at rt for 1 h. Afterward, the reaction was filtered and the filtrate was concentrated in vacuum to give the crude **10**, which was purified by recrystallization. Recrystallization system: methanol. ¹H NMR (DMSO-*d*₆) δ 1.69 (m, 4H, CH₂CH₂CH₂CH₂S), 2.02 (t, 2H, CH₂CO), 3.25 (t, 2H, CH₂S), 6.72 (s, 1H, C5-H), 7.39–7.48 (m, 3H, benzene rings), 7.73–7.83 (m, 4H, benzene rings), 8.14 (m, 2H, benzene rings), 8.69 (s, 1H, NHOH), 10.37 (s, 1H, NHOH), 12.6 (s, 1H, uracil NH). MS (ESI), *m/z*: 396 [M + H].

***N*-Hydroxy-5-(3,4-dihydro-4-oxo-6-phenyl-2-pyrimidinylthio)pentanamide (1).** ¹H NMR (DMSO-*d*₆) δ 1.65 (m, 4H, CH₂CH₂CH₂S), 1.97 (t, 2H, CH₂CO), 3.21 (t, 2H, CH₂S), 6.65 (s, 1H, C5-H), 7.48 (m, 3H, benzene ring), 8.04 (m, 2H, benzene ring), 8.70 (s, 1H, NHOH), 10.34 (s, 1H, NHOH), 12.68 (s, 1H, NH uracil ring).

***N*-Hydroxy-6-(3,4-dihydro-4-oxo-6-phenyl-2-pyrimidinylthio)hexanamide (2).** ¹H NMR (DMSO-*d*₆) δ 1.38 (m, 2H, CH₂CH₂CH₂S), 1.52 (m, 2H, CH₂CH₂CO), 1.70 (m, 2H, CH₂CH₂S), 1.94 (t, 2H, CH₂CO), 3.19 (t, 2H, CH₂S), 6.65 (s, 1H, C5-H), 7.47 (m, 3H, benzene ring), 8.03 (m, 2H, benzene ring), 8.65 (s, 1H, NHOH), 10.35 (s, 1H, NHOH), 12.65 (s, 1H, NH uracil ring).

***N*-Hydroxy-6-(3,4-dihydro-4-oxo-6-benzyl-2-pyrimidinylthio)hexanamide (14).** ¹H NMR (DMSO-*d*₆) δ 1.27 (m, 2H, CH₂CH₂CH₂S), 1.44 (m, 2H, CH₂CH₂CO), 1.50 (m, 2H, CH₂CH₂S), 1.92 (t, 2H, CH₂CO), 3.01 (t, 2H, CH₂S), 3.72 (s, 2H, PhCH₂), 5.92 (s, 1H, C5-H), 7.24 (m, 5H, benzene ring), 8.66 (s, 1H, NHOH), 10.33 (s, 1H, NHOH), 12.45 (s, 1H, NH uracil ring).

***N*-Hydroxy-5-(3,4-dihydro-4-oxo-6-benzyl-2-pyrimidinylthio)pentanamide (15).** ¹H NMR (DMSO-*d*₆) δ 1.52 (m, 4H, CH₂CH₂CH₂S), 2.03 (t, 2H, CH₂CO), 3.03 (t, 2H, CH₂S), 3.72 (s, 2H, PhCH₂), 5.91 (s, 1H, C5-H), 7.23 (m, 5H, benzene ring), 8.68 (s, 1H, NHOH), 10.34 (s, 1H, NHOH), 12.35 (s, 1H, NH uracil ring).

General Procedure for the Synthesis of 6-(3,4-Dihydro-4-oxo-6-substituted-2-pyrimidinylthio)-alkanoic Acids (22a-r). Example: 5-((4-([1,1'-biphenyl]-4-yl)-6-oxo-1,6-dihydropyrimidin-2-yl)thio)hexanoic acid (**22k**). A mixture of ethyl 5-((4-([1,1'-biphenyl]-4-

yl)-6-oxo-1,6-dihydropyrimidin-2-yl)thio)hexanoate (**21k**) (1.1 mmol), 2 N KOH (8.8 mmol), and EtOH (5 mL) was stirred at room temperature for 18 h. The solution was poured into water (50 mL) and extracted with ethyl acetate (2 X 20 mL). HCl (2 N) was added to the aqueous layer until the pH 5, and the precipitate was filtered and recrystallized to yield the title compound **22k** as a pure solid. ¹H NMR (DMSO-*d*₆) δ 1.32 (m, 2H, CH₂CH₂CH₂S), 1.49 (m, 2H, CH₂CH₂CO), 1.61 (m, 2H, CH₂CH₂S), 1.93 (t, 2H, CH₂CO), 3.06 (t, 2H, CH₂S), 6.07 (s, 1H, C5-H, uracil), 7.39–7.48 (m, 3H, benzene rings), 7.73–7.83 (m, 4H, benzene rings), 8.14 (m, 2H, benzene rings), 12.2 (s, 1H, COOH).

General Procedure for the Synthesis of Ethyl ω-(3,4-Dihydro-4-oxo-6-substituted-2-pyrimidinylthio)alkanoates (21a-n). **Example: Ethyl 6-(6-Benzyl-3,4-dihydro-4-oxopyrimidin-2-ylthio)hexanoate (21n).** A mixture of 6-benzyl-4-hydroxy-2-mercaptopyrimidine (**20n**) (9.16 mmol, 2.0 g), ethyl 6-bromohexanoate (10 mmol, 1.8 mL), and anhydrous potassium carbonate (10 mmol, 1.4 g) in 3 mL of anhydrous DMF was stirred at room temperature for 1 h. After treatment with cold water (100 mL), the precipitate which formed was filtered and washed to furnish **21n** (1.6 g), which was purified by crystallization from MeOH. Yield: 49%; mp: 104-106 °C; recrystallization solvent: MeOH; ¹H NMR (CDCl₃) δ 1.25 (t, 3H, CH₂CH₃), 1.40 (m, 2H, CH₂CH₂CH₂CO), 1.63 (m, 4H, CH₂CH₂CO and CH₂CH₂S), 2.28 (t, 2H, CH₂CO), 3.13 (t, 2H, CH₂S), 3.80 (s, 2H, PhCH₂), 4.13 (q, 2H, CH₂CH₃), 5.96 (s, 1H, H C₅), 7.28 (m, 5H, benzene ring), 12.87 (s, 1H, NH). Anal. C, H, N, S.

General procedure for the synthesis of derivatives of the 6-substituted 2-thiouracils (18a-g). **Example: Example: 6-(benzyl)-3,4-dihydro-2-thioxopyrimidin-4(3H)-one (19h).** Sodium metal (23.70 mmol) was dissolved in 21 mL of absolute ethanol, and thiourea (16.6 mmol) and **18h** (11.80 mmol) were added to the clear solution. The mixture was heated at reflux for 12 h. After the completion of reaction the mixture was cooled, the solvent was distilled in vacuo at 40-50 °C until dry and the residue was dissolved in water (15 mL) and made acidic with 2 N HCl. The resulting precipitate was filtered under reduced pressure, washed with diethyl ether, and vacuum dried at 80 °C for 12 h to give title compound **19h** as a pure white solid which was further purified by crystallization from ethanol. Yield: 68%; mp: 242-245 °C; recrystallization solvent: ethanol. ¹H NMR (DMSO) δ 3.28 5.04 (s, 2H, PhCH₂), 5.78 (s, 1H, C₅-H), 7.40 (m, 5H, benzene ring), 12.38 (s, 1H, NH), 12.43 (s, 1H, NH).

General procedure for the synthesis of ethyl β-ketoesters (18a-j). **Example: ethyl 3-oxo-4-phenylbutanoate (18h).** Triethylamine (48.00 mmol) and magnesium chloride (37.50

mmol) were added to a stirred suspension of potassium ethyl malonate (31.50 mmol) in acetonitrile (50 mL), and stirring was continued at room temperature for 2 h. Then, a solution of phenylacetyl imidazolidine [prepared from phenylacetic acid (15.00 mmol) and *N,N*-carbonyldiimidazole (CDI, 18.00 mmol)] in acetonitrile (15 mL) was added and the reaction mixture was stirred overnight at room temperature. 13% HCl (90 mL) was cautiously added while keeping the temperature below 25°C and the resulting clear mixture was stirred for a further 15 min. The organic layer was separated from aqueous mixture and evaporated; then the residue was treated with ethyl acetate (30 mL). The aqueous layer was extracted with ethyl acetate (3 x 30 mL), and the organic phases were combined, washed with saturated sodium bicarbonate solution (3 x 30 mL) and brine (3 x 30 mL), dried, and concentrated to give **18h** as a yellow oil. Yield: 88%. ¹H NMR (CDCl₃) δ 1.22 (t, 3H, OCH₂CH₃), 3.50 (m, 2H, COCH₂CO), 4.13 (q, 2H, OCH₂CH₃), 4.77 (s, 2H, PhCH₂), 7.35 (m, 5H, benzene ring).

6.4 Biological Evaluation and Results

6.4.1 Phenotypic screening of epigenetic modulators against 3D7

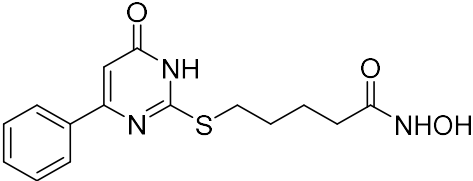
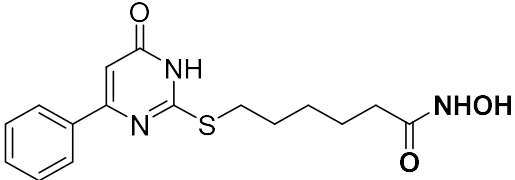
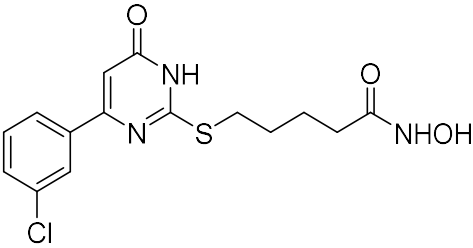
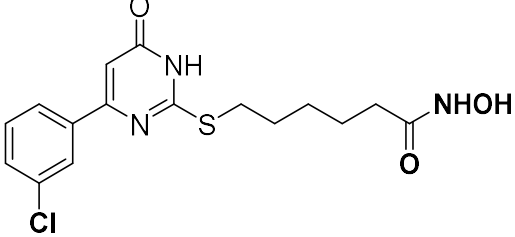
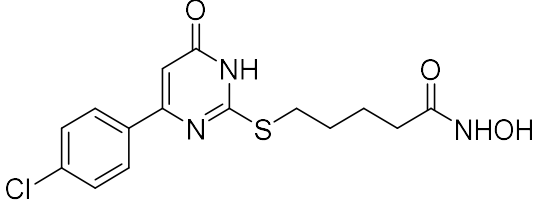
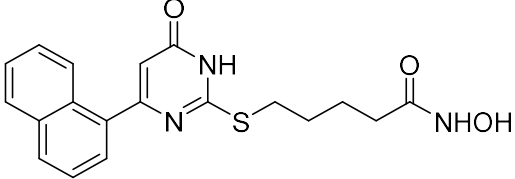
In this target-based screening, the antiparasmodial activities of the selected HDAC and Sirtuin inhibitors were initially assessed at 10 μM against the *P. falciparum* 3D7 strain. As shown in Table 6.1, 8 compounds inhibited parasite growth between 50 and 100%, and 1 compound showed an inhibition of parasite growth lower than 5%. The 8 compounds were then tested in dose response assays to determine their IC₅₀ values (50% or half maximal inhibitory concentration). The most potent compound showing IC₅₀ values of 79.38 was the UBHA-based HDACi, MC1746, bearing selectivity for classes I/IIb of HDACs (Table 6.1).

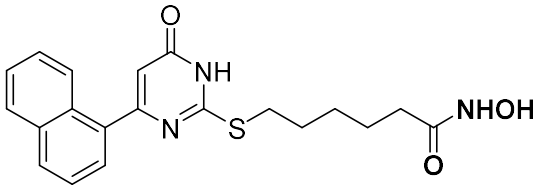
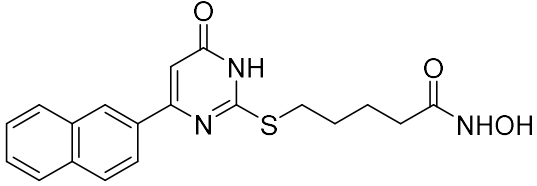
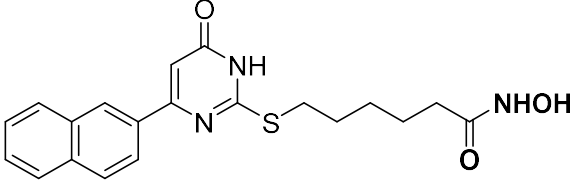
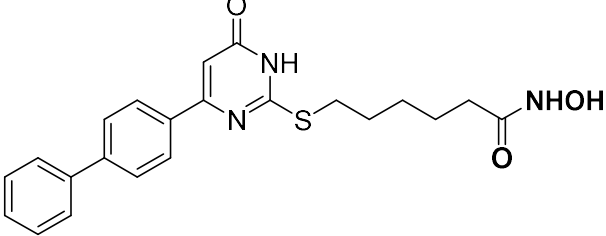
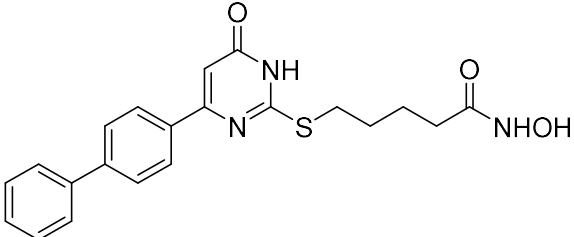
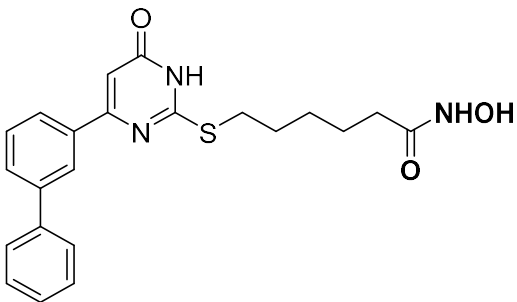
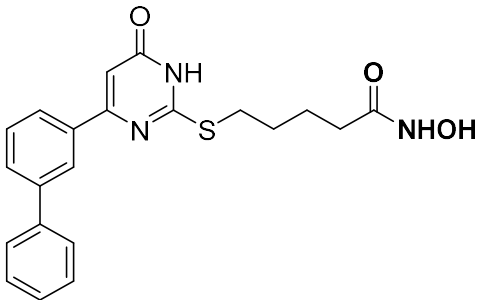
6.4.2 Antiparasmodial activity of analogues derived from active compounds (focused screening)

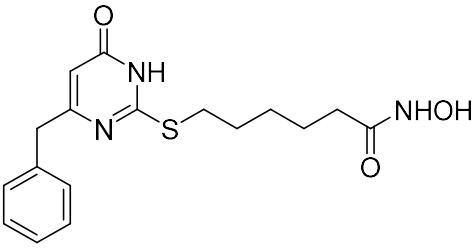
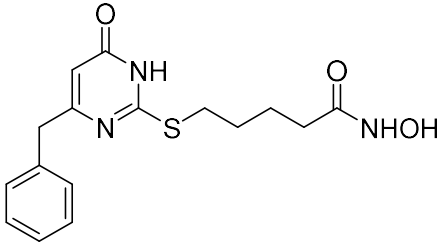
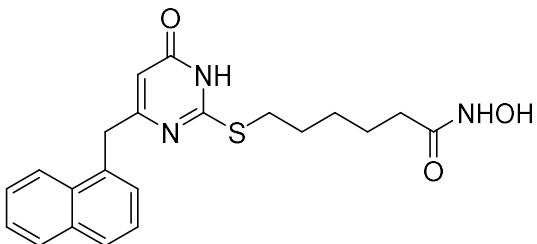
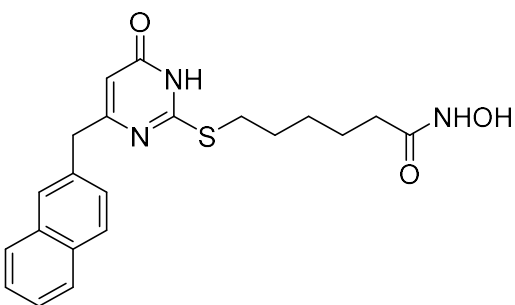
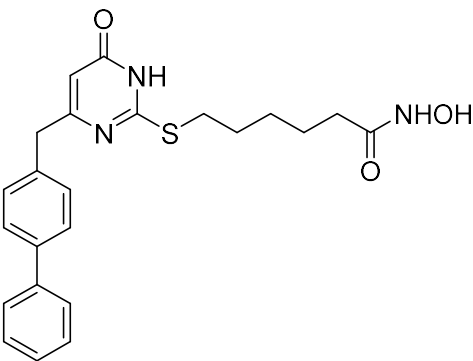
In order to optimize the potency of the active compounds primarily tested, further a small series of analogues were tested belonging to the HDACi which gave the highest *Plasmodium* growth arrest in the first screen, i.e. MC1746 (focused screening). They were first screened at 10 μM for their ability to inhibit 3D7 parasite growth. Several compounds showed an inhibition of parasite growth greater than 50%; more specifically, among the screened compounds, 5 compounds displayed 96-100% inhibition of parasite growth (Table 6.3). For the new analogues, IC₅₀ values were then determined as previously described (Table 6.3). About the new tested HDACi, several new analogues exhibited IC₅₀ values < 100 nM, moreover, three compounds (**8**, **10** and **11**) showed IC₅₀ values lower than the corresponding

prototype, in particular **11** displayed the highest antiplasmodial potency with IC₅₀ value of 4.21 (Table 6.3). Thus, from the results obtained by the two screenings, we selected **11** for further experiments.

Table 6.3: Percentage of growth inhibition at 10 μ M and IC₅₀ values on 3D7 of the hit and its newly synthesized analogues. ND: not determined. IC₅₀ values were not determined when the percentage of inhibition at 10 μ M was lower than 50%.

Compounds	Structures	% of inh. at 10 μ M	IC ₅₀ (nM)
1		80.23	88.98 \pm 3.12
2		76.00	98.58 \pm 2.11
3 MC1716		98.01	88.61 \pm 2.16
4		90.30	108.01 \pm 5.12
5 MC1714		92.05	87.6 \pm 5.28
6		75.24	104.87 \pm 5.19

7		65.98	110 ± 6.21
8 MC1745		97.92	25.17 ± 4.98
9 MC1746		97.44	79.38 ± 0.73
10 MC1738		97.44	50.89 ± 5.01
11 MC1742		96.12	4.21 ± 0.39
12		78.20	90.39 ± 4.69
13		83.45	81.97 ± 3.41

14		66.65	114.19 ± 5.91
15		70.00	109.47 ± 4.91
16		76.07	98.69 ± 5.56
17		68.04	106.94 ± 6.01
18		88.95	85.81 ± 4.85

6.4.3 Antiplasmodial activity against W2, a multiresistant strain

Several criteria have been proposed for defining hits and leads in the development of drugs for diseases such as malaria. To be validated as a hit for antiplasmodial activity, a selected compound should be active against multidrug-resistant strains [728]. To this end, the growth inhibition of the multidrug-resistant W2 strain [729] has been tested along with the sensitive 3D7 strain. Under the experimental conditions used throughout this study, chloroquine had an IC₅₀ value of 21.5 nM (± 1.6) and 290 nM (± 6) for 3D7 and W2 strains,

respectively, which is consistent with previous reports [598]. As far as MC1742 is considered, the IC₅₀ value obtained for W2 (6.6 nM) as close to that obtained for 3D7 (4.2 nM) strain. Altogether, these results suggest that MC1742 is a very promising candidate as hit/early lead compound for antimalarial treatment.

6.4.4 Selectivity Index (SI) on primary activated cells (splenic murine cells) and on eukaryotic cell line (HFF)

The high selectivity of a compound for *Plasmodium* is one of the criterion that has to be addressed to exclude potential toxic effects and to validate a compound as a hit (greater than 10-fold selectivity between the half maximal cytotoxic concentration for mammalian cell line and the IC₅₀ value for *Plasmodium* [728]. To assess the selectivity index (SI) of MC1742, a cytotoxicity assay on a murine splenic primary cell line and a human foreskin fibroblast cell line (HFF) was performed. As shown in Table 6.4, testing the cytotoxicity of this compound on HFF cell line showed SI = 783. The same assay performed on primary murine cells revealed SI value of 186, which was less selective in this test.

Table 6.4: MC1742 selectivity

		Mammalian cells				
		3D7	Splenic cells		HFF	
Epi-target	Compd	IC ₅₀ (nM)	IC ₅₀ (nM)	SI	IC ₅₀ (nM)	SI
HDAC	MC1742	4.21 ± 0.39	785 ± 78	186	3295 ± 247	783

SI – selectivity index; mammalian cell IC₅₀/*P. falciparum* IC₅₀.

4.4.5 Pharmacokinetic analysis

Based on criteria including *P. falciparum* IC₅₀ values (<50 nM) on both sensitive and multidrug-resistant strains, selectivity indexes on primary murine cells and HFF cell line (> 100-fold) and the new promising chemical structure, MC1742 was selected for pharmacokinetic (PK) studies. A (2-hydroxypropyl)-beta-cyclodextrin (HP-β-CD)-based formulation, suitable for both intravenous (i.v.) and *per os* (p.o.) administration, was selected for these PK studies. For MC1742, 2 mice were administered with one single dose (50 mg/kg) either intravenously or p.o.. Blood was collected at 3 different time points (15, 60 and 180 min for i.v and 30, 60 and 180 min p.o). Plasma samples were analysed and concentrations are summarized in Table 6.5. MC1742 administered at a 50 mg/kg dose was well tolerated. The 15 min i.v. samples showed quite high MC1742 plasma concentrations, but the compound concentration decreased rapidly with time. P.o. and i.v. plasma samples at 1 h post administration showed MC1742 concentrations between 0.5 and 2.2 μM and after 3 h between 43 and 300 nM.

Table 6.5: Pharmacokinetic parameters of MC1742 administered intravenously or orally to mice.

Compound/Dose	Administration					
	i.v.			Per os		
	Time (min)	Concentrations (μ M)		Time (min)	Concentrations (μ M)	
		Mouse 1	Mouse 2		Mouse 3	Mouse 4
MC1742 50 mg/kg	15	15.2	10.7	30	2.43	0.67
	60	2.16	1.67	60	0.90	0.48
	180	0.044	0.043	180	0.30	0.070

6.4.6 Effect on histones of treated *P. falciparum* parasites

To determine whether MC1742 has an effect on parasite histone acetylation levels, we treated parasites with a concentration of 3-fold its IC₅₀ value, collected samples after 5 h incubation and performed histone acetylation-specific Western blots on the treated parasites samples (Fig. 6.3).

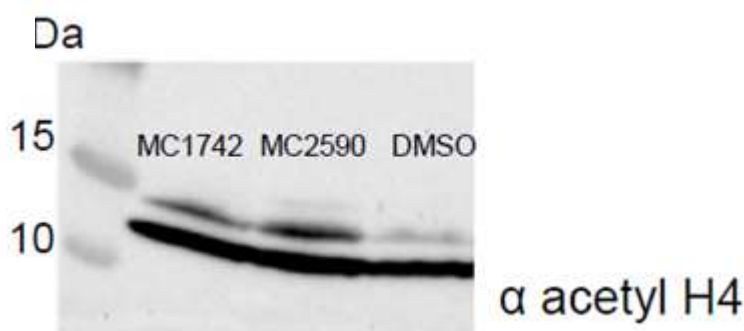


Fig. 6.3: Hyper-acetylation, WB; Histone acetylation levels in treated parasites. Asynchronous *P. falciparum* parasites were grown in 3-fold of the IC₅₀ values of MC1742, MC2590 and in DMSO for 5 hours for immunoblotting with anti H3 CT and anti-acetyl H4.

6.4.7 *In vivo* antimalarial activity in *P. berghei* infected mice

In order to comply with “early leads” criteria for malaria treatment, compounds should present oral efficacy [728]. From the above PK studies, it appears that the plasma concentrations of the selected compounds, when compared to their IC₅₀ values, could provide enough exposure to affect parasite growth. To examine the oral efficacy, the Peters 4-day suppressive test [730], which indicates the capacity of compounds to reduce or to completely inhibit blood parasite growth was carried out. Groups of 6 BALB/c mice were infected intraperitoneally (i.p) with 10⁶ *P. berghei* ANKA parasites and treated as depicted in Fig. 6.4A. On day 4 post infection, parasitemia levels in treated groups were compared to vehicle control groups.

In the group treated orally with MC1742 at 50 mg/kg, none of the mice showed a reduction of parasitemia (Fig. 6.4B, Exp. 1). The efficacy of MC1742 was then assessed by a combination of oral and i.v route as the PK studies revealed that the concentration of MC1742 was higher in the plasma samples after 15 and 60 min when administered i.v. (12.95 and 1.91 μ M, respectively) compared to *per os* (1.55 and 0.69 μ M, respectively, Table 6.5). Data presented in Fig. 6.4B (Exp. 2) showed that the combined route treatment of mice twice a day, one *per os* and one i.v., still did not have any effect on blood stage infection.

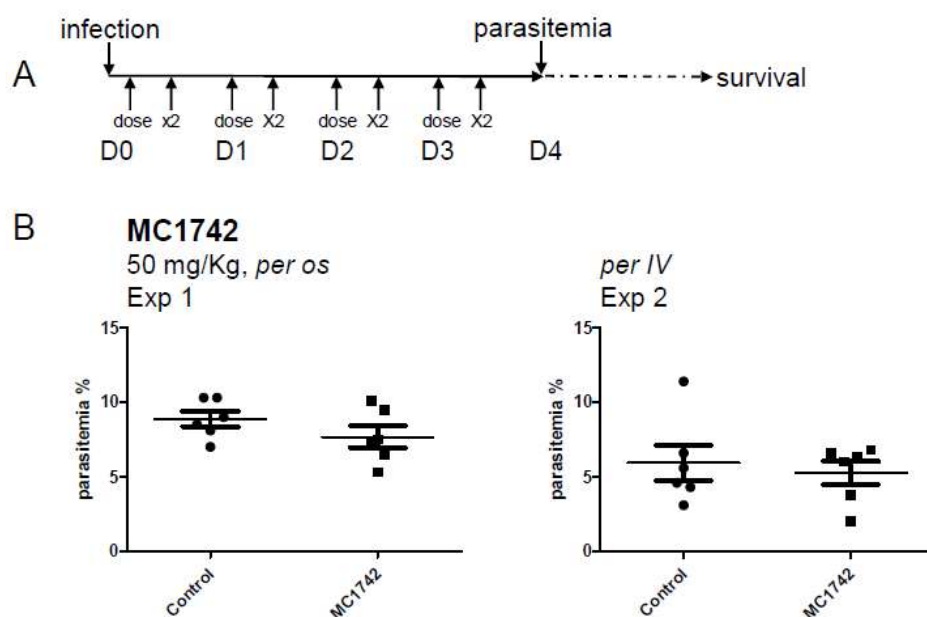


Fig. 6.4: Treatment of BALB/c male mice infected with *P. berghei* ANKA strain with MC1742 administered orally show total parasites clearance at Day 4 of the suppressive Peter's test. For each compound, 2 independent experiments, Exp 1 and Exp 2, were performed. Fifteen BALB/c mice were infected i.p. with 10^6 RBC infected with *P. berghei* ANKA strain. (A) Six mice were given *per os* the compound at the appropriate concentration, twice a day, 6 mice were given *per os* DMSO (7%), the vehicle and negative control and 3 mice were given *per os* CQ at 10 mg/kg, the positive control once a day, for 4 days. For MC1742, in Exp 2, mice received also 2 administrations: one *per os* and one *per iv*. On Day 4, parasitemia was determined for each mouse on a blood smear (and mouse survival was followed thereafter). Each dot represents one mouse. (B) Parasitemia at Day 4 for MC1742 (50 mg/kg) and the control-treated groups. The data in panels B, C, D and E are means \pm SEM.

6.5 Discussion and Conclusion

The key role played by epigenetic modifications, well known to be involved in transcriptional regulation in *Plasmodium*, provided a strong boost to research efforts on epigenetic inhibitors. Nonetheless, the clinical treatment of parasitic infections is quite different from that of other diseases, such as cancer, because most morbidity and mortality associated with parasitic diseases occur in resource-constrained regions of the world, with children, pregnant women, and immune-compromised people being at highest risk. Moreover, the coinfection of people in these regions with different infective agents (e.g., HIV)

is quite common and needs to be taken into account due to potential drug–drug interactions. Consequently, the main features that a HDACi, as any other new antiparasitic drug, should have before being considered for clinical use include: (1) high potency and selectivity in vivo for parasite over normal host cells, (2) activity against organisms resistant to currently employed drug(s), (3) an elevated degree of safety for use also in children and pregnant women, (4) low cost, to potentially treat hundreds of millions of deprived people, (5) oral bioavailability and effective pharmacokinetic profiles that allow single daily doses, and (6) hopefully, pharmacokinetics compatible with those of potential partner drugs to prevent or limit the development of drug resistance.

To progress class I/II HDACi toward clinical trials as potential antiparasitic drugs, a high level of potency and selectivity for parasites versus host cells is essential. From a medicinal chemistry point of view, there is opportunity to optimize the chemical structures of the currently available class I/II HDACi for therapeutic use against parasites by modifying each one of the four portions (CAP, CU, linker, and ZBG) of the general pharmacophoric model for class I/II HDAC inhibition. The zinc-coordinating residues in HDACs and the tubular cavity between the zinc and the surface of HDAC enzymes are relatively well-conserved between human and parasite enzymes [264, 578-579], and the linker moiety of HDACi is not able to be varied a great deal, being restricted by the size and shape of the active site tunnel. Moreover, the length of the linker group has been found to be a major structural determinant for the antimalarial and antileishmanial activities of two classes of nonpeptide macrocyclic HDACi that displayed the maximal antileishmanial activity in analogues with linkers comprising eight or nine methylene units [268, 629], whereas the best antimalarial potency was observed for analogues with five or six methylene unit spacers. The CAP group involved in the interaction with the rim at the entrance of the catalytic tunnel has more scope for variation and exploitation, and it is to be expected that most attempts to improve the activity and/or selectivity of the future antiparasitic HDACi will focus on this.

Therefore, in an attempt to identify HDAC inhibitors with potent and selective antimalarial activity, we examined a first series of HDAC inhibitors, including uracil-based hydroxamides (UBHAs, MC1746 and MC1761) (Fig. 6.1). Antiparasitic activity revealed MC1746, the only HDACi selective towards classes I and IIb of HDACs, as the most potent compound, with IC_{50} value of 79.38 nM against *Pf3D7* sensitive strains (Table 6.1). On the

other hand, none of the sirtuin inhibitors exhibited appreciable parasite growth inhibition (in general IC_{50} values $> 1 \mu M$).

To further generate structure-activity relationships on MC1746, another small group of analogues (Table 6.2) were synthesized and evaluated their HDAC inhibitory activity against *P. falciparum*. From this series, 4 analogues of MC1742 (MC1716, MC1738, MC1745 and MC1746) were found to be active against *P. falciparum* (Table 6.2). Respect to MC1742, the new analogues were different for the C6-uracil substitution [various aryl or aryl methyl instead of 4-biphenyl group], or for the length of the spacer between the sulphur atom and the hydroxamide [5 instead of 4 methylene groups], or for both. Similar to MC1746, the new analogues showed the selectivity for class I/IIb HDACs inhibition. When tested against 3D7, several analogues showed a better potency respect to the hit/MC1746, where MC1742 was the most potent derivative with IC_{50} values of 4 and 6 nM against *Pf*3D7 sensitive and W2 multidrug resistant strains, respectively.

From our previous work, in the UBHA general structure, the introduction of benzyl/phenyl moiety at the C6 position of the uracil group furnished highly active derivatives, depending on either the size of the linear spacer or the methylenecinnamyl regioisomer connecting the uracil with the hydroxamate group. Likewise, compounds with a linear, polymethylene spacer between the uracil and the hydroxamate showed the highest activity with the insertion of 4 to 5 carbon units. By increasing this number to 7 carbon units as well as by introducing shorter, linear HSs in the UBHA general formula, a decrease of inhibiting activity was recorded. Particularly, the corresponding unsaturated analogues failed in inhibiting HDACs. This study also showed that the C₆ phenyl substituted analogues performed better activity toward *P. falciparum* compared to the C₆ benzyl ones. Indeed, the C₆ benzyl/phenyl substitution with bulkier aromatic rings, in general, led to derivatives with better parasite inhibitory activity. In fact, as far as the C₆ phenyl substituted analogues are considered, the 4'-biphenyl showed the best parasite inhibitory activity followed by 2-naphthyl whilst the *meta* and *para* chloro-substituted phenyl displayed moderate inhibitory activity. Interestingly, in all compounds, when we compare the linear HSs of the tested compounds, compounds having 4 carbon unit showed a better potency in comparison to 5 carbon unit compounds, for example, MC1742 vs MC1738 ($IC_{50} = 6.03$ vs 50.89) and MC1745 vs MC1746 ($IC_{50} = 25.17$ vs 79.38).

In the light of potential role of MC1742 to inhibit HDACs, its role was explored on Histone H4 acetylation in *P. falciparum*. Treated parasites with MC1742 clearly exhibit increased H4 acetylation, supporting that this compound acts as parasite HDACs inhibitor. The toxicity of MC1742 against murine primary cells and human cell line revealed SI values of 186 and 783, respectively. These data, together with the PK studies, prompted us to examine MC1742 in a rodent model of malaria infection. Mice treated with MC1742 did not show any reduction of parasitemia at day 4 post infection and thereafter either after an oral administration or after a combination of oral/i.v. injections. In mice treated with chloroquine at 10 mg/kg, no blood stage parasites were detected. It is unlikely that the lack of *in vivo* activity could be linked to differences in targeted HDAC enzymes as they are well conserved between *P. falciparum* and *P. berghei* (60 up to 95% aa identity). The failure of MC1742 to cure mice at doses up to 50 mg/kg twice a day may be due to a too short exposure of parasites to the compound, even after 4-days treatment. Another possibility may be related to the mouse model in which *P. berghei* could be less sensitive *in vivo* due to genetic redundancy and /or to a tighter control of the target expression level. This could be further explored by additional studies using *P. falciparum*-infected *humanized SCID* mice receiving human erythrocytes [731]. This approach could also point out whether metabolism of human versus mouse erythrocytes could affect the antiparasitic activity of the compound. However, in the context of hydroxamate-based drugs, it is noteworthy that several and convergent studies reported that they showed high potencies *in vitro* when compared to approved drugs, but yet exhibited poor antimalarial activities [620, 630, 732].

In general, MC1742's lack of *in vivo* activity was unexpected considering its best ever *in vitro* activity against *Pf3D7* sensitive and W2 multidrug resistant strains compared to the previously reported HDAC inhibitors (see Table 4.3).

6.6 Methods

6.6.1 Determination of *in vitro* activity against *P. falciparum*

Growth inhibition assay performed on *P. falciparum* 3D7 line using SYBR Green I was described in detail in Fréville *et al.* [733]. Briefly, *in vitro* cultured *P. falciparum* 3D7 line infected erythrocytes (0.5% parasitemia, 1% haematocrit) were seeded in duplicate wells into 96-well tissue culture plates containing vehicle control (DMSO, <0.5%), positive control (chloroquine, Sigma Aldrich) or test compound and incubated under standard *P. falciparum* culture conditions for 48 h. Cultures were stained for 30 minutes in the dark with SYBR Green

I 1X (Invitrogen) diluted in 20 mM Tris pH 8.8, 138 mM NaCl, and fixed with 1% paraformaldehyde. Fixed parasitized red blood cells (RBC) were stored at 4°C in the dark until flow cytometry analysis. Parasite growth was assessed by flow cytometry on a BD FACS Cantoll (BD Biosciences). Cell pairs were excluded from the analysis using a forward scatter (FSC)-width *versus* FSC-area dot plot. Infected and uninfected erythrocytes were gated on the basis of their FSC and side scatter (SSC) signals. Fluorescence analysis (Green fluorescence FITC) was performed using BD FACSDiva software (version 6.1.3, BD Biosciences) on a total of 200,000 acquired events. Fluorescence was observed on a two-parameter dot plot (FITC-FSC). Fluorescence of non-infected RBC was adjusted to plot between 10^0 and 10^2 .

For testing the inhibitory effects on *P. falciparum*, a drug-sensitive (3D7) and drug-resistant (W2) line were used. For both *P. falciparum* cell lines growth inhibition was initially assessed at 10 μ M in two independent assays. Compounds showing more than 50% inhibition at 10 μ M were then tested in dose response assays to determine 50% growth inhibition (IC_{50}) values on Pf3D7. All IC_{50} values were calculated using log-linear interpolation with mean values (\pm SD) determined over two independent experiments [734].

6.6.2 In vivo experiments

Parasite clearing was examined in an acute infection murine model. To test the anti-malarial effect *in vivo*, the Peter's test was followed using BALB/c male mice infected with *P. berghei* ANKA strain parasites [730]. The compounds were administered *per os*, twice a day for 4 days (D0 to D3). Each experiment comprised 3 groups of mice: a first group of 6 mice was given the compound to be tested at the appropriate concentration determined by the PK studies, *i. e.* 50 mg/kg for MC1742; a second group of 6 mice, the negative control (DMSO, 7%) and the third group of 3 mice, the positive control (CQ at 10 mg/kg, once a day). The experiment lasted for 4 days. At Day 0, the mice were all infected i.p. with 10^6 parasitized red blood cells with *P. berghei* ANKA strain. At Day 4, the parasitemia was determined for each mouse on blood smears. Mice parasitemia was followed thereafter for 2 weeks. For each compound, the experiment was repeated twice.

All animal experiments were approved by the animal ethics committee, in accordance with the French National Regulations. In this study, infected animals with at least 2 clinical signs (respiratory distress, lethargy, piloerection, anemia and body loss weight) were euthanized and this time point is denoted as time of death.

7. DESIGN, SYNTHESIS AND PRELIMINARY BIOLOGICAL VALIDATION OF *SCHISTOSOMA MANSONI* SIRT2 INHIBITORS

7.1 Research Project

Most of the current efforts to identify new drug leads for schistosomiasis and other neglected parasitic diseases rely on the screening of random compound libraries directly on the parasite maintained in culture (phenotypic screening). The recent publication of the genome sequences of a variety of parasites including the three-main species of schistosomes that infect humans [735-737] now means that approaches targeting specific gene products or pathways can be envisaged. These can include enzymes with activities specific to the parasite, or at least not found in the human host [738], metabolic bottlenecks, or molecules that are targeted in other pathologies. Nevertheless, the use of high-throughput screening of extensive compound libraries represents a complementary strategy that has recently been used with success to generate inhibitors of human Sirts 1, 2 and 3 that show nanomolar IC₅₀ inhibitory values, although they are not selective [711]. It is to be expected that the application of both high-throughput and structure-based screening strategies will rapidly lead to the identification of both selective and potent sirtuin inhibitors. It has been reported that sirtuins have vital role in parasite survival by catalyzing the deacetylation reaction of acetylated lysine residues of nuclear histones and other substrates, with NAD⁺ as a cofactor [708]. Altogether, five sirtuins were found to be encoded in *S. mansoni* genome, which are orthologues of the human sirtuins SIRT1, SIRT2, SIRT5, SIRT6 and SIRT7. The encoded sirtuins are expressed at all stages of *S. mansoni* life cycle; suggesting that schistosome sirtuins could be potential therapeutic targets and validate screening for selective sirtuin inhibitors as a strategy for the development of new drugs against schistosomiasis.

Previous work showed strong effects of hSirt2 inhibitors on both worm life span and reproduction. The molecular features of SmSirt2 as well as its use for the development of new targets for schistosomiasis were explored in some recent studies [709-710]. The schistosome sirtuins, while showing overall conservation of essential catalytic domain residues [686], also show significant differences. The solution of crystal structures of schistosome sirtuins bound to inhibitors would represent a significant advance for the development of selective inhibitors [706]. Indeed, in a recent study, fluorescence-based assays were optimized for *S. mansoni* Sirt2 that allowed a pilot screen with inhibitors showing IC₅₀ values of <50 μ M and docking studies rationalizing the binding of hits to the target using a homology model of the enzyme

[712]. All these efforts constituent a very good foundation for further development of *SmSirt2* inhibitors.

GSK published for the first time the outcome from a parallel high throughput screening of a pharma compound collection (1.8 million compounds) against three kinetoplastids: *Leishmania donovani*, *Trypanosoma cruzi* and *Trypanosoma brucei*. Three corresponding kinetoplastid chemical boxes of, 200 compounds each were assembled, encompassing a wide variety of potential targets, such as kinases, proteases, and cytochromes as well as potential host-pathogen interaction targets. After the setup of the three chemical boxes, they were made public with all the relevant data to encourage the search for new potent drugs. These chemical boxes prompted us to apply for *Schistosoma mansoni* based on the basic idea that, like *T. cruzi*, *T. brucei* and *L. donovani*, *Schistosoma mansoni* is a parasite with a complex life cycle during which many morphological changes are expected that may be partially determined by epigenetic modulators. In our attempt to identify *smSIRT2* inhibitors (perhaps with the help of our collaborator Prof. Jung), the three chemical boxes were then tested on *smSirt2* and, from the assays carried out, some compounds are emerged with a discrete activity on the target enzyme. We thus decided to work on a particular compound: TCMDC-143295 (Fig. 7.1), as the starting point for development of novel *smSIRT2* inhibitors. TCMDC-143295 is a pyrimido[4,5-d]pyrimidine with three amino groups, one of which in turn substituted, of which an IC_{50} value of $23.7 \pm 9.6 \mu M$ was calculated that we considered it to be a good starting point for our next optimization work. All biological evaluations have been done at Prof. Jung's lab at the Institute of Pharmacy, Albert-Ludwigs-University of Freiburg, Germany.

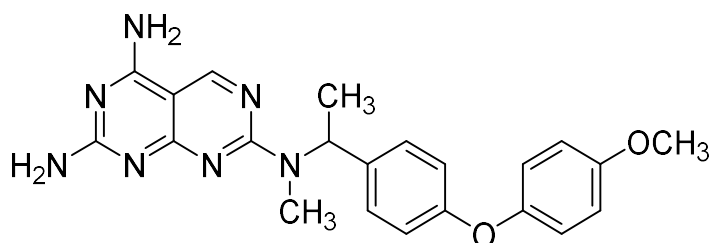


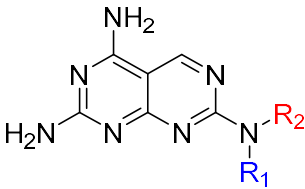
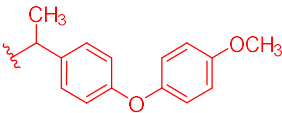
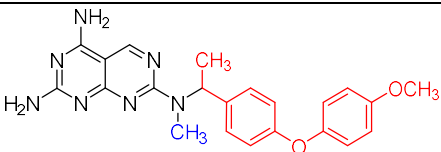
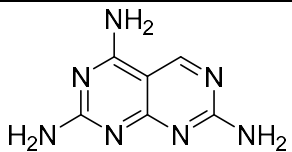
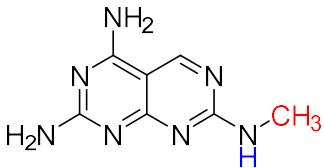
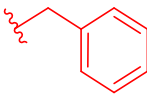
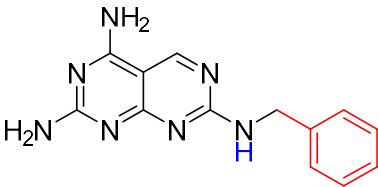
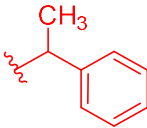
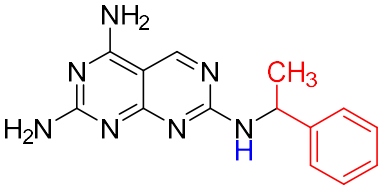
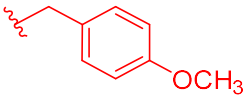
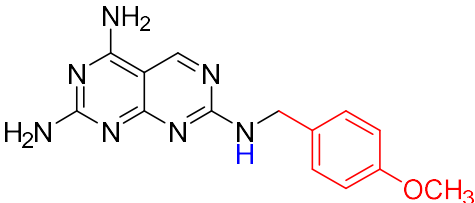
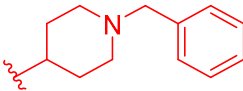
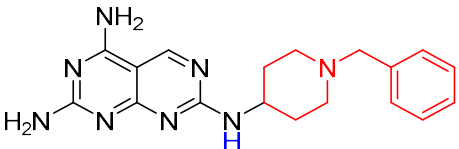
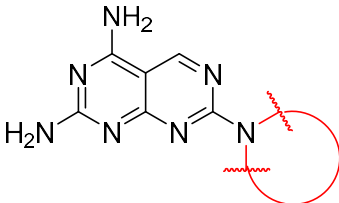
Fig. 7.1: Chemical structure of TCMDC-143295

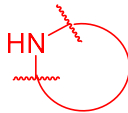
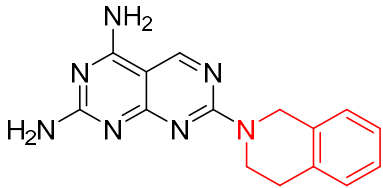
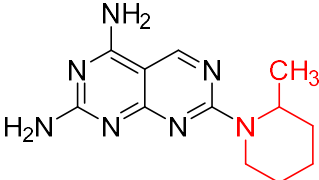
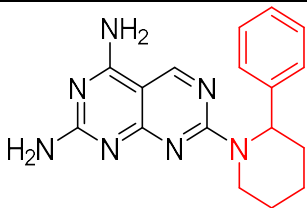
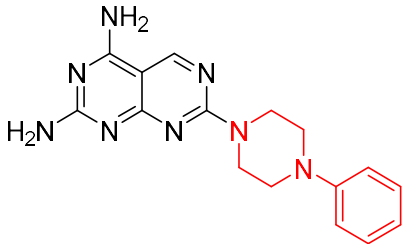
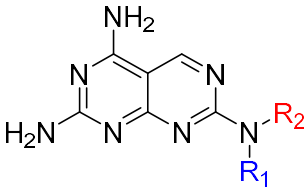
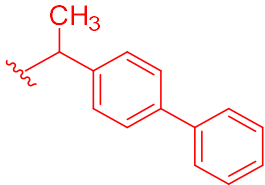
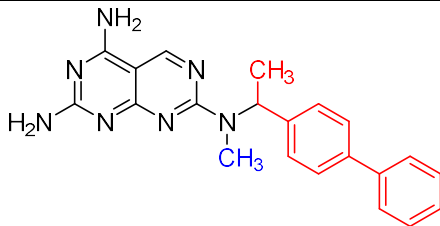
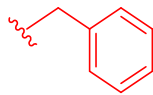
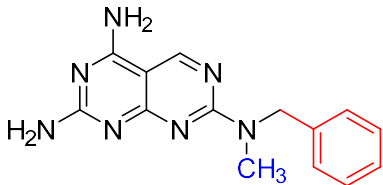
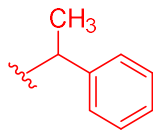
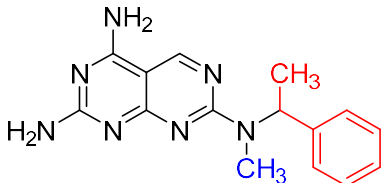
Starting from the prototype, we decided to synthesize analogues characterized by a simplified structure. Being the starting molecule characterized by a structure that is already quite important from the point of view of dimensions, it was thought to embark on a

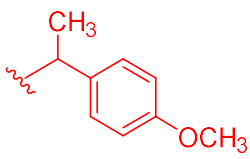
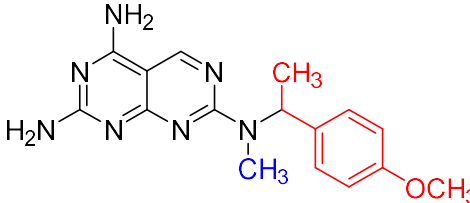
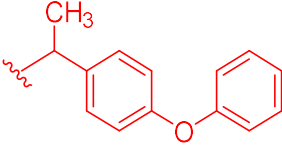
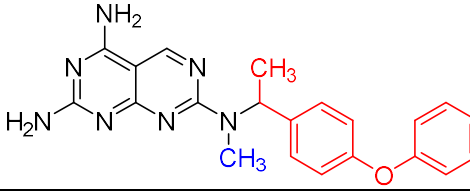
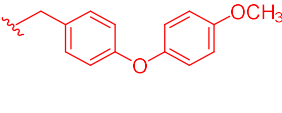
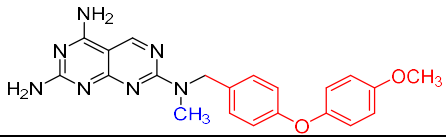
"molecular striptease" pathway that, through progressive de-construction, would allow us to identify analogues with the smallest molecular portion that retain or improve the inhibitory activity against *smSirt2*. In particular, the idea was to maintain the pyrimido[4,5-d]pyrimidine portion (which could be important for the activity, perhaps mimicking the adenosine portion of NAD⁺) with the two free amine groups.

Extensive structure-activity relationship (SAR) studies have been applied on the N⁷-(1-(4-(4-methoxyphenoxy)phenyl)ethyl)-N⁷-methylpyrimido[4,5-d]pyrimidine-2,4,7-triamine (TCMDC-143295) to obtain new hit compounds showing potent and selective inhibition of *smSirt2*. In particular, in a first stage of the project, the influence of substituents at the N⁷ position of the *bispyrimidine* ring of TCMDC-143295 has been explored by replacing the substituents on the prototype basically by substituents with smaller structures (Table 7.1). In general, the newly synthesized analogues in this attempt can be represented by four groups: (i) the N⁷ position of the *bispyrimidine* is a primary amine, i.e., no substituents (**2**, **MC4222**), (ii) the N⁷ position of the *bispyrimidine* is a secondary amine, i.e., no methyl group at the N⁷ position (**3-7**, **MC4262**, **MC4261**, **MC4189**, **MC4234**, **MC4265**); (iii) the N⁷ position of the *bispyrimidine* is a tertiary amine and is a part of a cyclic structure (**8-11**, **MC4232**, **MC4235**, **MC4269**, **MC4236**); and (iv) the N⁷ position of the *bispyrimidine* is a tertiary amine, i.e., with methyl group at the N⁷ position, (**1**, **12-17**, **MC4223**, **MC4268**, **MC4180**, **MC4210**, **MC4231**, **MC4211**, **MC4233**).

Table 7.1: The newly synthesised derivatives in the first round of optimazation

				
Sr. No	Lab code	R ₁	R ₂	Structure
1	MC4223	CH ₃		
2	MC4222	H	H	
3	MC4262	H	CH ₃	
4	MC4261	H		
5	MC4189	H		
6	MC4234	H		
7	MC4265	H		
				

Sr. No	Lab code			Structure
8	MC4232	1,2,3,4-tetrahydroisoquinoline		
9	MC4235	2-methylpiperidine		
10	MC4269	2-phenylpiperidine		
11	MC4236	1-phenylpiperazine		
				
S.No	Lab code	R ₁	R ₂	Structure
12	MC4268	CH ₃		
13	MC4180	CH ₃		
14	MC4210	CH ₃		

15	MC4231	CH ₃		
16	MC4211	CH ₃		
17	MC4233	CH ₃		

Surprisingly, when the final compounds were subjected to enzymatic assays for their inhibitory activity of *sm*SIRT2 and hSIRT2 at Prof. Jung's laboratory, we noticed that majority of the newly synthesized compounds displayed no activity against both *sm*SIRT2 and hSirt2 inhibition. Only MC4233 and MC4211 showed some activity against *sm*SIRT2. From this attempt, we learnt that smaller substituents or no substituents at N⁷ position of the *bispyrimidine* yielded analogues devoid of activity. Though the changes made to the prototype did not allow derivative with better activity against *sm*SIRT2, on the other hand, this attempt highlights the core SARs of the molecule which intern could be useful input for the next optimization process. In particular, it was possible to notice that the diphenyl ether portion is indispensable for activity against the parasite's enzyme as well as presence of *para* methoxy in the second phenyl moiety.

In light of the above observations, in the second part of the project, we decided to keep the N⁷-methyl. Indeed, the alpha carbon at N⁷ position has been replaced with larger steric groups compared the prototype to increase molecular constraint while the portion of diphenyl ether, given its importance, remained almost unchanged, though we investigate the effect of other heteroatoms instead of oxygen, or increasing the linkage or replacing the second phenyl with bulky groups (Table 7.2). Thus, in the second round of modification, we decided to keep the methyl group at N⁷ position of the *bispyrimidine* (R₁ = CH₃), except in the case of MC4314 (R₁ = H), in any way we did modification at four regions of the molecule (Fig. 7.2): (i) removing the methyl group at N⁷ position of the *bispyrimidine* (**18**, **MC4314**); (ii) introduction of bulky groups at α-carbon of the N⁷ position of *bispyrimidine* (R₂), i.e., replacing

methyl group by ethyl (**19**, **MC4315**), isopropyl (**20**, **MC4313**) or phenyl (**21**, **MC4318**) group; (iii) substitution of the oxygen linkage between the two phenyls (**X**) by sulfur (**22**, **MC4304**) or nitrogen (**23**, **MC4316**); or increase this linkage by one carbon (**24**, **MC4320**); (iv) substitution of the 4-methoxyphenyl part the molecule (**R₃**) by 3,4-dimethoxyphenyl (**25**, **MC4310**), 3,5-dimethoxyphenyl (**26**, **MC4319**), 3,4,5-trimethoxyphenyl (**27**, **MC4309**), 4-trifluoromethoxyphenyl (**28**, **MC4311**), 3-methoxyphenyl (**29**, **MC4298**), 4-benzoyloxyphenyl (**30**, **MC4312**), or 4-methoxynaphthalenyl (**31**, **MC4323**).

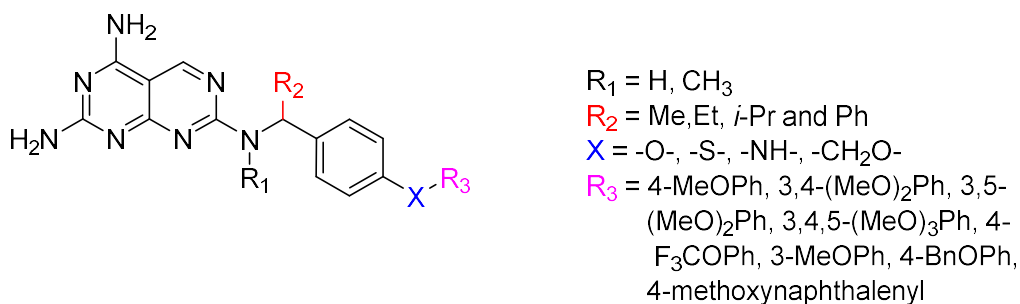
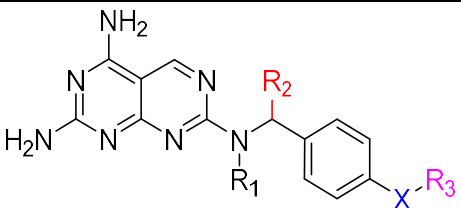
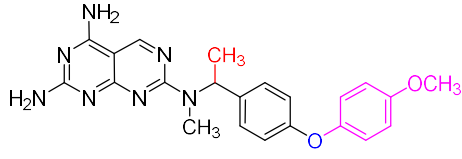
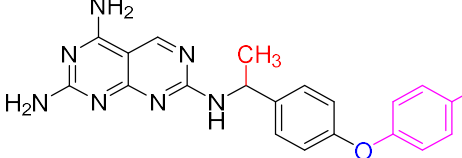
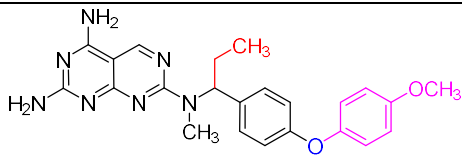
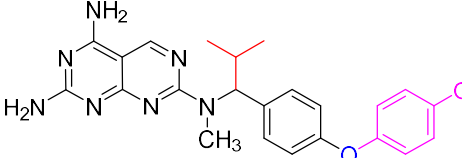
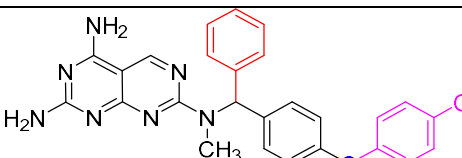
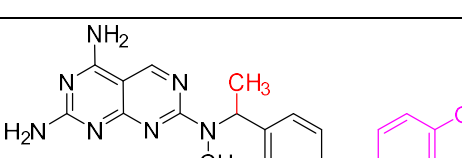
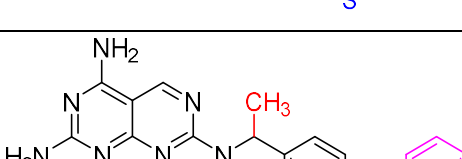


Fig. 7.2: Designed analogues for the second round of optimization

Table 7.2: The newly synthesised derivatives in the second round of optimization

						
Sr. No	Cpd	R ₁	R ₂	X	R ₃	Structures
1	MC4223	Me	Me	O	4-MeOPh	
18	MC4314	H	Me	O	4-MeOPh	
19	MC4315	Me	Et	O	4-MeOPh	
20	MC4313	Me	<i>i</i> -Pr	O	4-MeOPh	
21	MC4318	Me	Ph	O	4-MeOPh	
22	MC4304	Me	Me	S	4-MeOPh	
23	MC4316	Me	Me	N	4-MeOPh	

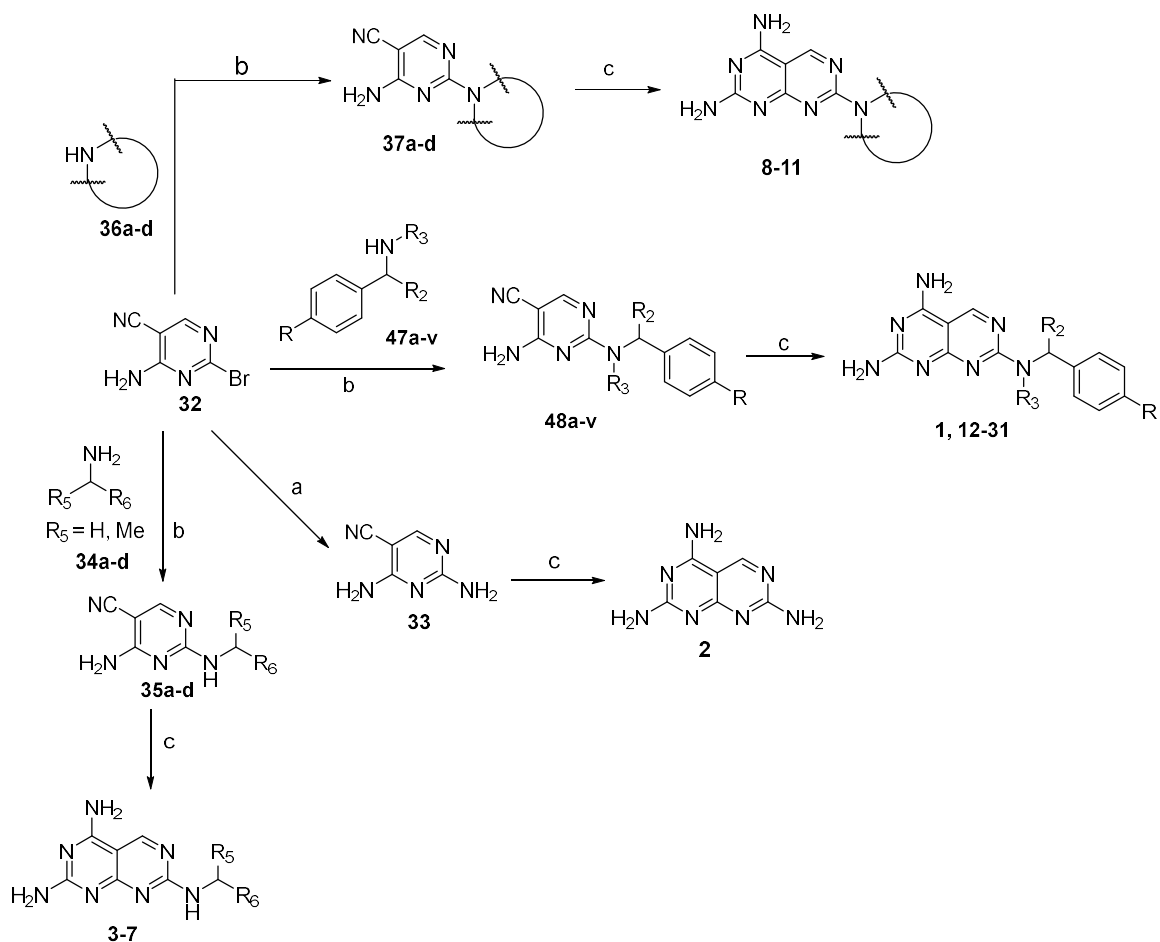
24	MC4320	Me	Me	CH ₂ O	4-MeOPh	
25	MC4310	Me	Me	O	3,4-(MeO) ₂ Ph	
26	MC4319	Me	Me	O	3,5-(MeO) ₂ Ph	
27	MC4309	Me	Me	O	3,4,5-(MeO) ₃ Ph	
28	MC4311	Me	Me	O	4-F ₃ COPh	
29	MC4298	Me	Me	O	3-MeOPh	
30	MC4312	Me	Me	O	4-BnOPh	
31	MC4323	Me	Me	O	4-Methoxynaphthalen-1-yl	
Store all compounds at -20 °C and dissolve them in DMSO.						

7.2 Chemistry

The final compounds (**1**, **3-31**) were prepared from condensation of the free base guanine and the key pyrimidine intermediates (**33**, **35a-e**, **37a-d**, **48a-v**) that are appropriately substituted at N² position of the pyrimidine ring according to Scheme 1. While

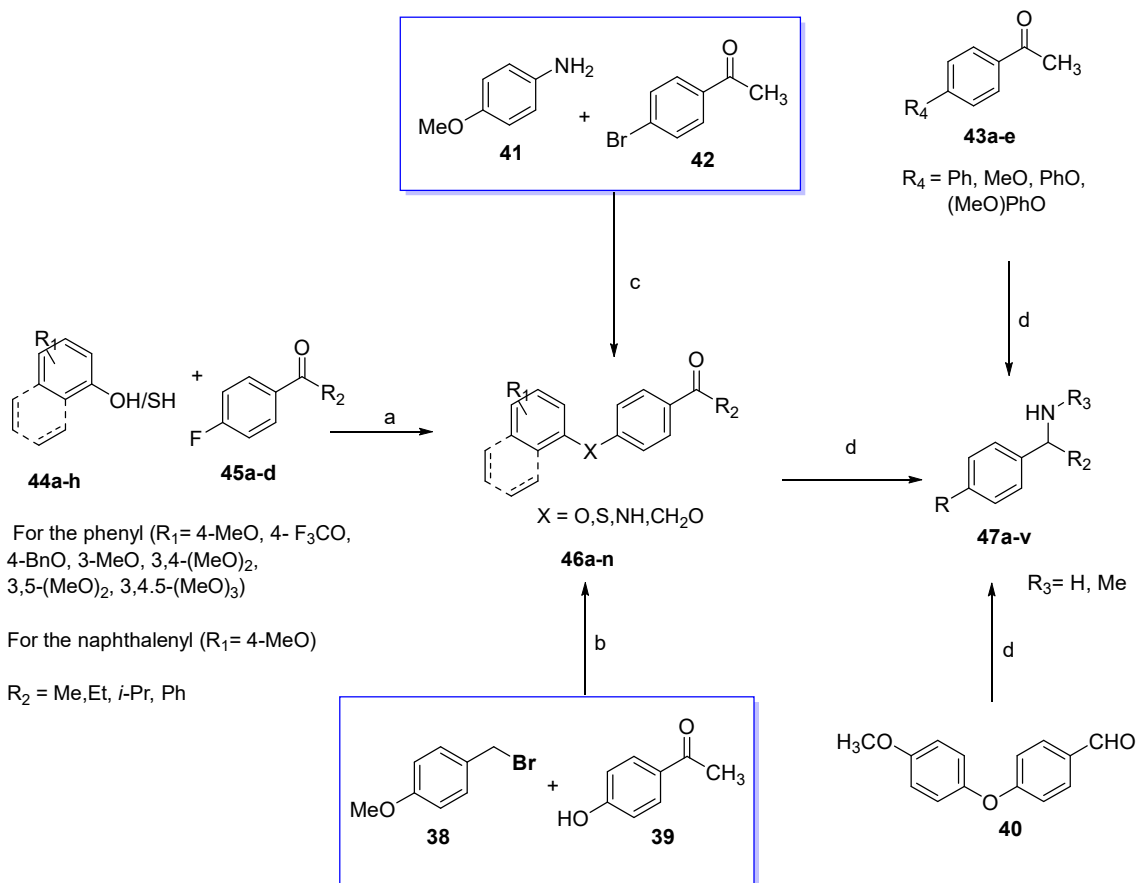
compound **2** was prepared by refluxing guanidine and the unsubstituted pyrimidine (**33**), which in turn was prepared from 4-amino-2-bromopyrimidine-5-carbonitrile (**32**) by treating with 7 M methanolic solution of NH_3 . On the other hand, the displacement reaction between **32** and the commercially available amines (**34a-e** and **36a-d**) in 2-MeOEtOH in the presence of Et_3N afforded the intermediates **35a-f** and **37a-d**, respectively. Similar displacement reaction between **32** and **47a-v** also gave the intermediates **48a-v**. Except compound **47b** and **g**, which are commercially available, the other amines (**47a,c-f**, and **h-v**) were synthesized starting from the appropriately substituted carbonyl compounds (**40**, **43a-e** and **46a-n**) by treating with a 2 M solution methylamine in anhydrous MeOH in the presence of $\text{Ti}(\text{O}i\text{-Pr})_4$, and a subsequent addition of the reducing agent NaBH_4 yielded the aforementioned amine intermediates (Scheme 2). While compound **40** and **43a-e** are commercially available, compounds **46a-n** are prepared according to Scheme 2 using three different procedures based on the nature of the connection unit (**X**). Compounds **46a-k**, having oxygen/sulfur as connecting unit (**X** = **O**, **S**), were synthesized from the appropriate naphthols/phenols (**44a-h**) and *para*-fluoro substituted ketones (**45a-c**) in the presence of anhydrous K_2CO_3 in dry DMF, while 1-(4-((4-methoxybenzyl)oxy)phenyl)ethan-1-one (**46l**), $-\text{CH}_2\text{O}-$ as connecting unit, was prepared by refluxing 1-(bromomethyl)-4-methoxybenzene (**38**) and 1-(4-hydroxyphenyl)ethan-1-one (**39**) together with K_2CO_3 and NaI in dry CH_3CN . Finally, the reaction of 4-methoxyaniline (**41**) and 1-(4-bromophenyl)ethan-1-one (**42**) in the presence of K_2CO_3 , $\text{Pd}_2(\text{dba})_3$ and Xphos in dry toluene yielded 1-(4-((4-methoxyphenyl)amino)phenyl)ethan-1-one (**46m**). Table 7.3. depicts the chemical and physical data of the final compounds.

Scheme 1^a



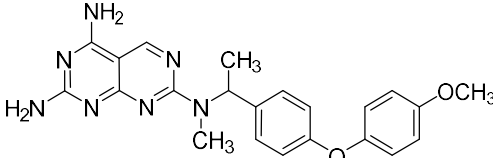
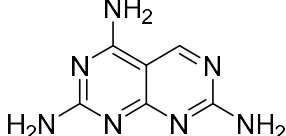
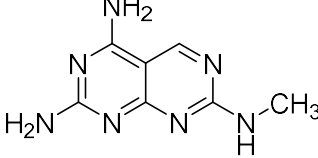
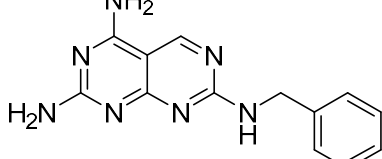
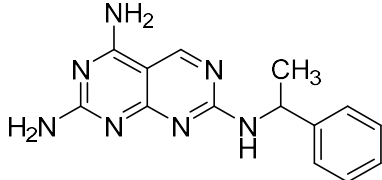
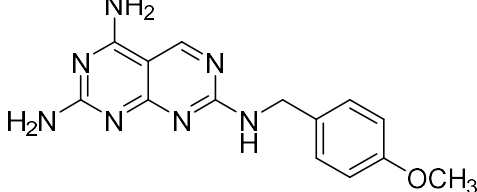
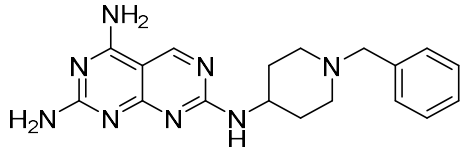
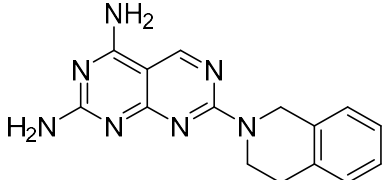
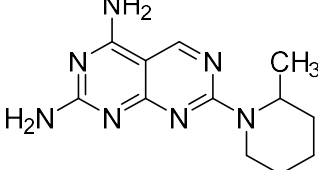
^a **Reagents and conditions:** (a) 7M methanolic NH₃, TEA, 2-MeOEtOH, 80 °C; (b) TEA, 2-MeOEtOH, 80 °C, 2.5 h; (c) guanidine, dry 2-MeOEtOH, 150 °C, 4.5 h

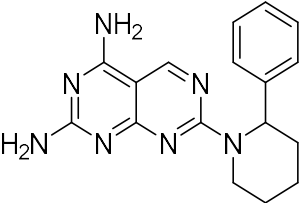
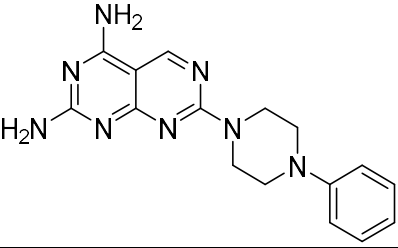
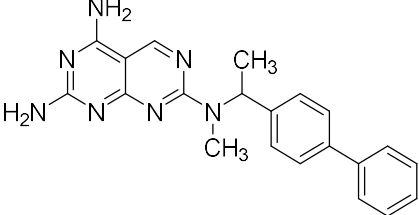
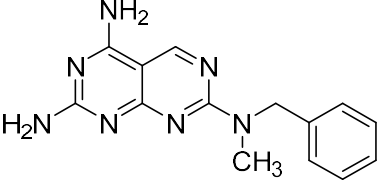
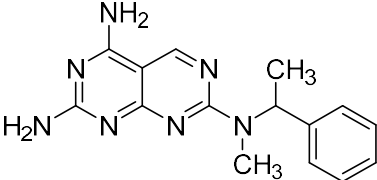
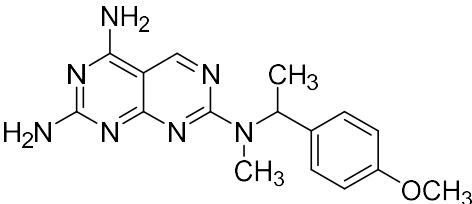
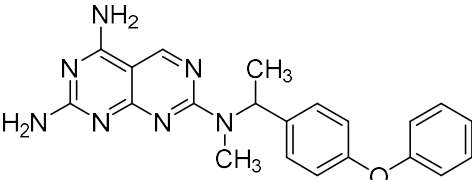
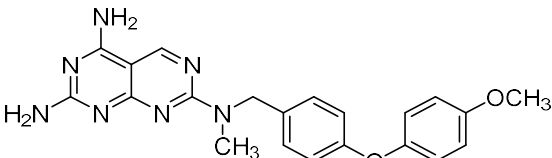
Scheme 2^a

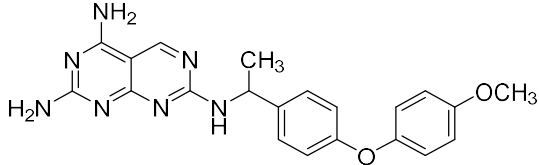
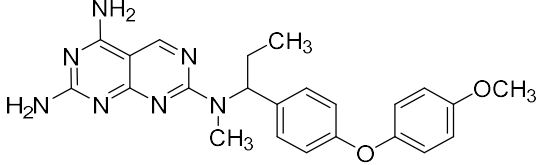
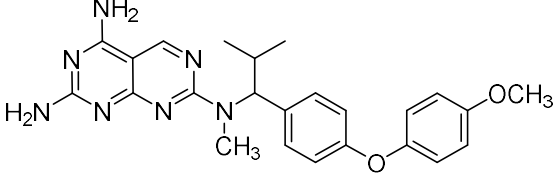
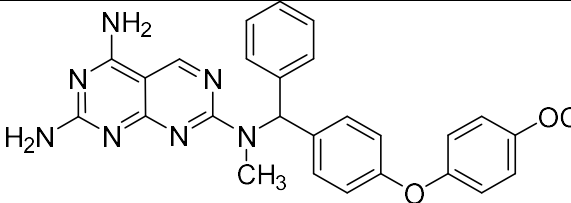
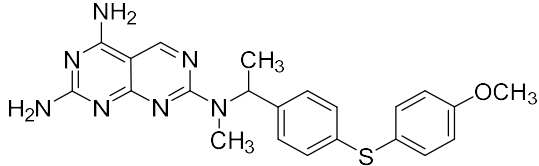
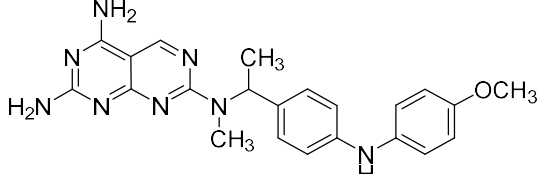
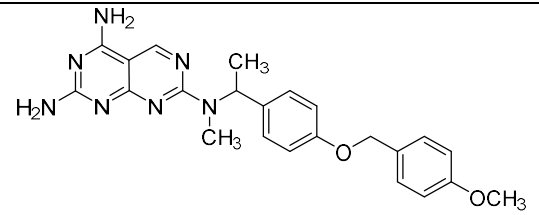
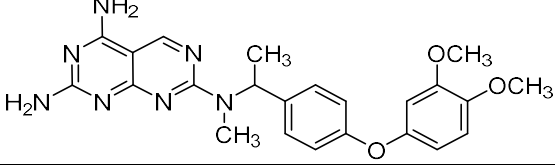
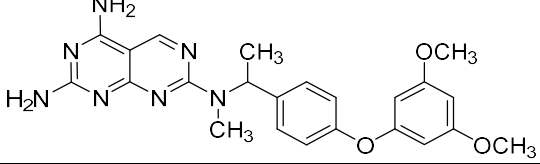


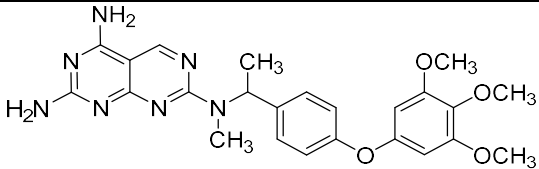
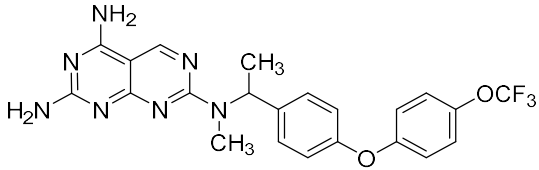
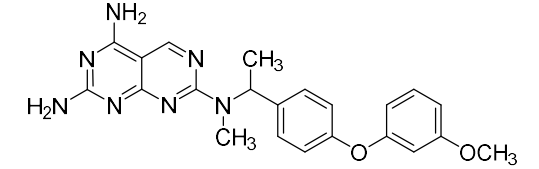
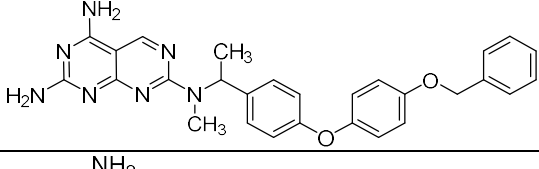
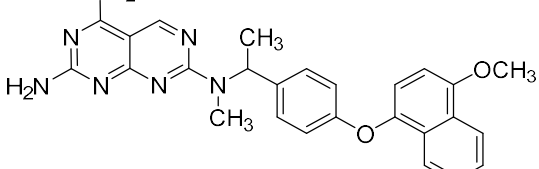
Reagents and conditions: (a) K_2CO_3 , dry DMF, 175°C ; (b) K_2CO_3 , NaI, dry CH_3CN , 95°C , 2.5 h; (c) K_2CO_3 , $\text{Pd}_2(\text{dba})_3$, Xphos, dry toluene, 140°C , 48 h; (d) (i) 2M methylamine, $\text{Ti}(\text{Oi-Pr})_4$, dry MeOH, N_2 , 5.5 h, rt; (ii) NaBH_4 , 0°C -rt.

Table 7.3. Physico-chemical data of compounds **1-31**

Sr. No	Cpd	Structure	MW	Mpt (°C)	Yield (%)
1	MC4223		417.47	181-184	60.0
2	MC4222		177.17	>300	68.5
3	MC4262		191.20	>300	70.1
4	MC4261		267.30	>300	75.4
5	MC4189		281.32	>300	68.3
6	MC4234		297.32	>300	82.7
7	MC4265		350.43	205-208	75.3
8	MC4232		293.33	278-280	70.6
9	MC4235		259.32	>300	52.8

10	MC4269		321.39	188-190	61.1
11	MC4236		322.38	>300	62.8
12	MC4268		371.45	>300	57.1
13	MC4180		281.323	275-277	65.2
14	MC4210		295.350	192-194	76.8
15	MC4231		325.376	184-187	60.1
16	MC4211		387.45	185-187	41.9
17	MC4233		403.45	244-247	68.0

18	MC4314		403.45	> 300	82.5
19	MC4315		431.50	186-190	60.7
20	MC4313		445.53	162-167	64
21	MC4318		479.54	248-250	58.8
22	MC4304		433.53	160-163	72.9
23	MC4316		416.49	146-149	52.1
24	MC4320		431.50	225-228	78.1
25	MC4310		447.50	185-188	69.2
26	MC4319		447.50	233-235	75.6

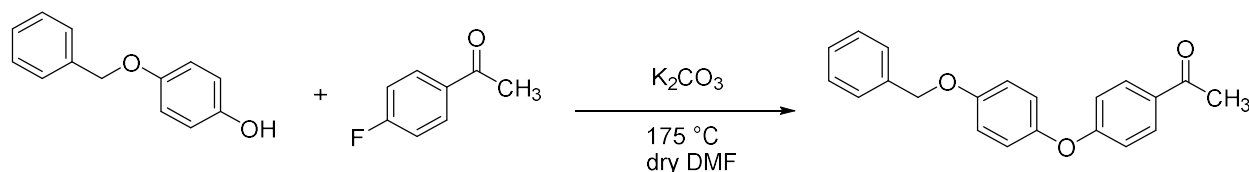
27	MC4309		477.53	172-176	67.1
28	MC4311		471.44	140-143	58.3
29	MC4298		417.47	152-154	47.4
30	MC4312		493.57	129-132	77.8
31	MC4323		467.53	>300	71.9

7.3 Experimental Section

Chemistry: melting points were determined on a Buchi 530 melting point apparatus. ¹H-NMR spectra were recorded at 400 MHz using a Bruker AC 400 spectrometer; chemical shifts are reported in δ (ppm) units relative to the internal reference tetramethylsilane (Me₄Si). Mass spectra were recorded on a API-TOF Mariner by Perspective Biosystem (Stratford, Texas, USA), samples were injected by an Harvard pump using a flow rate of 5–10 μ L/min, infused in the Electrospray system. All compounds were routinely checked by TLC and ¹H-NMR. TLC was performed on aluminum-backed silica gel plates (Merck DC, Alufolien Kieselgel 60 F₂₅₄) with spots visualized by UV light or using a KMnO₄ alkaline solution. All solvents were reagent grade and, when necessary, were purified and dried by standard methods. Concentration of solutions after reactions and extractions involved the use of a rotary evaporator operating at reduced pressure of \sim 20 Torr. Organic solutions were dried over anhydrous sodium sulfate. Elemental analysis has been used to determine purity of the described compounds, that is > 95%. Analytical results are within 0.40% of the theoretical values. All chemicals were purchased from Sigma Aldrich s.r.l., Milan (Italy) or from TCI Europe N.V., Zwijndrecht (Belgium), and were of the highest purity. As a rule, samples prepared for physical and

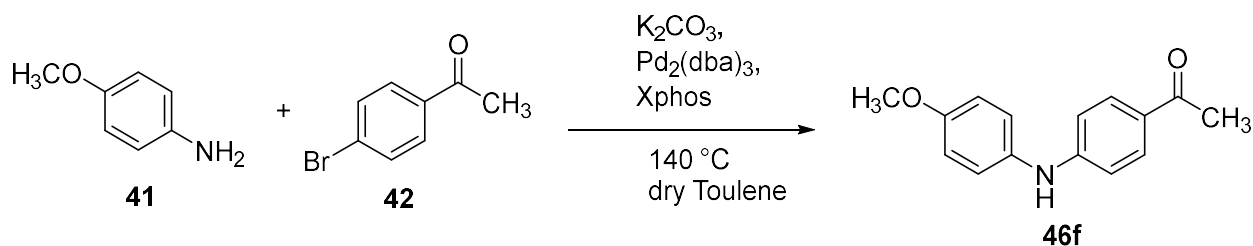
biological studies were dried in high vacuum over P2O5 for 20h at temperatures ranging from 25 to 40 °C, depending on the sample melting point.

General procedure for the synthesis of intermediates 46a-e and h-n. Example: 1-(4-(4-(benzyloxy)phenoxy)phenyl)ethan-1-one (46m).



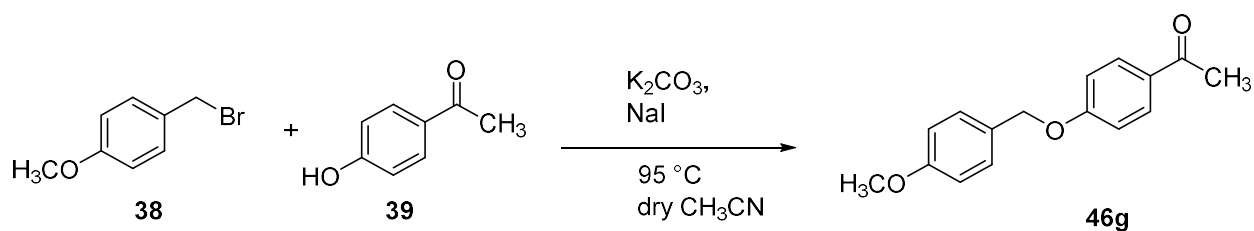
A mixture of 4-(benzyloxy)phenol (**44c**) (1 eq, 2.5 mmol), 1-(4-fluorophenyl)ethan-1-one (**45a**) (1 eq., 2.5 mmol) and K_2CO_3 (1.2 eq, 3 mmol) in anhydrous DMF (2.5 mL) was refluxed at 175 °C. After 2 h, another 0.2 eq. of **45a** and 0.25 eq. of K_2CO_3 were added and further 6 h stirring the reaction was completed and stopped by quenching with 20 mL of NaClss. Subsequently, extraction with EtOAc (5 x 20 mL) and washed with NaClss (2 x 5 mL) of NaClss. The organic phase thus was dried over Na_2SO_4 , filtered and evaporated. The crude was subjected to SiO_2 column purification using a mobile phase consisting of EtOAc/PE (1: 7) to afford **46m** as a white solid. Yield = 70.8%

General procedure for the synthesis of intermediate: 1-(4-((4-methoxyphenyl)amino)phenyl)ethan-1-one (46f).



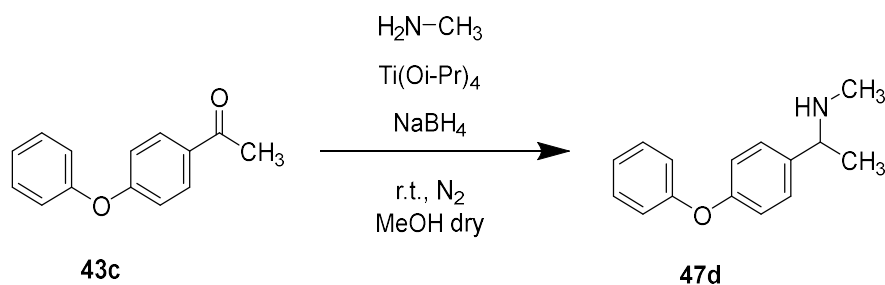
A mixture of 4-methoxyaniline (**41**) (1.2 eq, 3.014 mmol, 5 mL) and 4-(4-bromophenyl)ethan-1-one (**42**) (1 eq, 2.5 mmol) in the presence of K_2CO_3 , $Pd_2(dba)_3$ and Xphos in dry toluene was refluxed at 140 °C and left to stir for 48h. After this time, the reaction was stopped and diluted with 20 mL of EtOAc. Then the mixture was filtered using double filter paper with subsequent washing with chloroform. The combined organic phase was evaporated and the resulting crude was purified Chromatographed using SiO_2 with eluent of EtOA/Hexane/ $CHCl_3$ (15:70:15) to afford **46f** as a dark-brown oil. Yield: 66.01%

General procedure for the synthesis of intermediate: 1-(4-((4-methoxyphenyl)amino)phenyl)ethan-1-one (46g).



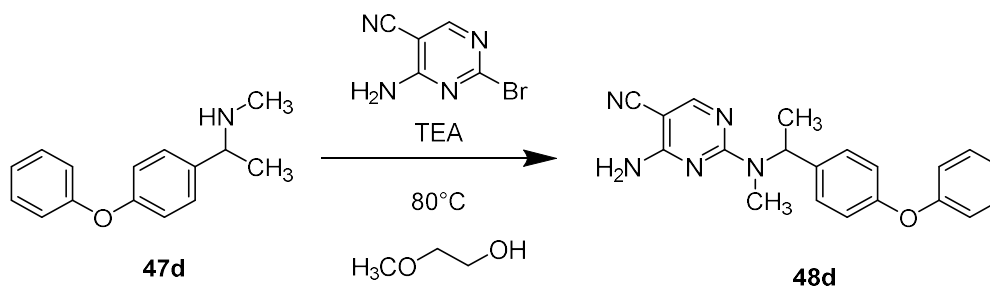
A mixture of 4 (methoxy)benzyl bromide (**38**) (1.2 eq., 3.6 mmol.) and 1-(4-hydroxyphenyl)ethan-1-one (**39**) (1 eq, 3 mmol) in anhydrous CH₃CN (15 mL) was reacted in the presence of K₂CO₃ (1.5 eq, 4.5 mmol) and NaI (1.1 eq, 3.3 mmol) at 95 °C. After 5 h, the reaction was finished and quenched with 20 mL of water. Following extraction with EtOAc (5 x 20 mL) and washing with NaClss (2 x 5 mL), the organic layer was dried over Na₂SO₄, filtered and evaporated. The crude was subjected to SiO₂ column purification using a mobile phase consisting of EeOAc/PE (1:8) to afford **46g** as a white solid. Yield = 57.58%.

General procedure for the synthesis of intermediates 47a, c-f, and h-v. Example: *N*-methyl-1-(4-phenoxyphenyl) ethan-1-amine (47d).



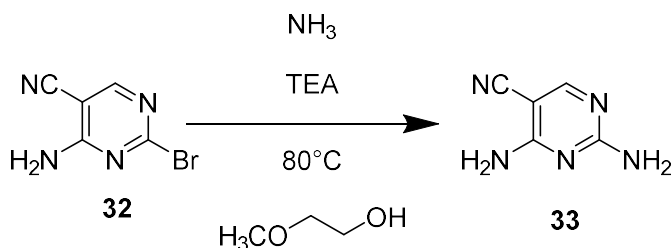
A mixture of 1-(4-phenoxyphenyl) ethan-1-one (**43c**) (1 eq, 2 mmol), methylamine 2 M in methanol (3 eq, 6 mmol) and Ti(Oi-Pr)₄ (1.3 eq., 2.6 mmol) in anhydrous methanol (5 ml) was reacted under nitrogen and rt for 5 h 30min, subsequently, NaBH₄ (1.1eq, 2.2mmol) was added at 0 °C and kept the reaction string at rt for another 2 h. Then, the reaction was stopped by quenching with distilled H₂O (20 mL) and acidified with 1M HCl (12 mL) until a pH of 1-2. The resulting suspension was filtered on celite and washed with a mixture of water and EtOAc. The filtrate was extracted with 20 ml of EtOAc. Following basification of the aqueous layer to pH 10-12 using 10% NaOH (5 mL), it was further extracted with EtOAc (3 x 30 mL). The combined EtOAc layer was dried over anhydrous Na₂SO₄, filtered and evaporated. The resulting oily crude was then purified by silica chromatography eluting with a mixture of CHCl₃: MeOH: NH₃ (45: 1: 0.1) to obtain the pure *N*-methyl-1-(4-phenoxyphenyl)ethan-1-amine (**47d**) as an oil.

General procedure for the synthesis of intermediates 35a-f, 37a-d, 48a-v. Example: 4-amino-2- (methyl (1-(4-phenoxyphenyl) ethyl)amino)-pyrimidine-5-carbonitrile (48d).



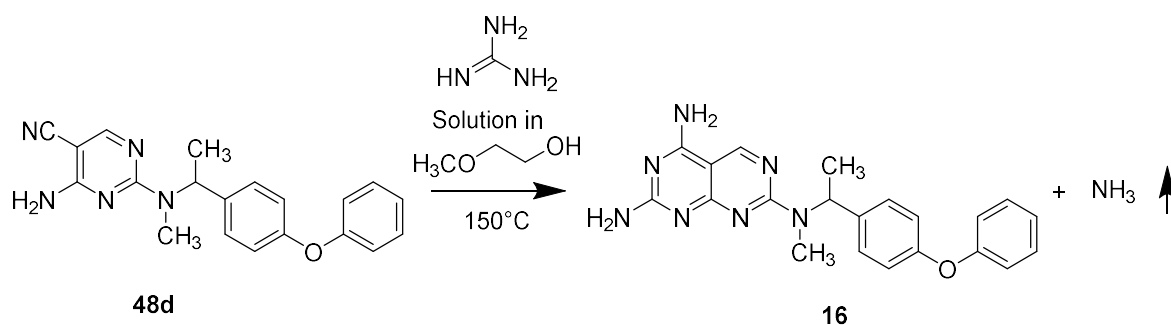
N-methyl-1- (4-phenoxyphenyl) ethan-1-amine (**47d**) (1.2 eq, 1.2 mmol), 4-amino-2-bromopyrimidine-5-carbonitrile (**32**) (1 eq, 1.0 mmol), TEA (1.6 eq, 1.6 mmol) and 2-MeOEtOH (2.0 mL, equal to [c] = 0.5 M) were added to a vial and heated at 80 ° C. After 2.5h, the reaction was stopped and transferred into round bottom flask and evaporated. To the crude 60 mL of EtOAc was added and washed with 0.1 N KHSO₄ (2x3 mL) counter extracted with EtOAc. The combined organic layer was dried over Na₂SO₄, filtered and evaporated. The crude was purified by silica column eluting with a mixture of CHCl₃:n-Hexane (80:20) to give 4-amino-2- (methyl(1-(4-phenoxyphenyl)ethyl)amino)pyrimidine-5-carbonitrile (**48d**).

Synthesis of the intermediate of 2,4-diaminopyrimidine-5-carbonitrile (33)



A mixture of 7 M methanolic solution of NH₃ (1.3 eq), 4-amino-2-bromopyrimidine-5-carbonitrile (**32**) (1.0 eq), TEA (1.6 eq) and 2-MeOEtOH (2 mL) was refluxed at 80 ° C in a vial for 2.5 h. The reaction content was transferred into round bottom flask and evaporated and dissolved with 60 mL of EtOAc, followed by washing with 0.1 N KHSO₄ (2x3 mL) and counter extraction with EtOAc. The combined organic layer was dried over Na₂SO₄, filtered and evaporated to give a pure compound **33**.

General procedure for the synthesis of final compounds (1-30). Example: Synthesis of N⁷-methyl-N⁷- (1- (4-phenoxyphenyl) ethyl) pyrimido [4,5-d] pyrimidine-2,4,7-triamine (16)



4-Amino-2-(methyl (1-(4-phenoxyphenyl)ethyl) amino) pyrimidine-5-carbonitrile (**48d**) (1eq, 0.829 mmol) was reacted with a 0.73M free base guanidine solution (3.5 eq, 2.901 mmol) in 2-MeOEtOH anhydrous previously prepared. The reaction is conducted in an oil bath at a temperature of 150 ° C. After 4.5 h, the reaction content was transferred into a round bottom flask and evaporated. To the crude 10 mL of distilled H₂O are added and the extracted with EtOAc (5x40 mL). The organic phase was dried over Na₂SO₄, filtered and evaporated. The resulting crude was purified by silica column eluting with a mixture of CHCl₃:MeOH:NH₃ (20:1:0.1). After trituration with Et₂O and string for 45 minutes, it was filtered to yield a pure N⁷-methyl-N⁷-(1-(4-phenoxyphenyl) ethyl) pyrimido[4,5-d] pyrimidine-2,4,7-triamine (**16**) as white solid. ¹H NMR (400 MHz, DMSO- d₆) δ 8.96 (s, 1H, CH pyrimidine), 7.40-7.30 (m, 6H, NH₂ in pos. 4 pyrimido-pyrimidine and CH aromatic), 7.15-7.11 (m, 1H, CH aromatic), 7.01-6.97 (m, 4H, CH aromatic), 6.49 (s, 2H, NH₂ in pos. 2 pyrimido-pyrimidine), 6.30 (m, 1H, CHCH₃), 2.84 (s, 3H, N-CH₃), 1.53 (d, 3H, CHCH₃). MS (ESI) *m/z*: 378.18 [M]⁺.

N⁷-(1-(4-(4-Methoxyphenoxy)phenyl)ethyl)-N⁷-methylpyrimido[4,5-d]pyrimidine-2,4,7-triamine (1, 4223). ¹H NMR (400 MHz, DMSO- d₆) δ 8.95 (s, 1H, CH pyrimidine), 7.54 (s, 2H, NH₂ in pos. 4 pyrimido-pyrimidine), 7.27-7.25 (m, 2H, CH aromatic), 7.00-6.94 (m, 4H, CH aromatic), 6.90-6.87 (m, 2H, CH aromatic), 6.49 (s, 2H, NH₂ in pos. 2 pyrimido-pyrimidine), 6.28 (m, 1H, CHCH₃), 3.74 (s, 3H, OCH₃), 2.82 (s, 3H, N-CH₃), 1.51 (d, 3H, CHCH₃), MS (ESI) *m/z*: 417.19 [M]⁺.

Pyrimido[4,5-d]pyrimidine-2,4,7-triamine (2, MC4222). ¹H NMR (400 MHz, DMSO- d₆) δ 8.86 (s, 1H, CH pyrimidine), 7.31 (s, 2H, NH₂ in pos. 4 pyrimido-pyrimidine), 6.71 (s, 2H, NH₂ in pos. 7 pyrimido-pyrimidine), 6.44 (s, 2H, NH₂ in pos. 2 pyrimido-pyrimidine), MS (ESI) *m/z*: 177.08 [M]⁺.

N⁷-Methylpyrimido[4,5-d]pyrimidine-2,4,7-triamine (3, MC4262). ¹H NMR (400 MHz, DMSO- d₆) δ 8.85 (s, 1H, C-H pyrimidine), 7.3-7.1 (m, 3H, NH + NH₂ in pos. 4 pyrimido-pyrimidine), 6.45 (s, 2H, NH₂ in pos. 2 pyrimido-pyrimidine), 2.8 (s, 3H, NHCH₃), MS (ESI) *m/z*:

191.09 [M]⁺.

N⁷-Benzylpyrimido[4,5-d]pyrimidine-2,4,7-triamine (4, MC4261). ¹H NMR (400 MHz, DMSO- d₆) δ 8.85 (s, 1H, CH pyrimidine), 7.8 (sb, 1H, NH) 7.40-7.20 (m, 7H, NH₂ in pos. 4 pyrimido-pyrimidine + CH aromatic), 6.4 (s, 2H, NH₂ in pos. 2 pyrimido-pyrimidine), 4.5 (s, 2H, CH₂), MS (ESI) *m/z*: 267.12 [M]⁺.

N⁷-(1-Phenylethyl)pyrimido[4,5-d]pyrimidine-2,4,7-triamine (5, MC4189). ¹H NMR (400 MHz, DMSO- d₆) δ 8.85 (s, 1H, CH pyrimidine), 7.81-7.79 (sb, 1H, NH) 7.39-7.37 (m, 2H, NH₂ in pos. 4 pyrimido-pyrimidine), 7.30-7.27 (m, 4H, CH aromatic), 7.19-7.16 (m, 1H, CH aromatic), 6.44 (s, 2H, NH₂ in pos. 2 pyrimido-pyrimidine), 5.14 (m, 1H, CHCH₃), 1.42 (d, 3H, CHCH₃), MS (ESI) *m/z*: 281.14 [M]⁺.

N⁷-(4-Methoxybenzyl)pyrimido[4,5-d]pyrimidine-2,4,7-triamine (6, MC4234). ¹H NMR (400 MHz, DMSO-d₆) δ 8.86 (s, 1H, CH pyrimidine), 7.67 (sb, 1H, NH) 7.31-7.24 (m, 4H, NH₂ in pos. 4 pyrimido-pyrimidine + CH aromatic), 6.86-6.84 (m, 2H, CH aromatic), 6.46 (s, 2H, NH₂ in pos. 2 pyrimido-pyrimidine), 4.43-4.41 (m, 2H, CH₂), 3.60 (s, 3H, OCH₃), MS (ESI) *m/z*: 297.13 [M]⁺.

N⁷-(1-Benzylpiperidin-4-yl)pyrimido[4,5-d]pyrimidine-2,4,7-triamine (7, MC4265). ¹H NMR (400 MHz, DMSO- d₆) δ 8.84 (s, 1H, CH pyrimidine), 7.35-7.29 (m, 5H, NH + NH₂ in pos. 4 pyrimido-pyrimidine + CH aromatic), 7.27-7.26 (m, 2H, CH aromatic) 7.25-7.18 (m, 1H, CH aromatic), 6.40 (s, 2H, NH₂ in pos. 2 pyrimido-pyrimidine), 3.74 (s, 1H, CH piperidine), 3.46 (s, 2H, CH₂-Ph), 2.81-2.79 (m, 2H, CH₂ piperidine), 2.01 (t, 2H, CH₂ piperidine), 1.84-1.82 (m, 2H, CH₂ piperidine), 1.54-1.46 (m, 2H, CH₂ piperidine), MS (ESI) *m/z*: 350.20 [M]⁺.

7-(3,4-Dihydroisoquinolin-2(1H)-yl)pyrimido[4,5-d]pyrimidine-2,4-diamine (8, MC4232). ¹H NMR (400 MHz, DMSO- d₆) δ 8.97 (s, 1H, CH pyrimidine), 7.43 (s, 2H, NH₂ in pos. 4 pyrimido-pyrimidine), 7.25-7.18 (m, 4H, CH aromatic), 6.51 (s, 2H, NH₂ in pos. 2 pyrimido-pyrimidine), 4.92 (s, 2H, CH₂ piperidine), 4.03 (t, 2H, CH₂ piperidine), 2.86 (t, 2H, CH₂ piperidine), MS (ESI) *m/z*: 293.14 [M]⁺.

7-(2-Methylpiperidin-1-yl)pyrimido[4,5-d]pyrimidine-2,4-diamine (9, MC4235). ¹H NMR (400 MHz, DMSO- d₆) δ 8.90 (s, 1H, CH pyrimidine), 7.34 (s, 2H, NH₂ in pos. 4 pyrimido-pyrimidine), 6.43 (s, 2H, NH₂ in pos. 2 pyrimido-pyrimidine), 5.10 (m, 1H, CH piperidine), 4.69-4.66 (m, 1H, CH pyrimidine), 2.92-2.85 (m, 1H, CH piperidine), 1.70-1.58 (m, 5H, CH piperidine), 1.38-1.24 (m, 1H, CH piperidine), 1.14 (d, 3H, CHCH₃), MS (ESI) *m/z*: 259.15 [M]⁺.

7-(2-Phenylpiperidin-1-yl)pyrimido[4,5-d]pyrimidine-2,4-diamine (10, MC4269). ¹H NMR (400 MHz, DMSO- d₆) δ 8.93 (s, 1H, CH pyrimidine), 7.40 (sb, 2H, NH₂ in pos. 4 pyrimido-pyrimidine), 7.35-7.32 (m, 2H, CH aromatic), 7.23-7.18 (m, 3H, CH aromatic), 6.48 (s, 2H, NH₂ in pos. 2 pyrimido-pyrimidine), 6.19 (m, 1H, CH piperidine), 4.84-4.81 (m, 1H, CH piperidine), 2.84-2.81 (m, 1H, CH piperidine), 2.45-2.41 (m, 1H, CH piperidine), 1.84 (m, 1H, CH piperidine), 1.63-1.61 (m, 2H, CH₂ piperidine), 1.48-1.36 (m, 2H, CH₂ piperidine), MS (ESI) *m/z*: 321.17 [M]⁺.

7-(4-Phenylpiperazin-1-yl)pyrimido[4,5-d]pyrimidine-2,4-diamine (11, MC4236). ¹H NMR (400 MHz, DMSO- d₆) δ 8.96 (s, 1H, CH pyrimidine), 7.43 (s, 2H, NH₂ in pos. 4 pyrimido-pyrimidine), 7.26-7.22 (m, 2H, CH aromatic) 7.01-6.99 (m, 2H, CH aromatic), 6.83-6.79 (m, 1H, CH aromatic), 6.52 (s, 2H, NH₂ in pos. 2 pyrimido-pyrimidine), 3.95 (m, 4H, CH₂ piperazine), 3.20-3.19 (m, 4H, CH₂ piperazine), MS (ESI) *m/z*: 322.17 [M]⁺.

N⁷-(1-([1,1'-Biphenyl]-4-yl)ethyl)-N⁷-methylpyrimido[4,5-d]pyrimidine-2,4,7-triamine (12, MC4268).

¹H NMR (400 MHz, DMSO- d₆) δ 8.97 (s, 1H, CH pyrimidine), 7.66-7.63 (m, 4H, NH₂ in pos. 4 pyrimido-pyrimidine + CH aromatic), 7.48-7.39 (m, 7H, CH aromatic), 6.51 (s, 2H, NH₂ in pos. 4 pyrimido-pyrimidine), 6.35 (s, 1H, CHCH₃), 2.87 (s, 3H, N-CH₃), 1.59 (d, 3H, CHCH₃), MS (ESI) *m/z*: 371.19 [M]⁺.

N⁷-Benzyl-N⁷-methylpyrimido[4,5-d]pyrimidine-2,4,7-triamine (13, MC4180). ¹H NMR (400 MHz, DMSO- d₆) δ 8.94 (s, 1H, CH pyrimidine), 7.33-7.24 (m, 7H, NH₂ in pos. 4 pyrimido-pyrimidine + CH aromatic), 6.49 (s, 2H, NH₂ in pos. 2 pyrimido-pyrimidine), 4.90 (s, 2H, CH₂), 3.09 (s, 3H, N-CH₃), MS (ESI) *m/z*: 281.14 [M]⁺.

N⁷-Methyl-N⁷-(1-phenylethyl)pyrimido[4,5-d]pyrimidine-2,4,7-triamine (14, 4210). ¹H NMR (400 MHz, DMSO- d₆) δ 8.96 (s, 1H, CH pyrimidine), 7.34-7.28 (m, 7H, NH₂ in pos. 4 pyrimido-pyrimidine and CH aromatic), 6.48 (s, 2H, NH₂ in pos. 2 pyrimido-pyrimidine), 6.32-6.31 (m, 1H, CHCH₃), 2.82 (s, 3H, N-CH₃), 1.54 (d, 3H, CHCH₃), MS (ESI) *m/z*: 295.15 [M]⁺.

N⁷-(1-(4-Methoxyphenyl)ethyl)-N⁷-methylpyrimido[4,5-d]pyrimidine-2,4,7-triamine (15, MC4231). ¹H NMR (400 MHz, DMSO- d₆) δ 8.95 (s, 1H, CH pyrimidine), 7.40-7.39 (s broad, 2H, NH₂ in pos. 4 pyrimido-pyrimidine), 7.22-7.20 (m, 2H, CH aromatic), 6.90-6.88 (m, 2H, CH aromatic), 6.48 (s, 2H, NH₂ in pos. 2 pyrimido-pyrimidine), 6.26 (s, 1H, CHCH₃), 3.73 (s, 3H, OCH₃) 2.78 (s, 3H, N-CH₃), 1.49 (d, 3H, CHCH₃), MS (ESI) *m/z*: 325.17 [M]⁺.

N⁷-(4-(4-Methoxyphenoxy)benzyl)-N⁷-methylpyrimido[4,5-d]pyrimidine-2,4,7-

triamine (17, MC4233). ¹H NMR (400 MHz, DMSO- d₆) δ 8.94 (s, 1H, CH pyrimidine), 7.54-7.23 (m, 4H, NH₂ in pos. 4 pyrimido-pyrimidine + CH aromatic), 6.99-6.86 (m, 6H, CH aromatic), 6.50 (s, 2H, NH₂ in pos. 2 pyrimido-pyrimidine), 4.85 (s, 2H, CH₂), 3.74 (s, 3H, OCH₃), 3.08 (s, 3H, N-CH₃), MS (ESI) *m/z*: 403.18 [M]⁺.

N⁷-(1-(4-(4-Methoxyphenoxy)phenyl)ethyl)pyrimido[4,5-d]pyrimidine-2,4,7-triamine (18, MC4314). ¹H NMR (400 MHz, DMSO-d₆) δ 8.85 (s, 1H, CH pyrimidine), 7.78-7.768 (m, 1H, NH), 7.36-7.33 (d, 4H, CH aromatic), 6.98-6.85, (m, 4H, aromatic CH), 6.85-6.83 (d, 2H, NH₂ in pos. 4 pyrimido-pyrimidine), 6.45 (s, 2H, NH₂ in pos. 2 pyrimido-pyrimidine), 5.13 (m, 1H, CHCH₃), 3.91 (s, 3H, OCH₃) 1.42 (s, 3H, CHCH₃), MS (ESI) *m/z*: 403.18 [M]⁺.

N⁷-(1-(4-(4-Methoxyphenoxy)phenyl)propyl)-N⁷-methylpyrimido[4,5-d]pyrimidine-2,4,7-triamine (19, MC4315). ¹H NMR (400 MHz, DMSO-d₆) δ 8.95 (s, 1H, CH pyrimidine), 7.38-7.30 (d, 4H, CH arom.), 7.00-6.94 (m, 4H, aromatic CH), 6.89-6.86 (d, 2H, NH₂ in pos. 4 pyrimido-pyrimidine), 6.48 (sb, 2H, NH₂ in pos. 2 pyrimidopyrimidine), 6.01 (d, 1H, CHCH₂CH₃), 3.74 (s, 3H, OCH₃), 2.82-2.79 (m, 3H, N-CH₃), 2.07-1.89 (m, 2H, CH₂CH₃), 0.86 (m, 3H, CH₂CH₃), MS (ESI) *m/z*: 431.21 [M]⁺.

N⁷-(1-(4-(4-Methoxyphenoxy)phenyl)-2-methylpropyl)-N⁷-methylpyrimido[4,5-d]pyrimidine-2,4,7-triamine (20, MC4313). ¹H NMR (400 MHz, DMSO-d₆) δ 8.95-8.91 (d, 1H, CH pyrimidine), 7.42-7.36 (m, 4H, CH arom.), 7.00-6.93 (m, 4H, aromatic CH), 6.87-6.85 (d, 2H, NH₂ in position 4 pyrimido-pyrimidine), 6.46 (sb, 2H, NH₂ in pos. 2-pyrimidopyrimidine), 5.84-5.81 (d, 1H, CH-iPr), 3.74 (s, 3H, OCH₃), 2.89-2.81 (d, 3H, N-CH₃), 2.51-2.50 (m, 1H CH-iPr), 0.89-0.83 (m, 6H, CH₃-iPr), MS (ESI) *m/z*: 445.22 [M]⁺.

N⁷-((4-(4-Methoxyphenoxy)phenyl)(phenyl)methyl)-N⁷-methylpyrimido[4,5-d]pyrimidine-2,4,7-triamine (21, MC4318). ¹H NMR (400 MHz, DMSO-d₆) δ 8.97 (s, 1H, CH pyrimidine), 7.43-7.23 (m, 6H, NH₂ in pos. 4 pyrimidopyrimidine, CH aromatic), 7.18-7.13 (m, 4H, CH aromatic), 7.04-6.90 (m, 6H, CH aromatic, CH-Ph), 6.52 (sb, 2H, NH₂ in pos. 2 pyrimidopyrimidine), 3.93 (s, 3H, OCH₃), 2.89 (s, 3H, N-CH₃), MS (ESI) *m/z*: 479.21 [M]⁺.

N⁷-(1-(4-((4-Methoxyphenyl)thio)phenyl)ethyl)-N⁷-methylpyrimido[4,5-d]pyrimidine-2,4,7-triamine (22, MC4304). ¹H NMR (400 MHz, DMSO-d₆) δ 8.95 (s, 1H, CH pyrimidine), 7.54 (sb, 2H, NH₂ in position 4 pyrimido-pyrimidine) 7.27-7.25 (m, 2H, CH aromatic), 7.00-6.94 (m, 4H, aromatic CH), 6.90-6.87 (m, 2H, CH aromatic), 6.49 (sb, 2H, NH₂ in position 2 pyrimido-pyrimidine), 6.28 (m, 1H, CHCH₃), 3.74 (s, 3H, OCH₃), 2.82 (s, 3H, NCH₃), 1.51 (s, 3H, CHCH₃), MS (ESI) *m/z*: 433.17 [M]⁺.

***N*⁷-(1-(4-((4-Methoxyphenyl)amino)phenyl)ethyl)-*N*⁷-methylpyrimido[4,5-d]pyrimidine-2,4,7-triamine (23, MC4316).** ¹H NMR (400 MHz, DMSO-d₆) δ 8.95 (s, 1H, CH pyrimidine), 7.83 (s, 1H, Ph-NH-Ph), 7.38-7.37 (sb, 2H, NH₂ in pos. 4-pyrimidopyrimidine), 7.1-7.08 (d, 2H, CH aromatic), 7.03-7.01 (d, 2H, CH aromatic), 6.89-6.83 (m, 4H, CH aromatic), 6.46 (sb, 2H, NH₂ in pos. 2 pyrimidopyrimidine), 6.23 (m, 1H, CHCH₃), 3.70 (s, 3H, OCH₃), 2.79 (s, 3H, N-CH₃) 1.47-1.46 (d, 3H, CHCH₃), MS (ESI) *m/z*: 416.21 [M]⁺.

***N*⁷-(1-(4-((4-Methoxybenzyl)oxy)phenyl)ethyl)-*N*⁷-methylpyrimido[4,5-d]pyrimidine-2,4,7-triamine (24, MC4320).** ¹H NMR (400 MHz, DMSO-d₆) δ 8.95 (s, 1H, CH pyrimidine), 7.37-7.35 (d, 4H, CH aromatic), 7.21-7.20 (sb, 2H, NH₂ in pos. 4-pyrimidopyrimidine), 6.96-6.92 (t, 4H, CH arom.), 6.47 (sb, 2H, NH₂ in pos. 2-pyrimidopyrimidine), 6.26 (m, 1H, CHCH₃), 4.99 (s, 2H, O-CH₂-Ph) 3.76 (s, 3H, OCH₃), 2.79 (s, 3H, N-CH₃), 1.50-1.49 (d, 3H, CHCH₃), MS (ESI) *m/z*: 431.21 [M]⁺.

***N*⁷-(1-(4-(3,4-Dimethoxyphenoxy)phenyl)ethyl)-*N*⁷-methylpyrimido[4,5-d]pyrimidine-2,4,7-triamine (25, MC4310).** ¹H NMR (400 MHz, DMSO-d₆) δ 8.96 (s, 1H, CH pyrimidine), 7.39 (sb, 2H, NH₂ in pos. 4 pyrimidopyrimidine), 7.27-7.25 (sb, 2H, NH₂ in position 2 pyrimidopyrimidine), 6.95-6.89 (m, 3H, CH aromatic), 6.74-6.73 (m, 1H, CH arom.), 6.53-6.48 (m, 3H, CH arom.), 6.29 (s, 1H, CHCH₃), 3.74-3.72 (d, 6H, OCH₃), 2.82 (s, 3H, N-CH₃), 1.52-1.50 (d, 3H, CHCH₃), MS (ESI) *m/z*: 447.20 [M]⁺.

***N*⁷-(1-(4-(3,5-Dimethoxyphenoxy)phenyl)ethyl)-*N*⁷-methylpyrimido[4,5-d]pyrimidine-2,4,7-triamine (26, MC4319).** ¹H NMR (400 MHz, DMSO-d₆) δ 8.96 (s, 1H, CH pyrimidine), 7.39 (sb, 2H, NH₂ in pos. 4 pyrimidopyrimidine) 7.31-7.29 (m, 2H, CH aromatic), 7.00-6.98 (m, 2H, CH aromatic), 6.48 (sb, 2H, NH₂ in position 2 pyrimido-pyrimidine), 6.79-6.83 (m, 1H, CH arom.), 6.59-6.61 (m, 2H, CH arom.), 6.31 (s, 1H, CHCH₃), 3.74-3.72 (d, 6H, OCH₃), 2.82 (s, 3H, N-CH₃), 1.52-1.50 (d, 3H, CHCH₃), MS (ESI) *m/z*: 447.20 [M]⁺.

***N*⁷-Methyl-*N*⁷-(1-(4-(3,4,5-trimethoxyphenoxy)phenyl)ethyl)pyrimido[4,5-d]pyrimidine-2,4,7-triamine (27, MC4309).** ¹H NMR (400 MHz, DMSO-d₆) δ 8.96 (s, 1H, CH pyrimidine), 7.40 (sb, 2H, NH₂ in pos. 4 pyrimidopyrimidine), 7.29-7.27 (d, 2H, CH aromatic), 6.96-6.94 (m, 2H, CH aromatic), 6.48 (sb, 2H, NH₂ in pos. 2 pyrimidopyrimidine), 6.39 (s, 2H, CH aromatic), 6.30 (m, 1H, CHCH₃), 3.71 (s, 6H, m-OCH₃), 3.63 (s, 3H, p-OCH₃), 2.82 (s, 3H, N-CH₃), 1.52-1.51 (d, 3H, CHCH₃), MS (ESI) *m/z*: 477.21 [M]⁺.

***N*⁷-Methyl-*N*⁷-(1-(4-(4-(trifluoromethoxy)phenoxy)phenyl)ethyl)pyrimido[4,5-d]pyrimidine-2,4,7-triamine (28, MC4311).** ¹H NMR (400 MHz, DMSO-d₆) δ 8.96 (s, 1H, CH

pyrimidine), 7.38-7.32 (m, 6H, NH₂ in position 4 pyrimidopyrimidine, CH arom.), 7.10-7.03 (m, 4H, CH arom.), 6.49 (sb, 2H, NH₂ in pos. Pyrimidopyrimidine), 6.31 (sb, 1H, CHCH₃), 2.85 (s, 3H, N-CH₃), 1.54-1.53 (m, 3H, CHCH₃), MS (ESI) *m/z*: 471.16 [M]⁺.

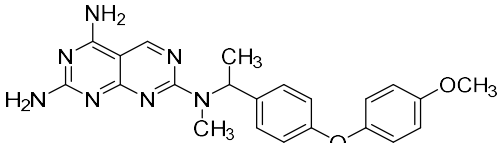
***N*⁷-(1-(4-(3-Methoxyphenoxy)phenyl)ethyl)-*N*⁷-methylpyrimido[4,5-d]pyrimidine-2,4,7-triamine (29, MC4298).** ¹H NMR (400 MHz, DMSO-d₆) δ 8.94 (s, 1H, CH pyrimidine), 7.54 (s, 2H, NH₂ in position 4 pyrimido-pyrimidine) 7.27-7.25 (m, 2H, CH aromatic), 7.00-6.94 (m, 4H, aromatic CH), 6.90-6.87 (m, 2H, CH aromatic), 6.49 (s, 2H, NH₂ in position 2 pyrimido-pyrimidine), 6.28 (m, 1H, CHCH₃), 3.74 (s, 3H, OCH₃), 2.82 (s, 3H, N-CH₃), 1.51 (d, 3H, CHCH₃), MS (ESI) *m/z*: 417.19 [M]⁺.

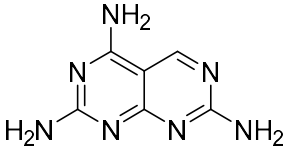
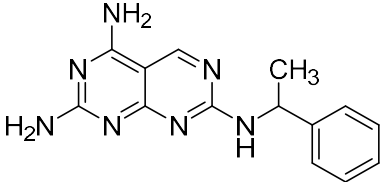
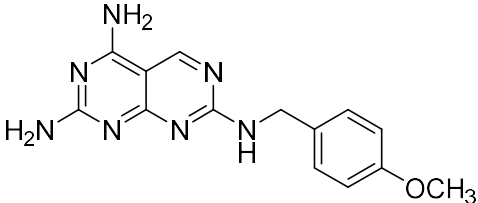
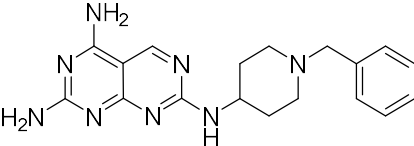
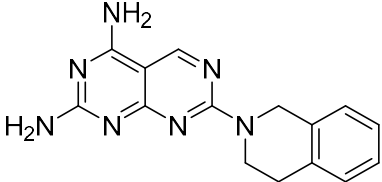
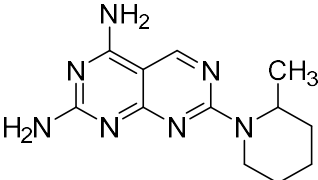
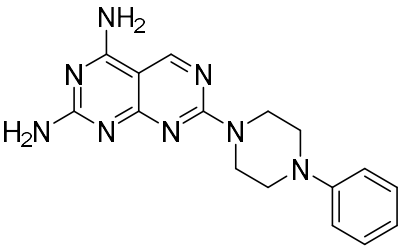
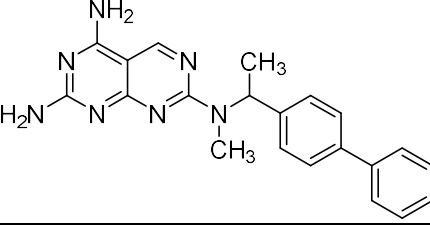
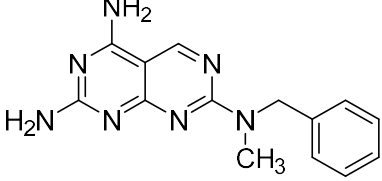
***N*⁷-(1-(4-(4-(Benzyloxy)phenoxy)phenyl)ethyl)-*N*⁷-methylpyrimido[4,5-d]pyrimidine-2,4,7-triamine (30, MC4312).** ¹H NMR (400 MHz, DMSO-d₆) δ 8.96 (s, 1H, CH pyrimidine), 7.47-7.38 (m, 5H, CH aromatic), 7.35-7.34 (d, 2H, NH₂ in position 4 pyrimido-pyrimidine), 7.28-7.25 (d, 2H, CH₂ aromatic), 7.04-6.97 (m, 4H, aromatic CH), 6.90-6.88 (m, 2H, CH aromatic), 6.48 (sb, 2H, NH₂ in position 2 pyrimidopyrimidine), 6.28 (s, 1H, CHCH₃), 5.08 (s, 2H, OCH₂-Ph), 2.81 (s, 3H, NCH₃), 1.52-1.51 (d, 3H, CHCH₃), MS (ESI) *m/z*: 493.22 [M]⁺.

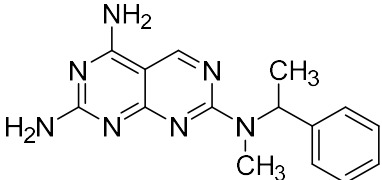
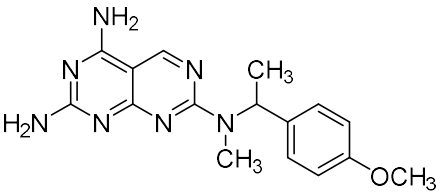
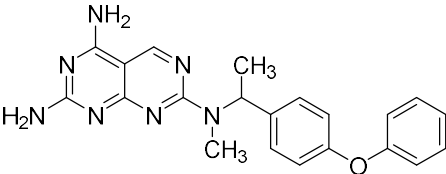
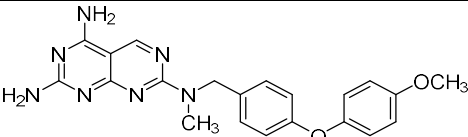
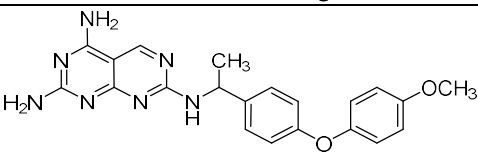
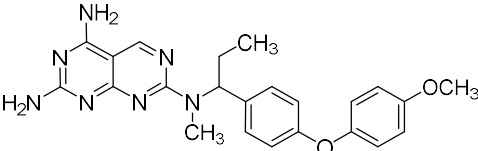
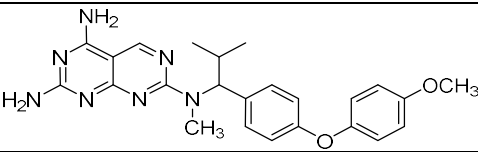
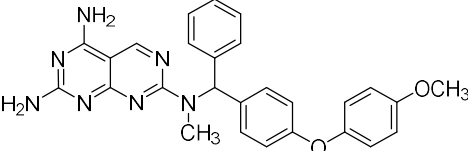
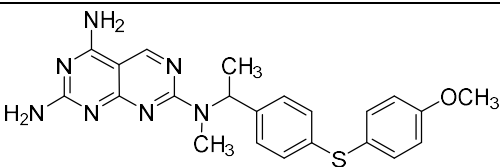
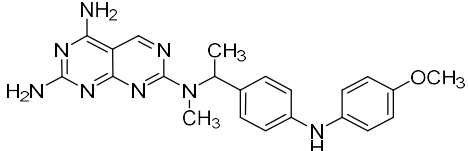
***N*⁷-(1-(4-((4-Methoxynaphthalen-1-yl)oxy)phenyl)ethyl)-*N*⁷-methylpyrimido[4,5-d]pyrimidine-2,4,7-triamine (31, MC4323).** ¹H NMR (400 MHz, DMSO-d₆) δ 8.95 (s, 1H, CH pyrimidine) 8.21-8.19 (t, 1H, aromatic CH), 7.91-7.88 (t, 1H, aromatic CH), 7.587-53 (m, 2H, CH aromatic), 7.38 (sb, 2H, NH₂ in position 4 pyrimidopyrimidine), 7.30-7.24 (t, 2H, CH arom.), 7.09-7.07 (d, 1H, CH arom.), 6.96-6.89 (m, 3H, aromatic CH), 6.46 (sb, 2H, NH₂ in pos. 2 pyrimido-pyrimidine), 6.28 (m, 1H, CHCH₃), 3.98 (s, 3H, OCH₃), 2.82 (s, 3H, N-CH₃), 1.51-1.49 (d, 3H, CHCH₃), MS (ESI) *m/z*: 467.21 [M]⁺.

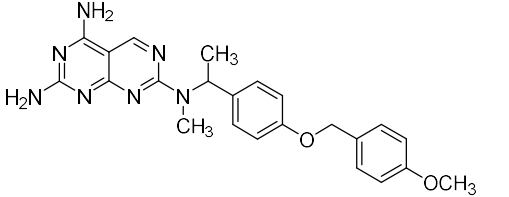
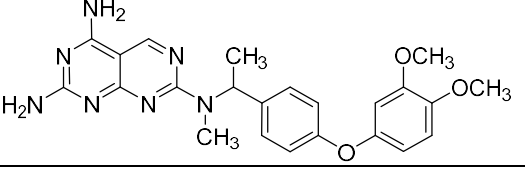
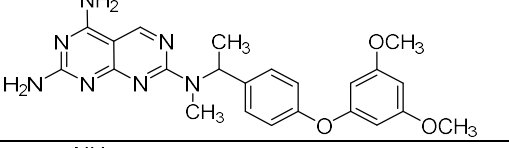
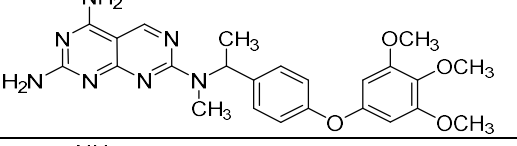
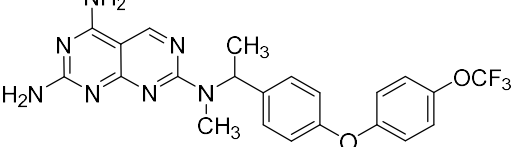
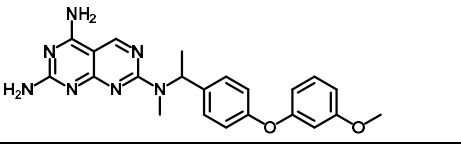
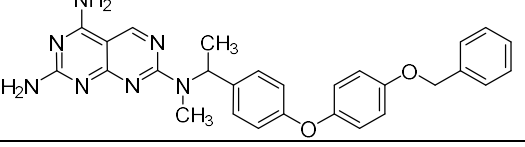
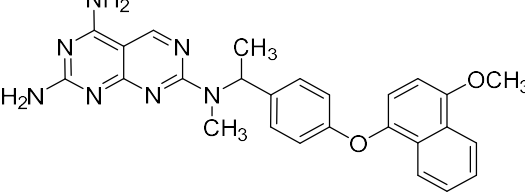
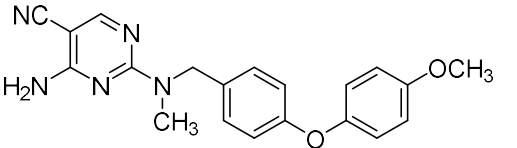
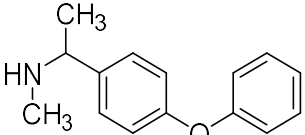
7.4 Biological evaluation, results and discussion

The inhibitory effects of the newly synthesized compounds on *smSirt2* and *hSirt2* deacetylase activity were tested through continuous fluorescence assay. The residual *smSirt2* and *hSirt2* activity in presence of 25 μM of the candidate inhibitors was evaluated (Table 7.4).

Table 7.4: Enzymatic inhibition of selected compounds derived from the prototype at 25 μM				
	Lab code	Structure	% inh. <i>smSIRT2</i> at 25 μM	% inh. <i>hSIRT2</i> at 25 μM
1	MC4223		62.6% ± 1.1% IC ₅₀ =23.7 ± 9.6 μM	21.9% ± 0.6%

2	MC4222		-14.1% ± 4.7%	-16.4% ± 3.7%
5	MC4189		0.9% ± 7.2%	-0.8% ± 4.4%
6	MC4234		-13.7% ± 1.8%	-18.35% ± 5.1%
7	MC4265		-7.9%	23.2 %
8	MC4232		-4.4% ± 0.7%	-5.2% ± 5.7%
9	MC4235		-6.6% ± 3.5%	-3.9% ± 8.1%
11	MC4236		-8.8% ± 8.7%	-10.9% ± 5.6%
12	MC4268		24.8%	9.3%
13	MC4180		-0.5% ± 2.4%	1.8% ± 3.7%

14	MC4210		-1.1% ± 6.8%	-4.4% ± 5.5%
15	MC4231		3.2% ± 1.4	-11.1% ± 4.6%
16	MC4211		27.6% ± 2.8%	5.0% ± 4.5%
17	MC4233		14.0 % ± 3.3%	4.2% ± 0.1%
18	MC4314		37.5%	21.0%
19	MC4315		IC ₅₀ = 12.8 ± 0.8 μM*	49.6%
20	MC4313		37.9%	57.4%
21	MC4318		IC ₅₀ = 2.34 ± 0.2 μM*	63.4%
22	MC4304		IC ₅₀ = 14.9 ± 0.9 μM*	45.9%
23	MC4316		52.9%	40.8%

24	MC4320		18.4%	30.6%
25	MC4310		IC ₅₀ = 44.7 ± 4.4 μM*	35.3%
26	MC4319		IC ₅₀ = 12.5 ± 1.1 μM*	7.4%
27	MC4309		52.2%	29.2%
28	MC4311		20.3%	37.5%
29	MC4298		IC ₅₀ = 23.1 ± 1.4 μM*	33.8%
30	MC4312		40.3%	70.4%
31	MC4323		46.2%	61.7%
Intermediate compounds tested along the final one				
48g	MC4238		2.0% ± 2.6%	-18.1% ± 7.6%
47c	MC4239		-9.9% ± 1.1%	4.9% ± 0.6%

In the first part of this project, extensive structure-activity relationship (SAR) studies have been applied on the N⁷-(1-(4-(4-methoxyphenoxy)phenyl)ethyl)-N⁷-methylpyrimido[4,5-

d]pyrimidine-2,4,7-triamine (TCMDC-143295) to obtain new hit compounds showing potent and selective inhibition of *smSirt2*; in particular, the influence of substituents at the N⁷ position of the *bispyrimidine* ring of TCMDC-143295 has been investigated by replacing the substituents on the prototype basically by substituents with smaller structures. Unfortunately, none of the newly synthesized compounds showed better *smSirt2* inhibitory activity compared to the prototype. Together with these final compounds, we tested also the pyrimidine intermediate, MC4238, and the amine intermediate, MC4239; but neither of them did not show any *smSirt2* inhibitory activity. In general, the tested compounds, except for three compounds MC4233, MC4211 and MC4268 which showed modest *smSirt2* inhibitory activities, showed either very poor or no activity against both *smSirt2* and hSirt2. Noticeably, replacing the substituent at the N⁷ position of the *bispyrimidine* ring of TCMDC-143295 basically by substituents with smaller structures strongly decreased or totally abolished both *smSirt2* and hSirt2 inhibitory activity. More accurately, no substituents at the N⁷ position of *bispyrimidine* (**MC4222**), or no methyl group at the N⁷ position of *bispyrimidine* (**MC4189**, **MC4261**, **MC4234**, **MC4262**, **MC4265**, **MC4314**), or the N⁷ position of *bispyrimidine* is a tertiary amine and is a part of a cyclic structure (**MC4236**, **MC4269**, **MC4235**, **MC4232**), resulted in significant reduction or total loss of activity toward *smSirt2*. In the light of these data, one methyl group and another larger substituent, N⁷ position of pyrimido[4,5-d]pyrimidine appear to be essential for the maintenance of inhibitory activity against *smSIRT2*.

In the second round of modification, we decided to keep the methyl group at the N⁷ position of *bispyrimidine* ring, however, introduction of bulky groups at α -carbon of the N⁷ position of *bispyrimidine*, i.e., replacing methyl group by ethyl (**MC4315**), isopropyl (**MC4313**) or phenyl (**MC4318**) group; led to compounds with better *smSirt2* inhibitory activity (**MC4315** and **MC4318**) or slightly lower *smSirt2* inhibitory activity (**MC4313**) compared to the prototype. In this regard, substitution of the methyl group with ethyl or phenyl group gave analogues with improved potency. Nevertheless, this improved potency came at the expense of poor selectivity over the hSirt2. Compared to the prototype, analogues with bulky group at α -carbon of the N⁷ position of *bispyrimidine* ring showed also improved hSirt2 inhibitory activity.

On the other hand, substitution of the oxygen linkage between the two phenyls by sulfur afforded compound (**MC4304**) with improved potency toward both *smSirt2* and *hSirt2* activity while replacing it with nitrogen gave compound (**MC4316**) with comparable potency but low selectivity over *hSirt2* compared to the prototype. Likewise, increasing this linkage by one carbon resulted in analogue (**MC4320**) characterized by weak *smSirt2* activity but comparable *hSirt2* activity in comparison to the prototype.

Furthermore, several modifications have been made on the etheric phenyl such as shifting the methoxy group from *para* to *meta* gave compound **MC4298**, having the same potency against *smSirt2* but higher potency toward *hSirt2* compared to the prototype. The introduction of additional methoxy groups, for example, 3,4-dimethoxyphenyl instead of 4-methoxyphenyl resulted in derivative **MC4310** that showed low potency and selectivity over *hSirt2* in comparison to the prototype, whereas replacement of the 4-methoxyphenyl by 3,4,5-trimethoxyphenyl led to compound **MC4309** with similar potency and selectivity compared to the prototype. Interestingly, the substitution of 4-methoxyphenyl by 3,5-dimethoxyphenyl produced analogue **MC4319** which is characterized with good potency and the best selectivity over *hSirt2* in comparison to the prototype. This is one of the most promising compound from the series with modest *smSirt2* activity ($IC_{50} = 12.5 \mu M$) and almost devoid of activity against *hSirt2* (7.4% inh. @ 25 μM). Finally, replacement of 4-methoxyphenyl by 4-trifluoromethoxyphenyl resulted in a 3-fold loss of potency against *smSirt2* and selectivity over *hSirt2* (**MC4311**), whilst replacement of 4-methoxyphenyl by 4-benzoyloxyphenyl (**MC4312**) or 4-methoxynaphthalenyl (**MC4323**) led to modest reduction of potency against *smSirt2* but more than 3-fold active toward *hSirt2* in comparison to the prototype. Fig. 7.3 represents the IC_{50} curves of selected compounds.

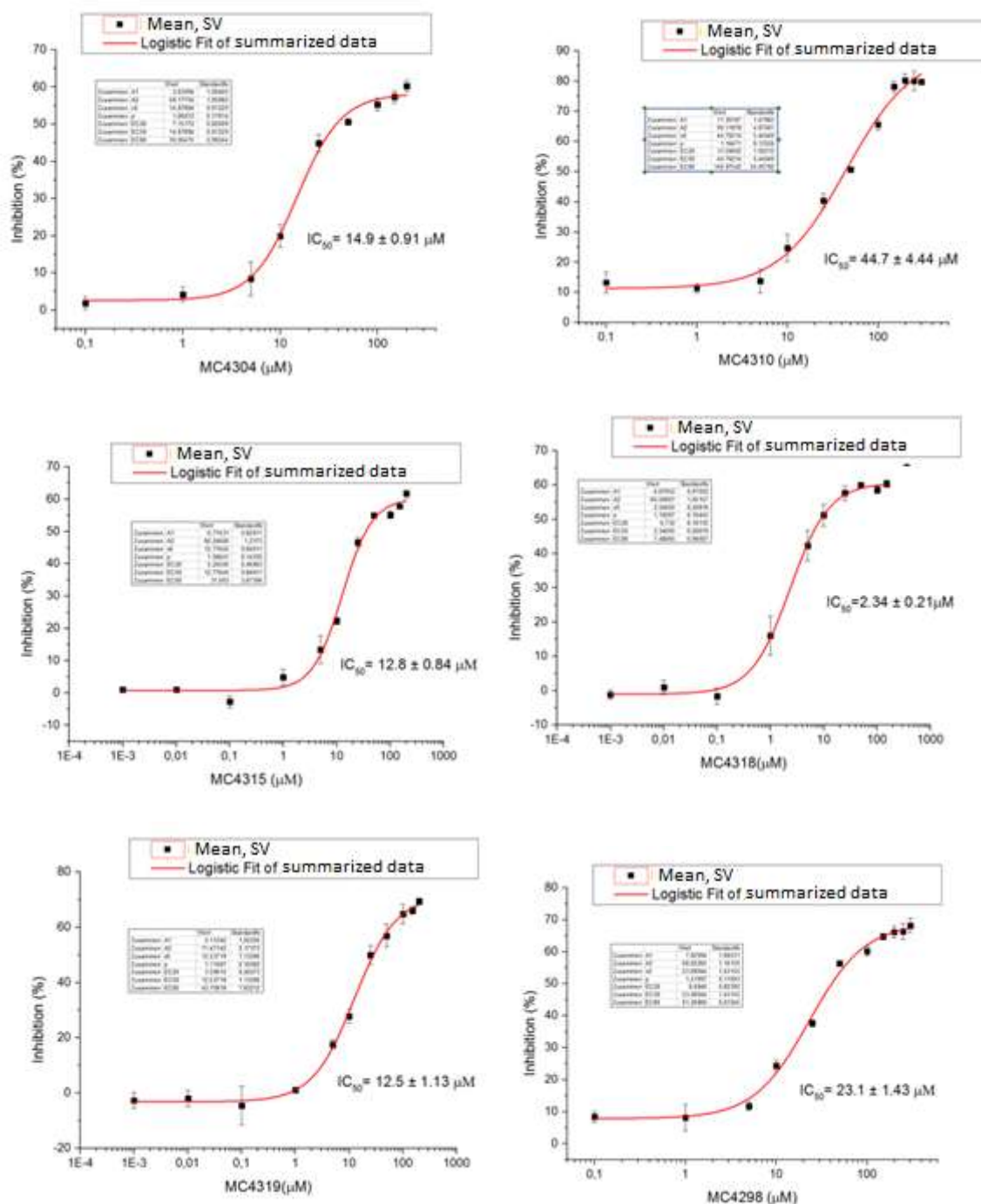


Fig. 7.3: The IC_{50} curves of selected compounds.

7.5 Conclusion and perspectives

Sirtuins are crucial regulators of cellular processes, two of which, energy metabolism and the DNA repair response, determine their potential importance as therapeutic targets. In the case of parasitic diseases, it is evident that the inhibition of sirtuins is sufficient to cause detrimental effects to the parasite and that species selectivity and/or enhanced bioavailability to the parasitic organism is most important. The differences in the catalytic domains of

schistosome sirtuins compared with their human counterparts are likely to be sufficient to allow the development of selective inhibitors, but this requires verification by molecular modeling and, where possible, x-ray crystallographic studies. However, high-throughput screening of recombinant enzymes can also allow the detection of inhibitors with novel scaffolds and warheads that are selective. Using the later approach, a fluorescent-based enzyme assay was developed by our collaborators and this led to the identification of novel compounds targeting *smSirt2*. From the screening series disclosed here we select one compound/hit, TCMDC-143295, as initial structural feature and represents a novel *smSirt2* inhibition template that provides the possibility to develop potent and selective inhibitors for the therapy of schistosomiasis. Consequently, extensive structure-activity relationship (SAR) studies have been applied on TCMDC-143295 (MC4223) to obtain new hit compounds showing potent and selective inhibition of *smSirt2*; in particular, the influence of substituents at the N⁷ position of the *bispyrimidine* ring of TCMDC-143295 has been investigated. Unfortunately, in the first round of SAR optimization, none of the newly synthesized compounds showed better *smSirt2* inhibitory activity compared to the prototype. In light of the above observations, in the second part of the project, we decided to keep the N⁷-methyl. Indeed, the alpha carbon at N⁷ position has been replaced with larger steric groups compared prototype to increase molecular constraint while the portion of diphenyl ether, given its importance, remained almost unchanged. Enzymatic assays of the tested compounds showed that several compounds exhibit a relatively better potency and selectivity toward *smSirt2*, indicating that the inhibition of some of these new analogues could be some potential leads for further SAR optimizations. Central to this optimization was the inclusion of a methyl or bulky groups at the alpha carbon of N⁷ position of *bispyrimidine* ring and dimethoxy group at the phenyl moiety as well as replacement of the ether with thioether linkage.

Thus, while we recognize that both potency toward *smSirt2* and selectivity over *hSirt2* still needs optimization, there are strong indications that the high selectivity by **MC4319** with respect to *hSirt2* and good potency by **MC4304** and **MC4318** that we have already obtained are more important for potential further SAR optimization of new derivatives with better potency toward *smSirt2* and selectivity over *hSirt2*.

A best strategy could be to synthesize new derivatives based on the above observations, specifically, further exploring the different SAR approaches, perhaps by combination, that had already led to better potency toward *smSirt2* and selectivity over *hSirt2*, in particular, it would

be a good of intervening on the other portion of the molecule without, for now, touching the pyrimido[4,5-d]pyrimidine nucleus. The above results suggest that the ether linkage between the two phenyls is flexible and it could be replaced with sulphones, sulfoxides, amides or methylene groups in obtaining derivatives with target biological profile. It would be also nice to see the effects of methylthio instead of methoxy on the ethereal phenyl. Further goal of future projects will be to investigate the importance of carbon chiral alpha at N⁷. Indeed, it is thought to be possible to functionalize the N² of pyrimido[4,5-d]pyrimidine by using condensation reactions with appropriately substituted guanidine (Fig. 7.4).

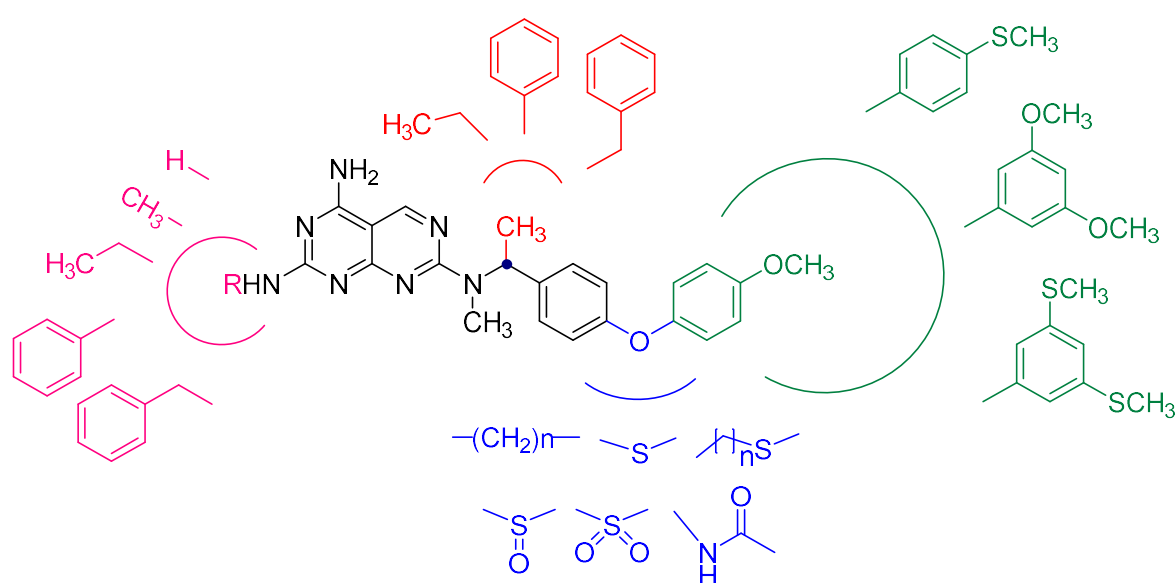


Fig. 7.4: Suggested possible future modifications for further SAR optimization on MC4223/TCMDC-143295

7.6 Methods

Coupled Enzymatic Deacetylation Assay: the deacetylase activity of *smSirt2* was assayed using a described coupled enzymatic reaction, preciously optimized for assay of hSirt2.[739-740] This assay is based on fluorescence measurements and uses a synthetic substrate, Z-Acetyl-Lysine-Amino-methylcumarin (ZMAL), that mimics the peptide containing an acetylated lysine residue. *smSIRT2* will deacylated ZMAL, thus leading to the liberation of the lysine amino-terminal group (ZML), which is recognized only in the deacylated state, by trypsin. Trypsin mediates the lysis of amide bonds, leading therefore to the release of Amino-methylcumarin (AMC), which is fluorescent (Fig. 7.5). As negative control, sample without the inhibitor was used (in this case *smSIRT2* will deacylated lysine and trypsin will split the peptide bond), while nicotinamide (which acts as SIRT4 inhibitor) was employed as a positive control,

finally only enzyme in DMSO was used as a blank control in order to identify hypothetical contamination. Briefly, smSirt2 (60 ng/ μ L), NAD⁺ (500 μ M), ZMAL (10.5 μ M), the potential inhibitor (dissolved in DMSO at various concentrations), and the FdL-developer (Trypsin 1mg/mL and nicotinamide 8 mM). The assay employed 384 wells (Greiner Bio-One) with a reaction volume of 20 μ l per well and all tests were performed at least in duplicate. The concentration of both smSIRT2 and NAD⁺ was prepared by dissolving in a buffer of 50mM TRIS, 137mM NaCl, 2.7mM KCl, 1mM MgCl₂, 0.5mM DTT, 0.015% Triton X-100, pH 8.0. while ZMAL was prepared from 12.6 mM DMSO solutions which were diluted with the same buffer until the concentration became 10.5 μ M. On the other hand, the FdL-developer (stop solution) was composed of 50mM TRIS, 100mM NaCl, 6.7% (v / v) DMSO, 1mg / mL trypsin, 8mM nicotinamide, pH 8.0.

Thus, ZMAL, smSIRT2, NAD⁺ and a hypothetical inhibitor dissolved in DMSO at various concentrations were incubated at 37 °C for 1h. In the presence of its cofactor, NAD⁺, smSIRT2 is able to deacetylase ZMAL to the formation of AMC, but in the presence of smSIRT2 inhibitor, this activity is blocked or become less depending on the power of the smSIRT2 inhibitory activity. Then, a solution containing/buffer trypsin and nicotinamide, was added and the plates were incubated at 37 °C for another 20 min. The action of trypsin leads to the formation of AMC and Z-lysine, where AMC is the source of fluorescence signal in the assay. Then the fluorescence intensity was measured in a microplate reader (BMG Polarstar, λ_{ex} 365 nm, λ_{em} 465 nm). The amount of inhibition was determined with respect to the mixture with only DMSO. IC₅₀ values were determined with Graphpad Prism software using a non-linear regression to fit the dose–response curve.

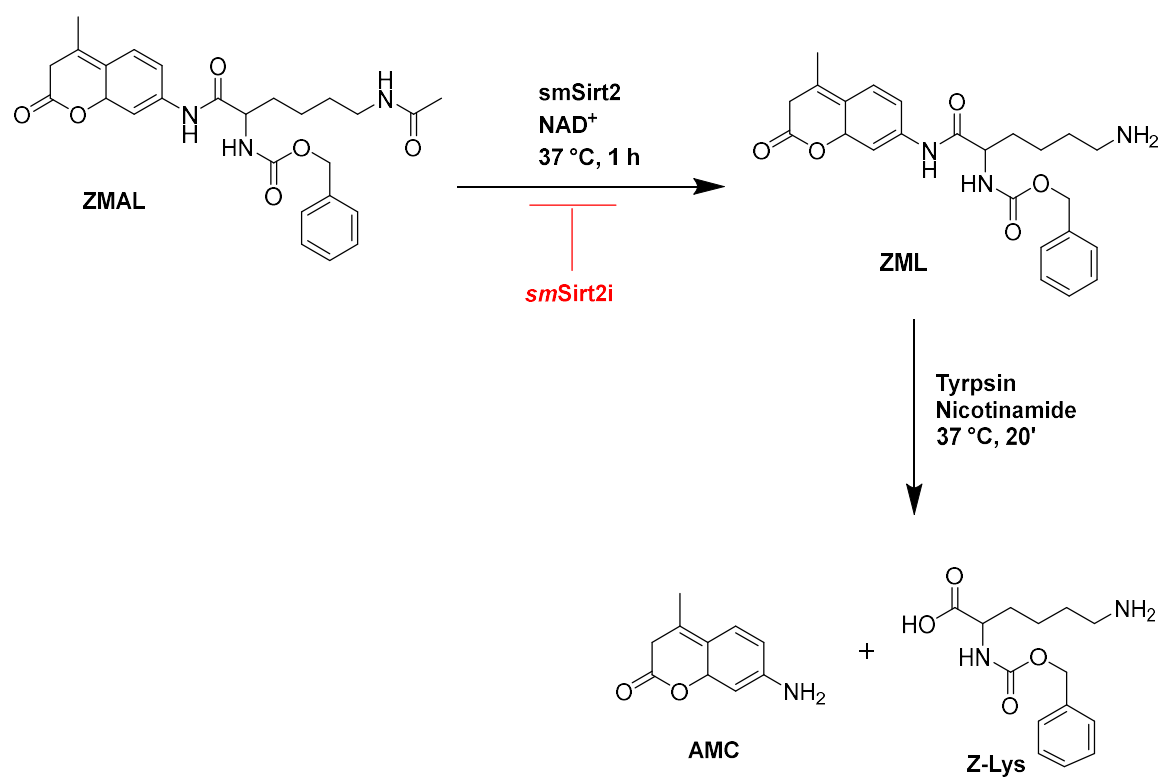


Fig. 7.5: Graphic representation of the deacetylation of the substrate ZMAL during the assay

8. DESIGN AND SYNTHESIS OF TRANSLCYCPROMINE-BASED LSD1 INHIBITORS POTENTIALLY ACTIVE AGAINST *SCHISTOSOMA MANSONI*

8.1 Research Project

The role of epigenetic mechanisms in the control of gene transcription in schistosomes, and hence in bio-logical processes like development and reproduction, has gained a momentum in epigenetics. Epi-drugs, including LSD1 inhibitors, were characterized and studied in recent years as potential new drug targets, with the strategy of testing known anti-cancer drugs to kill schistosomes [264, 686, 699, 702-703, 708-709, 741]. Here, we proposed a new series of LSD1 inhibitors based on the *trans* 2-phenylcyclopropylamine (*trans*-2-PCPA), which is a useful lead to develop several highly potent small-molecules active toward various cancer cell lines, as a potentially active against *S. mansoni* parasites. The rationale of the approach is based on the fact that the parasite shares some of the characteristics of malignant cells, such as high levels of metabolic activity and of cell division, an effective host immune evasion, and an intense oxidative metabolism [684]. In addition, *in silico* analyses [742] have pointed to a large number of *S. mansoni* histone binding partners potentially involved in the regulation of gene expression, DNA replication, cell death, cellular growth and proliferation [742], thus suggesting that drug-induced histone modifications could affect these cellular processes in the parasite. Insights into schistosome epigenetic mechanisms has been gained from studies aimed at developing such strategies, including for example the characterization of the actions of inhibitors of histone modifying enzymes (HMEs), or from transcript knockdown studies. For example, during the previous EC-funded project (SEtTREND) transcript knockdown by RNA interference was used to identify three HMEs, SmHDAC8, SmLSD1 and SmPRMT3 as valid targets in *Schistosoma mansoni* and three of them were found to be essential to the survival and/or development of the parasite within its mammalian host. Studies on these three HMEs have been continued during another EC-funded project (A-ParaDDisE) in which our group involved in.

The results from both SEtTREND and A-ParaDDisE prompted us, as part of the FP7 A-ParaDDisE Project, to prepare a small group of LSD1 inhibitors (**1-9**, **11**, **15**, **19-24**, Table 8.1) potentially active against *S. mansoni*. The resulting compounds have been tested against *Schistosoma* at Prof. Fantappi  's lab (in Brazil). Interestingly, preliminary data indicate that most of the tested compounds were relatively toxic to the juvenile stage of schistosomula (the ideal target to control schistosomiasis because no eggs are involved in this stage) and to

a lesser extent to adult worms. Among these tested compounds, MC3935, an analogue of the 2-phenylcyclopropylamine (Fig. 8.1), was found to be extremely toxic to both schistosomula and adults. A subsequent treatment of *S. mansoni* with MC3935 led to induced tegumental and muscle abnormalities as well as the presence of apoptotic and necrotic vesicles and granules. Induction of apoptosis cause the death of the parasite after treatment and extensive alterations to reproductive systems were also observed in adult schistosomes treated with these inhibitors. These inhibitors resulted in hypermethylation of histone 3 at lysine 4 (H3K4), which is the specific target of this enzyme, that showed the aforementioned alterations in the parasites are in fact as a result of inhibition of LSD1. RNASeq analysis of adult worms treated with the LSD1 inhibitor showed that 2709 and 938 genes were differentially expressed in males and females, respectively. While, 270 genes were differentially expressed in schistosomula treated with the inhibitor. Downregulated genes in male worms included those involved in drug pumps and cytoskeleton formation, whereas in female's transmembrane transporter genes were downregulated. Notch signaling pathway genes were upregulated in female worms and schistosomula.

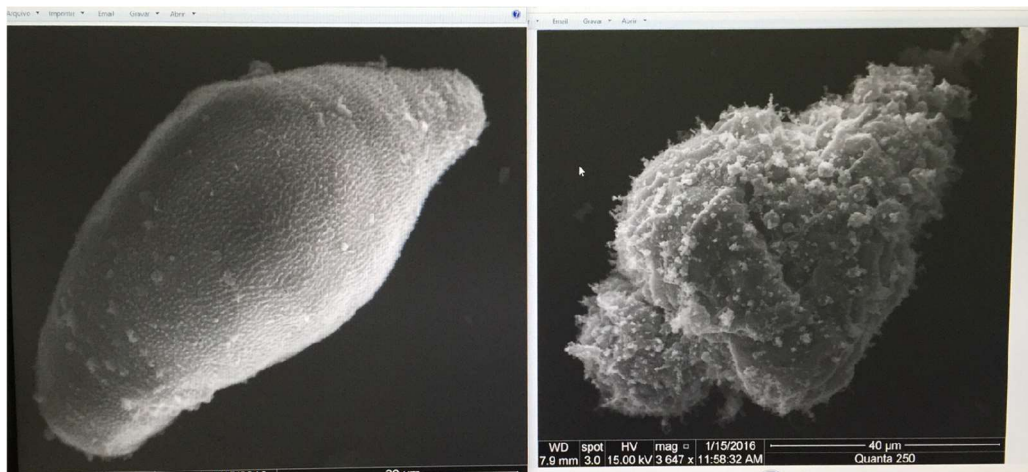


Fig. 8.1: Effect of MC3935 on the tegument of *S. mansoni* after treatment with 25 µM for 48h.

These compounds deserved further investigation, more specifically, MC3935 is an interested compound with magnificent antischistosomal activities that needs further medicinal chemistry exploration. Hence, we decided to synthesized a small group of compounds by chemical modifications of MC3935 in order to improve its potency and selectivity over human LSD1 activity. As result, during my stay in Prof. Ganesan's lab at the

University of East Anglia, Norwich, I prepared small series of MC3935 analogues (**10**, **12-14**, **16-18**, **25** and **26**, Table 8.1). In this regard, the new analogues were designed by two modification approaches on MC3935: (i) moving the ethynyl from *para* to *meta* position(**GS4**), or substituting the ethynyl group with other alkynyl (**GS3** and **GS5-7**) or alkyl (**GS1** and **GS2**) groups; and (ii) moving the amido (CONH) from *para* to *meta* and varying the aroyl groups (**GS8** and **GS9**) (Fig. 8.2).

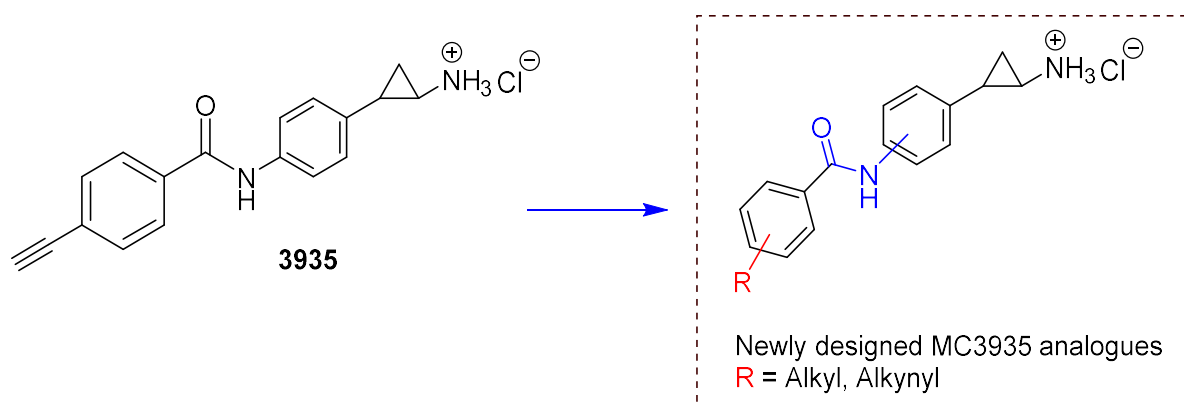


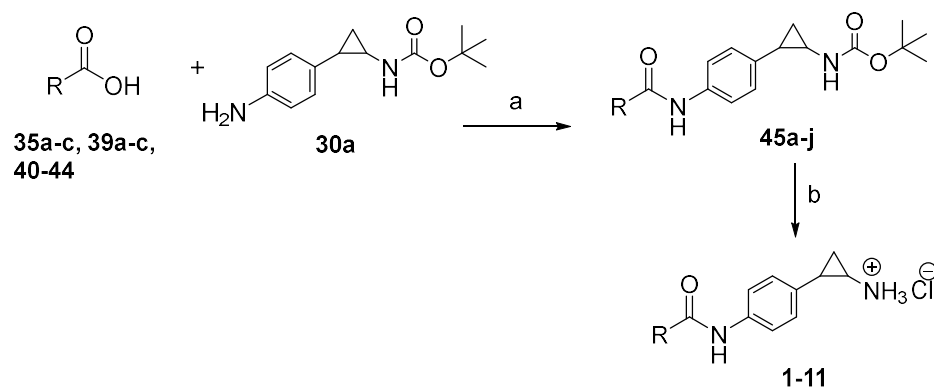
Fig. 8.2: Structure of MC3935 and its proposed potential analogues

8.2 Chemistry

The *trans*-2-(3/4-nitrophenyl)cyclopropylcarboxylic acids (**28a,b**) were prepared by treating the commercially available *trans*-2-phenylcyclopropylcarboxylic acid (**27**) with 69.5% HNO₃. To a suspension of *trans*-2-(3/4-nitrophenyl) cyclopropylcarboxylic acid in anhydrous toluene was added TEA, DPPA, *tert*-butanol and *di-tert*-butyl dicarbonate and refluxed under nitrogen to afford *trans-tert*-butyl-2-(3/4-nitrophenyl) cyclopropylcarbamates (**29a,b**) [743]. The key intermediate *trans-tert*-butyl-2-(3/4-aminophenyl) cyclopropylcarbamates (**30a,b**) were prepared by hydrogenation of *trans-tert*-butyl-2-(3/4-nitrophenyl) cyclopropylcarbamate in MeOH in the presence of 10% Pd/C under nitrogen condition (Scheme 3). Subsequently, the synthesis of the final compounds **1-26** was carried out following two routes. According to Scheme 1, the appropriate acids, prepared as Scheme 4 and 5 (**35a-c**, **39a-c**) or commercially available (**40-44**), were activated by benzotriazol-1-yl-oxytripyrrolidinophosphonium hexafluorophosphate (PyBOP) or 1-(3-dimethylaminopropyl)-3-ethylcarbodiimide (EDC), in the presence triethylamine and condensed with *tert*-butyl *N*-[2-(4-aminophenyl)cyclopropyl]carbamate **30a** to afford their corresponding carbamates **45a-j**. The final compounds **1-11** were smoothly obtained by removing Boc protection with hydrochloric acid in dioxane. On the other hand, the final compounds **12-26** were prepared

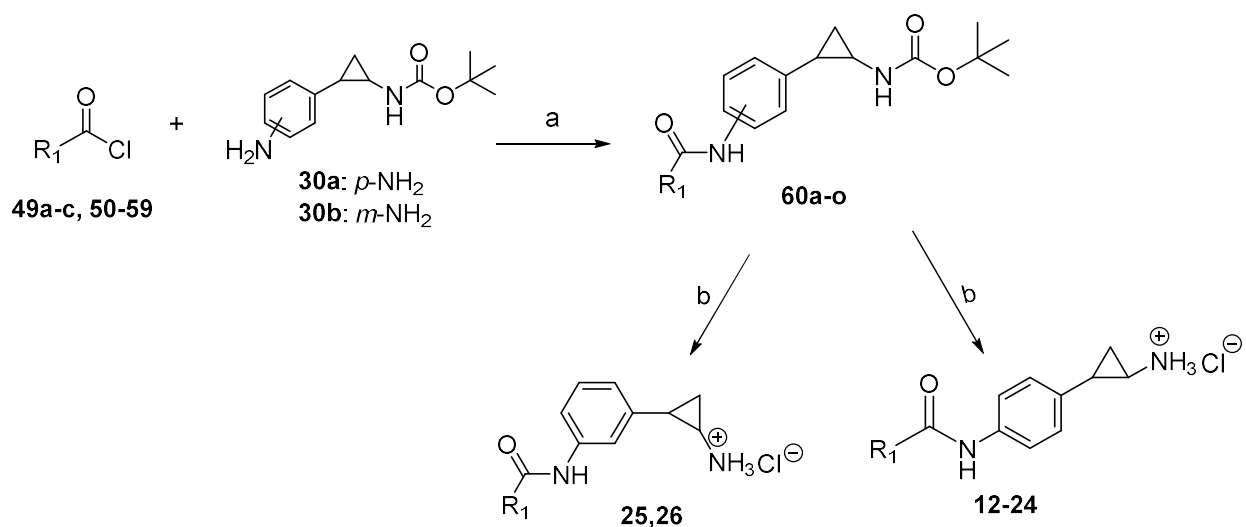
according to Scheme 2. Where, the key intermediates **30a,b** were treated with the appropriate aroyl/benzyl chlorides, which were prepared as scheme 6 (**49a-c**) or commercially available (**50-59**), in the presence of TEA and dry DCM to give the intermediates, *trans tert*-butyl 2-(4-aroyle/benzyl)aminophenyl)cyclopropyl carbamates (**60a-o**).¹ Finally, cleavage of the Boc group by the addition of 4 N hydrochloric acid in dioxane/tetrahydrofuran yielded the final compounds, *trans tert*-butyl 2-(4-aroyle/benzyl)aminophenyl)cyclopropylamine hydrochlorides (**12-26**) [744]. The aroyl chloride intermediates (**49a-c**) were synthesized starting from methyl-4-iodobenzoate (**46**), which was treated with the appropriate alkynes in the presence of $\text{PdCl}_2(\text{PPh}_3)_2$ and CuI in dry DMF/THF to provide the corresponding substituted *para*-alkyne-benzoates (**47a-c**) [745-746]. The resulting esters were dissolved in MeOH, treated with aqueous 2 N LiOH and heated under reflux to give the carboxylic acids (**48a-c**). Further the appropriate carboxylic acid was heated under reflux with excess thionyl chloride to furnish the aroyl chlorides (**49a-c**). Table 8.1 depicts the physico-chemical data of the final compounds **1-26**.

Scheme 1^a



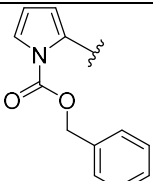
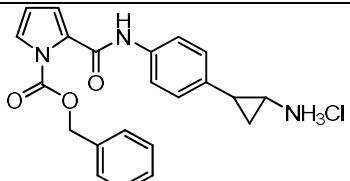
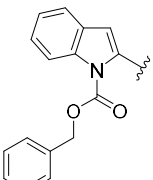
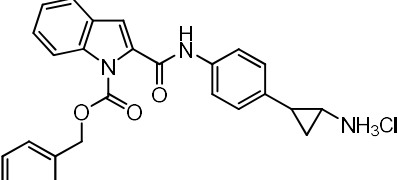
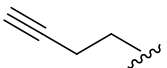
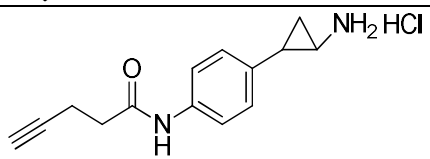
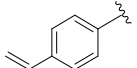
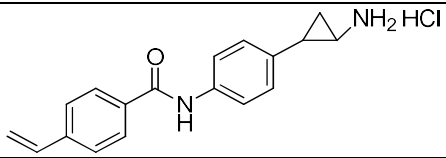
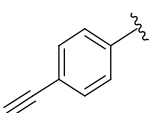
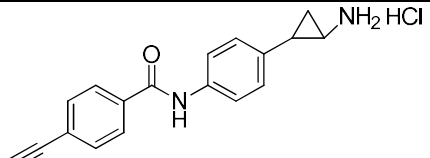
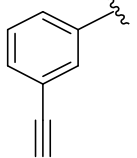
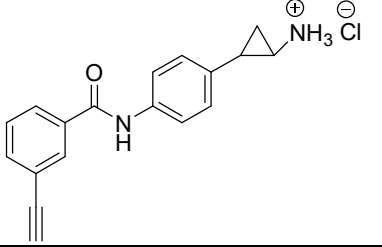
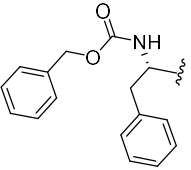
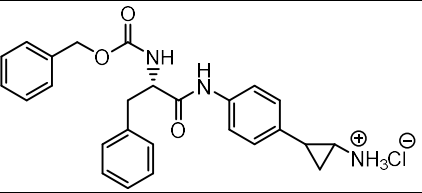
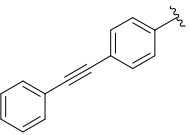
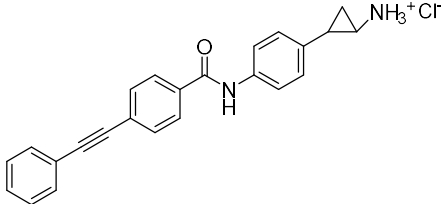
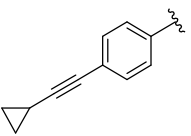
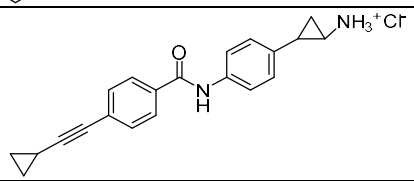
^a **Reagents and conditions:** (a) PyBop, Et₃N, dry DMF, N₂ atmosphere, overnight, rt; (b) 4 N HCl in dioxane, anhydrous THF, 24-48 h, 0 °C-rt.

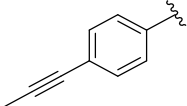
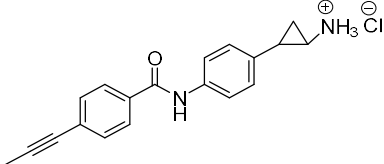
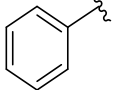
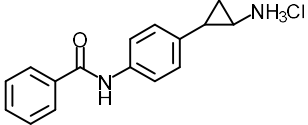
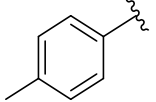
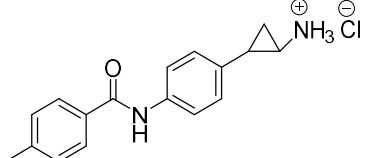
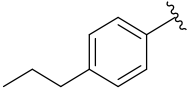
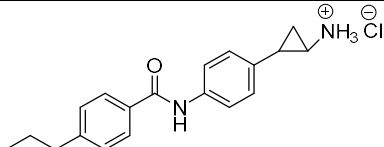
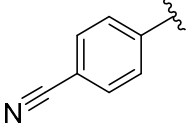
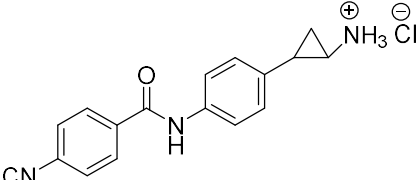
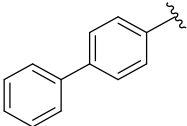
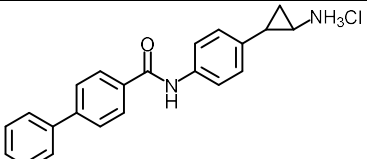
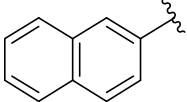
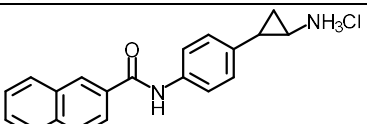
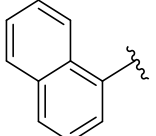
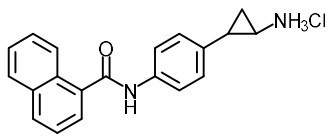
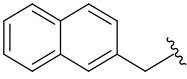
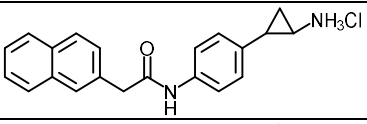
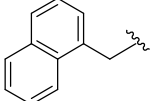
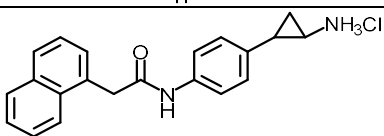
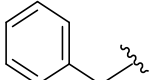
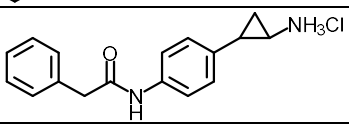
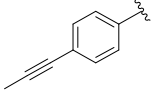
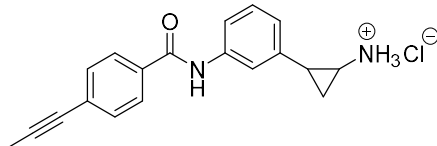
Scheme 2^a

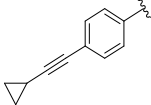
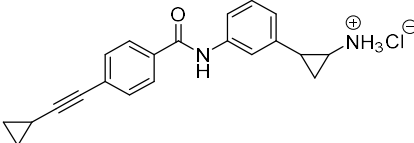


^a **Reagents and conditions:** (a) Et₃N, anhydrous DCM, 2-4 h, 0 °C-rt; (b) 4 N HCl in dioxane, anhydrous THF, 24-48 h, 0 °C-rt.

Table 8.1. Physico-chemical data of compounds 1-26						
Sr. No	Lab Code	R	Structure	M.W.	M.P. (°C)	Yield (%)
1	MC33 71			523.03	195-197	77
2	MC33 84			572.53	190-192	79
3	MC34 73			523.03	186-189	78
4	MC34 13			411.89	177-179	62

5	MC32 88			411.89	192-194	61
6	MC33 82			461.95	202-204	63
7	MC39 37			264.75	>250	75
8	MC39 34			314.81	>250	80
9	MC39 35			312.79 3	>250	86
10	GS4			312.80	>250	70
11	MC32 05			465.98	218-220	70
Cm pd	Lab Code	R ₁		M.W.	M.P. (°C)	Yield
12	GS5			388.90	>250	69
13	GS6			352.86	>250	72

14	GS7			326.82	>250	78
15	MC25 84			288.78	210- 212	83
16	GS1			302.80	>250	86
17	GS2			330.86	>250	79
18	GS3			313.79	>250	65
19	MC26 52			364.87	>250	85
20	MC26 53			338.84	>250	81
21	MC26 34			338.84	>250	76
22	MC26 46			352.86	238- 240	84
23	MC26 45			352.86	240- 242	78
24	MC26 39			302.80	180- 182	73
25	GS8			326.82	>250	75

26	GS9			352.86	>250	60
----	-----	-----------------------------------------------------------------------------------	------------------------------------------------------------------------------------	--------	------	----

8.3 Experimental Section

Chemistry. Melting points were determined on a Buchi 530 melting point apparatus. ^1H -NMR spectra were recorded at 400 MHz using a Bruker AC 400 spectrometer; chemical shifts are reported in δ (ppm) units relative to the internal reference tetramethylsilane (Me_4Si). Mass spectra were recorded on a API-TOF Mariner by Perspective Biosystem (Stratford, Texas, USA), samples were injected by an Harvard pump using a flow rate of 5–10 $\mu\text{L}/\text{min}$, infused in the Electrospray system. All compounds were routinely checked by TLC and ^1H -NMR. TLC was performed on aluminum-backed silica gel plates (Merck DC, Alufolien Kieselgel 60 F_{254}) with spots visualized by UV light or using a KMnO_4 alkaline solution. All solvents were reagent grade and, when necessary, were purified and dried by standard methods. Concentration of solutions after reactions and extractions involved the use of a rotary evaporator operating at reduced pressure of ~ 20 Torr. Organic solutions were dried over anhydrous sodium sulfate. Elemental analysis has been used to determine purity of the described compounds, that is $> 95\%$. Analytical results are within 0.40% of the theoretical values. All chemicals were purchased from Sigma Aldrich s.r.l., Milan (Italy) or from TCI Europe N.V., Zwijndrecht (Belgium), and were of the highest purity. As a rule, samples prepared for physical and biological studies were dried in high vacuum over P_2O_5 for 20h at temperatures ranging from 25 to 40 $^\circ\text{C}$, depending on the sample melting point.

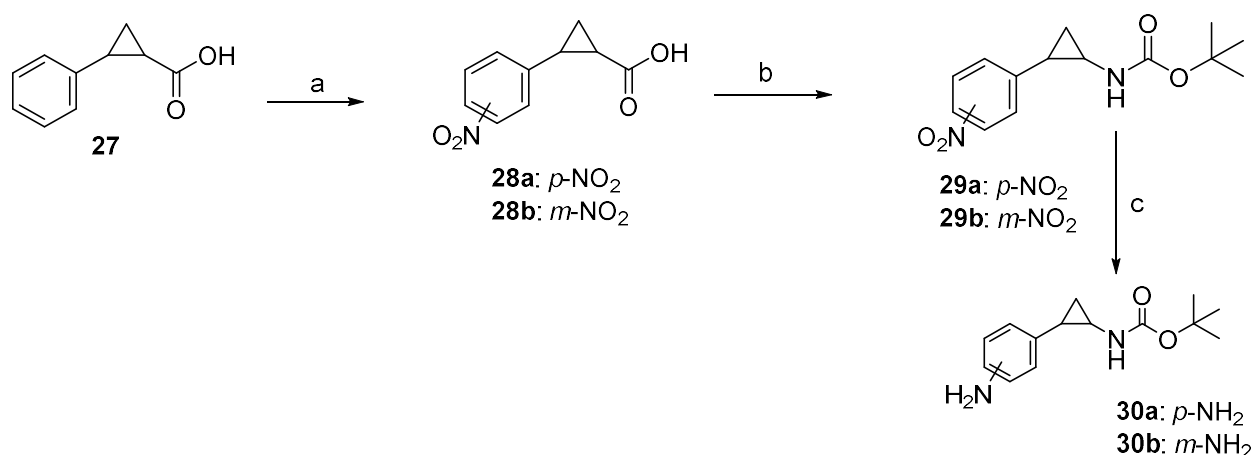
General Procedure for the synthesis of 2- (3/4-nitrophenyl) cyclopropylcarboxylic acids (28a,b, Scheme 3). **Example: *trans* 2-(4-nitrophenyl)cyclopropylcarboxylic acid (28a).** The commercially available *trans* -2-phenylcyclopropylcarboxylic **27** (1 eq) was treated with 69.5% nitric acid solution (15 eq) and left to stir at rt for 7 h. After completion of the reaction, it was filtered and washed with water to give the *trans* 2-(4-Nitrophenyl)cyclopropylcarboxylic and *trans* 2-(3-Nitrophenyl)cyclopropylcarboxylic (4:1). Crystallization of the resulting solid from benzene affords the pure *trans* 2-(4-nitrophenyl)cyclopropylcarboxylic **28a** as a white solid. ^1H NMR (DMSO, 400 MHz): δ 1.44–1.48 (m, 1H, CHH cyclopropane), 1.51–1.56 (m, 1H, CHH cyclopropane), 1.96–2.00 (m, 1H, CHCOOH cyclopropane), 2.54–2.59 (m, 1H, PhCH

cyclopropane), 7.44–7.46 (d, 2H, benzene protons), 8.11–8.13 (d, 2H, benzene protons), 12.47 (bs, 1H, COOH).

General Procedure for the Synthesis of *trans tert*-Butyl 2-(3/4-Nitrophenyl)cyclopropyl Carbamates (29ab, Scheme 3): example *trans tert*-butyl 2-(4-nitrophenyl)cyclopropyl carbamate (29a). A solution of *trans* 2-(4-Nitrophenyl)cyclopropylcarboxylic **28a** (12.5 mmol, 2.56 g) in dry toluene (75 mL), triethylamine (16.25 mmol, 2.26 mL), diphenylphosphoryl azide (15 mmol; 3.23 mL) and *tert*-butanol (24 mmol, 5 mL) was stirred at 90 °C under N₂ atmosphere for 18 h. Afterwards, di-*tert*-butyldicarbonate (18.75 mmol, 4.1 g) was added, and the reaction was continued at 90 °C for further 2 h. The solvent was removed under vacuum and dissolved with a 100 mL EtOAc and extracted with 50 mL of H₂O and 50 mL of saturated NaHCO₃. After drying with Na₂SO₄ and evaporation, the resulting residue was purified on flash chromatography by silica gel eluting with ethyl acetate/*n*-hexane to give pure *trans tert*-butyl 2-(4-nitrophenyl)cyclopropyl carbamate **29a** as a white solid. ¹H NMR (CDCl₃, 400 MHz, δ ; ppm) δ 1.10–1.15 (m, 1H, CHH cyclopropane), 1.19–1.23 (m, 1H, CHH cyclopropane), 1.39 (s, 9H, C(CH₃)₃), 2.40–2.45 (m, 1H, CHNH cyclopropane), 2.62–2.67 (m, 1H, PhCH cyclopropane), 4.96 (bs, 1H, NHCO), 7.29–7.31 (d, 2H, benzene protons), 7.84–7.86 (d, 2H, benzene protons).

General procedure for the synthesis of *trans tert*-Butyl 2-(3/4-amophenyl)cyclopropyl Carbamate (30a,b, Scheme 3): example *trans tert*-Butyl 2-(4-Aminophenyl)cyclopropyl Carbamate (30a). To a solution *trans tert*-butyl 2-(4-nitrophenyl)cyclopropyl carbamate **29a** (6.72 mmol, 1.87 g) in methanol (100 mL), 10% Pd/C (100 mg) was added at nitrogen atmosphere. The reaction mixture was stirred under hydrogen gas at room temperature for 4 h. After completion, the reaction mixture was filtered off through a Celite bed, and the filtrate was concentrated. The crude was subjected to flash column chromatography using ethyl acetate/hexane as eluting system to provide the *trans tert*-butyl 2-(4-amminophenyl)cyclopropyl carbamate **30a** as an oil. ¹H NMR (CDCl₃, 400 MHz, δ ; ppm) δ 0.98–1.01 (m, 1H, CHH cyclopropane), 1.17–1.21 (m, 1H, CHH cyclopropane), 1.38 (s, 9H, C(CH₃)₃), 1.85–1.90 (m, 1H, CHNH cyclopropane), 2.55–2.57 (m, 1H, PhCH cyclopropane), 3.49 (bs, 2H, –NH₂), 4.73 (bs, 1H, NHCO), 6.52–6.54 (d, 2H, benzene protons), 6.88–8.90 (d, 2H, benzene protons).

Scheme 3



Reagents and conditions: (a) 69.5% HNO₃, rt; (b) (i) Et₃N, DPPA, *tert*-BuOH, anhydrous toluene, N₂ atmosphere, 16 h, 90 °C; (ii) di-*tert*-butyl dicarbonate, 2 h, 90 °C; (c) H₂, 10% Pd/C, anhydrous MeOH, 5 h, rt.

General procedures for preparation of *tert*-butyl 3/4-morpholino/(4-methylpiperazin-1-yl)-3/4-nitrobenzoate (32a-c) Scheme 4. Example: *tert*-Butyl 4-(4-methylpiperazin-1-yl)-3-nitrobenzoate (32b). A suspension of 2.0 g (7.8 mmol) *tert* butyl 4-chloro-3-nitro-benzoate **31**, 3.22 g (23.3 mmol) of dry K₂CO₃) and 2.58 mL (23.3 mmol) of *N*-methylpiperazine was stirred in 10 mL of dry DMF at 90 °C for 5 h in a sealed tube. Then, the reaction mixture was quenched with water and extracted with EtOAc. The combined organic phases were washed with brine, dried over Na₂SO₄, concentrated and the residue was purified on silica gel (eluent: EtOAc) and recrystallized from toluene to obtain 2.3 g (92%) of intermediate **32b** as a yellow solid. ¹H NMR (CDCl₃, 400 MHz) δ, 1.61 (s, 9H, -COOC(CH₃)₃), 2.38 (s, 3H, -NCH₃), 3.20 (t, 4H, -PhN(CH₂)₂), 2.58 (t, 4H, -CH₃N(CH₂)₂), 7.07-7.10 (d, 1H, aromatic proton), 8.03-8.06 (d, 1H, aromatic proton), 8.37 (s, 1H, aromatic proton); MS (EI) *m/z*: 321.17 [M]⁺; m.p. 138- 140°C.

***tert*-butyl 3/4-amino-3/4-morpholino/(4-methylpiperazin-1-yl)benzoate (33a-c) Scheme 4. Example: *tert*-Butyl 3-amino-4-(4-methylpiperazin-1-yl)benzoate (33b).** A suspension of 0.80 g (2.5 mmol) of the *tert*-butyl nitrobenzoate **32b** in 30 mL MeOH and 0.13 g (0.12 mmol) of 10% palladium on carbon were placed in a Parr apparatus and was hydrogenated at 50 psi and 25 °C for 5 h. The palladium was then filtered off and the MeOH was evaporated to afford an oily residue that was first purified on silica gel (eluent: CHCl₃/MeOH, 10:1, v:v) and then recrystallized from cyclohexane to provide 0.29 g (65%) of the *tert*-butyl 4-amino-benzoate **33b** as a yellow solid. ¹H NMR (CDCl₃, 400 MHz) δ 1.58 (s, 9H, -COOC(CH₃)₃), 2.38 (s, 3H, -N(CH₃)), 2.61 (t, 4H, -CH₃N(CH₂)₂), 2.98 (t, 4H, -PhN(CH₂)₂), 3.96

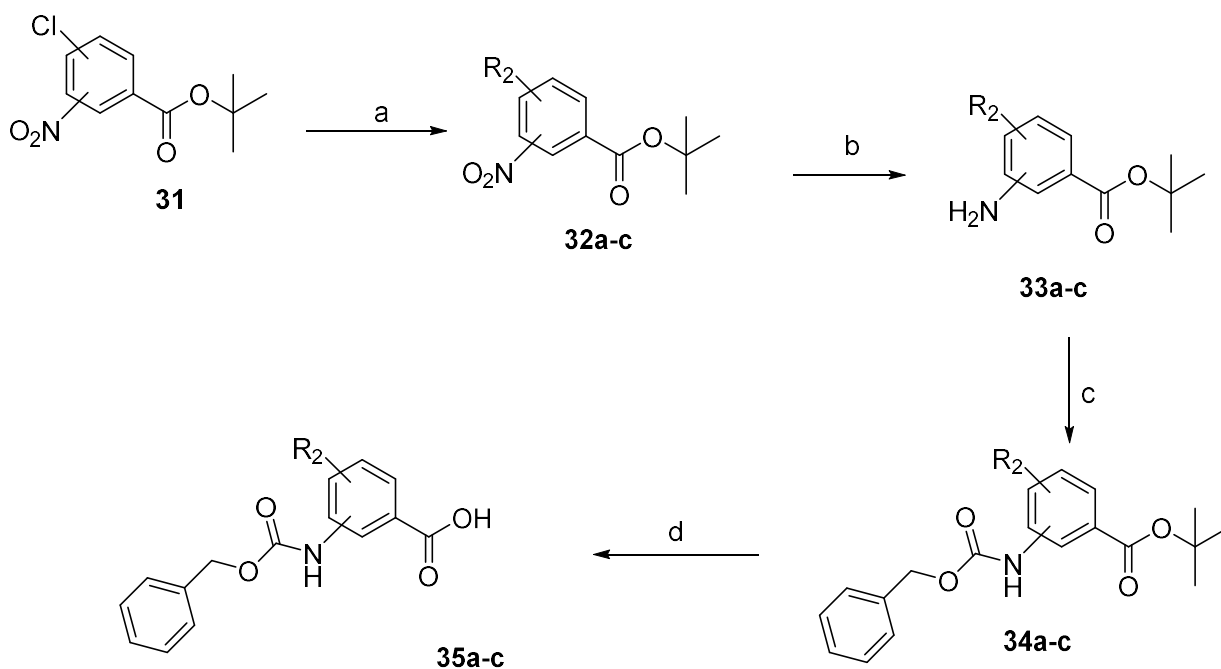
(s, 2H, Ph(NH₂)), 6.99-7.00 (d, 1H, aromatic proton), 7.36 (d, 1H, aromatic proton), 7.41-7.43 (dd, 1H, aromatic proton),; MS (EI) *m/z*: 291.19 [M]⁺; m.p. 114-116°C.

***tert*-butyl 3/4-(benzyloxycarbonylamino)-3/4-morpholino/(4-methylpiperazin-1-yl)benzoate (34a-c) Scheme 4. Example: *tert*-Butyl 3-(benzyloxycarbonylamino)-4-(4-methylpiperazin-1-yl)benzoate (34b).**

Benzyl chloroformate (2.1 mmol, 0.3 mL) was slowly added at 0 °C to a solution of 0.50 g (1.72 mmol) of *tert*-butyl 4-amino-3-(4-methylpiperazin-1-yl)benzoate (**33b**) in 10 mL of THF and 0.29 mL (2.1 mmol) of TEA. After stirring at RT for 1.5 h the solution was then quenched with water (20 mL) and extracted with CH₂Cl₂ (3 x 20 mL). The organic phases were washed with brine, dried over Na₂SO₄ and concentrated to afford a residue that was purified on silica gel (eluent EtOAc/CHCl₃, 1:1, v:v) providing 0.53 g (65%) of the *tert*-butyl benzoate **34b**. ¹H NMR (CDCl₃, 400 MHz) δ 1.60 (s, 9H, -COOC(CH₃)₃), 2.20 (s, 3H, -N(CH₃)), 2.61 (t, 4H, CH₃N(CH₂)₂), 2.92 (t, 4H, -PhN(CH₂)₂), 5.28 (s, 2H, -COOCH₂Ph), 7.15-7.17 (d, 1H, aromatic proton), 7.37-7.47 (m, 5H, -CH₂Ph), 7.69-7.71 (m, 2H, aromatic proton), 8.69 (br s, 1H, -PhNHCOO),; MS (EI) *m/z*: 425.23 [M]⁺.

3/4-(benzyloxycarbonylamino)-3/4-morpholino/(4-methylpiperazin-1-yl)benzoic acid (35a-c) Scheme 4. Example: 3-(benzyloxycarbonylamino)-4-(4-methylpiperazin-1-yl)benzoic acid (35b). A solution of 0.20 g (0.47 mmol) of *tert*-butyl benzoate **34b**, and 0.72 mL (9.4 mmol) of TFA in 5 mL of dry CH₂Cl₂ was stirred at RT overnight. The solvent was then removed and the resulting solid was first triturated with 10 mL Et₂O and then crystallized from acetonitrile to give 0.13 g (76%) of the benzoic acid **35b** as a colorless solid. ¹H NMR (DMSO-*d*₆, 400 MHz) δ 2.86 (s, 3H, -N(CH₃)), 3.08 (t, 4H, CH₃N(CH₂)₂), 3.20 (t, 4H, -PhN(CH₂)₂), 5.22 (s, 2H, -COOCH₂Ph), 7.22-7.25 (d, 1H, aromatic proton), 7.36-7.38 (d, 2H, aromatic protons), 7.40-7.46 (m, 3H, aromatic protons), 7.66-7.68 (d, 1H, aromatic proton), 8.36 (s, 1H, aromatic proton), 9.85 (br s, 1H, -PhNHCOO), 12.84 (br s, 1H, -COOH); MS (EI) *m/z*: 369.17 [M]⁺; m.p. 205-207°C.

Scheme 4^a



^a **Reagents and conditions:** (a) morpholine or 4-methylpiperazine, K₂CO₃, DMF, 90 °C, 5 h; (b) 10% Pd-C, MeOH, Parr apparatus, 50 psi, 25 °C, 5h; (c) Benzyl chloroformate, TEA, THF, RT 1.5 h; (d) TFA, CH₂Cl₂, RT, overnight.

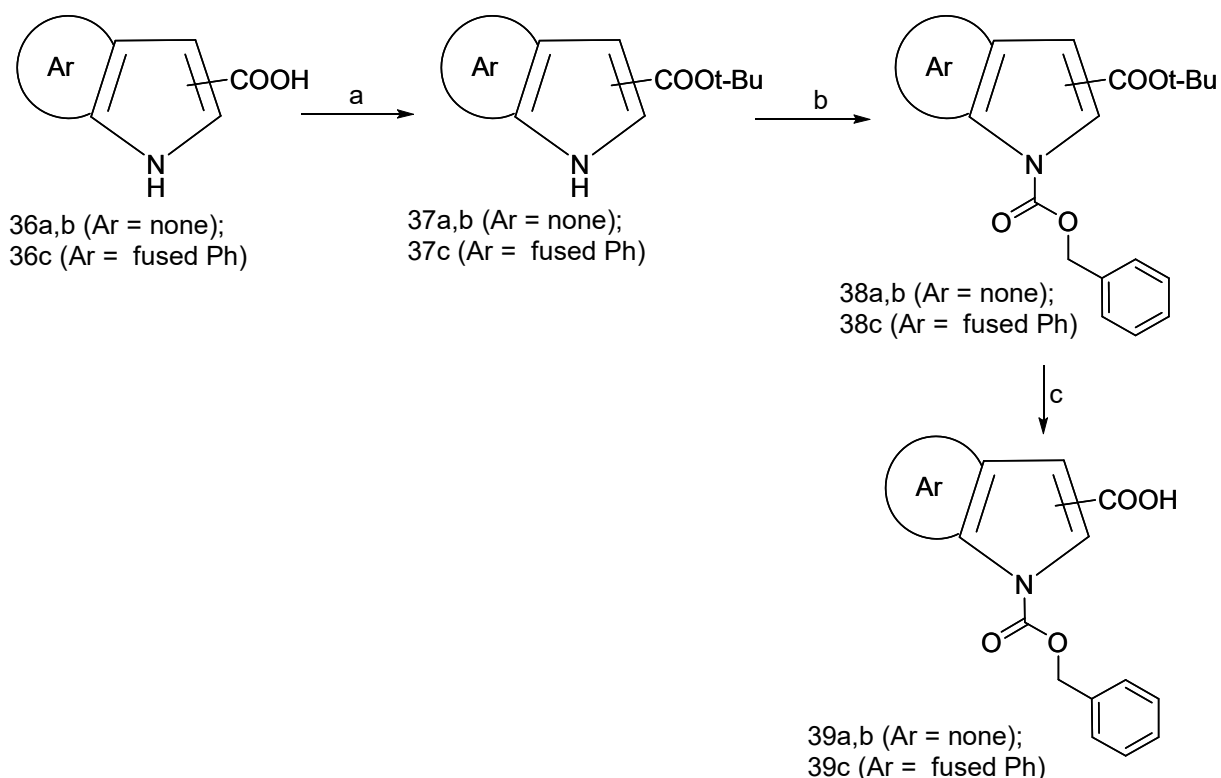
General procedure for the synthesis of the *tert*-butyl 1*H*-pyrrole and -1*H*-indole-2- and -3-carboxylates (37-c, Scheme 5). Example: *tert*-butyl 1*H*-pyrrole-3-carboxylate (37a). A mixture of 1*H*-pyrrole-3-carboxylic acid **36a** (1.0 mmol, 0.11 g) and *N,N*-dimethylformamide di-*tert*-butyl acetal (3.96 mmol, 0.80 g, 0.95 mL) in anhydrous benzene (15 mL) was stirred at 80 °C for 1 h. Afterwards, the solvent was evaporated and the residue obtained was purified by column chromatography (SiO₂ eluting with ethyl acetate/petroleum ether 1:9) to provide the pure **37a**. ¹H NMR (CDCl₃, 400 MHz, δ; ppm) δ 1.63 (s, 9H, (CH₃)₃), 6.78 (s, 1H, pyrrole proton), 7.12 (s, 1H, pyrrole proton), 7.46 (s, 1H, pyrrole proton), 11.3 (bs, 1H, NH pyrrole). MS (EI) *m/z*: 167.09 [M]⁺.

General procedure for the synthesis of the 1-benzyl 2- and 3-*tert*butyl 1*H*-pyrrole- and 1*H*-indole-1,2- and -1,3-dicarboxylates 38a-c (Scheme 5). Example: 1-benzyl 3-*tert*-butyl 1*H*-pyrrole-1,3- dicarboxylate (38a). *Tert*-butyl 1*H*-pyrrole-3-carboxylate **37a** (0.63 mmol, 0.14 g) in dry THF (2 mL) was added to a solution of NaH (0.94 mmol, 0.04 g) in dry THF (3 mL) at 0 °C, and the mixture was stirred at room temperature for 30 min, followed by the addition of benzyl chloroformate (0.94 mmol, 0.13 mL), and the reaction was stirred for 1 h further. The reaction was then quenched with water (20 mL) and extracted with chloroform (3 × 30 mL). The organic layers were washed with saturated sodium chloride solution (2 × 15 mL), dried

with anhydrous sodium sulfate and concentrated. The residue was purified by chromatographic column on silica gel eluting with ethyl acetate/*n*-hexane 1:10 to afford the pure **38a**. ^1H NMR (CDCl_3 , 400 MHz, δ ; ppm) δ 1.63 (s, 9H, $(\text{CH}_3)_3$), 5.27 (s, 2H, CH_2), 6.48 (s, 1H, pyrrole proton), 7.02 (s, 1H, pyrrole proton), 7.33- 7.36 (m, 3H, benzene protons), 7.54- 7.56 (m, 2H, benzene protons), 8.03 (s, 1H, pyrrole proton. MS (EI) m/z : 401.13 $[\text{M}]^+$.

General procedure for the synthesis of the 1- (benzyloxycarbonyl)-1*H*-pyrrole- and -1*H*-indole-2- and -3- carboxylic acids **39a-c (Scheme 5). Example: 1- (benzyloxycarbonyl)-1*H*-pyrrole-3-carboxylic acid (**39a**). 1-Benzyl 3-*tert*-butyl 1*H*-pyrrole-1,3-dicarboxylate **38a** (0.64 mmol, 0.22 g) was added to a solution of trifluoroacetic acid (0.77 mmol, 0.05 mL) in dry dichloromethane (3 mL). The resulting mixture was stirred for 5 h at room temperature. The reaction was then quenched with water (30 mL) and extracted with ethyl acetate (3×30 mL). The organic layers were washed with saturated sodium chloride solution (2×15 mL), dried with anhydrous sodium sulfate and concentrated in vacuo. The precipitated colorless solid was filtered, washed with petroleum ether and dried to afford the pure **39a**. ^1H NMR ($\text{DMSO}-d_6$, 400 MHz, δ ; ppm) δ 5.45 (s, 2H, CH_2), 6.78 (s, 1H, pyrrole proton), 7.12 (s, 1H, pyrrole proton), 7.43-7.46 (m, 3H, benzene protons), 7.64-7.66 (m, 2H, benzene protons), 8.33 (s, 1H, pyrrole proton), 12.09 (bs, 1H, COOH); MS (EI) m/z : 245.07 $[\text{M}]^+$.**

Scheme 5^a



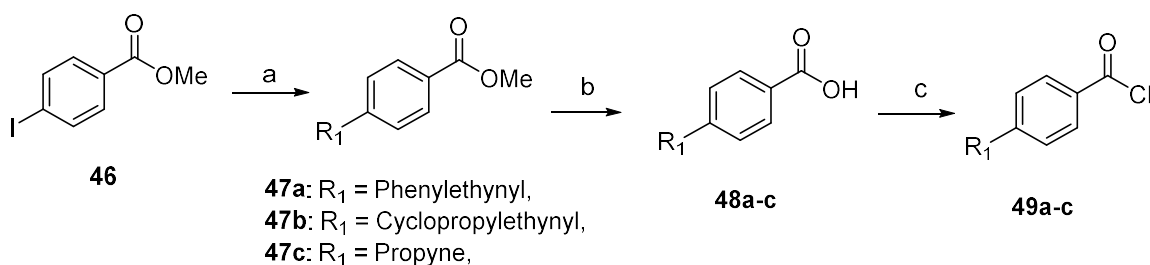
^a **Reagents and conditions:** (a) *N,N*-dimethylformamide di-*tert*-butyl acetal, toluene, 1 h, 80 °C; (b) 60% NaH, dry THF, benzyl chloroformate, 1 h, rt; (c) trifluoroacetic acid, dry DCM, 5 h, rt.

General procedure for Sonogashira reaction in liquid phase compounds 47a-c (Scheme 6): example methyl- 4-cyclopropylethynyl-benzoate (47b). Methyl-4-iodobenzoate **46** (2.50 mmol; 655 mg), triethylamine (25 mmol; 3.5 mL), CuI (5 mol %), PdCl₂(PPh₃)₂ (5 mol %), and ethynylcyclopropane (3.25 mmol) were dissolved in dry DMF (10 mL). After the mixture was stirred at 70 °C overnight, it was quenched with EtOAc and filtrated on Celite. The EtOAc solution was washed with water and brine, and the organic layer was dried over MgSO₄ and evaporated. The residue was purified by flash chromatography (ethyl acetate/hexane) to give methyl- 4-cyclopropylethynyl-benzoate **47b** as a white solid. ¹H NMR (400 MHz, CDCl₃): δ 0.75-0.77 (m, 2H, CH₂ cyclopropyl), 0.82-0.85 (m, 2H, CH₂ cyclopropyl), 1.38-1.42 (m, 1H CH cyclopropyl), 3.83 (s, 3H, CH₃), 7.33-7.36 (d, 2H, benzene protons), 7.85-7.88 (d, 2H, benzene protons).

General Procedure for the Preparation of 4-(Alkynyl)benzoic acids 48a-c (Scheme 6): example 4-(phenylethynyl)benzoic acid (48a). Methyl 4-(phenylethynyl)benzoate **47a** (2.27 mmol, 1 eq) was dissolved in a 60 mL of methanol/water (3:1), 2 N LiOH (6.81 mmol, 3 eq) was added thereto, and the mixture was stirred at room temperature for 5 min, and heated under reflux for overnight. The reaction mixture was allowed to cool to room temperature, and the solvent was evaporated under reduced pressure. The residue was suspended in water, and the suspension was acidified with 1 N HCl solution (pH = 2-4), and stirred at room temperature for 30 min. The obtained suspension was filtered, washed with water, and dried to obtain 4-(phenylethynyl)benzoic acid **48a** as a white solid. ¹H NMR (400 MHz, CDCl₃): δ 7.45-7.47 (m, 3H, benzene protons), 7.59-7.61 (m, 2H, benzene protons), 7.66-7.69 (d, 2H, benzene protons), 7.96-7.99 (d, 2H, benzene protons), 13.19 (bs, 1H, OH).

General Procedure for the preparation of aroyl chlorides 49a-c (Scheme 6): example 4-propynebenzoyl chloride (49c). A mixture of 4-phenylethynyl benzoic acid **48c** (3 mmol) in excess of SOCl₂ with two drops of *N,N*-dimethylformamide was refluxed at 85 °C for 3 h with nitrogen purge before the SOCl₂ was distilled off and purified by flash chromatography with DCM to afford 4-propynebenzoyl chloride **49c** as a low melting yellowish-solid. ¹H NMR (400 MHz, CDCl₃): δ 2.03 (s, 3H, CH₃), 7.41-7.43 (d, 2H, benzene protons), 7.95-7.98 (d, 2H, benzene protons).

Scheme 6^a



^a **Reagents and conditions:** (a) alkyne, 5% $\text{PdCl}_2(\text{PPh}_3)_2$, 5% CuI , Et_3N , dry THF/DMF, overnight, rt-70 °C; (b) 2 N LiOH , $\text{MeOH}:\text{H}_2\text{O}$, (3:1) overnight, rt; (c) SOCl_2 , 3 h reflux.

General procedures for the preparation of carbamates (45a-j) according to Method 1 (Scheme 1). Example: *tert*-Butyl ((1*R*,2*S*)-2-(4-((*R*)-2-(((Benzyloxy)carbonyl)amino)-3-phenylpropanamido)phenyl) cyclopropyl)carbamate **45j**. Triethylamine (0.89 mmol, 0.12 mL) and *N*-ethyl-*N'*-(3-dimethylaminopropyl)carbodiimide hydrochloride (0.89 mmol, 0.39 g) were added to a solution of *N*-benzyloxycarbonyl-D-phenylalanine **44** (0.74 mmol, 0.22 g) and *N*-hydroxybenzotriazole (0.89 mmol, 0.12 g) in dry dichloromethane (5 mL), and the mixture was stirred over a period of 1h. After this time, the compound **30a** [*tert*-butyl ((1*R*,2*S*)-2-(4-aminophenyl)cyclopropyl)carbamate, 0.81 mmol, 0.2 g] was added, and the stirring was continued for 1 h. The reaction was poured into water (50 mL) and extracted with dichloromethane (3 × 10 mL). The organic layers were washed with saturated sodium chloride solution (3 × 10 mL), dried with anhydrous sodium sulfate and concentrated. The residue was purified by chromatographic column on silica gel eluting with ethyl acetate/*n*-hexane 1/2 to afford the pure **45j** as a colorless solid. ^1H NMR (CDCl_3 , 400 MHz, δ ; ppm) δ 0.87-0.89 (m, 1H, CHH cyclopropane), 1.05-1.07 (m, 1H, CHH cyclopropane), 1.47 (s, 9H, $\text{C}(\text{CH}_3)_3$), 1.99-2.01 (m, 1H, PhCH), 2.67-2.69 (m, 1H, CHNH), 3.08-3.13 (m, 2H, PhCH_2CH), 4.54-4.56 (m, 1H, PhCH_2CH), 4.89 (bs, 1H, $\text{NHCOOC}(\text{CH}_3)_3$), 5.10 (s, 2H, $\text{PhCH}_2\text{OCONH}$), 5.60 (bs, 1H, NHCOOBn), 7.03-7.05 (d, 2H, benzene protons), 7.21-7.34 (m, 12H, benzene protons), 7.77 (bs, 1H, PhNHCOCH); MS (EI) m/z : 529.26 $[\text{M}]^+$.

General Procedure for the Synthesis of *trans tert*-butyl 2-(3/4-aroyle/benzyl)aminophenyl)cyclopropyl carbamates 60a-o (Method 2, Scheme 2). Example: *trans tert*-butyl (2-(4-(4-propylbenzamido)phenyl)cyclopropyl)carbamate (**60f**).

Triethylamine (0.846 mmol; 0.120 mL; 1.5 equiv) and 4-propyl-benzoyl chloride **52** (0.677 mmol; 0.130 mL; 1.2 equiv) were added dropwise to a cooled (0 °C) solution of *trans tert*-butyl 2-(4-aminophenyl)cyclopropylcarbamate **30a** (0.564 mmol; 140 mg; 1.0 equiv) in dry dichloromethane (5 mL). The mixture was stirred at room temperature for 2.3 h,

afterwards the reaction was quenched with saturated NaHCO_3 (30 mL) and extracted with EtOAc (3×30 mL), washed with saturated NaHCO_3 and Na_2CO_3 solution and dried with sodium sulfate. The solvent was removed under vacuum and the residue purified by flash chromatography on silica gel 60 eluting with ethyl acetate:hexane system to provide pure *trans tert*-butyl (2-(4-(4-propylbenzamido)phenyl)cyclopropyl)carbamate **60f** as white solid. ^1H NMR (CDCl_3 , 400 MHz): δ 0.86–0.90 (t, 3H, $\text{CH}_2\text{CH}_2\text{CH}_3$), 1.05–1.09 (m, 1H, *CHH* cyclopropane), 1.18 (s, 1H, *CHH* cyclopropane), 1.39 (s, 9H, $\text{COO}(\text{CH}_3)_3$), 1.57–1.63 (m, 2H, $\text{CH}_2\text{CH}_2\text{CH}_3$), 1.94–1.99 (m, 1H, $\text{CHNHCOO}(\text{CH}_3)_3$ cyclopropane), 2.56–2.60 (t, 2H, $\text{CH}_2\text{CH}_2\text{CH}_3$), 2.62–2.64 (m, 1H, *PhCH* cyclopropane), 4.78 (bs, 1H, $\text{NHCOO}(\text{CH}_3)_3$), 7.06–7.08 (d, 2H, benzene protons), 7.20–7.22 (d, 2H, benzene protons), 7.45–7.47 (d, 2H, benzene protons), 7.68 (bs, 1H, NHCOPh), 7.70–7.72 (d, 2H, benzene protons). MS (EI) m/z : 395.23 $[\text{M}]^+$.

General Procedure for the preparation of the final compounds 1-26 (Scheme 1 and 2): example *trans* 2-(4-(4-cyanobenzamido)phenyl)cyclopropylamine hydrochloride (18, GS3).

trans tert-Butyl (2-(4-(4-cyanobenzamido)phenyl)cyclopropyl)carbamate **60g** (95.5 mg, 0.253 mmol; 1.0 equiv) was dissolved in dry tetrahydrofuran (6 mL) and the solution was stirred at 0 °C. Then 4 N HCl in 1,4-dioxane (4.1 mL; 16.45 mmol; 65 equiv) was added dropwise and the mixture was allowed to warm at room temperature. After 48 h, when conversion was complete, the suspension was filtered and washed with dry THF and then with dry Et_2O to afford **18** as a hydrochloride salt. ^1H NMR ($\text{DMSO}-d_6$, 400 MHz, δ ; ppm) δ 1.17–1.22 (m, 1H, *CHH* cyclopropane), 1.36–1.34 (m, 1H, *CHH* cyclopropane), 2.32–2.34 (m, 1H, CHNH_2), 2.77–2.82 (m, 1H, *PhCH*), 7.15–7.17 (d, 2H, benzene protons), 7.70–7.72 (d, 2H, benzene protons), 8.01–8.03 (d, 2H, benzene protons), 8.10–8.12 (d, 2H, benzene protons), 8.46 (bs, 3H, NH_3^+), 10.51 (bs, 1H, CONH).

Benzyl *N*-[5-[[4-*trans*-2-aminocyclopropyl]phenyl]carbamoyl]-2-morpholinophenyl] carbamate hydrochloride (1, MC3371). Yield: 77%. ^1H NMR ($\text{DMSO}-d_6$, 400 MHz) δ 1.21 (m, 1H, *-CHH* cyclopropane), 1.38 (m, 1H, *-CHH* cyclopropane), 2.33 (m, 1H, *-CHNH}_2), 2.89 (t, 4H, *-N(CH}_2)_2*), 3.88 (m, 4H, *-O(CH}_2)_2*), 5.27 (s, 2H, *-NHCOOCH}_2\text{Ph}*), 7.15–7.18 (d, 2H, aromatic protons), 7.32–7.46 (m, 5H, aromatic protons), 7.71–7.73 (d, 2H, aromatic protons), 7.79–7.86 (m, 2H, aromatic protons), 8.03–8.05 (d, 1H, aromatic proton), 8.58 (br s, 3H, *-NH}_3^+*) 8.75 (br s, 1H, *-NHCOOCH}_2\text{Ph}*), 10.30 (br s, 1H, *-PhCONH*), 11.13 (br s, 1H, *-NH}^+*); MS (ESI) m/z : 487 $[(\text{M}+\text{H})^+]$.*

Benzyl *N*-[5-[[4-*trans*-2-aminocyclopropyl]phenyl]carbamoyl]-2-(4-methylpiperazin-1-yl)phenyl]carbamate dihydrochloride (2, MC3384). ¹H NMR (DMSO-*d*₆, 400 MHz) δ 1.20 (m, 1H, *CHH* cyclopropane), 1.39 (m, 1H, -*CHH* cyclopropane), 2.34 (m, 1H, -*CHNH*₂), 2.83 (t, 4H, -CH₃N(CH₂)₂), 3.15 (m, 4H, -PhN(CH₂)₂), 3.33 (s, 3H, -NCH₃), 5.23 (s, 2H, -NHCOOCH₂Ph), 7.15-7.18 (d, 2H, aromatic protons), 7.30-7.48 (m, 5H, aromatic protons), 7.70-7.72 (d, 2H, aromatic protons), 7.79-7.86 (m, 2H, aromatic protons), 8.01-8.03 (d, 1H, aromatic proton), 8.56 (br s, 3H, -NH₃⁺), 8.74 (br s, 1H, -NHCOOCH₂Ph), 10.27 (br s, 1H, -PhCONH), 11.12 (br s, 1H, -NH⁺); MS (ESI) *m/z*: 500 ([M+H]⁺).

Benzyl *N*-[4-[[4-*trans*-2-aminocyclopropyl]phenyl]carbamoyl]-2-morpholinophenyl]carbamate hydrochloride (3, MC3473). Yield: 78%. ¹H NMR (DMSO-*d*₆, 400 MHz) δ 1.22 (m, 1H, -*CHH* cyclopropane), 1.38 (m, 1H, -*CHH* cyclopropane), 2.33 (m, 1H, -*CHNH*₂), 2.88 (t, 4H, -N(CH₂)₂), 3.79 (m, 4H, -O(CH₂)₂), 5.22 (s, 2H, -NHCOOCH₂Ph), 7.14-7.16 (d, 1H, aromatic proton), 7.31-7.46 (m, 6H, aromatic protons), 7.69-7.71 (d, 1H, aromatic proton), 7.74-7.83 (m, 3H, aromatic protons), 7.94-8.02 (m, 2H, aromatic protons), 8.47 (br s, 3H, -NH₃⁺), 8.61 (br s, 1H, -NHCOOCH₂Ph), 10.15 (br s, 1H, -PhCONH); MS (EI) *m/z*: 486.23 [M]⁺.

***trans* benzyl 3-((4-(2-aminocyclopropyl)phenyl)carbamoyl)-1Hpyrrole-1-carboxylate hydrochloride (4, MC3413).** Mp, 177-179 °C (acetonitrile/methanol); yield, 62%. ¹H NMR (DMSO-*d*₆, 400 MHz, δ; ppm) δ 1.33-1.35 (m, 2H, CH₂ cyclopropane), 2.27 (m, 1H, CHNH₂HCl), 2.77-2.78 (m, 1H, PhCH), 5.46 (s, 2H, CH₂), 6.79 (s, 1H, pyrrole proton), 7.11-7.13 (d, 2H benzene protons), 7.41-7.47 (m, 4H, benzene and pyrrole protons), 7.52-7.54 (d, 2H, benzene protons), 7.64-7.66 (d, 2H, benzene protons), 8.33 (bs, 3H, NH₃⁺), 9.91 (bs, 1H, CONH) ppm; ¹³C NMR (DMSO-*d*₆, 100 MHz, δ; ppm) δ 17.2, 25.6, 34.3, 66.3, 102.4, 109.8, 115.0, 118.9, 121.0 (2C), 125.2 (2C), 127.0 (2C), 127.8, 128.7 (2C), 134.6, 136.4, 137.9, 150.1, 164.9 ppm; MS (EI) *m/z*: 375.16 [M]⁺

***trans* benzyl 2-((4-(2-aminocyclopropyl)phenyl)carbamoyl)-1Hpyrrole-1-carboxylate hydrochloride (5, MC3288).** Mp, 192-194 °C (methanol); yield, 61%. ¹H NMR (DMSO-*d*₆, 400 MHz, δ; ppm) δ 1.33-1.35 (m, 2H, CH₂ cyclopropane), 2.28 (m, 1H, CHNH₂HCl), 2.76-2.78 (m, 1H, PhCH), 5.57 (s, 2H, CH₂), 6.79 (s, 1H, pyrrole proton), 6.91 (s, 1H, pyrrole proton), 7.11-7.13 (d, 2H benzene protons), 7.39-7.43 (m, 4H, benzene and pyrrole protons), 7.52-7.54 (d, 2H, benzene protons), 7.64-7.66 (d, 2H, benzene protons), 8.31 (bs, 3H, NH₃⁺), 10.01 (bs, 1H, CONH) ppm; ¹³C NMR (DMSO-*d*₆, 100 MHz, δ; ppm) δ 17.2, 25.6, 34.3, 66.1, 109.0, 110.8,

121.0 (2C), 124.0, 124.7, 125.2 (2C) 127.1 (2C), 127.7, 128.6 (2C), 134.5, 136.1, 137.6, 150.3, 162.7 ppm; MS (EI) m/z : 375.18 $[M]^+$.

trans benzyl 2-((4-(2-aminocyclopropyl)phenyl)carbamoyl)-1Hindole-1-carboxylate hydrochloride (6, MC3382). Mp, 202-204 °C (methanol); yield, 63%. ^1H NMR (DMSO- d_6 , 400 MHz, δ ; ppm) δ 1.31-1.33 (m, 2H, CH_2 cyclopropane), 2.26 (m, 1H, CHNH_2HCl), 2.74-2.75 (m, 1H, PhCH), 5.44 (s, 2H, CH_2), 7.28-7.31 (m, 2H, benzene and indole protons), 7.31-7.43 (m, 4H benzene and indole protons), 7.47-7.52 (d, 2H, benzene protons), 7.59-7.61 (d, 2H, benzene protons), 7.69-7.71 (d, 2H, benzene protons), 7.94-7.96 (d, 1H, benzene proton), 8.14 (s, 1H, indole proton), 8.30 (bs, 3H, NH_3^+), 9.99 (bs, 1H, CONH) ppm; ^{13}C NMR (DMSO- d_6 , 100 MHz, δ ; ppm) δ 17.2, 25.6, 34.3, 66.3, 114.4, 115.8, 119.9, 121.2 (2C), 123.9, 124.1, 125.6 (2C), 127.0 (2C), 127.5, 127.9, 128.9 (2C), 134.1, 136.0, 136.9, 137.9, 144.1, 150.0, 162.3 ppm; MS (EI) m/z : 425.17 $[M]^+$.

trans 2-(4-(3-Ethynylbenzamido)phenyl)cyclopropylamine hydrochloride (10, GS4): ^1H NMR (DMSO- d_6 , 400 MHz, δ ; ppm) δ 1.16–1.21 (m, 1H, CHH cyclopropane), 1.34–1.40 (m, 1H, CHH cyclopropane), 2.28–2.32 (m, 1H, CHNH_2), 2.76–2.79 (m, 1H, PhCH), 4.33 (s, 1H, CH acetylene), 7.14–7.16 (d, 2H, benzene protons), 7.53–7.57 (t, 1H, benzene protons), 7.68–7.72 (t, 3H, benzene protons), 7.96–7.98 (d, 1H, benzene protons), 8.05 (s, 1H, benzene protons), 8.42 (bs, 3H, NH_3^+), 10.33 (bs, 1H, CONH).

Benzyl ((R)-1-((4-((1S,2R)-2-aminocyclopropyl)phenyl)amino)-1-oxo-3-phenylpropan-2-yl)carbamate Hydrochloride (11, MC3205). ^1H NMR (DMSO- d_6 , 400 MHz, δ ; ppm) δ 1.12-1.17 (m, 1H, CHH cyclopropane), 1.36-1.40 (m, 1H, CHH cyclopropane), 2.27-2.32 (m, 1H, CHNH_2), 2.74-2.78 (m, 1H, PhCH), 2.83-2.88 (m, 1H, PhCHHCH), 2.99-3.04 (m, 1H, PhCHHCH), 4.38-4.42 (t, 1H, $\text{PhCH}_2\text{CHCONH}$), 4.96 (s, 2H, $\text{PhCH}_2\text{OCONH}$), 7.09-7.33 (m, 12H, benzene protons and NHCOOBn), 7.53-7.55 (d, 2H, benzene protons), 7.70-7.72 (d, 1H, benzene proton), 8.47 (bs, 1H, NH_3^+), 10.19 (bs, 1H, CONH); MS (EI) m/z : 465.18 $[M]^+$.

trans 2-(4-(4-Phenylethynylbenzamido)phenyl)cyclopropylamine hydrochloride (12, GS5): ^1H NMR (DMSO- d_6 , 400 MHz, δ ; ppm) δ 1.18–1.21 (m, 1H, CHH cyclopropane), 1.35–1.40 (m, 1H, CHH cyclopropane), 2.29–2.33 (m, 1H, CHNH_2), 2.78–2.81 (m, 1H, PhCH), 15–7.17 (d, 2H, benzene protons), 7.46–7.47 (m, 3H, benzene protons), 7.60–7.62 (m, 2H, benzene protons), 7.71–7.74 (m, 4H, benzene protons), 8.01–8.03 (d, 2H, benzene protons), 8.38 (bs, 3H, NH_3^+), 10.34 (bs, 1H, CONH).

trans 2-(4-(4-Cyclopropylethynylbenzamido)phenyl)cyclopropylamine hydrochloride (13, GS6): ^1H NMR (DMSO- d_6 , 400 MHz, δ ; ppm) δ 0.78 (s, 2H, CH_2 cyclopropane acetylene), 0.92–0.93 (d, 2H, CH_2 cyclopropane acetylene), 1.16–1.20 (m, 1H, CHH cyclopropane), 1.35–1.39 (m, 1H, CHH cyclopropane), 1.55–1.62 (m, 1H, CH cyclopropane acetylene), 2.29–2.33 (m, 1H, CHNH), 2.78–2.80 (m, 1H, PhCH), 7.13–7.15 (d, 2H, benzene protons), 7.49–7.51 (d, 2H, benzene protons), 7.69–7.71 (d, 2H, benzene protons), 7.90–7.92 (d, 2H, benzene protons), 8.38 (bs, 3H, NH_3^+), 10.26 (bs, 1H, CONH).

trans 2-(4-(4-Propynylbenzamido)phenyl)cyclopropylamine hydrochloride (14, GS7): ^1H NMR (DMSO- d_6 , 400 MHz, δ ; ppm) δ 1.16–1.21 (m, 1H, CHH cyclopropane), 1.34–1.38 (m, H, CHH cyclopropane), 2.09 (s, 3H, CH_3), 2.31–2.33 (m, 1H, CHNH), 2.77–2.79 (m, 1H, PhCH), 7.13–7.15 (d, 2H, benzene protons), 7.52–7.54 (d, 2H, benzene protons), 7.69–7.72 (d, 2H, benzene protons), 7.91–7.93 (d, 2H, benzene protons), 8.40 (bs, 3H, NH_3^+), 10.27 (bs, 1H, CONH).

trans 2-(4-(4-Methylbenzamido)phenyl)cyclopropylamine hydrochloride (16, GS1): ^1H NMR (DMSO- d_6 , 400 MHz, δ ; ppm) δ 1.16–1.22 (m, 1H, CHH cyclopropane), 1.34–1.39 (m, 1H, CHH cyclopropane), 2.28–2.33 (m, 1H, CHNH $_2$), 2.39 (s, 3H, CH_3), 2.77–2.80 (m, 1H, PhCH), 7.13–7.15 (d, 2H, benzene protons), 7.32–7.34 (d, 2H, benzene protons), 7.70–7.72 (d, 2H, benzene protons), 7.86–7.88 (d, 2H, benzene protons), 8.42 (bs, 3H, NH_3^+), 10.15 (bs, 1H, CONH).

trans 2-(4-(4-Propylbenzamido)phenyl)cyclopropylamine hydrochloride (17, GS2): ^1H NMR (DMSO- d_6 , 400 MHz, δ ; ppm) δ 0.88–0.92 (t, 3H, $\text{CH}_2\text{CH}_2\text{CH}_3$), 1.16–1.21 (m, 1H, CHH cyclopropane), 1.33–1.38 (m, 1H, CHH cyclopropane), 1.57–1.67 (m, 2H, $\text{CH}_2\text{CH}_2\text{CH}_3$), 2.27–2.32 (m, 1H, CHNH $_2$), 2.61–2.65 (t, 2H, $\text{CH}_2\text{CH}_2\text{CH}_3$), 2.76–2.80 (m, 1H, PhCH), 7.12–7.14 (d, 2H, benzene protons), 7.33–7.35 (d, 2H, benzene protons), 7.69–7.71 (d, 2H, benzene protons), 7.86–7.88 (d, 2H, benzene protons), 8.38 (bs, 3H, NH_3^+), 10.15 (bs, 1H, CONH).

trans 2-(3-(4-Propynylbenzamido)phenyl)cyclopropylamine hydrochloride (25, GS8): ^1H NMR (DMSO- d_6 , 400 MHz, δ ; ppm) δ 1.14–1.19 (m, 1H, CHH cyclopropane), 1.26–1.31 (m, H, CHH cyclopropane), 2.09 (s, 3H, CH_3), 2.43–2.47 (m, 1H, CHNH), 2.79–2.81 (m, 1H, PhCH), 7.07–7.08 (d, 1H, benzene protons), 7.21–7.29 (m, 2H, benzene protons), 7.33–7.35 (m, 1H, benzene protons), 7.52–7.55 (d, 2H, benzene protons), 8.02–8.04 (d, 2H, benzene protons), 8.39 (bs, 3H, NH_3^+), 10.21 (bs, 1H, CONH).

trans 2-(3-(4-Cyclopropylethynylbenzamido)phenyl)cyclopropylamine hydrochloride (26, GS9): ^1H NMR ($\text{DMSO-}d_6$, 400 MHz, δ ; ppm) δ 0.79-80 (d, 2H, CH_2 cyclopropane acetylene), 0.94-0.96 (m, 2H, CH_2 cyclopropane acetylene), 1.15-1.19 (m, 1H, CHH cyclopropane), 1.28-1.31 (m, 1H, CHH cyclopropane), 1.58-1.63 (m, 1H, CH cyclopropane acetylene), 2.44-2.47 (m, 1H, CHNH), 2.81-2.82 (m, 1H, PhCH), 7.08-7.09 (d, 1H, benzene protons), 7.22-7.30 (m, 2H, benzene protons), 7.34-7.35 (d, 1H, benzene protons), 7.51-7.53 (d, 2H, benzene protons), 8.02-8.04 (d, 2H, benzene protons), 8.38 (bs, 3H, NH_3^+), 10.21 (bs, 1H, CONH).

8.4 Conclusion and perspectives

At this stage of the analysis of the results obtained with different LSD1 inhibitors in schistosomes, it is too early to draw hard and fast conclusions, as we are still waiting for biological results from Prof. Fantappi . However, some of the tested LSD1 inhibitors, including MC3935, have striking effects on the morphology of adults and schistosomula. Indeed, these effects are correlated with the downregulation of genes involved in egg shell formation and transmembrane transporters. Besides, effects on signaling pathways and genes involved in cell differentiation and cell fate determination are affected. This suggests that LSD1 inhibitors affect parasite development pathways. Taking into account the preliminary effect of MC3935 on *S. mansoni*, it has been demonstrated, as expected, that histone demethylase inhibitors are essential and attractive targets for development of new antischistosomal agents.

Indeed, several patents described LSD1 inhibitors, predominantly *N*-alkylated compounds, have been reported with excellent potency and selectivity against LSD1 over MAOs. In fact, the first two of the *N*-alkylated compounds, GSK2879552 and ORY-1001, have already been advanced to clinical trials for the treatment of cancer and neurodegenerative diseases. Hence, it would be wise to further explore the effect of *N*-alkylation of MC3935 and related derivatives on their activity against *S. mansoni* (Fig. 8.3).

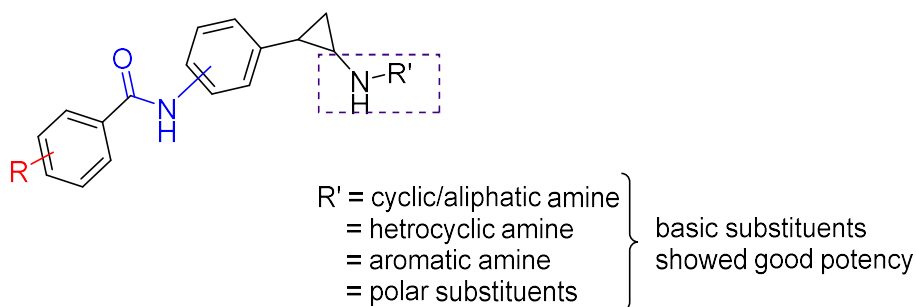


Fig. 8.3: Suggested further modifications on MC3935 and other analogues.

ACKNOWLEDGEMENTS

First and foremost, I would like to thank my supervisor Prof. Antonello Mai, for giving me the opportunity to undertake my PhD and for helping me to grow up both professionally and personally, as active member of his research group. I will never forget his support and for providing me numerous opportunities to learn and develop as a chemist.

I am deeply thankful to Dr. Dante Rotili for his guidance, encouragement and profitable contribution of ideas in drug synthesis. It was a real privilege and an honour for me to share of his exceptional knowledge of scientific but also of his extraordinary professionalism.

I would also like to express my sincere thanks to Dr. Sergio Valente for his advices and constant support throughout my PhD study.

I am thankful to Prof. A. Ganesan, for providing me the opportunity to work in his laboratory and for his support and encouragement during my stay. I would also like to thank all the members of Genesan's lab group of School of Pharmacy, University of East Anglia for all the support and a good working atmosphere provided to me.

I will always be grateful to "Neverlab" group members with whom I shared this beautiful experience for their unconditional help, insightful discussions, and friendship. In particular, I would like to thank Alessia L, Mariantonieta F, Daniela T, Clemens Z, Julia S, Roberta M and all the members/students, past and present, of my lab in Rome (Neverlab): thank you for all the time spent together and for mutual support. Probably without them this experience wouldn't be the same.

Finally, very special thanks to 'Sapienza' University of Rome for the financial support.

BIBIOLOGRAPHY

1. Waddington, C. H., The epigenotype. *Endeavour* **1942**, 1, 18–20.
2. Waddington, C. H., *The Strategy of the Genes* Allen & Unwin: London, **1957**.
3. Bird, A., Perceptions of epigenetics. *Nature* **2007**, 447 (7143), 396–8.
4. Russo, V. E. A., Martienssen, R. A. & Riggs, A. D. , *Epigenetic Mechanisms of Gene Regulation*. Cold Spring Harbor Laboratory Press: Woodbury, **1996**.
5. Sollars, V.; Lu, X.; Xiao, L., *et al.*, Evidence for an epigenetic mechanism by which Hsp90 acts as a capacitor for morphological evolution. *Nature Genetics* **2003**, 33 (1), 70–4.
6. Luger, K.; Mader, A. W.; Richmond, R. K.; Sargent, D. F.; Richmond, T. J., Crystal structure of the nucleosome core particle at 2.8 Å resolution. *Nature* **1997**, 389 (6648), 251–60.
7. Perri, F.; Longo, F.; Giuliano, M., *et al.*, Epigenetic control of gene expression: Potential implications for cancer treatment. *Critical Reviews in Oncology/Hematology* **2017**, 111, 166–172.
8. Grewal, S. I.; Moazed, D., Heterochromatin and epigenetic control of gene expression. *Science* **2003**, 301 (5634), 798–802.
9. Venkatesh, S.; Workman, J. L., Histone exchange, chromatin structure and the regulation of transcription. *Nature reviews. Molecular Cell Biology* **2015**, 16 (3), 178–89.
10. Suzuki, M. M.; Bird, A., DNA methylation landscapes: provocative insights from epigenomics. *Nature Reviews Genetics* **2008**, 9 (6), 465–76.
11. Chen, Q. W.; Zhu, X. Y.; Li, Y. Y.; Meng, Z. Q., Epigenetic regulation and cancer (review). *Oncology Reports* **2014**, 31 (2), 523–32.
12. Baylin, S. B.; Jones, P. A., A decade of exploring the cancer epigenome - biological and translational implications. *Nature Reviews Cancer* **2011**, 11 (10), 726–34.
13. Berger, S. L., The complex language of chromatin regulation during transcription. *Nature* **2007**, 447 (7143), 407–12.
14. Kouzarides, T., Chromatin modifications and their function. *Cell* **2007**, 128 (4), 693–705.
15. Dawson, M. A.; Kouzarides, T., Cancer epigenetics: from mechanism to therapy. *Cell* **2012**, 150 (1), 12–27.
16. Falkenberg, K. J.; Johnstone, R. W., Histone deacetylases and their inhibitors in cancer, neurological diseases and immune disorders. *Nature Reviews Drug Discovery* **2014**, 13 (9), 673–91.
17. Jones, P. A.; Baylin, S. B., The epigenomics of cancer. *Cell* **2007**, 128 (4), 683–92.
18. Bernstein, B. E.; Meissner, A.; Lander, E. S., The mammalian epigenome. *Cell* **2007**, 128 (4), 669–81.
19. Zhang, B.; Pan, X.; Cobb, G. P.; Anderson, T. A., microRNAs as oncogenes and tumor suppressors. *Developmental Biology* **2007**, 302 (1), 1–12.
20. Jiang, C.; Pugh, B. F., Nucleosome positioning and gene regulation: advances through genomics. *Nature Reviews Genetics* **2009**, 10 (3), 161–72.
21. Jones, P. A.; Baylin, S. B., The fundamental role of epigenetic events in cancer. *Nature Reviews Genetics* **2002**, 3 (6), 415–28.
22. Egger, G.; Liang, G.; Aparicio, A.; Jones, P. A., Epigenetics in human disease and prospects for epigenetic therapy. *Nature* **2004**, 429 (6990), 457–63.
23. Arrowsmith, C. H.; Bountra, C.; Fish, P. V.; Lee, K.; Schapira, M., Epigenetic protein families: a new frontier for drug discovery. *Nature Reviews Drug Discovery* **2012**, 11 (5), 384–400.
24. Meaney, M. J., Epigenetics and the biological definition of gene x environment interactions. *Child Development* **2010**, 81 (1), 41–79.
25. Kelly, T. K.; De Carvalho, D. D.; Jones, P. A., Epigenetic modifications as therapeutic targets. *Nature Biotechnology* **2010**, 28 (10), 1069–78.
26. Meaney, M. J.; Ferguson-Smith, A. C., Epigenetic regulation of the neural transcriptome: the meaning of the marks. *Nature Neuroscience* **2010**, 13 (11), 1313–8.
27. Portela, A.; Esteller, M., Epigenetic modifications and human disease. *Nature Biotechnology* **2010**, 28 (10), 1057–68.

28. Dawson, M. A.; Kouzarides, T.; Huntly, B. J., Targeting epigenetic readers in cancer. *The New England Journal of Medicine* **2012**, 367 (7), 647-57.
29. Kaminskas, E.; Farrell, A.; Abraham, S., *et al.*, Approval summary: azacitidine for treatment of myelodysplastic syndrome subtypes. *Clinical Cancer Research : an official journal of the American Association for Cancer Research* **2005**, 11 (10), 3604-8.
30. Kaminskas, E.; Farrell, A. T.; Wang, Y. C.; Sridhara, R.; Pazdur, R., FDA drug approval summary: azacitidine (5-azacytidine, Vidaza) for injectable suspension. *The Oncologist* **2005**, 10 (3), 176-82.
31. Daigle, S. R.; Olhava, E. J.; Therkelsen, C. A., *et al.*, Potent inhibition of DOT1L as treatment of MLL-fusion leukemia. *Blood* **2013**, 122 (6), 1017-25.
32. Yu, W.; Chory, E. J.; Wernimont, A. K., *et al.*, Catalytic site remodelling of the DOT1L methyltransferase by selective inhibitors. *Nature communications* **2012**, 3, 1288.
33. McCabe, M. T.; Ott, H. M.; Ganji, G., *et al.*, EZH2 inhibition as a therapeutic strategy for lymphoma with EZH2-activating mutations. *Nature* **2012**, 492 (7427), 108-12.
34. Knutson, S. K.; Wigle, T. J.; Warholic, N. M., *et al.*, A selective inhibitor of EZH2 blocks H3K27 methylation and kills mutant lymphoma cells. *Nature Chemical Biology* **2012**, 8 (11), 890-6.
35. Bonham, K.; Hemmers, S.; Lim, Y. H., *et al.*, Effects of a novel arginine methyltransferase inhibitor on T-helper cell cytokine production. *The FEBS Journal* **2010**, 277 (9), 2096-108.
36. Kleinschmidt, M. A.; de Graaf, P.; van Teeffelen, H. A.; Timmers, H. T., Cell cycle regulation by the PRMT6 arginine methyltransferase through repression of cyclin-dependent kinase inhibitors. *PLoS One* **2012**, 7 (8), e41446.
37. Pande, V., Understanding the Complexity of Epigenetic Target Space. *J Med Chem* **2016**, 59 (4), 1299-307.
38. Robertson, K. D., DNA methylation and human disease. *Nature Reviews Genetics* **2005**, 6 (8), 597-610.
39. Du, J.; Johnson, L. M.; Jacobsen, S. E.; Patel, D. J., DNA methylation pathways and their crosstalk with histone methylation. *Nature reviews. Molecular Cell Biology* **2015**, 16 (9), 519-32.
40. Gros, C.; Fahy, J.; Halby, L., *et al.*, DNA methylation inhibitors in cancer: recent and future approaches. *Biochimie* **2012**, 94 (11), 2280-2296.
41. Castillo-Aguilera, O.; Depreux, P.; Halby, L.; Arimondo, P. B.; Goossens, L., DNA Methylation Targeting: The DNMT/HMT Crosstalk Challenge. *Biomolecules* **2017**, 7 (1).
42. Yoo, C. B.; Jones, P. A., Epigenetic therapy of cancer: past, present and future. *Nature Reviews Drug Discovery* **2006**, 5 (1), 37-50.
43. Comb, M.; Goodman, H. M., CpG methylation inhibits proenkephalin gene expression and binding of the transcription factor AP-2. *Nucleic Acids Research* **1990**, 18 (13), 3975-82.
44. Inamdar, N. M.; Ehrlich, K. C.; Ehrlich, M., CpG methylation inhibits binding of several sequence-specific DNA-binding proteins from pea, wheat, soybean and cauliflower. *Plant Molecular Biology* **1991**, 17 (1), 111-23.
45. Jin, B.; Li, Y.; Robertson, K. D., DNA Methylation: Superior or Subordinate in the Epigenetic Hierarchy? *Genes & Cancer* **2011**, 2 (6), 607-617.
46. Ehrlich, M., DNA methylation in cancer: too much, but also too little. *Oncogene* **2002**, 21 (35), 5400-13.
47. Bestor, T.; Laudano, A.; Mattaliano, R.; Ingram, V., Cloning and sequencing of a cDNA encoding DNA methyltransferase of mouse cells. The carboxyl-terminal domain of the mammalian enzymes is related to bacterial restriction methyltransferases. *Journal of Molecular Biology* **1988**, 203 (4), 971-83.
48. Cheng, X.; Blumenthal, R. M., Mammalian DNA methyltransferases: a structural perspective. *Structure* **2008**, 16 (3), 341-50.
49. Bestor, T. H., The DNA methyltransferases of mammals. *Human Molecular Genetics* **2000**, 9 (16), 2395-2402.
50. Probst, A. V.; Dunleavy, E.; Almouzni, G., Epigenetic inheritance during the cell cycle. *Nature reviews. Molecular Cell Biology* **2009**, 10 (3), 192-206.

51. Goll, M. G.; Kirpekar, F.; Maggert, K. A., *et al.*, Methylation of tRNA^{Asp} by the DNA methyltransferase homolog Dnmt2. *Science* **2006**, *311* (5759), 395-8.
52. Kareta, M. S.; Botello, Z. M.; Ennis, J. J.; Chou, C.; Chedin, F., Reconstitution and mechanism of the stimulation of de novo methylation by human DNMT3L. *The Journal of Biological Chemistry* **2006**, *281* (36), 25893-902.
53. Egger, G.; Jeong, S.; Escobar, S. G., *et al.*, Identification of DNMT1 (DNA methyltransferase 1) hypomorphs in somatic knockouts suggests an essential role for DNMT1 in cell survival. *Proceedings of the National Academy of Sciences of the United States of America* **2006**, *103* (38), 14080-5.
54. Riggs, A. D.; Xiong, Z., Methylation and epigenetic fidelity. *Proceedings of the National Academy of Sciences of the United States of America* **2004**, *101* (1), 4-5.
55. Klimasauskas, S.; Kumar, S.; Roberts, R. J.; Cheng, X., HhaI methyltransferase flips its target base out of the DNA helix. *Cell* **1994**, *76* (2), 357-69.
56. Verdine, G. L., The flip side of DNA methylation. *Cell* **1994**, *76* (2), 197-200.
57. de Lera, A. R.; Ganesan, A., Epigenetic polypharmacology: from combination therapy to multitargeted drugs. *Clinical Epigenetics* **2016**, *8*, 105.
58. Hargreaves, D. C.; Crabtree, G. R., ATP-dependent chromatin remodeling: genetics, genomics and mechanisms. *Cell Res* **2011**, *21* (3), 396-420.
59. Richmond, T. J.; Davey, C. A., The structure of DNA in the nucleosome core. *Nature* **2003**, *423* (6936), 145-50.
60. Tan, S.; Davey, C. A., Nucleosome structural studies. *Current Opinion in Structural Biology* **2011**, *21* (1), 128-36.
61. Woodcock, C. L.; Ghosh, R. P., Chromatin higher-order structure and dynamics. *Cold Spring Harbor Perspectives in Biology* **2010**, *2* (5), a000596.
62. Levenson, J. M.; Sweatt, J. D., Epigenetic mechanisms in memory formation. *Nature Reviews Neuroscience* **2005**, *6* (2), 108-18.
63. Anderson, J. D.; Widom, J., Sequence and position-dependence of the equilibrium accessibility of nucleosomal DNA target sites. *Journal of Molecular Biology* **2000**, *296* (4), 979-87.
64. Lowary, P. T.; Widom, J., New DNA sequence rules for high affinity binding to histone octamer and sequence-directed nucleosome positioning. *Journal of Molecular Biology* **1998**, *276* (1), 19-42.
65. Widom, J., Role of DNA sequence in nucleosome stability and dynamics. *Q Rev Biophys* **2001**, *34* (3), 269-324.
66. Segal, E.; Widom, J., From DNA sequence to transcriptional behaviour: a quantitative approach. *Nature Reviews Genetics* **2009**, *10* (7), 443-56.
67. Shogren-Knaak, M.; Ishii, H.; Sun, J. M., *et al.*, Histone H4-K16 acetylation controls chromatin structure and protein interactions. *Science* **2006**, *311* (5762), 844-7.
68. Fierz, B.; Chatterjee, C.; McGinty, R. K., *et al.*, Histone H2B ubiquitylation disrupts local and higher-order chromatin compaction. *Nature Chemical Biology* **2011**, *7* (2), 113-119.
69. Zentner, G. E.; Henikoff, S., Regulation of nucleosome dynamics by histone modifications. *Nature Structural & Molecular Biology* **2013**, *20* (3), 259-266.
70. Patel, D. J.; Wang, Z., Readout of epigenetic modifications. *Annual Review of Biochemistry* **2013**, *82*, 81-118.
71. Rando, O. J.; Winston, F., Chromatin and transcription in yeast. *Genetics* **2012**, *190* (2), 351-87.
72. Papamichos-Chronakis, M.; Peterson, C. L., Chromatin and the genome integrity network. *Nature Reviews Genetics* **2013**, *14* (1), 62-75.
73. Clapier, C. R.; Cairns, B. R., The Biology of Chromatin Remodeling Complexes. *Annual Review of Biochemistry* **2009**, *78* (1), 273-304.
74. Boyer, L. A.; Logie, C.; Bonte, E., *et al.*, Functional delineation of three groups of the ATP-dependent family of chromatin remodeling enzymes. *The Journal of Biological Chemistry* **2000**, *275* (25), 18864-70.

75. Rothbart, S. B.; Strahl, B. D., Interpreting the language of histone and DNA modifications. *Biochimica et Biophysica Acta (BBA) - Gene Regulatory Mechanisms* **2014**, 1839 (8), 627-643.
76. Bannister, A. J.; Kouzarides, T., Regulation of chromatin by histone modifications. *Cell Research* **2011**, 21 (3), 381-395.
77. Strahl, B. D.; Allis, C. D., The language of covalent histone modifications. *Nature* **2000**, 403 (6765), 41-5.
78. Yun, M.; Wu, J.; Workman, J. L.; Li, B., Readers of histone modifications. *Cell Res* **2011**, 21 (4), 564-78.
79. Shliaha, P. V.; Baird, M. A.; Nielsen, M. M., *et al.*, Characterization of Complete Histone Tail Proteoforms Using Differential Ion Mobility Spectrometry. *Analytical Chemistry* **2017**.
80. Bowman, G. D.; Poirier, M. G., Post-translational modifications of histones that influence nucleosome dynamics. *Chemical Reviews* **2015**, 115 (6), 2274-95.
81. Avvakumov, N.; Nourani, A.; Côté, J., Histone Chaperones: Modulators of Chromatin Marks. *Molecular Cell* **2011**, 41 (5), 502-514.
82. Murawska, M.; Brehm, A., CHD chromatin remodelers and the transcription cycle. *Transcription* **2011**, 2 (6), 244-53.
83. Josling, G. A.; Selvarajah, S. A.; Petter, M.; Duffy, M. F., The role of bromodomain proteins in regulating gene expression. *Genes* **2012**, 3 (2), 320-43.
84. Petty, E.; Pillus, L., Balancing chromatin remodeling and histone modifications in transcription. *Trends in Genetics* **2013**, 29 (11), 621-629.
85. Hansen, J. C.; Nyborg, J. K.; Luger, K.; Stargell, L. A., Histone chaperones, histone acetylation, and the fluidity of the chromogenome. *Journal of Cellular Physiology* **2010**, 224 (2), 289-99.
86. Liu, W. H.; Churchill, M. E., Histone transfer among chaperones. *Biochemical Society transactions* **2012**, 40 (2), 357-63.
87. Das, C.; Tyler, J. K., Histone exchange and histone modifications during transcription and aging. *Biochimica et Biophysica Acta* **2013**, 1819 (3-4), 332-42.
88. Olsen, C. A., Expansion of the lysine acylation landscape. *Angewandte Chemie (International ed. in English)* **2012**, 51 (16), 3755-6.
89. Cosgrove, M. S.; Boeke, J. D.; Wolberger, C., Regulated nucleosome mobility and the histone code. *Nature Structural & Molecular Biology* **2004**, 11 (11), 1037-43.
90. Cosgrove, M. S.; Wolberger, C., How does the histone code work? *Biochemistry and Cell Biology* **2005**, 83 (4), 468-76.
91. Mersfelder, E. L.; Parthun, M. R., The tale beyond the tail: histone core domain modifications and the regulation of chromatin structure. *Nucleic Acids Research* **2006**, 34 (9), 2653-62.
92. Ning, B.; Li, W.; Zhao, W.; Wang, R., Targeting epigenetic regulations in cancer. *Acta Biochimica et Biophysica Sinica* **2016**, 48 (1), 97-109.
93. Murray, K., The Occurrence of ϵ -N-Methyl Lysine in Histones. *Biochemistry* **1964**, 3 (1), 10-15.
94. Chen, D.; Ma, H.; Hong, H., *et al.*, Regulation of transcription by a protein methyltransferase. *Science* **1999**, 284 (5423), 2174-7.
95. Paik, W. K.; Kim, S., ϵ -N-dimethyllysine in histones. *Biochemical and Biophysical Research Communications* **1967**, 27 (4), 479-483.
96. Gershey, E. L.; Haslett, G. W.; Vidali, G.; Allfrey, V. G., Chemical studies of histone methylation. Evidence for the occurrence of 3-methylhistidine in avian erythrocyte histone fractions. *The Journal of Biological Chemistry* **1969**, 244 (18), 4871-7.
97. Greer, E. L.; Shi, Y., Histone methylation: a dynamic mark in health, disease and inheritance. *Nature Reviews Genetics* **2012**, 13 (5), 343-357.
98. Strahl, B. D.; Ohba, R.; Cook, R. G.; Allis, C. D., Methylation of histone H3 at lysine 4 is highly conserved and correlates with transcriptionally active nuclei in Tetrahymena. *Proceedings of the National Academy of Sciences of the United States of America* **1999**, 96 (26), 14967-72.
99. van Holde, K. E., The First Hundred Years. In *Springer Series in Molecular Biology*, Springer New York: 1989; pp 1-15.

100. Zheng, Q.; Simel, E. J.; Klein, P. E.; Royer, M. T.; Houtz, R. L., Expression, purification, and characterization of recombinant ribulose-1,5-bisphosphate carboxylase/oxygenase large subunit neptisin-methyltransferase. *Protein Expression and Purification* **1998**, *14* (1), 104-12.
101. Polevoda, B.; Martzen, M. R.; Das, B.; Phizicky, E. M.; Sherman, F., Cytochrome c methyltransferase, Ctm1p, of yeast. *The Journal of Biological Chemistry* **2000**, *275* (27), 20508-13.
102. McGrath, J.; Trojer, P., Targeting histone lysine methylation in cancer. *Pharmacology & Therapeutics* **2015**, *150*, 1-22.
103. Barski, A.; Cuddapah, S.; Cui, K., *et al.*, High-Resolution Profiling of Histone Methylations in the Human Genome. *Cell* **2007**, *129* (4), 823-837.
104. Lee, J.-S.; Smith, E.; Shilatifard, A., The Language of Histone Crosstalk. *Cell* **2010**, *142* (5), 682-685.
105. Fraga, M. F.; Ballestar, E.; Villar-Garea, A., *et al.*, Loss of acetylation at Lys16 and trimethylation at Lys20 of histone H4 is a common hallmark of human cancer. *Nature genetics* **2005**, *37* (4), 391-400.
106. Wang, Z.; Patel, D. J., Small molecule epigenetic inhibitors targeted to histone lysine methyltransferases and demethylases. *Quarterly Reviews of Biophysics* **2013**, *46* (04), 349-373.
107. Helin, K.; Dhanak, D., Chromatin proteins and modifications as drug targets. *Nature* **2013**, *502* (7472), 480-488.
108. Iwase, S.; Xiang, B.; Ghosh, S., *et al.*, ATRX ADD domain links an atypical histone methylation recognition mechanism to human mental-retardation syndrome. *Nature Structural & Molecular Biology* **2011**, *18* (7), 769-776.
109. Zhang, Y.; Reinberg, D., Transcription regulation by histone methylation: interplay between different covalent modifications of the core histone tails. *Genes & Development* **2001**, *15* (18), 2343-60.
110. Baxter, C. S.; Byvoet, P., Intercalating agents as probes of the spatial relationship between chromatin components. *Biochemical and Biophysical Research Communications* **1975**, *63* (1), 286-91.
111. Byvoet, P.; Shepherd, G. R.; Hardin, J. M.; Noland, B. J., The distribution and turnover of labeled methyl groups in histone fractions of cultured mammalian cells. *Archives of Biochemistry and Biophysics* **1972**, *148* (2), 558-67.
112. Turner, B. M., Memorable transcription. *Nature Cell Biology* **2003**, *5* (5), 390-3.
113. Rice, J. C.; Allis, C. D., Histone methylation versus histone acetylation: new insights into epigenetic regulation. *Current Opinion in Cell Biology* **2001**, *13* (3), 263-73.
114. Copeland, R. A.; Solomon, M. E.; Richon, V. M., Protein methyltransferases as a target class for drug discovery. *Nature Reviews Drug Discovery* **2009**, *8* (9), 724-32.
115. Shi, Y.; Lan, F.; Matson, C., *et al.*, Histone Demethylation Mediated by the Nuclear Amine Oxidase Homolog LSD1. *Cell* **2004**, *119* (7), 941-953.
116. Feng, Q.; Wang, H.; Ng, H. H., *et al.*, Methylation of H3-Lysine 79 Is Mediated by a New Family of HMTases without a SET Domain. *Current Biology* **2002**, *12* (12), 1052-1058.
117. Herz, H.-M.; Garruss, A.; Shilatifard, A., SET for life: biochemical activities and biological functions of SET domain-containing proteins. *Trends in Biochemical Sciences* **2013**, *38* (12), 621-639.
118. Sims, R. J., 3rd; Nishioka, K.; Reinberg, D., Histone lysine methylation: a signature for chromatin function. *Trends in Genetics : TIG* **2003**, *19* (11), 629-39.
119. Kouzarides, T., Histone methylation in transcriptional control. *Current Opinion in Genetics & Development* **2002**, *12* (2), 198-209.
120. Lachner, M.; Jenuwein, T., The many faces of histone lysine methylation. *Current Opinion in Cell Biology* **2002**, *14* (3), 286-98.
121. Marmorstein, R., Structure of SET domain proteins: a new twist on histone methylation. *Trends Biochem Sci* **2003**, *28* (2), 59-62.
122. Schneider, R.; Bannister, A. J.; Kouzarides, T., Unsafe SETs: histone lysine methyltransferases and cancer. *Trends Biochem Sci* **2002**, *27* (8), 396-402.
123. Xiao, B.; Jing, C.; Wilson, J. R., *et al.*, Structure and catalytic mechanism of the human histone methyltransferase SET7/9. *Nature* **2003**, *421* (6923), 652-6.

124. Patnaik, D.; Chin, H. G.; Esteve, P. O., *et al.*, Substrate specificity and kinetic mechanism of mammalian G9a histone H3 methyltransferase. *The Journal of Biological Chemistry* **2004**, 279 (51), 53248-58.
125. Swalm, B. M.; Knutson, S. K.; Warholc, N. M., *et al.*, Reaction coupling between wild-type and disease-associated mutant EZH2. *ACS Chemical Biology* **2014**, 9 (11), 2459-64.
126. Santos-Rosa, H.; Schneider, R.; Bannister, A. J., *et al.*, Active genes are tri-methylated at K4 of histone H3. *Nature* **2002**, 419 (6905), 407-11.
127. Bedford, M. T.; Clarke, S. G., Protein arginine methylation in mammals: who, what, and why. *Molecular Cell* **2009**, 33 (1), 1-13.
128. Di Lorenzo, A.; Bedford, M. T., Histone arginine methylation. *FEBS Lett* **2011**, 585 (13), 2024-31.
129. Hadjikyriacou, A.; Yang, Y.; Bedford, M.; Clarke, S., Characterization of the activity and biological function of human protein arginine methyltransferase 9 (PRMT9). *The FASEB Journal* **2015**, 29 (1 Supplement), LB211.
130. Tschiersch, B.; Hofmann, A.; Krauss, V., *et al.*, The protein encoded by the Drosophila position-effect variegation suppressor gene Su(var)3-9 combines domains of antagonistic regulators of homeotic gene complexes. *The EMBO Journal* **1994**, 13 (16), 3822-31.
131. Smith, B. C.; Denu, J. M., Chemical mechanisms of histone lysine and arginine modifications. *Biochimica et Biophysica Acta* **2009**, 1789 (1), 45-57.
132. Shepherd, G. R.; Hardin, J. M.; Noland, B. J., Methylation of lysine residues of histone fractions in synchronized mammalian cells. *Archives of Biochemistry and Biophysics* **1971**, 143 (1), 1-5.
133. Jenuwein, T., Re-SET-ting heterochromatin by histone methyltransferases. *Trends in Cell Biology* **2001**, 11 (6), 266-73.
134. Ahmad, K.; Henikoff, S., The histone variant H3.3 marks active chromatin by replication-independent nucleosome assembly. *Molecular Cell* **2002**, 9 (6), 1191-200.
135. Karytinis, A.; Forneris, F.; Profumo, A., *et al.*, A Novel Mammalian Flavin-dependent Histone Demethylase. *Journal of Biological Chemistry* **2009**, 284 (26), 17775-17782.
136. Tian, X.; Fang, J., Current Perspectives on Histone Demethylases. *Acta Biochimica et Biophysica Sinica* **2007**, 39 (2), 81-88.
137. Forneris, F.; Binda, C.; Vanoni, M. A.; Mattevi, A.; Battaglioli, E., Histone demethylation catalysed by LSD1 is a flavin-dependent oxidative process. *FEBS Letters* **2005**, 579 (10), 2203-2207.
138. Dong, C.; Zhang, H.; Xu, C.; Arrowsmith, C. H.; Min, J., Structure and function of dioxygenases in histone demethylation and DNA/RNA demethylation. *IUCr* **2014**, 1 (6), 540-549.
139. Rotili, D.; Mai, A., Targeting Histone Demethylases: A New Avenue for the Fight against Cancer. *Genes & Cancer* **2011**, 2 (6), 663-679.
140. Thinnis, C. C.; England, K. S.; Kawamura, A., *et al.*, Targeting histone lysine demethylases — Progress, challenges, and the future. *Biochimica et Biophysica Acta (BBA) - Gene Regulatory Mechanisms* **2014**, 1839 (12), 1416-1432.
141. Hakimi, M. A.; Bochar, D. A.; Chenoweth, J., *et al.*, A core-BRAF35 complex containing histone deacetylase mediates repression of neuronal-specific genes. *Proceedings of the National Academy of Sciences* **2002**, 99 (11), 7420-7425.
142. Zhen, C. Y.; Tatavosian, R.; Huynh, T. N., *et al.*, Live-cell single-molecule tracking reveals co-recognition of H3K27me3 and DNA targets polycomb Cbx7-PRC1 to chromatin. *eLife* **2016**, 5.
143. Battaglioli, E.; Andres, M. E.; Rose, D. W., *et al.*, REST Repression of Neuronal Genes Requires Components of the hSWI{middle dot}SNF Complex. *Journal of Biological Chemistry* **2002**, 277 (43), 41038-41045.
144. You, A.; Tong, J. K.; Grozinger, C. M.; Schreiber, S. L., CoREST is an integral component of the CoREST- human histone deacetylase complex. *Proceedings of the National Academy of Sciences* **2001**, 98 (4), 1454-1458.
145. Aravind, L.; Iyer, L. M., The SWIRM domain: a conserved module found in chromosomal proteins points to novel chromatin-modifying activities. *Genome Biology* **2002**, 3 (8), Research0039.

146. Stavropoulos, P.; Blobel, G.; Hoelz, A., Crystal structure and mechanism of human lysine-specific demethylase-1. *Nature Structural & Molecular Biology* **2006**, *13* (7), 626-32.
147. Yang, M.; Gocke, C. B.; Luo, X., *et al.*, Structural Basis for CoREST-Dependent Demethylation of Nucleosomes by the Human LSD1 Histone Demethylase. Protein Data Bank, Rutgers University: **2006**.
148. Forneris, F.; Binda, C.; Battaglioli, E.; Mattevi, A., LSD1: oxidative chemistry for multifaceted functions in chromatin regulation. *Trends in Biochemical Sciences* **2008**, *33* (4), 181-189.
149. Chen, Y.; Yang, Y.; Wang, F., *et al.*, Crystal structure of human histone lysine-specific demethylase 1 (LSD1). *Proceedings of the National Academy of Sciences of the United States of America* **2006**, *103* (38), 13956-61.
150. Shi, Y.-J.; Matson, C.; Lan, F., *et al.*, Regulation of LSD1 Histone Demethylase Activity by Its Associated Factors. *Molecular Cell* **2005**, *19* (6), 857-864.
151. Andres, M. E.; Burger, C.; Peral-Rubio, M. J., *et al.*, CoREST: a functional corepressor required for regulation of neural-specific gene expression. *Proceedings of the National Academy of Sciences of the United States of America* **1999**, *96* (17), 9873-8.
152. Lee, M. G.; Wynder, C.; Cooch, N.; Shiekhhattar, R., An essential role for CoREST in nucleosomal histone 3 lysine 4 demethylation. *Nature* **2005**.
153. Culhane, J. C.; Cole, P. A., LSD1 and the chemistry of histone demethylation. *Current Opinion in Chemical Biology* **2007**, *11* (5), 561-568.
154. Forneris, F.; Binda, C.; Vanoni, M. A.; Battaglioli, E.; Mattevi, A., Human Histone Demethylase LSD1 Reads the Histone Code. *Journal of Biological Chemistry* **2005**, *280* (50), 41360-41365.
155. Garcia-Bassets, I.; Kwon, Y.-S.; Telese, F., *et al.*, Histone Methylation-Dependent Mechanisms Impose Ligand Dependency for Gene Activation by Nuclear Receptors. *Cell* **2007**, *128* (3), 505-518.
156. Metzger, E.; Wissmann, M.; Yin, N., *et al.*, LSD1 demethylates repressive histone marks to promote androgen-receptor-dependent transcription. *Nature* **2005**, *437* (7057), 436-9.
157. Metzger, E.; Wissmann, M.; Schule, R., Histone demethylation and androgen-dependent transcription. *Current Opinion in Genetics & Development* **2006**, *16* (5), 513-7.
158. Baron, R.; Vellore, N. A., LSD1/CoREST is an allosteric nanoscale clamp regulated by H3-histone-tail molecular recognition. *Proceedings of the National Academy of Sciences of the United States of America* **2012**, *109* (31), 12509-14.
159. Wang, Y.; Zhang, H.; Chen, Y., *et al.*, LSD1 is a subunit of the NuRD complex and targets the metastasis programs in breast cancer. *Cell* **2009**, *138* (4), 660-72.
160. Shi, Y.; Sawada, J.; Sui, G., *et al.*, Coordinated histone modifications mediated by a CtBP co-repressor complex. *Nature* **2003**, *422* (6933), 735-8.
161. Hayami, S.; Kelly, J. D.; Cho, H. S., *et al.*, Overexpression of LSD1 contributes to human carcinogenesis through chromatin regulation in various cancers. *International Journal of Cancer* **2011**, *128* (3), 574-86.
162. Kauffman, E. C.; Robinson, B. D.; Downes, M. J., *et al.*, Role of androgen receptor and associated lysine-demethylase coregulators, LSD1 and JMJD2A, in localized and advanced human bladder cancer. *Molecular Carcinogenesis* **2011**, *50* (12), 931-44.
163. Kahl, P.; Gullotti, L.; Heukamp, L. C., *et al.*, Androgen receptor coactivators lysine-specific histone demethylase 1 and four and a half LIM domain protein 2 predict risk of prostate cancer recurrence. *Cancer Research* **2006**, *66* (23), 11341-7.
164. Harris, W. J.; Huang, X.; Lynch, J. T., *et al.*, The histone demethylase KDM1A sustains the oncogenic potential of MLL-AF9 leukemia stem cells. *Cancer Cell* **2012**, *21* (4), 473-87.
165. Schenk, T.; Chen, W. C.; Gollner, S., *et al.*, Inhibition of the LSD1 (KDM1A) demethylase reactivates the all-trans-retinoic acid differentiation pathway in acute myeloid leukemia. *Nature Medicine* **2012**, *18* (4), 605-11.
166. Hoffmann, I.; Roatsch, M.; Schmitt, M. L., *et al.*, The role of histone demethylases in cancer therapy. *Molecular Oncology* **2012**, *6* (6), 683-703.

167. Brasacchio, D.; Okabe, J.; Tikellis, C., *et al.*, Hyperglycemia induces a dynamic cooperativity of histone methylase and demethylase enzymes associated with gene-activating epigenetic marks that coexist on the lysine tail. *Diabetes* **2009**, *58* (5), 1229-36.
168. Yang, Z.; Jiang, J.; Stewart, M. D., *et al.*, AOF1 is a histone H3K4 demethylase possessing demethylase activity-independent repression function. *Cell Res* **2010**, *20* (3), 276-87.
169. Fang, R.; Barbera, A. J.; Xu, Y., *et al.*, Human LSD2/KDM1b/AOF1 regulates gene transcription by modulating intragenic H3K4me2 methylation. *Molecular Cell* **2010**, *39* (2), 222-33.
170. Ciccone, D. N.; Su, H.; Hevi, S., *et al.*, KDM1B is a histone H3K4 demethylase required to establish maternal genomic imprints. *Nature* **2009**, *461* (7262), 415-8.
171. van Essen, D.; Zhu, Y.; Sacconi, S., A feed-forward circuit controlling inducible NF-kappaB target gene activation by promoter histone demethylation. *Molecular Cell* **2010**, *39* (5), 750-60.
172. Klose, R. J.; Kallin, E. M.; Zhang, Y., JmjC-domain-containing proteins and histone demethylation. *Nature Reviews Genetics* **2006**, *7* (9), 715-27.
173. Loenarz, C.; Schofield, C. J., Expanding chemical biology of 2-oxoglutarate oxygenases. *Nature Chemical Biology* **2008**, *4* (3), 152-6.
174. Hewitson, K. S.; McNeill, L. A.; Riordan, M. V., *et al.*, Hypoxia-inducible factor (HIF) asparagine hydroxylase is identical to factor inhibiting HIF (FIH) and is related to the cupin structural family. *The Journal of Biological Chemistry* **2002**, *277* (29), 26351-5.
175. Takeuchi, T.; Yamazaki, Y.; Katoh-Fukui, Y., *et al.*, Gene trap capture of a novel mouse gene, jumonji, required for neural tube formation. *Genes & Development* **1995**, *9* (10), 1211-22.
176. Labbe, R. M.; Holowatyj, A.; Yang, Z. Q., Histone lysine demethylase (KDM) subfamily 4: structures, functions and therapeutic potential. *American Journal of Translational Research* **2013**, *6* (1), 1-15.
177. Johansson, C.; Tumber, A.; Che, K., *et al.*, The roles of Jumonji-type oxygenases in human disease. *Epigenomics* **2014**, *6* (1), 89-120.
178. Tsukada Y, F. J., Erdjument-Bromage H, Warren ME, Borchers CH, Tempst P, Zhang Y, Histone demethylation by a family of JmjC domain-containing proteins. *Nature* **2006**, pp 811–816.
179. Hopkinson, R. J.; Hamed, R. B.; Rose, N. R.; Claridge, T. D.; Schofield, C. J., Monitoring the activity of 2-oxoglutarate dependent histone demethylases by NMR spectroscopy: direct observation of formaldehyde. *Chembiochem : a European Journal of Chemical Biology* **2010**, *11* (4), 506-10.
180. Cloos, P. A.; Christensen, J.; Agger, K.; Helin, K., Erasing the methyl mark: histone demethylases at the center of cellular differentiation and disease. *Genes & Development* **2008**, *22* (9), 1115-40.
181. Pedersen, M. T.; Helin, K., Histone demethylases in development and disease. *Trends in Cell Biology* **2010**, *20* (11), 662-71.
182. McDonough, M. A.; Loenarz, C.; Chowdhury, R.; Clifton, I. J.; Schofield, C. J., Structural studies on human 2-oxoglutarate dependent oxygenases. *Current Opinion in Structural Biology* **2010**, *20* (6), 659-72.
183. Rose, N. R.; McDonough, M. A.; King, O. N.; Kawamura, A.; Schofield, C. J., Inhibition of 2-oxoglutarate dependent oxygenases. *Chemical Society Reviews* **2011**, *40* (8), 4364-97.
184. Hegg, E. L.; Que, L., Jr., The 2-His-1-carboxylate facial triad--an emerging structural motif in mononuclear non-heme iron(II) enzymes. *European Journal of Biochemistry* **1997**, *250* (3), 625-9.
185. Clifton, I. J.; McDonough, M. A.; Ehrismann, D., *et al.*, Structural studies on 2-oxoglutarate oxygenases and related double-stranded beta-helix fold proteins. *Journal of Inorganic Biochemistry* **2006**, *100* (4), 644-69.
186. Klose, R. J.; Zhang, Y., Regulation of histone methylation by demethylation and demethylation. *Nature reviews. Molecular Cell Biology* **2007**, *8* (4), 307-18.
187. Horton, J. R.; Upadhyay, A. K.; Qi, H. H., *et al.*, Enzymatic and structural insights for substrate specificity of a family of jumonji histone lysine demethylases. *Nature Structural & Molecular Biology* **2010**, *17* (1), 38-43.
188. Yang, Y.; Hu, L.; Wang, P., *et al.*, Structural insights into a dual-specificity histone demethylase ceKDM7A from *Caenorhabditis elegans*. *Cell Res* **2010**, *20* (8), 886-98.

189. Chen, Z.; Zang, J.; Whetstone, J., *et al.*, Structural Insights into Histone Demethylation by JMJD2 Family Members. *Cell* **2006**, *125* (4), 691-702.
190. Castermans, D.; Vermeesch, J. R.; Fryns, J. P., *et al.*, Identification and characterization of the TRIP8 and REEP3 genes on chromosome 10q21.3 as novel candidate genes for autism. *European Journal of Human Genetics* **2007**, *15* (4), 422-31.
191. Laumonnier, F.; Holbert, S.; Ronce, N., *et al.*, Mutations in PHF8 are associated with X linked mental retardation and cleft lip/cleft palate. *Journal of Medical Genetics* **2005**, *42* (10), 780-6.
192. Qiu, J.; Shi, G.; Jia, Y., *et al.*, The X-linked mental retardation gene PHF8 is a histone demethylase involved in neuronal differentiation. *Cell Res* **2010**, *20* (8), 908-18.
193. Verdone, L.; Caserta, M.; Di Mauro, E., Role of histone acetylation in the control of gene expression. *Biochemistry and Cell Biology* **2005**, *83* (3), 344-53.
194. Workman, J. L.; Kingston, R. E., Alteration of nucleosome structure as a mechanism of transcriptional regulation. *Annual Review of Biochemistry* **1998**, *67*, 545-79.
195. Allfrey VG, F. R., Mirsky AE, Acetylation and methylation of histones and their possible role in the regulation of RNA synthesis. *Proc Natl Acad Sci USA* 1964, pp 786–794.
196. Simon, R. P.; Robaa, D.; Alhalabi, Z.; Sippl, W.; Jung, M., KATching-Up on Small Molecule Modulators of Lysine Acetyltransferases. *J Med Chem* **2016**, *59* (4), 1249-70.
197. Zeng, L.; Zhou, M. M., Bromodomain: an acetyl-lysine binding domain. *FEBS Lett* **2002**, *513* (1), 124-8.
198. Jenuwein, T., Translating the Histone Code. *Science* **2001**, *293* (5532), 1074-1080.
199. Dhalluin, C.; Carlson, J. E.; Zeng, L., *et al.*, Structure and ligand of a histone acetyltransferase bromodomain. *Nature* **1999**, *399* (6735), 491-6.
200. Filippakopoulos, P.; Knapp, S., Targeting bromodomains: epigenetic readers of lysine acetylation. *Nature Reviews Drug Discovery* **2014**, *13* (5), 337-56.
201. Lange, M.; Kaynak, B.; Forster, U. B., *et al.*, Regulation of muscle development by DPF3, a novel histone acetylation and methylation reader of the BAF chromatin remodeling complex. *Genes & Development* **2008**, *22* (17), 2370-84.
202. Zeng, L.; Zhang, Q.; Li, S., *et al.*, Mechanism and regulation of acetylated histone binding by the tandem PHD finger of DPF3b. *Nature* **2010**, *466* (7303), 258-62.
203. Su, D.; Hu, Q.; Li, Q., *et al.*, Structural basis for recognition of H3K56-acetylated histone H3-H4 by the chaperone Rtt106. *Nature* **2012**, *483* (7387), 104-7.
204. Filippakopoulos P, P. S., Mangos M, Keates T, Lambert JP, Barsyte-Lovejoy D, Felletar I, Volkmer R, Müller S, Pawson T, Gingras AC, Arrowsmith CH, Knapp S, Histone recognition and large-scale structural analysis of the human bromodomain family. *Cell* **2012**, pp 214-231.
205. Marushige, K., Activation of chromatin by acetylation of histone side chains. *Proceedings of the National Academy of Sciences of the United States of America* **1976**, *73* (11), 3937-41.
206. Marmorstein, R.; Zhou, M. M., Writers and readers of histone acetylation: structure, mechanism, and inhibition. *Cold Spring Harbor Perspectives in Biology* **2014**, *6* (7), a018762.
207. Sterner, D. E.; Berger, S. L., Acetylation of Histones and Transcription-Related Factors. *Microbiology and Molecular Biology Reviews* **2000**, *64* (2), 435-459.
208. Lundby, A.; Lage, K.; Weinert, B. T., *et al.*, Proteomic analysis of lysine acetylation sites in rat tissues reveals organ specificity and subcellular patterns. *Cell Reports* **2012**, *2* (2), 419-31.
209. Hodawadekar, S. C.; Marmorstein, R., Chemistry of acetyl transfer by histone modifying enzymes: structure, mechanism and implications for effector design. *Oncogene* **2007**, *26* (37), 5528-40.
210. Brownell, J. E.; Zhou, J.; Ranalli, T., *et al.*, Tetrahymena Histone Acetyltransferase A: A Homolog to Yeast Gcn5p Linking Histone Acetylation to Gene Activation. *Cell* **1996**, *84* (6), 843-851.
211. Kleff, S.; Andrulis, E. D.; Anderson, C. W.; Sternglanz, R., Identification of a gene encoding a yeast histone H4 acetyltransferase. *The Journal of Biological Chemistry* **1995**, *270* (42), 24674-7.
212. Parthun, M. R.; Widom, J.; Gottschling, D. E., The major cytoplasmic histone acetyltransferase in yeast: links to chromatin replication and histone metabolism. *Cell* **1996**, *87* (1), 85-94.

213. Neuwald, A. F.; Landsman, D., GCN5-related histone N-acetyltransferases belong to a diverse superfamily that includes the yeast SPT10 protein. *Trends Biochem Sci* **1997**, 22 (5), 154-5.
214. Allis, C. D.; Berger, S. L.; Cote, J., *et al.*, New nomenclature for chromatin-modifying enzymes. *Cell* **2007**, 131 (4), 633-6.
215. Spencer, T. E.; Jenster, G.; Burcin, M. M., *et al.*, Steroid receptor coactivator-1 is a histone acetyltransferase. *Nature* **1997**, 389 (6647), 194-8.
216. Mizzen, C. A.; Yang, X.-J.; Kokubo, T., *et al.*, The TAFII250 Subunit of TFIID Has Histone Acetyltransferase Activity. *Cell* **1996**, 87 (7), 1261-1270.
217. Kawasaki, H.; Schiltz, L.; Chiu, R., *et al.*, ATF-2 has intrinsic histone acetyltransferase activity which is modulated by phosphorylation. *Nature* **2000**, 405 (6783), 195-200.
218. Doi, M.; Hirayama, J.; Sassone-Corsi, P., Circadian regulator CLOCK is a histone acetyltransferase. *Cell* **2006**, 125 (3), 497-508.
219. Heery, D. M.; Fischer, P. M., Pharmacological targeting of lysine acetyltransferases in human disease: a progress report. *Drug Discovery Today* **2007**, 12 (1-2), 88-99.
220. Renthall, W.; Nestler, E. J., Histone acetylation in drug addiction. *Seminars in Cell & Developmental Biology* **2009**, 20 (4), 387-94.
221. Ellis, L.; Atadja, P. W.; Johnstone, R. W., Epigenetics in cancer: targeting chromatin modifications. *Molecular Cancer Therapeutics* **2009**, 8 (6), 1409-20.
222. Esteller, M., Epigenetic changes in cancer. *F1000 biology reports* **2011**, 3, 9.
223. Geutjes, E. J.; Bajpe, P. K.; Bernards, R., Targeting the epigenome for treatment of cancer. *Oncogene* **2012**, 31 (34), 3827-44.
224. Peters, A. H.; Schwaller, J., Epigenetic mechanisms in acute myeloid leukemia. *Progress in drug research. Fortschritte der Arzneimittelforschung. Progres des recherches pharmaceutiques* **2011**, 67, 197-219.
225. Wang, L.; Gural, A.; Sun, X. J., *et al.*, The leukemogenicity of AML1-ETO is dependent on site-specific lysine acetylation. *Science* **2011**, 333 (6043), 765-9.
226. Esteller, M., Epigenetics in cancer. *The New England Journal of Medicine* **2008**, 358 (11), 1148-59.
227. Santer, F. R.; Hoschele, P. P.; Oh, S. J., *et al.*, Inhibition of the acetyltransferases p300 and CBP reveals a targetable function for p300 in the survival and invasion pathways of prostate cancer cell lines. *Molecular Cancer Therapeutics* **2011**, 10 (9), 1644-55.
228. Zhou, H. J.; Yan, J.; Luo, W., *et al.*, SRC-3 is required for prostate cancer cell proliferation and survival. *Cancer Research* **2005**, 65 (17), 7976-83.
229. Gojis, O.; Rudraraju, B.; Alifrangis, C., *et al.*, The role of steroid receptor coactivator-3 (SRC-3) in human malignant disease. *European journal of Surgical Oncology : the Journal of the European Society of Surgical Oncology and the British Association of Surgical Oncology* **2010**, 36 (3), 224-9.
230. Gojis, O.; Rudraraju, B.; Gudi, M., *et al.*, The role of SRC-3 in human breast cancer. *Nature reviews Clinical Oncology* **2010**, 7 (2), 83-9.
231. Barnes, P. J.; Adcock, I. M.; Ito, K., Histone acetylation and deacetylation: importance in inflammatory lung diseases. *The European Respiratory Journal* **2005**, 25 (3), 552-63.
232. Cereseto, A.; Manganaro, L.; Gutierrez, M. I., *et al.*, Acetylation of HIV-1 integrase by p300 regulates viral integration. *The EMBO Journal* **2005**, 24 (17), 3070-81.
233. He, L.; Sabet, A.; Djedjos, S., *et al.*, Metformin and insulin suppress hepatic gluconeogenesis through phosphorylation of CREB binding protein. *Cell* **2009**, 137 (4), 635-46.
234. Lopes da Rosa, J.; Boyartchuk, V. L.; Zhu, L. J.; Kaufman, P. D., Histone acetyltransferase Rtt109 is required for *Candida albicans* pathogenesis. *Proceedings of the National Academy of Sciences of the United States of America* **2010**, 107 (4), 1594-9.
235. Barneda-Zahonero, B.; Parra, M., Histone deacetylases and cancer. *Molecular Oncology* **2012**, 6 (6), 579-89.

236. de Ruijter, A. J.; van Gennip, A. H.; Caron, H. N.; Kemp, S.; van Kuilenburg, A. B., Histone deacetylases (HDACs): characterization of the classical HDAC family. *The Biochemical Journal* **2003**, 370 (Pt 3), 737-49.
237. Gallinari, P.; Di Marco, S.; Jones, P.; Pallaoro, M.; Steinkuhler, C., HDACs, histone deacetylation and gene transcription: from molecular biology to cancer therapeutics. *Cell Res* **2007**, 17 (3), 195-211.
238. Glozak, M. A.; Sengupta, N.; Zhang, X.; Seto, E., Acetylation and deacetylation of non-histone proteins. *Gene* **2005**, 363, 15-23.
239. Joshi, P.; Greco, T. M.; Guise, A. J., *et al.*, The functional interactome landscape of the human histone deacetylase family. *Molecular Systems Biology* **2013**, 9, 672.
240. Benedetti, R.; Conte, M.; Altucci, L., Targeting Histone Deacetylases in Diseases: Where Are We? *Antioxidants & Redox Signaling* **2015**, 23 (1), 99-126.
241. Verdin, E.; Dequiedt, F.; Kasler, H. G., Class II histone deacetylases: versatile regulators. *Trends in Genetics* **2003**, 19 (5), 286-93.
242. Kao, H. Y.; Verdel, A.; Tsai, C. C., *et al.*, Mechanism for nucleocytoplasmic shuttling of histone deacetylase 7. *The Journal of Biological Chemistry* **2001**, 276 (50), 47496-507.
243. McKinsey, T. A.; Zhang, C. L.; Lu, J.; Olson, E. N., Signal-dependent nuclear export of a histone deacetylase regulates muscle differentiation. *Nature* **2000**, 408 (6808), 106-11.
244. Wang, W. H.; Cheng, L. C.; Pan, F. Y., *et al.*, Intracellular trafficking of histone deacetylase 4 regulates long-term memory formation. *Anatomical record* **2011**, 294 (6), 1025-34.
245. Zhu, X.; Li, D.; Zhang, Z., *et al.*, Persistent phosphorylation at specific H3 serine residues involved in chemical carcinogen-induced cell transformation. *Molecular Carcinogenesis* **2017**, 56 (5), 1449-1460.
246. Deubzer, H. E.; Schier, M. C.; Oehme, I., *et al.*, HDAC11 is a novel drug target in carcinomas. *International Journal of Cancer* **2013**, 132 (9), 2200-8.
247. Gao, L., Cloning and Functional Characterization of HDAC11, a Novel Member of the Human Histone Deacetylase Family. *Journal of Biological Chemistry* **2002**, 277 (28), 25748-25755.
248. Dali-Youcef, N.; Lagouge, M.; Froelich, S., *et al.*, Sirtuins: the 'magnificent seven', function, metabolism and longevity. *Annals of Medicine* **2007**, 39 (5), 335-45.
249. North, B. J.; Verdin, E., Sirtuins: Sir2-related NAD-dependent protein deacetylases. *Genome Biology* **2004**, 5 (5), 224.
250. Taylor, D. M.; Maxwell, M. M.; Luthi-Carter, R.; Kazantsev, A. G., Biological and potential therapeutic roles of sirtuin deacetylases. *Cellular and Molecular Life Sciences* **2008**, 65 (24), 4000-18.
251. Carafa, V.; Nebbioso, A.; Altucci, L., Sirtuins and disease: the road ahead. *Frontiers in pharmacology* **2012**, 3, 4.
252. Michishita, E.; Park, J. Y.; Burneskis, J. M.; Barrett, J. C.; Horikawa, I., Evolutionarily conserved and nonconserved cellular localizations and functions of human SIRT proteins. *Molecular Biology of the Cell* **2005**, 16 (10), 4623-35.
253. New, M.; Olzscha, H.; La Thangue, N. B., HDAC inhibitor-based therapies: can we interpret the code? *Molecular Oncology* **2012**, 6 (6), 637-56.
254. Finnin, M. S.; Donigian, J. R.; Cohen, A., *et al.*, Structures of a histone deacetylase homologue bound to the TSA and SAHA inhibitors. *Nature* **1999**, 401 (6749), 188-93.
255. Grozinger, C. M.; Schreiber, S. L., Deacetylase enzymes: biological functions and the use of small-molecule inhibitors. *Chemistry & Biology* **2002**, 9 (1), 3-16.
256. Corminboeuf, C.; Hu, P.; Tuckerman, M. E.; Zhang, Y., Unexpected deacetylation mechanism suggested by a density functional theory QM/MM study of histone-deacetylase-like protein. *Journal of the American Chemical Society* **2006**, 128 (14), 4530-1.
257. Chen, K.; Zhang, X.; Wu, Y. D.; Wiest, O., Inhibition and mechanism of HDAC8 revisited. *Journal of the American Chemical Society* **2014**, 136 (33), 11636-43.
258. Christensen, D. P.; Dahllof, M.; Lundh, M., *et al.*, Histone deacetylase (HDAC) inhibition as a novel treatment for diabetes mellitus. *Molecular Medicine (Cambridge, Mass.)* **2011**, 17 (5-6), 378-90.

259. Ropero, S.; Esteller, M., The role of histone deacetylases (HDACs) in human cancer. *Molecular Oncology* **2007**, *1* (1), 19-25.
260. Dietz, K. C.; Casaccia, P., HDAC inhibitors and neurodegeneration: at the edge between protection and damage. *Pharmacological Research* **2010**, *62* (1), 11-7.
261. Dinarello, C. A., Anti-inflammatory Agents: Present and Future. *Cell* **2010**, *140* (6), 935-50.
262. Gray, S. G., Epigenetic treatment of neurological disease. *Epigenomics* **2011**, *3* (4), 431-50.
263. Manal, M.; Chandrasekar, M. J.; Gomathi Priya, J.; Nanjan, M. J., Inhibitors of histone deacetylase as antitumor agents: A critical review. *Bioorganic Chemistry* **2016**, *67*, 18-42.
264. Hailu, G. S.; Robaa, D.; Forgione, M., *et al.*, Lysine Deacetylase Inhibitors in Parasites: Past, Present, and Future Perspectives. *J Med Chem* **2017**, *60* (12), 4780-4804.
265. Rajak, H.; Singh, A.; Raghuwanshi, K., *et al.*, A structural insight into hydroxamic acid based histone deacetylase inhibitors for the presence of anticancer activity. *Current Medicinal Chemistry* **2014**, *21* (23), 2642-64.
266. Mottamal, M.; Zheng, S.; Huang, T. L.; Wang, G., Histone deacetylase inhibitors in clinical studies as templates for new anticancer agents. *Molecules (Basel, Switzerland)* **2015**, *20* (3), 3898-941.
267. Moradei, O.; Vaisburg, A.; Martell, R. E., Histone deacetylase inhibitors in cancer therapy: new compounds and clinical update of benzamide-type agents. *Curr Top Med Chem* **2008**, *8* (10), 841-58.
268. Mwakwari, S. C.; Patil, V.; Guerrant, W.; Oyeler, A. K., Macrocyclic histone deacetylase inhibitors. *Curr Top Med Chem* **2010**, *10* (14), 1423-40.
269. Li, J.; Li, G.; Xu, W., Histone deacetylase inhibitors: an attractive strategy for cancer therapy. *Current Medicinal Chemistry* **2013**, *20* (14), 1858-86.
270. Rajak, H.; Singh, A.; Dewangan, P. K., *et al.*, Peptide based macrocycles: selective histone deacetylase inhibitors with antiproliferative activity. *Current Medicinal Chemistry* **2013**, *20* (14), 1887-903.
271. Duvic, M.; Talpur, R.; Ni, X., *et al.*, Phase 2 trial of oral vorinostat (suberoylanilide hydroxamic acid, SAHA) for refractory cutaneous T-cell lymphoma (CTCL). *Blood* **2007**, *109* (1), 31-9.
272. VanderMolen, K. M.; McCulloch, W.; Pearce, C. J.; Oberlies, N. H., Romidepsin (Istodax, NSC 630176, FR901228, FK228, depsipeptide): a natural product recently approved for cutaneous T-cell lymphoma. *The Journal of Antibiotics* **2011**, *64* (8), 525-31.
273. Shi, Y.; Dong, M.; Hong, X., *et al.*, Results from a multicenter, open-label, pivotal phase II study of chidamide in relapsed or refractory peripheral T-cell lymphoma. *Annals of Oncology : Official Journal of the European Society for Medical Oncology* **2015**, *26* (8), 1766-71.
274. West, A. C.; Johnstone, R. W., New and emerging HDAC inhibitors for cancer treatment. *The Journal of Clinical Investigation* **2014**, *124* (1), 30-9.
275. Garnock-Jones, K. P., Panobinostat: first global approval. *Drugs* **2015**, *75* (6), 695-704.
276. Li, Y.; Seto, E., HDACs and HDAC Inhibitors in Cancer Development and Therapy. *Cold Spring Harbor Perspectives in Medicine* **2016**, *6* (10).
277. Mann, B. S.; Johnson, J. R.; Cohen, M. H.; Justice, R.; Pazdur, R., FDA approval summary: vorinostat for treatment of advanced primary cutaneous T-cell lymphoma. *The Oncologist* **2007**, *12* (10), 1247-52.
278. McDermott, J.; Jimeno, A., Belinostat for the treatment of peripheral T-cell lymphomas. *Drugs of Today (Barcelona, Spain : 1998)* **2014**, *50* (5), 337-45.
279. Richardson, P. G.; Laubach, J. P.; Lonial, S., *et al.*, Panobinostat: a novel pan-deacetylase inhibitor for the treatment of relapsed or relapsed and refractory multiple myeloma. *Expert Review of Anticancer Therapy* **2015**, *15* (7), 737-48.
280. Brunetto, A. T.; Ang, J. E.; Lal, R., *et al.*, First-in-human, pharmacokinetic and pharmacodynamic phase I study of Resminostat, an oral histone deacetylase inhibitor, in patients with advanced solid tumors. *Clinical Cancer Research : an official journal of the American Association for Cancer Research* **2013**, *19* (19), 5494-504.
281. Zhao, J.; Lawless, M. W., Resminostat: Opening the door to epigenetic treatments for liver cancer. *Hepatology (Baltimore, Md.)* **2016**, *63* (2), 668-9.

282. Galli, M.; Salmoiraghi, S.; Golay, J., *et al.*, A phase II multiple dose clinical trial of histone deacetylase inhibitor ITF2357 in patients with relapsed or progressive multiple myeloma. *Annals of Hematology* **2010**, *89* (2), 185-90.
283. Locatelli, S. L.; Cleris, L.; Stirparo, G. G., *et al.*, BIM upregulation and ROS-dependent necroptosis mediate the antitumor effects of the HDACi Givinostat and Sorafenib in Hodgkin lymphoma cell line xenografts. *Leukemia* **2014**, *28* (9), 1861-71.
284. Zorzi, A. P.; Bernstein, M.; Samson, Y., *et al.*, A phase I study of histone deacetylase inhibitor, pracinostat (SB939), in pediatric patients with refractory solid tumors: IND203 a trial of the NCIC IND program/C17 pediatric phase I consortium. *Pediatric Blood & Cancer* **2013**, *60* (11), 1868-74.
285. Choy, E.; Flamand, Y.; Balasubramanian, S., *et al.*, Phase 1 study of oral abexinostat, a histone deacetylase inhibitor, in combination with doxorubicin in patients with metastatic sarcoma. *Cancer* **2015**, *121* (8), 1223-30.
286. Morschhauser, F.; Terriou, L.; Coiffier, B., *et al.*, Phase 1 study of the oral histone deacetylase inhibitor abexinostat in patients with Hodgkin lymphoma, non-Hodgkin lymphoma, or chronic lymphocytic leukaemia. *Investigational New Drugs* **2015**, *33* (2), 423-31.
287. Venugopal, B.; Baird, R.; Kristeleit, R. S., *et al.*, A phase I study of quisinostat (JNJ-26481585), an oral hydroxamate histone deacetylase inhibitor with evidence of target modulation and antitumor activity, in patients with advanced solid tumors. *Clinical Cancer Research : an official journal of the American Association for Cancer Research* **2013**, *19* (15), 4262-72.
288. Zwergel, C.; Valente, S.; Jacob, C.; Mai, A., Emerging approaches for histone deacetylase inhibitor drug discovery. *Expert Opinion on Drug Discovery* **2015**, *10* (6), 599-613.
289. Banerji, U.; van Doorn, L.; Papadatos-Pastos, D., *et al.*, A phase I pharmacokinetic and pharmacodynamic study of CHR-3996, an oral class I selective histone deacetylase inhibitor in refractory solid tumors. *Clinical Cancer Research : an official journal of the American Association for Cancer Research* **2012**, *18* (9), 2687-94.
290. Shimizu, T.; LoRusso, P. M.; Papadopoulos, K. P., *et al.*, Phase I first-in-human study of CUDC-101, a multitargeted inhibitor of HDACs, EGFR, and HER2 in patients with advanced solid tumors. *Clinical Cancer Research : an official journal of the American Association for Cancer Research* **2014**, *20* (19), 5032-40.
291. Qian, C.; Lai, C. J.; Bao, R., *et al.*, Cancer network disruption by a single molecule inhibitor targeting both histone deacetylase activity and phosphatidylinositol 3-kinase signaling. *Clinical Cancer Research : an official journal of the American Association for Cancer Research* **2012**, *18* (15), 4104-13.
292. Knipstein, J.; Gore, L., Entinostat for treatment of solid tumors and hematologic malignancies. *Expert Opinion on Investigational Drugs* **2011**, *20* (10), 1455-67.
293. Younes, A.; Oki, Y.; Bociek, R. G., *et al.*, Mocetinostat for relapsed classical Hodgkin's lymphoma: an open-label, single-arm, phase 2 trial. *The Lancet Oncology* **2011**, *12* (13), 1222-8.
294. Pauer, L. R.; Olivares, J.; Cunningham, C., *et al.*, Phase I study of oral CI-994 in combination with carboplatin and paclitaxel in the treatment of patients with advanced solid tumors. *Cancer Investigation* **2004**, *22* (6), 886-96.
295. Santo, L.; Hideshima, T.; Kung, A. L., *et al.*, Preclinical activity, pharmacodynamic, and pharmacokinetic properties of a selective HDAC6 inhibitor, ACY-1215, in combination with bortezomib in multiple myeloma. *Blood* **2012**, *119* (11), 2579-89.
296. Dong, M.; Ning, Z. Q.; Xing, P. Y., *et al.*, Phase I study of chidamide (CS055/HBI-8000), a new histone deacetylase inhibitor, in patients with advanced solid tumors and lymphomas. *Cancer Chemotherapy and Pharmacology* **2012**, *69* (6), 1413-22.
297. Frye, R.; Myers, M.; Axelrod, K. C., *et al.*, Romidepsin: a new drug for the treatment of cutaneous T-cell lymphoma. *Clinical Journal of Oncology Nursing* **2012**, *16* (2), 195-204.
298. Bilen, M. A.; Fu, S.; Falchook, G. S., *et al.*, Phase I trial of valproic acid and lenalidomide in patients with advanced cancer. *Cancer Chemotherapy and Pharmacology* **2015**, *75* (4), 869-74.
299. Iannitti, T.; Palmieri, B., Clinical and experimental applications of sodium phenylbutyrate. *Drugs in R&D* **2011**, *11* (3), 227-49.

300. Guzman, M. L.; Yang, N.; Sharma, K. K., *et al.*, Selective activity of the histone deacetylase inhibitor AR-42 against leukemia stem cells: a novel potential strategy in acute myelogenous leukemia. *Molecular Cancer Therapeutics* **2014**, *13* (8), 1979-90.
301. Reid, T.; Valone, F.; Lipera, W., *et al.*, Phase II trial of the histone deacetylase inhibitor pivaloyloxymethyl butyrate (Pivanex, AN-9) in advanced non-small cell lung cancer. *Lung Cancer* **2004**, *45* (3), 381-6.
302. Klar, A. J.; Fogel, S.; Macleod, K., MAR1-a Regulator of the HMa and HMalpha Loci in SACCHAROMYCES CEREVISIAE. *Genetics* **1979**, *93* (1), 37-50.
303. Frye, R. A., Characterization of five human cDNAs with homology to the yeast SIR2 gene: Sir2-like proteins (sirtuins) metabolize NAD and may have protein ADP-ribosyltransferase activity. *Biochemical and Biophysical Research Communications* **1999**, *260* (1), 273-9.
304. Imai, S.; Armstrong, C. M.; Kaeberlein, M.; Guarente, L., Transcriptional silencing and longevity protein Sir2 is an NAD-dependent histone deacetylase. *Nature* **2000**, *403* (6771), 795-800.
305. Greiss, S.; Gartner, A., Sirtuin/Sir2 phylogeny, evolutionary considerations and structural conservation. *Molecules and cells* **2009**, *28* (5), 407-15.
306. Frye, R. A., Phylogenetic classification of prokaryotic and eukaryotic Sir2-like proteins. *Biochemical and Biophysical Research Communications* **2000**, *273* (2), 793-8.
307. Du, J.; Zhou, Y.; Su, X., *et al.*, Sirt5 is a NAD-dependent protein lysine demalonylase and desuccinylase. *Science* **2011**, *334* (6057), 806-9.
308. Carafa, V.; Rotili, D.; Forgione, M., *et al.*, Sirtuin functions and modulation: from chemistry to the clinic. *Clinical Epigenetics* **2016**, *8* (1).
309. Michan, S.; Sinclair, D., Sirtuins in mammals: insights into their biological function. *Biochemical Journal* **2007**, *404* (1), 1-13.
310. Martinez-Redondo, P.; Vaquero, A., The diversity of histone versus nonhistone sirtuin substrates. *Genes Cancer* **2013**, *4* (3-4), 148-63.
311. Tanno, M.; Sakamoto, J.; Miura, T.; Shimamoto, K.; Horio, Y., Nucleocytoplasmic shuttling of the NAD⁺-dependent histone deacetylase SIRT1. *The Journal of Biological Chemistry* **2007**, *282* (9), 6823-32.
312. North, B. J.; Verdin, E., Interphase nucleo-cytoplasmic shuttling and localization of SIRT2 during mitosis. *PLoS One* **2007**, *2* (8), e784.
313. Iwahara, T.; Bonasio, R.; Narendra, V.; Reinberg, D., SIRT3 functions in the nucleus in the control of stress-related gene expression. *Molecular and Cellular Biology* **2012**, *32* (24), 5022-34.
314. Scher, M. B.; Vaquero, A.; Reinberg, D., SirT3 is a nuclear NAD⁺-dependent histone deacetylase that translocates to the mitochondria upon cellular stress. *Genes & Development* **2007**, *21* (8), 920-8.
315. Schwer, B.; North, B. J.; Frye, R. A.; Ott, M.; Verdin, E., The human silent information regulator (Sir)2 homologue hSIRT3 is a mitochondrial nicotinamide adenine dinucleotide-dependent deacetylase. *The Journal of Cell Biology* **2002**, *158* (4), 647-57.
316. Kiran, S.; Chatterjee, N.; Singh, S., *et al.*, Intracellular distribution of human SIRT7 and mapping of the nuclear/nucleolar localization signal. *The FEBS Journal* **2013**, *280* (14), 3451-66.
317. Tan, M.; Peng, C.; Anderson, K. A., *et al.*, Lysine glutarylation is a protein posttranslational modification regulated by SIRT5. *Cell Metabolism* **2014**, *19* (4), 605-17.
318. Ahuja, N.; Schwer, B.; Carobbio, S., *et al.*, Regulation of insulin secretion by SIRT4, a mitochondrial ADP-ribosyltransferase. *The Journal of Biological Chemistry* **2007**, *282* (46), 33583-92.
319. Haigis, M. C.; Mostoslavsky, R.; Haigis, K. M., *et al.*, SIRT4 inhibits glutamate dehydrogenase and opposes the effects of calorie restriction in pancreatic beta cells. *Cell* **2006**, *126* (5), 941-54.
320. Liszt, G.; Ford, E.; Kurtev, M.; Guarente, L., Mouse Sir2 homolog SIRT6 is a nuclear ADP-ribosyltransferase. *The Journal of Biological Chemistry* **2005**, *280* (22), 21313-20.
321. Sebastian, C.; Satterstrom, F. K.; Haigis, M. C.; Mostoslavsky, R., From sirtuin biology to human diseases: an update. *The Journal of Biological Chemistry* **2012**, *287* (51), 42444-52.

322. Sebastian, C.; Mostoslavsky, R., The role of mammalian sirtuins in cancer metabolism. *Seminars in Cell & Developmental Biology* **2015**, *43*, 33-42.
323. Zhao, K.; Chai, X.; Clements, A.; Marmorstein, R., Structure and autoregulation of the yeast Hst2 homolog of Sir2. *Nature Structural Biology* **2003**, *10* (10), 864-71.
324. Tennen, R. I.; Berber, E.; Chua, K. F., Functional dissection of SIRT6: identification of domains that regulate histone deacetylase activity and chromatin localization. *Mechanisms of Ageing and Development* **2010**, *131* (3), 185-92.
325. Avalos, J. L.; Boeke, J. D.; Wolberger, C., Structural basis for the mechanism and regulation of Sir2 enzymes. *Molecular Cell* **2004**, *13* (5), 639-48.
326. Zhao, K.; Harshaw, R.; Chai, X.; Marmorstein, R., Structural basis for nicotinamide cleavage and ADP-ribose transfer by NAD(+)-dependent Sir2 histone/protein deacetylases. *Proceedings of the National Academy of Sciences of the United States of America* **2004**, *101* (23), 8563-8.
327. Smith, B. C.; Hallows, W. C.; Denu, J. M., Mechanisms and molecular probes of sirtuins. *Chemistry & Biology* **2008**, *15* (10), 1002-13.
328. Hawse, W. F.; Hoff, K. G.; Fatkins, D. G., *et al.*, Structural insights into intermediate steps in the Sir2 deacetylation reaction. *Structure (London, England : 1993)* **2008**, *16* (9), 1368-77.
329. Hu, P.; Wang, S.; Zhang, Y., Highly dissociative and concerted mechanism for the nicotinamide cleavage reaction in Sir2Tm enzyme suggested by ab initio QM/MM molecular dynamics simulations. *Journal of the American Chemical Society* **2008**, *130* (49), 16721-8.
330. Finkel, T.; Deng, C. X.; Mostoslavsky, R., Recent progress in the biology and physiology of sirtuins. *Nature* **2009**, *460* (7255), 587-91.
331. Smith, B. C.; Denu, J. M., Sir2 deacetylases exhibit nucleophilic participation of acetyl-lysine in NAD⁺ cleavage. *Journal of the American Chemical Society* **2007**, *129* (18), 5802-3.
332. Hoff, K. G.; Avalos, J. L.; Sens, K.; Wolberger, C., Insights into the sirtuin mechanism from ternary complexes containing NAD⁺ and acetylated peptide. *Structure* **2006**, *14* (8), 1231-40.
333. Reilmann, R.; Squitieri, F.; Priller, J., *et al.*, N02 Safety And Tolerability Of Selisistat For The Treatment Of Huntington's Disease: Results From A Randomised, Double-blind, Placebo-controlled Phase Ii Trial. *Journal of Neurology, Neurosurgery & Amp; Psychiatry* **2014**, *85* (Suppl 1), A102-A102.
334. Sussmuth, S. D.; Haider, S.; Landwehrmeyer, G. B., *et al.*, An exploratory double-blind, randomized clinical trial with selisistat, a SirT1 inhibitor, in patients with Huntington's disease. *British Journal of Clinical Pharmacology* **2015**, *79* (3), 465-76.
335. Westerberg, G.; Chiesa, J. A.; Andersen, C. A., *et al.*, Safety, pharmacokinetics, pharmacogenomics and QT concentration-effect modelling of the SirT1 inhibitor selisistat in healthy volunteers. *British Journal of Clinical Pharmacology* **2015**, *79* (3), 477-91.
336. Bitterman, K. J.; Anderson, R. M.; Cohen, H. Y.; Latorre-Esteves, M.; Sinclair, D. A., Inhibition of silencing and accelerated aging by nicotinamide, a putative negative regulator of yeast sir2 and human SIRT1. *The Journal of Biological Chemistry* **2002**, *277* (47), 45099-107.
337. Luo, J.; Nikolaev, A. Y.; Imai, S., *et al.*, Negative control of p53 by Sir2alpha promotes cell survival under stress. *Cell* **2001**, *107* (2), 137-48.
338. Medda, F.; Russell, R. J.; Higgins, M., *et al.*, Novel cambinol analogs as sirtuin inhibitors: synthesis, biological evaluation, and rationalization of activity. *J Med Chem* **2009**, *52* (9), 2673-82.
339. Medda, F.; Joseph, T. L.; Pirrie, L., *et al.*, N1-Benzyl substituted cambinol analogues as isozyme selective inhibitors of the sirtuin family of protein deacetylases. *MedChemComm* **2011**, *2* (7), 611-615.
340. Mahajan, S. S.; Scian, M.; Sripathy, S., *et al.*, Development of pyrazolone and isoxazol-5-one cambinol analogues as sirtuin inhibitors. *J Med Chem* **2014**, *57* (8), 3283-94.
341. Marshall, G. M.; Liu, P. Y.; Gherardi, S., *et al.*, SIRT1 promotes N-Myc oncogenesis through a positive feedback loop involving the effects of MKP3 and ERK on N-Myc protein stability. *PLoS Genetics* **2011**, *7* (6), e1002135.
342. Rotili, D.; Carafa, V.; Tarantino, D., *et al.*, Simplification of the tetracyclic SIRT1-selective inhibitor MC2141: coumarin- and pyrimidine-based SIRT1/2 inhibitors with different selectivity profile. *Bioorganic & Medicinal Chemistry* **2011**, *19* (12), 3659-68.

343. Yamagata, K.; Goto, Y.; Nishimasu, H., *et al.*, Structural basis for potent inhibition of SIRT2 deacetylase by a macrocyclic peptide inducing dynamic structural change. *Structure (London, England : 1993)* **2014**, 22 (2), 345-52.
344. Smith, B. C.; Denu, J. M., Acetyl-lysine analog peptides as mechanistic probes of protein deacetylases. *The Journal of Biological Chemistry* **2007**, 282 (51), 37256-65.
345. Kiviranta, P. H.; Suuronen, T.; Wallen, E. A., *et al.*, N(epsilon)-thioacetyl-lysine-containing tri-, tetra-, and pentapeptides as SIRT1 and SIRT2 inhibitors. *J Med Chem* **2009**, 52 (7), 2153-6.
346. He, B.; Hu, J.; Zhang, X.; Lin, H., Thiomyristoyl peptides as cell-permeable Sirt6 inhibitors. *Organic & Biomolecular Chemistry* **2014**, 12 (38), 7498-502.
347. Chen, B.; Wang, J.; Huang, Y.; Zheng, W., Human SIRT3 tripeptidic inhibitors containing N(epsilon)-thioacetyl-lysine. *Bioorganic & Medicinal Chemistry Letters* **2015**, 25 (17), 3481-7.
348. Fatkins, D. G.; Zheng, W., Substituting N(epsilon)-thioacetyl-lysine for N(epsilon)-acetyl-lysine in peptide substrates as a general approach to inhibiting human NAD(+)-dependent protein deacetylases. *International Journal of Molecular Sciences* **2008**, 9 (1), 1-11.
349. Huang, Y.; Liu, J.; Yan, L.; Zheng, W., Simple N(epsilon)-thioacetyl-lysine-containing cyclic peptides exhibiting highly potent sirtuin inhibition. *Bioorganic & Medicinal Chemistry Letters* **2016**, 26 (6), 1612-1617.
350. He, B.; Du, J.; Lin, H., Thiosuccinyl peptides as Sirt5-specific inhibitors. *Journal of the American Chemical Society* **2012**, 134 (4), 1922-5.
351. Morimoto, J.; Hayashi, Y.; Suga, H., Discovery of macrocyclic peptides armed with a mechanism-based warhead: isoform-selective inhibition of human deacetylase SIRT2. *Angewandte Chemie (International ed. in English)* **2012**, 51 (14), 3423-7.
352. Suzuki, T.; Asaba, T.; Imai, E., *et al.*, Identification of a cell-active non-peptide sirtuin inhibitor containing N-thioacetyl lysine. *Bioorganic & Medicinal Chemistry Letters* **2009**, 19 (19), 5670-2.
353. Asaba, T.; Suzuki, T.; Ueda, R., *et al.*, Inhibition of human sirtuins by in situ generation of an acetylated lysine-ADP-ribose conjugate. *Journal of the American Chemical Society* **2009**, 131 (20), 6989-96.
354. Mellini, P.; Kokkola, T.; Suuronen, T., *et al.*, Screen of pseudopeptidic inhibitors of human sirtuins 1-3: two lead compounds with antiproliferative effects in cancer cells. *J Med Chem* **2013**, 56 (17), 6681-95.
355. Kokkonen, P.; Rahnasto-Rilla, M.; Kiviranta, P. H., *et al.*, Peptides and Pseudopeptides as SIRT6 Deacetylation Inhibitors. *ACS Med Chem Lett* **2012**, 3 (12), 969-74.
356. Smith, B. C.; Denu, J. M., Mechanism-based inhibition of Sir2 deacetylases by thioacetyl-lysine peptide. *Biochemistry* **2007**, 46 (50), 14478-86.
357. Jamonnak, N.; Fatkins, D. G.; Wei, L.; Zheng, W., N(epsilon)-methanesulfonyl-lysine as a non-hydrolyzable functional surrogate for N(epsilon)-acetyl-lysine. *Organic & Biomolecular Chemistry* **2007**, 5 (6), 892-6.
358. Huhtiniemi, T.; Suuronen, T.; Lahtela-Kakkonen, M., *et al.*, N(epsilon)-Modified lysine containing inhibitors for SIRT1 and SIRT2. *Bioorganic & Medicinal Chemistry* **2010**, 18 (15), 5616-25.
359. Oki, M.; Aihara, H.; Ito, T., Role Of Histone Phosphorylation In Chromatin Dynamics And Its Implications in Diseases. In *Subcellular Biochemistry*, Springer Netherlands: pp 323-340.
360. Hu, S.; Xie, Z.; Onishi, A., *et al.*, Profiling the Human Protein-DNA Interactome Reveals ERK2 as a Transcriptional Repressor of Interferon Signaling. *Cell* **2009**, 139 (3), 610-622.
361. Cheung, P.; Allis, C. D.; Sassone-Corsi, P., Signaling to chromatin through histone modifications. *Cell* **2000**, 103 (2), 263-71.
362. Cruickshank, M. N.; Besant, P.; Ulgiati, D., The impact of histone post-translational modifications on developmental gene regulation. *Amino Acids* **2010**, 39 (5), 1087-105.
363. Houben, A.; Demidov, D.; Caperta, A. D., *et al.*, Phosphorylation of histone H3 in plants--a dynamic affair. *Biochimica et Biophysica Acta* **2007**, 1769 (5-6), 308-15.

364. Rogakou, E. P.; Pilch, D. R.; Orr, A. H.; Ivanova, V. S.; Bonner, W. M., DNA double-stranded breaks induce histone H2AX phosphorylation on serine 139. *The Journal of Biological Chemistry* **1998**, 273 (10), 5858-68.
365. Pickart, C. M., Back to the future with ubiquitin. *Cell* **2004**, 116 (2), 181-90.
366. Goldknopf, I. L.; Busch, H., Isopeptide linkage between nonhistone and histone 2A polypeptides of chromosomal conjugate-protein A24. *Proceedings of the National Academy of Sciences of the United States of America* **1977**, 74 (3), 864-8.
367. Adams, J., The proteasome: a suitable antineoplastic target. *Nature Reviews Cancer* **2004**, 4 (5), 349-60.
368. Hershko, A., Ubiquitin-mediated protein degradation. *The Journal of Biological Chemistry* **1988**, 263 (30), 15237-40.
369. Goldknopf, I. L.; Busch, H., Remarkable similarities of peptide fingerprints of histone 2A and nonhistone chromosomal protein A24. *Biochemical and Biophysical Research Communications* **1975**, 65 (3), 951-960.
370. Minsky, N.; Shema, E.; Field, Y., *et al.*, Monoubiquitinated H2B is associated with the transcribed region of highly expressed genes in human cells. *Nature Cell Biology* **2008**, 10 (4), 483-488.
371. Shema, E.; Tirosh, I.; Aylon, Y., *et al.*, The histone H2B-specific ubiquitin ligase RNF20/hBRE1 acts as a putative tumor suppressor through selective regulation of gene expression. *Genes & Development* **2008**, 22 (19), 2664-2676.
372. Zhu, Q.; Pao, G. M.; Huynh, A. M., *et al.*, BRCA1 tumour suppression occurs via heterochromatin-mediated silencing. *Nature* **2011**, 477 (7363), 179-184.
373. Hershko, A.; Ciechanover, A., THE UBIQUITIN SYSTEM. *Annual Review of Biochemistry* **1998**, 67 (1), 425-479.
374. Wang, H.; Zhai, L.; Xu, J., *et al.*, Histone H3 and H4 Ubiquitylation by the CUL4-DDB-ROC1 Ubiquitin Ligase Facilitates Cellular Response to DNA Damage. *Molecular Cell* **2006**, 22 (3), 383-394.
375. Jones, J. M.; Bhattacharyya, A.; Simkus, C., *et al.*, The RAG1 V(D)J recombinase/ubiquitin ligase promotes ubiquitylation of acetylated, phosphorylated histone 3.3. *Immunology Letters* **2011**, 136 (2), 156-162.
376. Doil, C.; Mailand, N.; Bekker-Jensen, S., *et al.*, RNF168 Binds and Amplifies Ubiquitin Conjugates on Damaged Chromosomes to Allow Accumulation of Repair Proteins. *Cell* **2009**, 136 (3), 435-446.
377. Stewart, G. S.; Panier, S.; Townsend, K., *et al.*, The RIDDLE Syndrome Protein Mediates a Ubiquitin-Dependent Signaling Cascade at Sites of DNA Damage. *Cell* **2009**, 136 (3), 420-434.
378. Huang, H.; Sabari, B. R.; Garcia, B. A.; Allis, C. D.; Zhao, Y., SnapShot: Histone Modifications. *Cell* **2014**, 159 (2), 458-458.e1.
379. Kim, J.; Guermah, M.; McGinty, R. K., *et al.*, RAD6-Mediated Transcription-Coupled H2B Ubiquitylation Directly Stimulates H3K4 Methylation in Human Cells. *Cell* **2009**, 137 (3), 459-471.
380. Moyal, L.; Lerenthal, Y.; Gana-Weisz, M., *et al.*, Requirement of ATM-Dependent Monoubiquitylation of Histone H2B for Timely Repair of DNA Double-Strand Breaks. *Molecular Cell* **2011**, 41 (5), 529-542.
381. Hassa, P. O.; Haenni, S. S.; Elser, M.; Hottiger, M. O., Nuclear ADP-Ribosylation Reactions in Mammalian Cells: Where Are We Today and Where Are We Going? *Microbiology and Molecular Biology Reviews* **2006**, 70 (3), 789-829.
382. Cohen-Armon, M.; Visochek, L.; Rozensal, D., *et al.*, DNA-Independent PARP-1 Activation by Phosphorylated ERK2 Increases Elk1 Activity: A Link to Histone Acetylation. *Molecular Cell* **2007**, 25 (2), 297-308.
383. Krishnakumar, R.; Kraus, W. L., PARP-1 Regulates Chromatin Structure and Transcription through a KDM5B-Dependent Pathway. *Molecular Cell* **2010**, 39 (5), 736-749.
384. Vaquero, A.; Loyola, A.; Reinberg, D., The constantly changing face of chromatin. *Science of Aging Knowledge Environment : SAGE KE* **2003**, 2003 (14), Re4.

385. Kraus, W. L.; Wong, J., Nuclear receptor-dependent transcription with chromatin. Is it all about enzymes? *European Journal of Biochemistry* **2002**, *269* (9), 2275-83.
386. Malik, N.; Smulson, M., A relationship between nuclear poly(adenosine diphosphate ribosylation) and acetylation posttranslational modifications. 1. Nucleosome studies. *Biochemistry* **1984**, *23* (16), 3721-5.
387. Melchior, F., SUMO--nonclassical ubiquitin. *Annual Review of Cell and Developmental Biology* **2000**, *16*, 591-626.
388. Seeler, J.-S.; Dejean, A., Nuclear and unclear functions of SUMO. *Nature Reviews Molecular Cell Biology* **2003**, *4* (9), 690-699.
389. Shiio, Y.; Eisenman, R. N., Histone sumoylation is associated with transcriptional repression. *Proceedings of the National Academy of Sciences* **2003**, *100* (23), 13225-13230.
390. Nathan, D., Histone sumoylation is a negative regulator in *Saccharomyces cerevisiae* and shows dynamic interplay with positive-acting histone modifications. *Genes & Development* **2006**, *20* (8), 966-976.
391. Klug, D. M.; Gelb, M. H.; Pollastri, M. P., Repurposing strategies for tropical disease drug discovery. *Bioorganic & Medicinal Chemistry Letters* **2016**, *26* (11), 2569-2576.
392. Njoroge, M.; Njuguna, N. M.; Mutai, P., *et al.*, Recent Approaches to Chemical Discovery and Development Against Malaria and the Neglected Tropical Diseases Human African Trypanosomiasis and Schistosomiasis. *Chemical Reviews* **2014**, *114* (22), 11138-11163.
393. Lozano, R.; Naghavi, M.; Foreman, K., *et al.*, Global and regional mortality from 235 causes of death for 20 age groups in 1990 and 2010: a systematic analysis for the Global Burden of Disease Study 2010. *The Lancet* **2012**, *380* (9859), 2095-2128.
394. Conteh, L.; Engels, T.; Molyneux, D. H., Socioeconomic aspects of neglected tropical diseases. *The Lancet* **2010**, *375* (9710), 239-247.
395. First malaria vaccine receives positive scientific opinion from EMA. *The Pharmaceutical Journal* **2015**.
396. Andrews, K. T.; Fisher, G.; Skinner-Adams, T. S., Drug repurposing and human parasitic protozoan diseases. *International Journal for Parasitology: Drugs and Drug Resistance* **2014**, *4* (2), 95-111.
397. Andrews, K. T.; Haque, A.; Jones, M. K., HDAC inhibitors in parasitic diseases. *Immunology and Cell Biology* **2011**, *90* (1), 66-77.
398. Escalante, A. A.; Ayala, F. J., Phylogeny of the malarial genus *Plasmodium*, derived from rRNA gene sequences. *Proceedings of the National Academy of Sciences* **1994**, *91* (24), 11373-11377.
399. Sutherland, Colin J.; Tanomsing, N.; Nolder, D., *et al.*, Two Nonrecombining Sympatric Forms of the Human Malaria Parasite *Plasmodium ovale* Occur Globally. *The Journal of Infectious Diseases* **2010**, *201* (10), 1544-1550.
400. Kumar, A.; Katiyar, S.; Agarwal, A.; Chauhan, P., Perspective in Antimalarial Chemotherapy. *Current Medicinal Chemistry* **2003**, *10* (13), 1137-1150.
401. Ashley, E.; McGready, R.; Proux, S.; Nosten, F., Malaria. *Travel Medicine and Infectious Disease* **2006**, *4* (3-4), 159-173.
402. Chuma, J. M.; Thiede, M.; Molyneux, C. S., Rethinking the economic costs of malaria at the household level: evidence from applying a new analytical framework in rural Kenya. *Malaria Journal* **2006**, *5* (1), 76.
403. Chuma, J.; Okungu, V.; Molyneux, C., Barriers to prompt and effective malaria treatment among the poorest population in Kenya. *Malaria Journal* **2010**, *9* (1), 144.
404. Anyanwu, P. E.; Fulton, J.; Evans, E.; Paget, T., Exploring the role of socioeconomic factors in the development and spread of anti-malarial drug resistance: a qualitative study. *Malaria Journal* **2017**, *16*, 203.
405. WHO, Roll Back Malaria. Global Malaria Action Plan. Geneva, 2008.
406. WHO, 10 fact sheets about malaria. Geneva, 2016.

407. Murhandarwati, E. E. H.; Fuad, A.; Sulistyawati, *et al.*, Change of strategy is required for malaria elimination: a case study in Purworejo District, Central Java Province, Indonesia. *Malaria Journal* **2015**, *14* (1).
408. Abdulla, S.; Salim, N.; Machera, F., *et al.*, Randomized, controlled trial of the long term safety, immunogenicity and efficacy of RTS,S/AS02D malaria vaccine in infants living in a malaria-endemic region. *Malaria Journal* **2013**, *12* (1), 11.
409. First Results of Phase 3 Trial of RTS,S/AS01 Malaria Vaccine in African Children. *New England Journal of Medicine* **2011**, *365* (20), 1863-1875.
410. Ridley, R. G., Medical need, scientific opportunity and the drive for antimalarial drugs. *Nature* **2002**, *415* (6872), 686-693.
411. White, N. J., The Treatment of Malaria. *New England Journal of Medicine* **1996**, *335* (11), 800-806.
412. Lim, P.; Alker, A. P.; Khim, N., *et al.*, Pfmldr1 copy number and artemisinin derivatives combination therapy failure in falciparum malaria in Cambodia. *Malaria Journal* **2009**, *8* (1), 11.
413. Enserink, M., MALARIA: Signs of Drug Resistance Rattle Experts, Trigger Bold Plan. *Science* **2008**, *322* (5909), 1776-1776.
414. Nayyar, G. M. L.; Breman, J. G.; Newton, P. N.; Herrington, J., Poor-quality antimalarial drugs in southeast Asia and sub-Saharan Africa. *The Lancet Infectious Diseases* **2012**, *12* (6), 488-496.
415. Dondorp, A. M.; Nosten, F.; Yi, P., *et al.*, Artemisinin Resistance in Plasmodium falciparum Malaria. *New England Journal of Medicine* **2009**, *361* (5), 455-467.
416. Dondorp, A. M.; Yeung, S.; White, L., *et al.*, Artemisinin resistance: current status and scenarios for containment. *Nature Reviews Microbiology* **2010**.
417. Learning to outwit malaria. *Bulletin of the World Health Organization* **2011**, *89* (1), 10-11.
418. Tanner, M.; de Savigny, D., Malaria eradication back on the table. *Bulletin of the World Health Organization* **2008**, *86* (2), 82-82.
419. Beutler, E., The hemolytic effect of primaquine and related compounds: a review. *Blood* **1959**, *14*, 103-39.
420. Guerra, C. A.; Howes, R. E.; Patil, A. P., *et al.*, The International Limits and Population at Risk of Plasmodium vivax Transmission in 2009. *PLoS Neglected Tropical Diseases* **2010**, *4* (8), e774.
421. Acharya, P.; Pallavi, R.; Chandran, S., *et al.*, A glimpse into the clinical proteome of human malaria parasites Plasmodium falciparum and Plasmodium vivax. *Proteomics Clinical Applications* **2009**, *3* (11), 1314-25.
422. Florens, L.; Washburn, M. P.; Raine, J. D., *et al.*, A proteomic view of the Plasmodium falciparum life cycle. *Nature* **2002**, *419* (6906), 520-526.
423. Foth, B. J.; Zhang, N.; Chahal, B. K., *et al.*, Quantitative time-course profiling of parasite and host cell proteins in the human malaria parasite Plasmodium falciparum. *Molecular & Cellular Proteomics* : MCP **2011**, *10* (8), M110.006411.
424. Kaiser, K.; Matuschewski, K.; Camargo, N.; Ross, J.; Kappe, S. H., Differential transcriptome profiling identifies Plasmodium genes encoding pre-erythrocytic stage-specific proteins. *Molecular Microbiology* **2004**, *51* (5), 1221-32.
425. Kappe, S. H.; Gardner, M. J.; Brown, S. M., *et al.*, Exploring the transcriptome of the malaria sporozoite stage. *Proceedings of the National Academy of Sciences of the United States of America* **2001**, *98* (17), 9895-900.
426. Khan, S. M.; Franke-Fayard, B.; Mair, G. R., *et al.*, Proteome analysis of separated male and female gametocytes reveals novel sex-specific Plasmodium biology. *Cell* **2005**, *121* (5), 675-87.
427. Lasender, E.; Janse, C. J.; van Gemert, G. J., *et al.*, Proteomic profiling of Plasmodium sporozoite maturation identifies new proteins essential for parasite development and infectivity. *PLoS Pathogens* **2008**, *4* (10), e1000195.
428. Greenwood, B. M.; Fidock, D. A.; Kyle, D. E., *et al.*, Malaria: progress, perils, and prospects for eradication. *The Journal of Clinical Investigation* **2008**, *118* (4), 1266-1276.

429. Doerig, C.; Rayner, J. C.; Scherf, A.; Tobin, A. B., Post-translational protein modifications in malaria parasites. *Nature Reviews Microbiology* **2015**, *13* (3), 160-72.
430. Gardiner, D. L.; Skinner-Adams, T. S.; Brown, C. L., *et al.*, Plasmodium falciparum: new molecular targets with potential for antimalarial drug development. *Expert Review of Anti-infective Therapy* **2009**, *7* (9), 1087-1098.
431. Josling, G. A.; Llinas, M., Sexual development in Plasmodium parasites: knowing when it's time to commit. *Nat Rev Micro* **2015**, *13* (9), 573-587.
432. Rosenberg, R.; Wirtz, R. A.; Schneider, I.; Burge, R., An estimation of the number of malaria sporozoites ejected by a feeding mosquito. *Trans R Soc Trop Med Hyg* **1990**, *84* (2), 209-12.
433. Bannister, L.; Mitchell, G., The ins, outs and roundabouts of malaria. *Trends in Parasitology* **2003**, *19* (5), 209-13.
434. Dixon, M. W.; Thompson, J.; Gardiner, D. L.; Trenholme, K. R., Sex in Plasmodium: a sign of commitment. *Trends in Parasitology* **2008**, *24* (4), 168-75.
435. Mantel, P. Y.; Hoang, A. N.; Goldowitz, I., *et al.*, Malaria-infected erythrocyte-derived microvesicles mediate cellular communication within the parasite population and with the host immune system. *Cell Host & Microbe* **2013**, *13* (5), 521-34.
436. Regev-Rudzki, N.; Wilson, D. W.; Carvalho, T. G., *et al.*, Cell-cell communication between malaria-infected red blood cells via exosome-like vesicles. *Cell* **2013**, *153* (5), 1120-33.
437. Billker, O.; Lindo, V.; Panico, M., *et al.*, Identification of xanthurenic acid as the putative inducer of malaria development in the mosquito. *Nature* **1998**, *392* (6673), 289-92.
438. Baruch, D. I.; Pasloske, B. L.; Singh, H. B., *et al.*, Cloning the P. falciparum gene encoding PfEMP1, a malarial variant antigen and adherence receptor on the surface of parasitized human erythrocytes. *Cell* **1995**, *82* (1), 77-87.
439. Smith, J. D.; Chitnis, C. E.; Craig, A. G., *et al.*, Switches in expression of Plasmodium falciparum var genes correlate with changes in antigenic and cytoadherent phenotypes of infected erythrocytes. *Cell* **1995**, *82* (1), 101-10.
440. Su, X.-z.; Heatwole, V. M.; Wertheimer, S. P., *et al.*, The large diverse gene family var encodes proteins involved in cytoadherence and antigenic variation of plasmodium falciparum-infected erythrocytes. *Cell* **1995**, *82* (1), 89-100.
441. Bull, P. C.; Lowe, B. S.; Kortok, M., *et al.*, Parasite antigens on the infected red cell surface are targets for naturally acquired immunity to malaria. *Nature Medicine* **1998**, *4* (3), 358-60.
442. Roberts, D. J.; Craig, A. G.; Berendt, A. R., *et al.*, Rapid switching to multiple antigenic and adhesive phenotypes in malaria. *Nature* **1992**, *357* (6380), 689-92.
443. Gray, D. J.; Ross, A. G.; Li, Y. S.; McManus, D. P., Diagnosis and management of schistosomiasis. *BMJ* **2011**, *342*, d2651-d2651.
444. Hotez, P. J.; Pecoul, B., "Manifesto" for Advancing the Control and Elimination of Neglected Tropical Diseases. *PLoS Neglected Tropical Diseases* **2010**, *4* (5), e718.
445. Holtfreter, M. C.; Mone, H.; Muller-Stover, I.; Mouahid, G.; Richter, J., Schistosoma haematobium infections acquired in Corsica, France, August 2013. *Euro surveillance : bulletin Europeen sur les maladies transmissibles = European communicable disease bulletin* **2014**, *19* (22).
446. de Laval, F.; Savini, H.; Biance-Valero, E.; Simon, F., Human schistosomiasis: an emerging threat for Europe. *Lancet (London, England)* **2014**, *384* (9948), 1094-5.
447. Brunet, J.; Pfaff, A. W.; Hansmann, Y., *et al.*, An unusual case of hematuria in a French family returning from Corsica. *International Journal of Infectious Diseases : IJID : official publication of the International Society for Infectious Diseases* **2015**, *31*, 59-60.
448. Kane, R. A.; Stothard, J. R.; Emery, A. M.; Rollinson, D., Molecular characterization of freshwater snails in the genus Bulinus: a role for barcodes? *Parasites & Vectors* **2008**, *1* (1), 15.
449. McCreesh, N.; Nikulin, G.; Booth, M., Predicting the effects of climate change on Schistosoma mansoni transmission in eastern Africa. *Parasites & Vectors* **2015**, *8*, 4.
450. Meltzer, E.; Schwartz, E., Schistosomiasis: Current Epidemiology and Management in Travelers. *Current Infectious Disease Reports* **2013**, *15* (3), 211-215.

451. WHO, Weekly Epidemiological Record Relevé Épidémiologique Hebdomadaire. 216; Vol. 91, pp 53-60.
452. Dömling, A.; Khoury, K., Praziquantel and Schistosomiasis. *ChemMedChem* **2010**, 5 (9), 1420-1434.
453. Standley, C. J.; Mugisha, L.; Dobson, A. P.; Stothard, J. R., Zoonotic schistosomiasis in non-human primates: past, present and future activities at the human-wildlife interface in Africa. *Journal of Helminthology* **2012**, 86 (2), 131-40.
454. WHO, Weekly Epidemiological Record Relevé Épidémiologique Hebdomadaire. 2015; Vol. 376, pp 25-32.
455. Colley, D. G.; Bustinduy, A. L.; Secor, W. E.; King, C. H., Human schistosomiasis. *The Lancet* **2014**, 383 (9936), 2253-2264.
456. Gobert, G. N.; Chai, M.; McManus, D. P., Biology of the schistosome lung-stage schistosomulum. *Parasitology* **2006**, 134 (04), 453.
457. He, Y. X.; Salafsky, B.; Ramaswamy, K., Comparison of skin invasion among three major species of *Schistosoma*. *Trends in Parasitology* **2005**, 21 (5), 201-3.
458. Curwen, R. S.; Wilson, R. A., Invasion of skin by schistosome cercariae: some neglected facts. *Trends in Parasitology* **2003**, 19 (2), 63-66.
459. Rheinberg, C. E.; Moné, H.; Caffrey, C. R., *et al.*, *Schistosoma haematobium*, *S. intercalatum*, *S. japonicum*, *S. mansoni*, and *S. rodhaini* in mice: relationship between patterns of lung migration by schistosomula and perfusion recovery of adult worms. *Parasitology Research* **1998**, 84 (4), 338-342.
460. Burke, M. L.; Jones, M. K.; Gobert, G. N., *et al.*, Immunopathogenesis of human schistosomiasis. *Parasite Immunology* **2009**, 31 (4), 163-176.
461. El Ridi, R. A. F.; Tallima, H. A. M., Novel Therapeutic and Prevention Approaches for Schistosomiasis: Review. *Journal of Advanced Research* **2013**, 4 (5), 467-478.
462. Andersson, K. L.; Chung, R. T., Hepatic schistosomiasis. *Current Treatment Options in Gastroenterology* **2007**, 10 (6), 504-512.
463. King, C. H.; Dickman, K.; Tisch, D. J., Reassessment of the cost of chronic helminthic infection: a meta-analysis of disability-related outcomes in endemic schistosomiasis. *The Lancet* **2005**, 365 (9470), 1561-1569.
464. Chitsulo, L.; Loverde, P.; Engels, D., Focus: Schistosomiasis. *Nature Reviews Microbiology* **2004**, 2 (1), 12-13.
465. Doenhoff, M. J.; Cioli, D.; Utzinger, J., Praziquantel: mechanisms of action, resistance and new derivatives for schistosomiasis. *Current Opinion in Infectious Diseases* **2008**, 21 (6), 659-667.
466. Cioli, D.; Pica-Mattoccia, L.; Basso, A.; Guidi, A., Schistosomiasis control: praziquantel forever? *Molecular and Biochemical Parasitology* **2014**, 195 (1), 23-29.
467. Gryseels, B.; Polman, K.; Clerinx, J.; Kestens, L., Human schistosomiasis. *The Lancet* **2006**, 368 (9541), 1106-1118.
468. Caffrey, C. R., Chemotherapy of schistosomiasis: present and future. *Current Opinion in Chemical Biology* **2007**, 11 (4), 433-439.
469. Doenhoff, M. J.; Kusel, J. R.; Coles, G. C.; Cioli, D., Resistance of *Schistosoma mansoni* to praziquantel: is there a problem? *Transactions of the Royal Society of Tropical Medicine and Hygiene* **2002**, 96 (5), 465-469.
470. Doenhoff, M. J.; Pica-Mattoccia, L., Praziquantel for the treatment of schistosomiasis: its use for control in areas with endemic disease and prospects for drug resistance. *Expert Review of Anti-infective Therapy* **2006**, 4 (2), 199-210.
471. Danso-Appiah, A.; De Vlas, S. J., Interpreting low praziquantel cure rates of *Schistosoma mansoni* infections in Senegal. *Trends in Parasitology* **2002**, 18 (3), 125-129.
472. Lawn, S. D.; Lucas, S. B.; Chiodini, P. L., Case report: *Schistosoma mansoni* infection: failure of standard treatment with praziquantel in a returned traveller. *Transactions of the Royal Society of Tropical Medicine and Hygiene* **2003**, 97 (1), 100-101.

473. Melman, S. D.; Steinauer, M. L.; Cunningham, C., *et al.*, Reduced Susceptibility to Praziquantel among Naturally Occurring Kenyan Isolates of *Schistosoma mansoni*. *PLoS Neglected Tropical Diseases* **2009**, *3* (8), e504.
474. Bonesso-Sabadini, P. I. P.; Dias, L. C. d. S., Altered Response of Strain of *Schistosoma mansoni* to Oxamniquine and Praziquantel. *Memórias do Instituto Oswaldo Cruz* **2002**, *97* (3), 381-385.
475. Couto, F. F. B.; Coelho, P. M. Z.; Araújo, N., *et al.*, *Schistosoma mansoni*: a method for inducing resistance to praziquantel using infected *Biomphalaria glabrata* snails. *Memórias do Instituto Oswaldo Cruz* **2011**, *106* (2), 153-157.
476. Fallon, P. G.; Doenhoff, M. J., Drug-Resistant Schistosomiasis: Resistance to Praziquantel and Oxamniquine Induced in *Schistosoma Mansoni* in Mice is Drug Specific. *The American Journal of Tropical Medicine and Hygiene* **1994**, *51* (1), 83-88.
477. Gardner, M. J.; Hall, N.; Fung, E., *et al.*, Genome sequence of the human malaria parasite *Plasmodium falciparum*. *Nature* **2002**, *419* (6906), 498-511.
478. Ay, F.; Bunnik, E. M.; Varoquaux, N., *et al.*, Multiple dimensions of epigenetic gene regulation in the malaria parasite *Plasmodium falciparum*: gene regulation via histone modifications, nucleosome positioning and nuclear architecture in *P. falciparum*. *Bioessays* **2015**, *37* (2), 182-94.
479. Cui, L.; Miao, J., Chromatin-Mediated Epigenetic Regulation in the Malaria Parasite *Plasmodium falciparum*. *Eukaryotic Cell* **2010**, *9* (8), 1138-1149.
480. Gupta, A. P.; Bozdech, Z., Epigenetic landscapes underlining global patterns of gene expression in the human malaria parasite, *Plasmodium falciparum*. *International Journal for Parasitology* **2017**.
481. Duffy, M. F.; Selvarajah, S. A.; Josling, G. A.; Petter, M., Epigenetic regulation of the *Plasmodium falciparum* genome. *Briefings in Functional Genomics* **2014**, *13* (3), 203-16.
482. Kirchner, S.; Power, B. J.; Waters, A. P., Recent advances in malaria genomics and epigenomics. *Genome Medicine* **2016**, *8* (1), 92.
483. Batugedara, G.; Lu, X. M.; Bunnik, E. M.; Le Roch, K. G., The Role of Chromatin Structure in Gene Regulation of the Human Malaria Parasite. *Trends in Parasitology* **2017**, *33* (5), 364-377.
484. Cortes, A.; Deitsch, K. W., Malaria Epigenetics. *Cold Spring Harbor Perspectives in Medicine* **2017**.
485. Coetzee, N.; Sidoli, S.; van Biljon, R., *et al.*, Quantitative chromatin proteomics reveals a dynamic histone post-translational modification landscape that defines asexual and sexual *Plasmodium falciparum* parasites. *Scientific Reports* **2017**, *7* (1), 607.
486. Choi, S.-W.; Keyes, M. K.; Horrocks, P., LC/ESI-MS demonstrates the absence of 5-methyl-2'-deoxycytosine in *Plasmodium falciparum* genomic DNA. *Molecular and Biochemical Parasitology* **2006**, *150* (2), 350-352.
487. Ponts, N.; Fu, L.; Harris, Elena Y., *et al.*, Genome-wide Mapping of DNA Methylation in the Human Malaria Parasite *Plasmodium falciparum*. *Cell Host & Microbe* **2013**, *14* (6), 696-706.
488. McNroy, G. R.; Beraldi, D.; Raiber, E. A., *et al.*, Enhanced Methylation Analysis by Recovery of Unsequenceable Fragments. *PLoS One* **2016**, *11* (3), e0152322.
489. Lopez-Rubio, J.-J.; Mancio-Silva, L.; Scherf, A., Genome-wide Analysis of Heterochromatin Associates Clonally Variant Gene Regulation with Perinuclear Repressive Centers in Malaria Parasites. *Cell Host & Microbe* **2009**, *5* (2), 179-190.
490. Salcedo-Amaya, A. M.; van Driel, M. A.; Alako, B. T., *et al.*, Dynamic histone H3 epigenome marking during the intraerythrocytic cycle of *Plasmodium falciparum*. *Proceedings of the National Academy of Sciences of the United States of America* **2009**, *106* (24), 9655-60.
491. Miao, J.; Fan, Q.; Cui, L., *et al.*, The malaria parasite *Plasmodium falciparum* histones: Organization, expression, and acetylation. *Gene* **2006**, *369*, 53-65.
492. Baum, J.; Papenfuss, A. T.; Mair, G. R., *et al.*, Molecular genetics and comparative genomics reveal RNAi is not functional in malaria parasites. *Nucleic Acids Research* **2009**, *37* (11), 3788-3798.
493. Kyes, S.; Horrocks, P.; Newbold, C., Antigenic variation at the infected red cell surface in malaria. *Annual Review of Microbiology* **2001**, *55*, 673-707.

494. Cortes, A.; Crowley, V. M.; Vaquero, A.; Voss, T. S., A view on the role of epigenetics in the biology of malaria parasites. *PLoS Pathogens* **2012**, *8* (12), e1002943.
495. Merrick, C. J.; Duraisingh, M. T., Epigenetics in Plasmodium: What Do We Really Know? *Eukaryotic Cell* **2010**, *9* (8), 1150-1158.
496. Bozdech, Z.; Llinas, M.; Pulliam, B. L., *et al.*, The transcriptome of the intraerythrocytic developmental cycle of Plasmodium falciparum. *PLoS Biol* **2003**, *1* (1), E5.
497. Le Roch, K. G.; Zhou, Y.; Blair, P. L., *et al.*, Discovery of gene function by expression profiling of the malaria parasite life cycle. *Science* **2003**, *301* (5639), 1503-8.
498. Llinas, M.; Bozdech, Z.; Wong, E. D.; Adai, A. T.; DeRisi, J. L., Comparative whole genome transcriptome analysis of three Plasmodium falciparum strains. *Nucleic Acids Research* **2006**, *34* (4), 1166-73.
499. Balaji, S., Discovery of the principal specific transcription factors of Apicomplexa and their implication for the evolution of the AP2-integrase DNA binding domains. *Nucleic Acids Research* **2005**, *33* (13), 3994-4006.
500. Fan, Q.; An, L.; Cui, L., Plasmodium falciparum Histone Acetyltransferase, a Yeast GCN5 Homologue Involved in Chromatin Remodeling. *Eukaryotic Cell* **2004**, *3* (2), 264-276.
501. Iyer, L. M.; Anantharaman, V.; Wolf, M. Y.; Aravind, L., Comparative genomics of transcription factors and chromatin proteins in parasitic protists and other eukaryotes. *International Journal for Parasitology* **2008**, *38* (1), 1-31.
502. Chandra, B. R.; Olivieri, A.; Silvestrini, F.; Alano, P.; Sharma, A., Biochemical characterization of the two nucleosome assembly proteins from Plasmodium falciparum. *Molecular and Biochemical Parasitology* **2005**, *142* (2), 237-247.
503. Gill, J.; Kumar, A.; Yogavel, M., *et al.*, Structure, localization and histone binding properties of nuclear-associated nucleosome assembly protein from Plasmodium falciparum. *Malaria Journal* **2010**, *9* (1), 90.
504. Yuda, M.; Iwanaga, S.; Shigenobu, S., *et al.*, Identification of a transcription factor in the mosquito-invasive stage of malaria parasites. *Molecular Microbiology* **2009**, *71* (6), 1402-14.
505. Silvestrini, F.; Bozdech, Z.; Lanfrancotti, A., *et al.*, Genome-wide identification of genes upregulated at the onset of gametocytogenesis in Plasmodium falciparum. *Mol Biochem Parasitol* **2005**, *143* (1), 100-10.
506. Raibaud, A.; Brahimi, K.; Roth, C. W.; Brey, P. T.; Faust, D. M., Differential gene expression in the ookinete stage of the malaria parasite Plasmodium berghei. *Mol Biochem Parasitol* **2006**, *150* (1), 107-13.
507. Sacci, J. B., Jr.; Ribeiro, J. M.; Huang, F., *et al.*, Transcriptional analysis of in vivo Plasmodium yoelii liver stage gene expression. *Mol Biochem Parasitol* **2005**, *142* (2), 177-83.
508. Tarun, A. S.; Peng, X.; Dumpit, R. F., *et al.*, A combined transcriptome and proteome survey of malaria parasite liver stages. *Proceedings of the National Academy of Sciences of the United States of America* **2008**, *105* (1), 305-10.
509. Kafsack, B. F. C.; Rovira-Graells, N.; Clark, T. G., *et al.*, A transcriptional switch underlies commitment to sexual development in malaria parasites. *Nature* **2014**, *507* (7491), 248-252.
510. Sinha, A.; Hughes, K. R.; Modrzynska, K. K., *et al.*, A cascade of DNA-binding proteins for sexual commitment and development in Plasmodium. *Nature* **2014**, *507* (7491), 253-257.
511. Flueck, C.; Bartfai, R.; Volz, J., *et al.*, Plasmodium falciparum Heterochromatin Protein 1 Marks Genomic Loci Linked to Phenotypic Variation of Exported Virulence Factors. *PLoS Pathogens* **2009**, *5* (9), e1000569.
512. Coleman, Bradley I.; Skillman, Kristen M.; Jiang, Rays H. Y., *et al.*, A Plasmodium falciparum Histone Deacetylase Regulates Antigenic Variation and Gametocyte Conversion. *Cell Host & Microbe* **2014**, *16* (2), 177-186.
513. Brancucci, Nicolas M. B.; Bertschi, Nicole L.; Zhu, L., *et al.*, Heterochromatin Protein 1 Secures Survival and Transmission of Malaria Parasites. *Cell Host & Microbe* **2014**, *16* (2), 165-176.

514. Cowman, A. F.; Crabb, B. S., Invasion of red blood cells by malaria parasites. *Cell* **2006**, *124* (4), 755-66.
515. Cortés, A.; Carret, C.; Kaneko, O., *et al.*, Epigenetic Silencing of Plasmodium falciparum Genes Linked to Erythrocyte Invasion. *PLoS Pathogens* **2007**, *3* (8), e107.
516. Josling, Gabrielle A.; Petter, M.; Oehring, Sophie C., *et al.*, A Plasmodium Falciparum Bromodomain Protein Regulates Invasion Gene Expression. *Cell Host & Microbe* **2015**, *17* (6), 741-751.
517. Chen, Q.; Fernandez, V.; Sundstrom, A., *et al.*, Developmental selection of var gene expression in Plasmodium falciparum. *Nature* **1998**, *394* (6691), 392-5.
518. Duffy, M. F.; Brown, G. V.; Basuki, W., *et al.*, Transcription of multiple var genes by individual, trophozoite-stage Plasmodium falciparum cells expressing a chondroitin sulphate A binding phenotype. *Molecular Microbiology* **2002**, *43* (5), 1285-1293.
519. Fernandez, V.; Chen, Q.; Sundstrom, A., *et al.*, Mosaic-like transcription of var genes in single Plasmodium falciparum parasites. *Mol Biochem Parasitol* **2002**, *121* (2), 195-203.
520. Mok, B. W.; Ribacke, U.; Rasti, N., *et al.*, Default Pathway of var2csa switching and translational repression in Plasmodium falciparum. *PLoS One* **2008**, *3* (4), e1982.
521. Ay, F.; Bunnik, E. M.; Varoquaux, N., *et al.*, Three-dimensional modeling of the P. falciparum genome during the erythrocytic cycle reveals a strong connection between genome architecture and gene expression. *Genome research* **2014**, *24* (6), 974-88.
522. Freitas-Junior, L. H.; Bottius, E.; Pirrit, L. A., *et al.*, Frequent ectopic recombination of virulence factor genes in telomeric chromosome clusters of P. falciparum. *Nature* **2000**, *407* (6807), 1018-22.
523. Crowley, V. M.; Rovira-Graells, N.; Ribas de Pouplana, L.; Cortes, A., Heterochromatin formation in bistable chromatin domains controls the epigenetic repression of clonally variant Plasmodium falciparum genes linked to erythrocyte invasion. *Molecular Microbiology* **2011**, *80* (2), 391-406.
524. Perez-Toledo, K.; Rojas-Meza, A. P.; Mancio-Silva, L., *et al.*, Plasmodium falciparum heterochromatin protein 1 binds to tri-methylated histone 3 lysine 9 and is linked to mutually exclusive expression of var genes. *Nucleic Acids Research* **2009**, *37* (8), 2596-2606.
525. Chookajorn, T.; Dzikowski, R.; Frank, M., *et al.*, Epigenetic memory at malaria virulence genes. *Proceedings of the National Academy of Sciences* **2007**, *104* (3), 899-902.
526. Lopez-Rubio, J. J.; Gontijo, A. M.; Nunes, M. C., *et al.*, 5' flanking region of var genes nucleate histone modification patterns linked to phenotypic inheritance of virulence traits in malaria parasites. *Molecular Microbiology* **2007**, *0* (0), 071119190133003-???
527. Duraisingh, M. T.; Voss, T. S.; Marty, A. J., *et al.*, Heterochromatin Silencing and Locus Repositioning Linked to Regulation of Virulence Genes in Plasmodium falciparum. *Cell* **2005**, *121* (1), 13-24.
528. Tonkin, C. J.; Carret, C. K.; Duraisingh, M. T., *et al.*, Sir2 Paralogues Cooperate to Regulate Virulence Genes and Antigenic Variation in Plasmodium falciparum. *PLoS Biology* **2009**, *7* (4), e1000084.
529. Jiang, L.; Mu, J.; Zhang, Q., *et al.*, PfSETvs methylation of histone H3K36 represses virulence genes in Plasmodium falciparum. *Nature* **2013**, *499* (7457), 223-227.
530. Ukaegbu, U. E.; Kishore, S. P.; Kwiatkowski, D. L., *et al.*, Recruitment of PfSET2 by RNA polymerase II to variant antigen encoding loci contributes to antigenic variation in P. falciparum. *PLoS pathogens* **2014**, *10* (1), e1003854.
531. Volz, J. C.; Bartfai, R.; Petter, M., *et al.*, PfSET10, a Plasmodium falciparum methyltransferase, maintains the active var gene in a poised state during parasite division. *Cell Host & Microbe* **2012**, *11* (1), 7-18.
532. Epp, C.; Li, F.; Howitt, C. A.; Chookajorn, T.; Deitsch, K. W., Chromatin associated sense and antisense noncoding RNAs are transcribed from the var gene family of virulence genes of the malaria parasite Plasmodium falciparum. *RNA* **2009**, *15* (1), 116-27.
533. Zhang, Q.; Siegel, T. N.; Martins, R. M., *et al.*, Exonuclease-mediated degradation of nascent RNA silences genes linked to severe malaria. *Nature* **2014**, *513* (7518), 431-5.

534. Amit-Avraham, I.; Pozner, G.; Eshar, S., *et al.*, Antisense long noncoding RNAs regulate gene activation in the malaria parasite *Plasmodium falciparum*. *Proceedings of the National Academy of Sciences* **2015**, *112* (9), E982-E991.
535. Lanzer, M.; Wertheimer, S. P.; de Bruin, D.; Ravetch, J. V., Chromatin structure determines the sites of chromosome breakages in *Plasmodium falciparum*. *Nucleic Acids Research* **1994**, *22* (15), 3099-3103.
536. Sullivan, W. J.; Naguleswaran, A.; Angel, S. O., Histones and histone modifications in protozoan parasites. *Cellular Microbiology* **2006**, *8* (12), 1850-1861.
537. Trelle, M. B.; Salcedo-Amaya, A. M.; Cohen, A. M.; Stunnenberg, H. G.; Jensen, O. N., Global Histone Analysis by Mass Spectrometry Reveals a High Content of Acetylated Lysine Residues in the Malaria Parasite *Plasmodium falciparum*. *Journal of Proteome Research* **2009**, *8* (7), 3439-3450.
538. Bonasio, R.; Tu, S.; Reinberg, D., Molecular signals of epigenetic states. *Science* **2010**, *330* (6004), 612-6.
539. Lasonder, E.; Treeck, M.; Alam, M.; Tobin, A. B., Insights into the *Plasmodium falciparum* schizont phospho-proteome. *Microbes Infect* **2012**, *14* (10), 811-9.
540. Treeck, M.; Sanders, J. L.; Elias, J. E.; Boothroyd, J. C., The phosphoproteomes of *Plasmodium falciparum* and *Toxoplasma gondii* reveal unusual adaptations within and beyond the parasites' boundaries. *Cell Host & Microbe* **2011**, *10* (4), 410-9.
541. Dastidar, E. G.; Dzek, K.; Krijgsveld, J., *et al.*, Comprehensive Histone Phosphorylation Analysis and Identification of Pf14-3-3 Protein as a Histone H3 Phosphorylation Reader in Malaria Parasites. *PLoS ONE* **2013**, *8* (1), e53179.
542. Issar, N.; Roux, E.; Mattei, D.; Scherf, A., Identification of a novel post-translational modification in *Plasmodium falciparum*: protein sumoylation in different cellular compartments. *Cellular microbiology* **2008**, *10* (10), 1999-2011.
543. Garcia, B. A.; Hake, S. B.; Diaz, R. L., *et al.*, Organismal differences in post-translational modifications in histones H3 and H4. *The Journal of Biological Chemistry* **2007**, *282* (10), 7641-55.
544. Bernstein, B. E.; Kamal, M.; Lindblad-Toh, K., *et al.*, Genomic maps and comparative analysis of histone modifications in human and mouse. *Cell* **2005**, *120* (2), 169-81.
545. Kim, T. H.; Barrera, L. O.; Zheng, M., *et al.*, A high-resolution map of active promoters in the human genome. *Nature* **2005**, *436* (7052), 876-880.
546. Nishida, H.; Suzuki, T.; Kondo, S., *et al.*, Histone H3 acetylated at lysine 9 in promoter is associated with low nucleosome density in the vicinity of transcription start site in human cell. *Chromosome Research : an international journal on the molecular, supramolecular and evolutionary aspects of chromosome biology* **2006**, *14* (2), 203-11.
547. Wang, Z.; Zang, C.; Rosenfeld, J. A., *et al.*, Combinatorial patterns of histone acetylations and methylations in the human genome. *Nature Genetics* **2008**, *40* (7), 897-903.
548. Bártfai, R.; Hoeijmakers, W. A. M.; Salcedo-Amaya, A. M., *et al.*, H2A.Z Demarcates Intergenic Regions of the *Plasmodium falciparum* Epigenome That Are Dynamically Marked by H3K9ac and H3K4me3. *PLoS Pathogens* **2010**, *6* (12), e1001223.
549. Cui, L.; Miao, J.; Furuya, T., *et al.*, PfGCN5-mediated histone H3 acetylation plays a key role in gene expression in *Plasmodium falciparum*. *Eukaryot Cell* **2007**, *6* (7), 1219-27.
550. Freitas-Junior, L. H.; Hernandez-Rivas, R.; Ralph, S. A., *et al.*, Telomeric Heterochromatin Propagation and Histone Acetylation Control Mutually Exclusive Expression of Antigenic Variation Genes in Malaria Parasites. *Cell* **2005**, *121* (1), 25-36.
551. Fastman, Y.; Noble, R.; Recker, M.; Dzikowski, R., Erasing the Epigenetic Memory and Beginning to Switch—The Onset of Antigenic Switching of var Genes in *Plasmodium falciparum*. *PLoS ONE* **2012**, *7* (3), e34168.
552. Merrick, C. J.; Huttenhower, C.; Buckee, C., *et al.*, Epigenetic Dysregulation of Virulence Gene Expression in Severe *Plasmodium falciparum* Malaria. *The Journal of Infectious Diseases* **2012**, *205* (10), 1593-1600.

553. Rovira-Graells, N.; Gupta, A. P.; Planet, E., *et al.*, Transcriptional variation in the malaria parasite *Plasmodium falciparum*. *Genome Research* **2012**, *22* (5), 925-938.
554. Voss, T. S.; Bozdech, Z.; Bártfai, R., Epigenetic memory takes center stage in the survival strategy of malaria parasites. *Current Opinion in Microbiology* **2014**, *20*, 88-95.
555. Rovira-Graells, N.; Crowley, V. M.; Bancells, C., *et al.*, Deciphering the principles that govern mutually exclusive expression of *Plasmodium falciparum* clag3 genes. *Nucleic Acids Research* **2015**, *43* (17), 8243-8257.
556. Karmodiya, K.; Pradhan, S. J.; Joshi, B., *et al.*, A comprehensive epigenome map of *Plasmodium falciparum* reveals unique mechanisms of transcriptional regulation and identifies H3K36me2 as a global mark of gene suppression. *Epigenetics & Chromatin* **2015**, *8* (1).
557. Sautel, C. F.; Cannella, D.; Bastien, O., *et al.*, SET8-Mediated Methylations of Histone H4 Lysine 20 Mark Silent Heterochromatic Domains in Apicomplexan Genomes. *Molecular and Cellular Biology* **2007**, *27* (16), 5711-5724.
558. Schotta, G., A silencing pathway to induce H3-K9 and H4-K20 trimethylation at constitutive heterochromatin. *Genes & Development* **2004**, *18* (11), 1251-1262.
559. Benetti, R.; Gonzalo, S.; Jaco, I., *et al.*, Suv4-20h deficiency results in telomere elongation and derepression of telomere recombination. *The Journal of Cell Biology* **2007**, *178* (6), 925-936.
560. Gupta, A. P.; Chin, W. H.; Zhu, L., *et al.*, Dynamic Epigenetic Regulation of Gene Expression during the Life Cycle of Malaria Parasite *Plasmodium falciparum*. *PLoS Pathogens* **2013**, *9* (2), e1003170.
561. Bunnik, E. M.; Polishko, A.; Prudhomme, J., *et al.*, DNA-encoded nucleosome occupancy is associated with transcription levels in the human malaria parasite *Plasmodium falciparum*. *BMC Genomics* **2014**, *15* (1), 347.
562. Ponts, N.; Harris, E. Y.; Prudhomme, J., *et al.*, Nucleosome landscape and control of transcription in the human malaria parasite. *Genome Research* **2010**, *20* (2), 228-238.
563. Kensche, Philip R.; Hoeijmakers, Wieteke Anna M.; Toenhake, Christa G., *et al.*, The nucleosome landscape of *Plasmodium falciparum* reveals chromatin architecture and dynamics of regulatory sequences. *Nucleic Acids Research* **2015**, *44* (5), 2110-2124.
564. Hoeijmakers, W. A.; Salcedo-Amaya, A. M.; Smits, A. H., *et al.*, H2A.Z/H2B.Z double-variant nucleosomes inhabit the AT-rich promoter regions of the *Plasmodium falciparum* genome. *Molecular Microbiology* **2013**, *87* (5), 1061-73.
565. Bischoff, E.; Vaquero, C., In silico and biological survey of transcription-associated proteins implicated in the transcriptional machinery during the erythrocytic development of *Plasmodium falciparum*. *BMC genomics* **2010**, *11* (1), 34.
566. Wade, P. A.; Pruss, D.; Wolffe, A. P., Histone acetylation: chromatin in action. *Trends in Biochemical Sciences* **1997**, *22* (4), 128-132.
567. Hassan, A. H.; Neely, K. E.; Workman, J. L., Histone Acetyltransferase Complexes Stabilize SWI/SNF Binding to Promoter Nucleosomes. *Cell* **2001**, *104* (6), 817-827.
568. Horrocks, P.; Wong, E.; Russell, K.; Emes, R. D., Control of gene expression in *Plasmodium falciparum* – Ten years on. *Molecular and Biochemical Parasitology* **2009**, *164* (1), 9-25.
569. Fan, Q.; An, L.; Cui, L., PfADA2, a *Plasmodium falciparum* homologue of the transcriptional coactivator ADA2 and its in vivo association with the histone acetyltransferase PfGCN5. *Gene* **2004**, *336* (2), 251-261.
570. Cui, L.; Miao, J.; Cui, L., Cytotoxic Effect of Curcumin on Malaria Parasite *Plasmodium falciparum*: Inhibition of Histone Acetylation and Generation of Reactive Oxygen Species. *Antimicrobial Agents and Chemotherapy* **2006**, *51* (2), 488-494.
571. Yang, X.-J.; Seto, E., The Rpd3/Hda1 family of lysine deacetylases: from bacteria and yeast to mice and men. *Nature Reviews Molecular Cell Biology* **2008**, *9* (3), 206-218.
572. Perrod, S.; Cockell, M. M.; Laroche, T., *et al.*, A cytosolic NAD-dependent deacetylase, Hst2p, can modulate nucleolar and telomeric silencing in yeast. *The EMBO Journal* **2001**, *20* (1-2), 197-209.

573. Gasser, S. M.; Cockell, M. M., The molecular biology of the SIR proteins. *Gene* **2001**, 279 (1), 1-16.
574. Andrews, K., Towards Histone Deacetylase Inhibitors as New Antimalarial Drugs. *Current Pharmaceutical Design* **2012**.
575. Rotili, D.; Simonetti, G.; Savarino, A., *et al.*, Non-cancer uses of histone deacetylase inhibitors: effects on infectious diseases and beta-hemoglobinopathies. *Curr Top Med Chem* **2009**, 9 (3), 272-91.
576. Aurrecochea, C.; Brestelli, J.; Brunk, B. P., *et al.*, PlasmoDB: a functional genomic database for malaria parasites. *Nucleic Acids Research* **2009**, 37 (Database), D539-D543.
577. Joshi, M. B.; Lin, D. T.; Chiang, P. H., *et al.*, Molecular cloning and nuclear localization of a histone deacetylase homologue in *Plasmodium falciparum*. *Molecular and Biochemical Parasitology* **1999**, 99 (1), 11-19.
578. Mukherjee, P.; Pradhan, A.; Shah, F.; Tekwani, B. L.; Avery, M. A., Structural insights into the *Plasmodium falciparum* histone deacetylase 1 (PfHDAC-1): A novel target for the development of antimalarial therapy. *Bioorganic & Medicinal Chemistry* **2008**, 16 (9), 5254-5265.
579. Andrews, K. T.; Tran, T. N.; Lucke, A. J., *et al.*, Potent Antimalarial Activity of Histone Deacetylase Inhibitor Analogues. *Antimicrobial Agents and Chemotherapy* **2008**, 52 (4), 1454-1461.
580. Patel, V.; Mazitschek, R.; Coleman, B., *et al.*, Identification and Characterization of Small Molecule Inhibitors of a Class I Histone Deacetylase from *Plasmodium falciparum*. *J Med Chem* **2009**, 52 (8), 2185-2187.
581. Merrick, C. J.; Dzikowski, R.; Imamura, H.; Chuang, J.; Deitsch, K.; Duraisingh, M.T., *Plasmodium falciparum* Sir2a histone deacetylase on clonal and longitudinal variation in expression of the var family of virulence genes. *International Journal for Parasitology* **2010**, 40, 35-43.
582. Chakrabarty, S. P.; Saikumari, Y. K.; Bopanna, M. P.; Balaram, H., Biochemical characterization of *Plasmodium falciparum* Sir2, a NAD⁺-dependent deacetylase. *Molecular and Biochemical Parasitology* **2008**, 158 (2), 139-151.
583. Merrick, C. J.; Duraisingh, M. T., *Plasmodium falciparum* Sir2: an Unusual Sirtuin with Dual Histone Deacetylase and ADP-Ribosyltransferase Activity. *Eukaryotic Cell* **2007**, 6 (11), 2081-2091.
584. Zhou, Y.; Hao, Q., *Plasmodium falciparum* Sir2A preferentially hydrolyzes medium and long chain fatty acyl lysine. Protein Data Bank, Rutgers University: **2011**.
585. Mancio-Silva, L.; Lopez-Rubio, J. J.; Claes, A.; Scherf, A., Sir2a regulates rDNA transcription and multiplication rate in the human malaria parasite *Plasmodium falciparum*. *Nature Communications* **2013**, 4, 1530.
586. Cheung, P.; Lau, P., Epigenetic Regulation by Histone Methylation and Histone Variants. *Molecular Endocrinology* **2005**, 19 (3), 563-573.
587. Fan, Q.; Miao, J.; Cui, L.; Cui, L., Characterization of PRMT1 from *Plasmodium falciparum*. *Biochemical Journal* **2009**, 421 (1), 107-118.
588. Cui, L.; Fan, Q.; Cui, L.; Miao, J., Histone lysine methyltransferases and demethylases in *Plasmodium falciparum*. *International Journal for Parasitology* **2008**, 38 (10), 1083-1097.
589. Volz, J.; Carvalho, T. G.; Ralph, S. A., *et al.*, Potential epigenetic regulatory proteins localise to distinct nuclear sub-compartments in *Plasmodium falciparum*. *International Journal for Parasitology* **2010**, 40 (1), 109-21.
590. Chen, P. B.; Ding, S.; Zanghi, G., *et al.*, *Plasmodium falciparum* PfSET7: enzymatic characterization and cellular localization of a novel protein methyltransferase in sporozoite, liver and erythrocytic stage parasites. *Scientific Reports* **2016**, 6, 21802.
591. Issar, N.; Ralph, S. A.; Mancio-Silva, L.; Keeling, C.; Scherf, A., Differential sub-nuclear localisation of repressive and activating histone methyl modifications in *P. falciparum*. *Microbes and Infection* **2009**, 11 (3), 403-407.
592. Shi, Y.; Whetstone, J. R., Dynamic regulation of histone lysine methylation by demethylases. *Molecular Cell* **2007**, 25 (1), 1-14.
593. Kutateladze, T. G., SnapShot: Histone Readers. *Cell* **2011**, 146 (5), 842-842.e1.

594. Wysocka, J.; Swigut, T.; Milne, T. A., *et al.*, WDR5 Associates with Histone H3 Methylated at K4 and Is Essential for H3 K4 Methylation and Vertebrate Development. *Cell* **2005**, *121* (6), 859-872.
595. De Silva, E. K.; Gehrke, A. R.; Olszewski, K., *et al.*, Specific DNA-binding by Apicomplexan AP2 transcription factors. *Proceedings of the National Academy of Sciences* **2008**, *105* (24), 8393-8398.
596. Flueck, C.; Bartfai, R.; Niederwieser, I., *et al.*, A Major Role for the Plasmodium falciparum ApiAP2 Protein PfSIP2 in Chromosome End Biology. *PLoS Pathogens* **2010**, *6* (2), e1000784.
597. Andrews, K. T.; Gupta, A. P.; Tran, T. N., *et al.*, Comparative Gene Expression Profiling of P. falciparum Malaria Parasites Exposed to Three Different Histone Deacetylase Inhibitors. *PLoS ONE* **2012**, *7* (2), e31847.
598. Malmquist, N. A.; Moss, T. A.; Mecheri, S.; Scherf, A.; Fuchter, M. J., Small-molecule histone methyltransferase inhibitors display rapid antimalarial activity against all blood stage forms in Plasmodium falciparum. *Proceedings of the National Academy of Sciences* **2012**, *109* (41), 16708-16713.
599. Malmquist, N. A.; Sundriyal, S.; Caron, J., *et al.*, Histone methyltransferase inhibitors are orally bioavailable, fast-acting molecules with activity against different species causing malaria in humans. *Antimicrob Agents Chemother* **2015**, *59* (2), 950-9.
600. Cui, L.; Miao, J.; Furuya, T., *et al.*, Histone Acetyltransferase Inhibitor Anacardic Acid Causes Changes in Global Gene Expression during In Vitro Plasmodium falciparum Development. *Eukaryotic Cell* **2008**, *7* (7), 1200-1210.
601. Srivastava, S.; Bhowmick, K.; Chatterjee, S., *et al.*, Histone H3K9 acetylation level modulates gene expression and may affect parasite growth in human malaria parasite Plasmodium falciparum. *The FEBS Journal* **2014**, *281* (23), 5265-78.
602. Lopez-Rubio, J. J.; Gontijo, A. M.; Nunes, M. C., *et al.*, 5' flanking region of var genes nucleate histone modification patterns linked to phenotypic inheritance of virulence traits in malaria parasites. *Molecular Microbiology* **2007**, *66* (6), 1296-1305.
603. Kumar, A.; Bhowmick, K.; Vikramdeo, K. S., *et al.*, Designing novel inhibitors against histone acetyltransferase (HAT: GCN5) of Plasmodium falciparum. *European J Med Chem* **2017**, *138*, 26-37.
604. Darkin-Rattray, S. J.; Gurnett, A. M.; Myers, R. W., *et al.*, Apicidin: A novel antiprotozoal agent that inhibits parasite histone deacetylase. *Proceedings of the National Academy of Sciences* **1996**, *93* (23), 13143-13147.
605. Hu, G.; Cabrera, A.; Kono, M., *et al.*, Transcriptional profiling of growth perturbations of the human malaria parasite Plasmodium falciparum. *Nature Biotechnology* **2009**, *28* (1), 91-98.
606. Chaal, B. K.; Gupta, A. P.; Wastuwidyaningtyas, B. D.; Luah, Y.-H.; Bozdech, Z., Histone Deacetylases Play a Major Role in the Transcriptional Regulation of the Plasmodium falciparum Life Cycle. *PLoS Pathogens* **2010**, *6* (1), e1000737.
607. Moore, P. S.; Barbi, S.; Donadelli, M., *et al.*, Gene expression profiling after treatment with the histone deacetylase inhibitor trichostatin A reveals altered expression of both pro- and anti-apoptotic genes in pancreatic adenocarcinoma cells. *Biochimica et Biophysica Acta* **2004**, *1693* (3), 167-76.
608. Peart, M. J.; Smyth, G. K.; van Laar, R. K., *et al.*, Identification and functional significance of genes regulated by structurally different histone deacetylase inhibitors. *Proceedings of the National Academy of Sciences* **2005**, *102* (10), 3697-3702.
609. Meinke, P. T.; Colletti, S. L.; Doss, G., *et al.*, Synthesis of Apicidin-Derived Quinolone Derivatives: Parasite-Selective Histone Deacetylase Inhibitors and Antiproliferative Agents. *J Med Chem* **2000**, *43* (25), 4919-4922.
610. Colletti, S. L.; Myers, R. W.; Darkin-Rattray, S. J., *et al.*, Broad spectrum antiprotozoal agents that inhibit histone deacetylase: structure-activity relationships of apicidin. Part 2. *Bioorganic & Medicinal Chemistry Letters* **2001**, *11* (2), 113-117.
611. Colletti, S. L.; Myers, R. W.; Darkin-Rattray, S. J., *et al.*, Broad spectrum antiprotozoal agents that inhibit histone deacetylase: structure-activity relationships of apicidin. Part 1. *Bioorganic & Medicinal Chemistry Letters* **2001**, *11* (2), 107-111.

612. Murray, P. J.; Kranz, M.; Ladlow, M., *et al.*, The synthesis of cyclic tetrapeptoid analogues of the antiprotozoal natural product apicidin. *Bioorganic & Medicinal Chemistry Letters* **2001**, *11* (6), 773-776.
613. Engel, J. A.; Jones, A. J.; Avery, V. M., *et al.*, Profiling the anti-protozoal activity of anti-cancer HDAC inhibitors against Plasmodium and Trypanosoma parasites. *International Journal for Parasitology: Drugs and Drug Resistance* **2015**, *5* (3), 117-126.
614. Tan, J.; Cang, S.; Ma, Y.; Petrillo, R. L.; Liu, D., Novel histone deacetylase inhibitors in clinical trials as anti-cancer agents. *Journal of Hematology & Oncology* **2010**, *3* (1), 5.
615. Azzi, A.; Cosseau, C.; Grunau, C., Schistosoma mansoni: Developmental arrest of miracidia treated with histone deacetylase inhibitors. *Experimental Parasitology* **2009**, *121* (3), 288-291.
616. Jones-Brando, L., Drugs used in the treatment of schizophrenia and bipolar disorder inhibit the replication of Toxoplasma gondii. *Schizophrenia Research* **2003**, *62* (3), 237-244.
617. Strobl, J. S.; Cassell, M.; Mitchell, S. M.; Reilly, C. M.; Lindsay, D. S., SCRIPTAID AND SUBEROYLANILIDE HYDROXAMIC ACID ARE HISTONE DEACETYLASE INHIBITORS WITH POTENT ANTI-TOXOPLASMA GONDII ACTIVITY IN VITRO. *Journal of Parasitology* **2007**, *93* (3), 694-700.
618. Andrews, K. T.; Walduck, A.; Kelso, M. J., *et al.*, Anti-malarial effect of histone deacetylation inhibitors and mammalian tumour cytodifferentiating agents. *International Journal for Parasitology* **2000**, *30* (6), 761-768.
619. Mai, A.; Cerbara, I.; Valente, S., *et al.*, Antimalarial and Antileishmanial Activities of Aroyl-Pyrrolyl-Hydroxyamides, a New Class of Histone Deacetylase Inhibitors. *Antimicrobial Agents and Chemotherapy* **2004**, *48* (4), 1435-1436.
620. Dow, G. S.; Chen, Y.; Andrews, K. T., *et al.*, Antimalarial Activity of Phenylthiazolyl-Bearing Hydroxamate-Based Histone Deacetylase Inhibitors. *Antimicrobial Agents and Chemotherapy* **2008**, *52* (10), 3467-3477.
621. Glaser, K. B.; Staver, M. J.; Waring, J. F., *et al.*, Gene expression profiling of multiple histone deacetylase (HDAC) inhibitors: defining a common gene set produced by HDAC inhibition in T24 and MDA carcinoma cell lines. *Molecular Cancer Therapeutics* **2003**, *2* (2), 151-63.
622. Mai, A.; Massa, S.; Rotili, D., *et al.*, Histone Deacetylation in Epigenetics: An Attractive Target for Anticancer Therapy. *ChemInform* **2005**, *36* (28).
623. Marfurt, J.; Chalfain, F.; Prayoga, P., *et al.*, Ex Vivo Activity of Histone Deacetylase Inhibitors against Multidrug-Resistant Clinical Isolates of Plasmodium falciparum and P. vivax. *Antimicrobial Agents and Chemotherapy* **2010**, *55* (3), 961-966.
624. Wheatley, N. C.; Andrews, K. T.; Tran, T. L., *et al.*, Antimalarial histone deacetylase inhibitors containing cinnamate or NSAID components. *Bioorganic & Medicinal Chemistry Letters* **2010**, *20* (23), 7080-7084.
625. Chen, Y.; Lopez-Sanchez, M.; Savoy, D. N., *et al.*, A Series of Potent and Selective, Triazolylphenyl-Based Histone Deacetylases Inhibitors with Activity against Pancreatic Cancer Cells and Plasmodium falciparum. *J Med Chem* **2008**, *51* (12), 3437-3448.
626. Agbor-Enoh, S.; Seudieu, C.; Davidson, E.; Dritschilo, A.; Jung, M., Novel Inhibitor of Plasmodium Histone Deacetylase That Cures P. berghei-Infected Mice. *Antimicrobial Agents and Chemotherapy* **2009**, *53* (5), 1727-1734.
627. Patil, V.; Guerrant, W.; Chen, P. C., *et al.*, Antimalarial and antileishmanial activities of histone deacetylase inhibitors with triazole-linked cap group. *Bioorganic & Medicinal Chemistry* **2010**, *18* (1), 415-425.
628. Mwakwari, S. C.; Guerrant, W.; Patil, V., *et al.*, Non-Peptide Macrocyclic Histone Deacetylase Inhibitors Derived from Tricyclic Ketolide Skeleton. *J Med Chem* **2010**, *53* (16), 6100-6111.
629. Guerrant, W.; Mwakwari, S. C.; Chen, P. C., *et al.*, A Structure-Activity Relationship Study of the Antimalarial and Antileishmanial Activities of Nonpeptide Macrocyclic Histone Deacetylase Inhibitors. *ChemMedChem* **2010**, *5* (8), 1232-1235.

630. Sumanadasa, S. D. M.; Goodman, C. D.; Lucke, A. J., *et al.*, Antimalarial Activity of the Anticancer Histone Deacetylase Inhibitor SB939. *Antimicrobial Agents and Chemotherapy* **2012**, *56* (7), 3849-3856.
631. Hansen, F. K.; Sumanadasa, S. D. M.; Stenzel, K., *et al.*, Discovery of HDAC inhibitors with potent activity against multiple malaria parasite life cycle stages. *European J Med Chem* **2014**, *82*, 204-213.
632. Hansen, F. K.; Skinner-Adams, T. S.; Duffy, S., *et al.*, Synthesis, Antimalarial Properties, and SAR Studies of Alkoxyurea-Based HDAC Inhibitors. *ChemMedChem* **2014**, *9* (3), 665-670.
633. Trenholme, K.; Marek, L.; Duffy, S., *et al.*, Lysine Acetylation in Sexual Stage Malaria Parasites Is a Target for Antimalarial Small Molecules. *Antimicrobial Agents and Chemotherapy* **2014**, *58* (7), 3666-3678.
634. Giannini, G.; Battistuzzi, G.; Vignola, D., Hydroxamic acid based histone deacetylase inhibitors with confirmed activity against the malaria parasite. *Bioorganic & Medicinal Chemistry Letters* **2015**, *25* (3), 459-461.
635. Itoh, Y.; Suzuki, T.; Kouketsu, A., *et al.*, Design, Synthesis, Structure–Selectivity Relationship, and Effect on Human Cancer Cells of a Novel Series of Histone Deacetylase 6-Selective Inhibitors. *J Med Chem* **2007**, *50* (22), 5425-5438.
636. Mai, A.; Altucci, L., Epi-drugs to fight cancer: From chemistry to cancer treatment, the road ahead. *The International Journal of Biochemistry & Cell Biology* **2009**, *41* (1), 199-213.
637. Mai, A.; Perrone, A.; Nebbioso, A., *et al.*, Novel uracil-based 2-aminoanilide and 2-aminoanilide-like derivatives: Histone deacetylase inhibition and in-cell activities. *Bioorganic & Medicinal Chemistry Letters* **2008**, *18* (8), 2530-2535.
638. Ontoria, J. M.; Paonessa, G.; Ponzi, S., *et al.*, Discovery of a Selective Series of Inhibitors of *Plasmodium falciparum* HDACs. *ACS Medicinal Chemistry Letters* **2016**, *7* (5), 454-459.
639. Gey, C.; Kyrylenko, S.; Hennig, L., *et al.*, Phloroglucinol Derivatives Guttiferone G, Aristoforin, and Hyperforin: Inhibitors of Human Sirtuins SIRT1 and SIRT2. *Angewandte Chemie International Edition* **2007**, *46* (27), 5219-5222.
640. Verotta, L.; Appendino, G.; Bombardelli, E.; Brun, R., In vitro antimalarial activity of hyperforin, a prenylated acylphloroglucinol. A structure-activity study. *Bioorganic & Medicinal Chemistry Letters* **2007**, *17* (6), 1544-8.
641. Prusty, D.; Mehra, P.; Srivastava, S., *et al.*, Nicotinamide inhibits *Plasmodium falciparum* Sir2 activity in vitro and parasite growth. *FEMS Microbiology Letters* **2008**, *282* (2), 266-272.
642. Chakrabarty, S. P.; Ramapanicker, R.; Mishra, R.; Chandrasekaran, S.; Balaram, H., Development and characterization of lysine based tripeptide analogues as inhibitors of Sir2 activity. *Bioorganic & Medicinal Chemistry* **2009**, *17* (23), 8060-8072.
643. Guizetti, J.; Scherf, A., Silence, activate, poise and switch! Mechanisms of antigenic variation in *Plasmodium falciparum*. *Cellular microbiology* **2013**, *15* (5), 718-26.
644. Ma, A.; Yu, W.; Li, F., *et al.*, Discovery of a selective, substrate-competitive inhibitor of the lysine methyltransferase SETD8. *J Med Chem* **2014**, *57* (15), 6822-33.
645. Ma, A.; Yu, W.; Xiong, Y., *et al.*, Structure-activity relationship studies of SETD8 inhibitors. *MedChemComm* **2014**, *5* (12), 1892-1898.
646. Chou, J. L.; Huang, R. L.; Shay, J., *et al.*, Hypermethylation of the TGF-beta target, ABCA1 is associated with poor prognosis in ovarian cancer patients. *Clinical Epigenetics* **2015**, *7*, 1.
647. Dembele, L.; Franetich, J. F.; Lorthiois, A., *et al.*, Persistence and activation of malaria hypnozoites in long-term primary hepatocyte cultures. *Nature Medicine* **2014**, *20* (3), 307-12.
648. Sundriyal, S.; Malmquist, N. A.; Caron, J., *et al.*, Development of diaminoquinazoline histone lysine methyltransferase inhibitors as potent blood-stage antimalarial compounds. *ChemMedChem* **2014**, *9* (10), 2360-2373.
649. Sundriyal, S.; Chen, P. B.; Lubin, A. S., *et al.*, Histone lysine methyltransferase structure activity relationships that allow for segregation of G9a inhibition and anti-*Plasmodium* activity. *MedChemComm* **2017**, *8* (5), 1069-1092.

650. Hernandez, D. C.; Lim, K. C.; McKerrow, J. H.; Davies, S. J., Schistosoma mansoni: sex-specific modulation of parasite growth by host immune signals. *Experimental Parasitology* **2004**, *106* (1-2), 59-61.
651. de Mendonça, R. L.; Escrivá, H.; Bouton, D.; Laudet, V.; Pierce, R. J., Hormones and Nuclear Receptors in Schistosome Development. *Parasitology Today* **2000**, *16* (6), 233-240.
652. Escobedo, G.; Roberts, C. W.; Carrero, J. C.; Morales-Montor, J., Parasite regulation by host hormones: an old mechanism of host exploitation? *Trends in Parasitology* **2005**, *21* (12), 588-593.
653. LoVerde, P. T.; Osman, A.; Hinck, A., Schistosoma mansoni: TGF- β signaling pathways. *Experimental Parasitology* **2007**, *117* (3), 304-317.
654. Oliveira, K. C.; Carvalho, M. L. P.; Venancio, T. M., *et al.*, Identification of the Schistosoma mansoni TNF-Alpha Receptor Gene and the Effect of Human TNF-Alpha on the Parasite Gene Expression Profile. *PLoS Neglected Tropical Diseases* **2009**, *3* (12), e556.
655. Siegel, D. A.; Tracy, J. W., Effect of Pairing In vitro on the Glutathione Level of Male Schistosoma mansoni. *The Journal of Parasitology* **1988**, *74* (4), 524.
656. Haseeb, M. A.; Fried, B.; Eveland, L. K., Schistosoma mansoni: Female-dependent lipid secretion in males and corresponding changes in lipase activity. *International Journal for Parasitology* **1989**, *19* (7), 705-709.
657. Kunz, W.; Gohr, L.; Grevelding, C., *et al.*, Schistosoma mansoni: control of female fertility by the male. *Memórias do Instituto Oswaldo Cruz* **1995**, *90* (2), 185-189.
658. Grevelding, C. G.; Sommer, G.; Kunz, W., Female-specific gene expression in Schistosoma mansoni is regulated by pairing. *Parasitology* **1997**, *115* (6), 635-640.
659. Beckmann, S.; Quack, T.; Burmeister, C., *et al.*, Schistosoma mansoni: signal transduction processes during the development of the reproductive organs. *Parasitology* **2010**, *137* (03), 497.
660. Beckmann, S.; Buro, C.; Dissous, C.; Hirzmann, J.; Grevelding, C. G., The Syk Kinase SmTK4 of Schistosoma mansoni Is Involved in the Regulation of Spermatogenesis and Oogenesis. *PLoS Pathogens* **2010**, *6* (2), e1000769.
661. Hahnel, S.; Quack, T.; Parker-Manuel, S. J., *et al.*, Gonad RNA-specific qRT-PCR analyses identify genes with potential functions in schistosome reproduction such as SmFz1 and SmFGFRs. *Frontiers in Genetics* **2014**, *5*.
662. Williams, D. L.; Sayed, A. A.; Bernier, J., *et al.*, Profiling Schistosoma mansoni development using serial analysis of gene expression (SAGE). *Experimental Parasitology* **2007**, *117* (3), 246-258.
663. Anderson, L.; Amaral, M. S.; Beckedorff, F., *et al.*, Schistosoma mansoni Egg, Adult Male and Female Comparative Gene Expression Analysis and Identification of Novel Genes by RNA-Seq. *PLoS Neglected Tropical Diseases* **2015**, *9* (12), e0004334.
664. Fitzpatrick, J. M.; Johnston, D. A.; Williams, G. W., *et al.*, An oligonucleotide microarray for transcriptome analysis of Schistosoma mansoni and its application/use to investigate gender-associated gene expression. *Molecular and Biochemical Parasitology* **2005**, *141* (1), 1-13.
665. Fitzpatrick, J. M.; Protasio, A. V.; McArdle, A. J., *et al.*, Use of Genomic DNA as an Indirect Reference for Identifying Gender-Associated Transcripts in Morphologically Identical, but Chromosomally Distinct, Schistosoma mansoni Cercariae. *PLoS Neglected Tropical Diseases* **2008**, *2* (10), e323.
666. Lepesant, J. M. J.; Cosseau, C.; Boissier, J., *et al.*, Chromatin structure changes around satellite repeats on the Schistosoma mansoni female sex chromosome suggest a possible mechanism for sex chromosome emergence. *Genome Biology* **2012**, *13* (2), R14.
667. Picard, M. A.; Boissier, J.; Roquis, D., *et al.*, Sex-Biased Transcriptome of Schistosoma mansoni: Host-Parasite Interaction, Genetic Determinants and Epigenetic Regulators Are Associated with Sexual Differentiation. *PLoS Negl Trop Dis* **2016**, *10* (9), e0004930.
668. Fantappie, M. R.; Gimba, E. R.; Rumjanek, F. D., Lack of DNA methylation in Schistosoma mansoni. *Exp Parasitol* **2001**, *98* (3), 162-6.
669. Geyer, K. K.; Chalmers, I. W.; Mackintosh, N., *et al.*, Cytosine methylation is a conserved epigenetic feature found throughout the phylum Platyhelminthes. *BMC Genomics* **2013**, *14*, 462.

670. Mansure, J. J.; Furtado, D. R.; de Oliveira, F. M., *et al.*, Cloning of a protein arginine methyltransferase PRMT1 homologue from *Schistosoma mansoni*: evidence for roles in nuclear receptor signaling and RNA metabolism. *Biochemical and Biophysical Research Communications* **2005**, 335 (4), 1163-72.
671. Diao, W.; Zhou, H.; Pan, W., *et al.*, Expression and immune characterization of a novel enzyme, protein arginine methyltransferase 1, from *Schistosoma japonicum*. *Parasitol Res* **2014**, 113 (3), 919-24.
672. Hermann, A.; Schmitt, S.; Jeltsch, A., The human Dnmt2 has residual DNA-(cytosine-C5) methyltransferase activity. *The Journal of Biological Chemistry* **2003**, 278 (34), 31717-21.
673. Geyer, K. K.; Rodriguez Lopez, C. M.; Chalmers, I. W., *et al.*, Cytosine methylation regulates oviposition in the pathogenic blood fluke *Schistosoma mansoni*. *Nature Communications* **2011**, 2, 424.
674. Raddatz, G.; Guzzardo, P. M.; Olova, N., *et al.*, Dnmt2-dependent methylomes lack defined DNA methylation patterns. *Proceedings of the National Academy of Sciences of the United States of America* **2013**, 110 (21), 8627-31.
675. Warnecke, P. M.; Stirzaker, C.; Song, J., *et al.*, Identification and resolution of artifacts in bisulfite sequencing. *Methods (San Diego, Calif.)* **2002**, 27 (2), 101-7.
676. Oliveira, K. C.; Carvalho, M. L.; Maracaja-Coutinho, V.; Kitajima, J. P.; Verjovski-Almeida, S., Non-coding RNAs in schistosomes: an unexplored world. *An Acad Bras Cienc* **2011**, 83 (2), 673-94.
677. Xue, X.; Sun, J.; Zhang, Q., *et al.*, Identification and characterization of novel microRNAs from *Schistosoma japonicum*. *PLoS One* **2008**, 3 (12), e4034.
678. Huang, J.; Hao, P.; Chen, H., *et al.*, Genome-wide identification of *Schistosoma japonicum* microRNAs using a deep-sequencing approach. *PLoS One* **2009**, 4 (12), e8206.
679. Hao, L.; Cai, P.; Jiang, N.; Wang, H.; Chen, Q., Identification and characterization of microRNAs and endogenous siRNAs in *Schistosoma japonicum*. *BMC Genomics* **2010**, 11, 55.
680. Wang, Z.; Xue, X.; Sun, J., *et al.*, An "in-depth" description of the small non-coding RNA population of *Schistosoma japonicum* schistosomulum. *PLoS Negl Trop Dis* **2010**, 4 (2), e596.
681. Simões, M. C.; Lee, J.; Djikeng, A., *et al.*, Identification of *Schistosoma mansoni* microRNAs. *BMC Genomics* **2011**, 12 (1).
682. Marco, A.; Kozomara, A.; Hui, J. H. L., *et al.*, Sex-Biased Expression of MicroRNAs in *Schistosoma mansoni*. *PLoS Neglected Tropical Diseases* **2013**, 7 (9), e2402.
683. Zhu, L.; Zhao, J.; Wang, J., *et al.*, MicroRNAs Are Involved in the Regulation of Ovary Development in the Pathogenic Blood Fluke *Schistosoma japonicum*. *PLOS Pathogens* **2016**, 12 (2), e1005423.
684. Pierce, R. J.; Dubois-Abdesselem, F.; Lancelot, J.; Andrade, L.; Oliveira, G., Targeting schistosome histone modifying enzymes for drug development. *Current Pharmaceutical Design* **2012**, 18 (24), 3567-78.
685. Oger, F.; Dubois, F.; Caby, S., *et al.*, The class I histone deacetylases of the platyhelminth parasite *Schistosoma mansoni*. *Biochemical and Biophysical Research Communications* **2008**, 377 (4), 1079-1084.
686. Lancelot, J.; Caby, S.; Dubois-Abdesselem, F., *et al.*, *Schistosoma mansoni* Sirtuins: Characterization and Potential as Chemotherapeutic Targets. *PLoS Neglected Tropical Diseases* **2013**, 7 (9), e2428.
687. Roquis, D.; Lepesant, J. M.; Picard, M. A., *et al.*, The Epigenome of *Schistosoma mansoni* Provides Insight about How Cercariae Poise Transcription until Infection. *PLoS Negl Trop Dis* **2015**, 9 (8), e0003853.
688. Roquis, D.; Rognon, A.; Chaparro, C., *et al.*, Frequency and mitotic heritability of epimutations in *Schistosoma mansoni*. *Molecular Ecology* **2016**, 25 (8), 1741-58.
689. Fneich, S.; Theron, A.; Cosseau, C., *et al.*, Epigenetic origin of adaptive phenotypic variants in the human blood fluke *Schistosoma mansoni*. *Epigenetics & Chromatin* **2016**, 9, 27.

690. Perrin, C.; Lepesant, J. M.; Roger, E., *et al.*, Schistosoma mansoni mucin gene (SmPoMuc) expression: epigenetic control to shape adaptation to a new host. *PLoS Pathogens* **2013**, *9* (8), e1003571.
691. Cabezas-Cruz, A.; Lancelot, J.; Caby, S.; Oliveira, G.; Pierce, R. J., Epigenetic control of gene function in schistosomes: a source of therapeutic targets? *Frontiers in Genetics* **2014**, *5*, 317.
692. de Moraes Maciel, R.; da Costa, R. F.; de Oliveira, F. M.; Rumjanek, F. D.; Fantappie, M. R., Protein acetylation sites mediated by Schistosoma mansoni GCN5. *Biochemical and Biophysical Research Communications* **2008**, *370* (1), 53-6.
693. de Moraes Maciel, R.; de Silva Dutra, D. L.; Rumjanek, F. D., *et al.*, Schistosoma mansoni histone acetyltransferase GCN5: linking histone acetylation to gene activation. *Mol Biochem Parasitol* **2004**, *133* (1), 131-5.
694. Bertin, B.; Oger, F.; Cornette, J., *et al.*, Schistosoma mansoni CBP/p300 has a conserved domain structure and interacts functionally with the nuclear receptor SmFtz-F1. *Mol Biochem Parasitol* **2006**, *146* (2), 180-91.
695. Fantappie, M. R.; Bastos de Oliveira, F. M.; de Moraes Maciel, R., *et al.*, Cloning of SmNCoA-62, a novel nuclear receptor co-activator from Schistosoma mansoni: assembly of a complex with a SmRXR1/SmNR1 heterodimer, SmGCN5 and SmCBP1. *International Journal for Parasitology* **2008**, *38* (10), 1133-47.
696. Carneiro, V. C.; de Abreu da Silva, I. C.; Torres, E. J., *et al.*, Epigenetic changes modulate schistosome egg formation and are a novel target for reducing transmission of schistosomiasis. *PLoS Pathogens* **2014**, *10* (5), e1004116.
697. Anderson, L.; Gomes, M. R.; daSilva, L. F., *et al.*, Histone deacetylase inhibition modulates histone acetylation at gene promoter regions and affects genome-wide gene transcription in Schistosoma mansoni. *PLOS Neglected Tropical Diseases* **2017**, *11* (4), e0005539.
698. Nakagawa, M.; Oda, Y.; Eguchi, T., *et al.*, Expression profile of class I histone deacetylases in human cancer tissues. *Oncology Reports* **2007**.
699. Dubois, F.; Caby, S.; Oger, F., *et al.*, Histone deacetylase inhibitors induce apoptosis, histone hyperacetylation and up-regulation of gene transcription in Schistosoma mansoni. *Molecular and Biochemical Parasitology* **2009**, *168* (1), 7-15.
700. Heimbürg, T.; Chakrabarti, A.; Lancelot, J., *et al.*, Structure-Based Design and Synthesis of Novel Inhibitors Targeting HDAC8 from Schistosoma mansoni for the Treatment of Schistosomiasis. *J Med Chem* **2016**, *59* (6), 2423-2435.
701. Kannan, S.; Melesina, J.; Hauser, A.-T., *et al.*, Discovery of Inhibitors of Schistosoma mansoni HDAC8 by Combining Homology Modeling, Virtual Screening, and in Vitro Validation. *Journal of Chemical Information and Modeling* **2014**, *54* (10), 3005-3019.
702. Marek, M.; Kannan, S.; Hauser, A.-T., *et al.*, Structural Basis for the Inhibition of Histone Deacetylase 8 (HDAC8), a Key Epigenetic Player in the Blood Fluke Schistosoma mansoni. *PLoS Pathogens* **2013**, *9* (9), e1003645.
703. Stolf, D. A.; Marek, M.; Lancelot, J., *et al.*, Molecular Basis for the Antiparasitic Activity of a Mercaptoacetamide Derivative That Inhibits Histone Deacetylase 8 (HDAC8) from the Human Pathogen Schistosoma mansoni. *Journal of Molecular Biology* **2014**, *426* (20), 3442-3453.
704. Utzinger, J.; Keiser, J.; Shuhua, X.; Tanner, M.; Singer, B. H., Combination Chemotherapy of Schistosomiasis in Laboratory Studies and Clinical Trials. *Antimicrobial Agents and Chemotherapy* **2003**, *47* (5), 1487-1495.
705. Horemans, A. M.; Tielens, A. G.; van den Bergh, S. G., The reversible effect of glucose on the energy metabolism of Schistosoma mansoni cercariae and schistosomula. *Mol Biochem Parasitol* **1992**, *51* (1), 73-9.
706. Lancelot, J.; Cabezas-Cruz, A.; Caby, S., *et al.*, Schistosome sirtuins as drug targets. *Future Medicinal Chemistry* **2015**, *7* (6), 765-82.
707. Religa, A. A.; Waters, A. P., Sirtuins of parasitic protozoa: in search of function(s). *Mol Biochem Parasitol* **2012**, *185* (2), 71-88.

708. Vergnes, B.; Sereno, D.; Madjidian-Sereno, N.; Lemesre, J.-L.; Ouaisi, A., Cytoplasmic SIR2 homologue overexpression promotes survival of Leishmania parasites by preventing programmed cell death. *Gene* **2002**, 296 (1-2), 139-150.
709. Singh, R.; Singh, S.; Pandey, P. N., In-silico analysis of Sirt2 from Schistosoma mansoni: structures, conformations, and interactions with inhibitors. *Journal of Biomolecular Structure & Dynamics* **2016**, 34 (5), 1042-51.
710. Singh, R.; Pandey, P. N., Molecular docking and molecular dynamics study on SmHDAC1 to identify potential lead compounds against Schistosomiasis. *Molecular Biology Reports* **2015**, 42 (3), 689-98.
711. Disch, J. S.; Evindar, G.; Chiu, C. H., *et al.*, Discovery of thieno[3,2-d]pyrimidine-6-carboxamides as potent inhibitors of SIRT1, SIRT2, and SIRT3. *J Med Chem* **2013**, 56 (9), 3666-79.
712. Schiedel, M.; Marek, M.; Lancelot, J., *et al.*, Fluorescence-Based Screening Assays for the NAD⁺-Dependent Histone Deacetylase smSirt2 from Schistosoma mansoni. *Journal of Biomolecular Screening* **2015**, 20 (1), 112-121.
713. Nimura, K.; Ura, K.; Kaneda, Y., Histone methyltransferases: regulation of transcription and contribution to human disease. *Journal of Molecular Medicine (Berlin, Germany)* **2010**, 88 (12), 1213-20.
714. Jelinic, P.; Stehle, J. C.; Shaw, P., The testis-specific factor CTCFL cooperates with the protein methyltransferase PRMT7 in H19 imprinting control region methylation. *PLoS Biol* **2006**, 4 (11), e355.
715. Choi, S.; Jung, C. R.; Kim, J. Y.; Im, D. S., PRMT3 inhibits ubiquitination of ribosomal protein S2 and together forms an active enzyme complex. *Biochimica et Biophysica Acta* **2008**, 1780 (9), 1062-9.
716. Shi, X.; Kachirskaia, I.; Yamaguchi, H., *et al.*, Modulation of p53 function by SET8-mediated methylation at lysine 382. *Molecular Cell* **2007**, 27 (4), 636-46.
717. Agger, K.; Cloos, P. A.; Christensen, J., *et al.*, UTX and JMJD3 are histone H3K27 demethylases involved in HOX gene regulation and development. *Nature* **2007**, 449 (7163), 731-4.
718. Ezhkova, E.; Lien, W. H.; Stokes, N., *et al.*, EZH1 and EZH2 cogovern histone H3K27 trimethylation and are essential for hair follicle homeostasis and wound repair. *Genes & Development* **2011**, 25 (5), 485-98.
719. Bissinger, E. M.; Heinke, R.; Spannhoff, A., *et al.*, Acyl derivatives of p-aminosulfonamides and dapsone as new inhibitors of the arginine methyltransferase hPRMT1. *Bioorganic & Medicinal Chemistry* **2011**, 19 (12), 3717-31.
720. Rosenthal, P. J., Antimalarial drug discovery: old and new approaches. *Journal of Experimental Biology* **2003**, 206 (21), 3735-3744.
721. Saraf, A.; Cervantes, S.; Bunnik, E. M., *et al.*, Dynamic and Combinatorial Landscape of Histone Modifications during the Intraerythrocytic Developmental Cycle of the Malaria Parasite. *Journal of Proteome Research* **2016**, 15 (8), 2787-801.
722. Rotili, D.; Simonetti, G.; Savarino, A., *et al.*, Non-Cancer Uses of Histone Deacetylase Inhibitors: Effects on Infectious Diseases and β-Hemoglobinopathies+. *Current Topics in Medicinal Chemistry* **2009**, 9 (3), 272-291.
723. Engel, J. A.; Jones, A. J.; Avery, V. M., *et al.*, Erratum to "Profiling the anti-protozoal activity of anti-cancer HDAC inhibitors against Plasmodium and Trypanosoma parasites" [Int. J. Parasitol. Drugs Drug Res. 5 (2015) 117–126]. *International Journal for Parasitology: Drugs and Drug Resistance* **2016**, 6 (3), 287.
724. Andrews, K.; Tran, T.; Wheatley, N.; Fairlie, D., Targeting Histone Deacetylase Inhibitors for Anti-Malarial Therapy. *Current Topics in Medicinal Chemistry* **2009**, 9 (3), 292-308.
725. Antonello Mai, S. M., Dante Rotili, Silvia Simeoni, Rino Ragno, Giorgia Botta, Angela Nebbioso, Marco Miceli, Lucia Altucci, and Gerald Brosch,, Synthesis and Biological Properties of Novel, Uracil-Containing Histone Deacetylase Inhibitors. *J. Med. Chem.* **2006**, 49, 6046-6056.
726. Mori K, K. K., Synthesis of trichostatin A, a potent differentiation inducer of Friend leukemic cells, and its antipode. *Tetrahedron* **1998**, 44, 6013-6020.

727. Mai, A. S., G.; Artico, M.; Ragno, R.; Massa, S.; Novellino, E.; Greco, G.; Lavecchia, A.; Musiu, C.; La Colla, M.; Murgioni, C.; La Colla, P.; Loddo, R., Structure-based design, synthesis, and biological evaluation of conformationally restricted novel 2-alkylthio-6-[1-(2,6-difluorophenyl)alkyl]-3,4-dihydro-5-alkylpyrimidin-4(3H)-ones as nonnucleoside inhibitors of HIV-1 reverse transcriptase. *J. Med. Chem.* **2001**, *44*, 2544-2554.
728. Katsuno, K.; Burrows, J. N.; Duncan, K., *et al.*, Hit and lead criteria in drug discovery for infectious diseases of the developing world. *Nature Reviews Drug Discovery* **2015**, *14* (11), 751-8.
729. Oduola, A. M.; Weatherly, N. F.; Bowdre, J. H.; Desjardins, R. E., Plasmodium falciparum: cloning by single-erythrocyte micromanipulation and heterogeneity in vitro. *Exp Parasitol* **1988**, *66* (1), 86-95.
730. Peters, W., The chemotherapy of rodent malaria, XXII. The value of drug-resistant strains of P. berghei in screening for blood schizontocidal activity. *Annals of Tropical Medicine and Parasitology* **1975**, *69* (2), 155-71.
731. Amaladoss, A.; Chen, Q.; Liu, M., *et al.*, De Novo Generated Human Red Blood Cells in Humanized Mice Support Plasmodium falciparum Infection. *PLoS ONE* **2015**, *10* (6), e0129825.
732. Chua, M. J.; Arnold, M. S. J.; Xu, W., *et al.*, Effect of clinically approved HDAC inhibitors on Plasmodium, Leishmania and Schistosoma parasite growth. *International Journal for Parasitology: Drugs and Drug Resistance* **2017**, *7* (1), 42-50.
733. Fréville, A.; Cailliau-Maggio, K.; Pierrot, C., *et al.*, Plasmodium falciparum encodes a conserved active inhibitor-2 for Protein Phosphatase type 1: perspectives for novel anti-plasmodial therapy. *BMC Biology* **2013**, *11*, 80-80.
734. Izumiyama, S.; Omura, M.; Takasaki, T.; Ohmae, H.; Asahi, H., Plasmodium falciparum: development and validation of a measure of intraerythrocytic growth using SYBR Green I in a flow cytometer. *Exp Parasitol* **2009**, *121* (2), 144-50.
735. Berriman, M.; Haas, B. J.; LoVerde, P. T., *et al.*, The genome of the blood fluke Schistosoma mansoni. *Nature* **2009**, *460* (7253), 352-8.
736. Zhou Y, Chen Y, Zhang L, *et al.* The Schistosoma japonicum genome reveals features of host-parasite interplay. *Nature* **2009**, *460* (7253), 345-351.
737. Young, N. D.; Jex, A. R.; Li, B., *et al.*, Whole-genome sequence of Schistosoma haematobium. *Nature Genetics* **2012**, *44* (2), 221-5.
738. Sayed, A. A.; Simeonov, A.; Thomas, C. J., *et al.*, Identification of oxadiazoles as new drug leads for the control of schistosomiasis. *Nature Medicine* **2008**, *14* (4), 407-12.
739. Smith, B. C.; Hallows, W. C.; Denu, J. M., A continuous microplate assay for sirtuins and nicotinamide-producing enzymes. *Anal Biochem* **2009**, *394* (1), 101-9.
740. Suenkel, B.; Steegborn, C., Recombinant Preparation, Biochemical Analysis, and Structure Determination of Sirtuin Family Histone/Protein Deacylases. *Methods Enzymol* **2016**, *573*, 183-208.
741. Ballante, F.; Reddy, D. R.; Zhou, N. J.; Marshall, G. R., Structural insights of SmKDAC8 inhibitors: Targeting Schistosoma epigenetics through a combined structure-based 3D QSAR, in vitro and synthesis strategy. *Bioorganic & Medicinal Chemistry* **2017**, *25* (7), 2105-2132.
742. Anderson L, P. R., Verjovski-Almeida S Schistosoma mansoni histones: from transcription to chromatin regulation; an in silico analysis. *Mol Biochem Parasitol* **2012**, *183*, 105-114.
743. Binda C, V. S., Romanenghi M, Pilotto S, Cirilli R, Karytinis A, Ciossani G, Botrugno OA, Forneris F, Tardugno M, Edmondson DE, Minucci S, Mattevi A, Mai A, Biochemical, structural, and biological evaluation of tranlylcypromine derivatives as inhibitors of histone demethylases LSD1 and LSD2. *Journal of the American Chemical Society* **2010**, pp 6827-6833.
744. Rotili, D.; Tomassi, S.; Conte, M., *et al.*, Pan-Histone Demethylase Inhibitors Simultaneously Targeting Jumonji C and Lysine-Specific Demethylases Display High Anticancer Activities. *J Med Chem* **2014**, *57* (1), 42-55.
745. Doebelin, C., *et al.*, Development of Dipeptidic hGPR54 Agonists. *ChemMedChem* **2016**, *11*, 2147-2154.

746. Gao, S., et al., Palladium-Catalyzed Dearomative Allylic Alkylation of Indoles with Alkynes To Synthesize Indolenines with C3-Quarternary Centers. *Org Lett* **2016**, *18*, 3906-3909.